Eco-evolutionary implications underlying the emergence of a derived reproductive mode in fire salamanders

André Filipe Plácido Lourenço
Biodiversity, Genetics, and Evolution
Department of Biology
2019
Orientador
Guillermo Velo-Antón, Auxiliary Researcher, CIBIO-InBIO/FCUP
Coorientador
Ian J. Wang, Assistant Professor, University of California, Berkeley

Nota prévia

Na elaboração desta tese, e nos termos do número 2 do Artigo 4º do Regulamento Geral dos Terceiros Ciclos de Estudos da Universidade do Porto e do Artigo 31º do D.L. 74/2006, de 24 de Março, com a nova redação introduzida pelo D.L. 230/2009, de 14 de Setembro, foi efetuado o aproveitamento total de um conjunto coerente de trabalhos de investigação já publicados em revistas internacionais indexadas e com arbitragem científica, os quais integram alguns dos capítulos da presente tese. Tendo em conta que os referidos trabalhos foram realizados com a colaboração de outros autores, o candidato esclarece que, em todos eles, participou ativamente na sua conceção, na obtenção e análise de dados, e discussão de resultados, bem como na elaboração da sua forma publicada.

Este trabalho foi apoiado pela Fundação para a Ciência e Tecnologia (FCT) através da atribuição da bolsa de doutoramento (PD/BD/106060/ 2015).

FCT
Fundação para a Ciência e a Tecnologia
MINISTÉRIO DA CIÊNCIA, TECNOLOGIA E ENSINO SUPERIOR

POPH
QUALIFICAR É CRESCER.

QREN
QUADRO DE REFERÊNCIA ESTRATÉGICO NACIONAL

GOVERNO DA REPÚBLICA PORTUGUESA

UNIÃO EUROPEIA
Fundo Social Europeu

Agradecimentos

A conclusão desta tese não teria sido possível sem a ajuda de várias pessoas, desde colegas de profissão até familiares e amigos. Algumas instituições também forneceram suporte (especialmente financeiro) que foi crucial para desenvolver todo o trabalho de campo e laboratorial incluído na presente tese doutoral.

Contrariando o formato habitual da secção de “Agradecimentos” em teses doutorais, as minhas primeiras palavras de agradecimento vão para os meus pais. Eles são os principais responsáveis por ter chegado a este ponto profissional da minha carreira. Eles deram-me amor, educação, conselhos de vida bastante importantes e não menos importante, apoiaram sempre as minhas decisões profissionais, mesmo sabendo que a área de investigação (e em particular da Biologia) acarretam alguns riscos. Por isto tudo, eles merecem este agradecimento especial. Espero um dia retribuir um centésimo daquilo que eles fizeram pela minha vida.

Em seguida, um agradecimento muito especial para o meu orientador principal, Guillermo Velo Antón. Ele ajudou-me a planear o meu doutoramento, demonstrou uma grande disponibilidade para discutir ideias sobre o meu trabalho, ajudou-me no meu trabalho de campo, reviu com bastante rapidez os incontáveis drafts de artigos e propostas de financiamento que enviei, esteve disponível para falar sobre temas de índole pessoal e foi um grande companheiro para beber cervejas. Por outras palavras, ele foi aquilo que, na minha perspectiva, deve de ser um orientador de doutoramento. Sem ele, jamais esta tese tería sido possível e portanto um “muchas gracías” a ti Guillermo. Continua a ser o investigador que és e mais tarde ou mais cedo irão dar-te o devido valor em Portugal, Espanha ou noutro lado qualquer.

I also have to thank my co-supervisor Ian Wang, who accepted me as his PhD student, kindly hosted my short-term stayings at University of California, Berkeley, and provided insightful opinions about the experimental design of my thesis and my manuscripts. Your teachings greatly helped me improve as a researcher.

Agradeço também às instituições de financiamento, nomeadamente, a Fundação para a Ciência e Tecnologia (FCT). A FCT não só forneceu financiamento individual (bolsa de doutoramento - PD/BD/106060/2015), mas também forneceu financiamento para suportar o meu trabalho de campo e laboratorial (EVOVIV: PTDC/BIA-EVF/3036/2012; SALOMICS: PTDC/BIA-EVL/28475/2017). Finalmente, também agradeço a outras instituições/programas que financiaram o meu trabalho, nomeadamente, aos fundos europeus do programa operacional de competitividade (FEDER; FCOMP-01-0124-FEDER-028325 and POCI-01-

0145-FEDER-006821) e também à British Herpetological Society que me ofereceu uma bolsa de Student Grant Scheme para financiar o meu trabalho de campo.

Esta tese também não teria sido terminada sem as instituições que me acolheram, nomedamente, o Centro de Investigação em Biodiversidade, Genética e Evolução (CIBIO-InBIO) da Universidade do Porto que forneceu as condições logistícas indispensáveis (gabinete, laboratórios e viaturas para realizar o trabalho de campo) ao término desta tese. Também agradeço ao polo universitário de Berkeley da Universidade da Califórnia por terem-me recebido.

Um muito obrigado também para os co-autores dos meus artigos – David Álvarez, Bernardo Antunes, João Gonçalves e Filipe Carvalho. Sem a vossa ajuda, os meus manuscritos teriam menos qualidade cientifíca. Agradeço também às pessoas que ajudaram na minha amostragem, uma vez que estiveram dispostas a dispender o seu tempo para ajudar a completar o meu doutoramento. Essas pessoas são: o Bernardo Antunes, Marco Dinis, Bárbara Santos, Clara Figueiredo Vásquez, Fábio Sousa, Lucía Ríos, Margarida Henrique, Aspassia Anagnostopoulou, Alessio Paoletti, Pedro Alves, Paulo Pereira, Sophia Rosa e Iria Pazos.

Também quero agradecer às pessoas que trabalham no Centro de Testagem Molecular (CTM) que tiveram muita paciência para aturar-me e demonstraram uma grande disponibilidade para ajudar e tirar as minhas dúvidas. Agradeço em especial à Susana Lopes pela ajuda na genotipagem dos microsatélites, à Patrícia Ribeiro e Sofia Mourão pela ajuda no laboratório e à Sara João pelo apoio logístico em relação ao material laboratorial. E como não podia deixar de ser, agradeço ao "rei" do CIBIO, o Sr. Bernardino, pelos transportes metro-Vairão, por resolver todos os problemas que ocorrem no CIBIO e, acima de tudo, pelo companheirismo.

Em seguida, gostaria de agradecer aos "miguxos" e "miguxas" pelos momentos de convivío, companheirismo, aconselhamento, bubadeiras, etc… Em especial gostaria de agradecer à Damas, Rita Monteiro, Pleno, Coelho, Jesus, Joana Amaral, Diana, Joana texugo, Joana Guimarães, Paulo, Hugo, Jessica, o bácaro do Passinhas, o porco do Duarte, o Luzpalo, Inês, João Gil, Ana Serrano, Cristina, Nádia, à Piranha, o Calistro, o Fainha e mais umas quantas pessoas (para salvaguardar caso me tenha esquecido de alguém). Vocês sabem que são batsante importantes na minha vida e por isso um muito obrigado especial a vocês todos!

Como não podia deixar de ser, a minha família é um pilar muito importante da minha vida. Agradeço aos meus familiares pela ajuda e por todos os momentos de convivío que permitiram-me relaxar e assim, encarar esta tese de uma maneira muito mais eficiente. Um

agradecimento especial à minha irmã Nela e aos “pigs” Zé e Francisco pelos momentos de parvoíce, entre outras coisas.

Finalmente, um MUITO OBRIGADO por tudo à minha bolachinha Barbara Correia. Obrigado não só pelo papel ativo que tiveste na concepção desta tese (ajudar-me no trabalho de campo, ler os meus incríveis drafts de artigos, emprestares-me o carro para trabalho de campo, etc…), mas também pelos momentos de preguiça no sofá, pelo apoio e carinho inestimáveis, pela compreensão ilimitada, pela (quase) inesgotável boa disposição para as minhas totozices e pelas aventuras partilhadas e por aquelas que irão ser partilhadas. Ah e claro, obrigado pelo Golias (ele agora é meu!). Espero poder continuar a partilhar esta viagem a que chamam “vida” contigo para sempre.

Resumo

A transição de um modo reprodutor ancestral ovíparo para um modo derivado vivíparo constitui uma grande inovação evolutiva que ocorreu várias vezes de forma independente em vertebrados em resposta a fortes pressões seletivas na descendência (ex: predação ou condições ambientais extremas). Estas mudanças nas estratégias reprodutoras causaram alterações profundas a nível fenotípico, ecológico e genético. A maior parte dos estudos que examinaram os efeitos das alterações nos modos reprodutores focaram-se nas mudanças fenotípicas e genéticas decorrentes da evolução de um modo reprodutor derivado, em particular, nos répteis. Os efeitos de um novo modo reprodutor na ecologia dos indivíduos e, por conseguinte, na evolução das populações, têm recebido pouca atenção pela comunidade científica, embora alguns estudos tenham explorado algumas das consequências eco-evolutivas subjacentes a um modo reprodutor derivado (ex: taxas de sobrevivência e colonização de ambientes instáveis mais elevada, mudanças na evolução de caracteres fenotípicos e nas taxas de diversificação de espécies). Um processo determinante para a dinâmica populacional e que está altamente correlacionado com a reprodução é a dispersão (e o fluxo génico). Considerando isto, as alterações biológicas e comportamentais subjacentes à reprodução podem modificar a maneira como os indivíduos dispersam pela paisagem, o que pode ter consequências para a conetividade genética. Apesar do possível efeito de alterações nos modos reprodutores na dispersão, este assunto tem sido muito pouco explorado.

As transições para o viviparismo ou pueriparismo (o último conceito é mais correto para anfíbios) causaram mudanças significativas no ciclo de vida dos anfíbios, o que faz deles bons sistemas para investigar os efeitos eco-evolutivos decorrentes de uma alteração no modo reprodutor. A maior parte dos anfíbios exibe um ciclo de vida bifásico, em que um estágio larvar aquático é seguido por uma metamorfose para juvenis terrestres. No entanto, alguns anfíbios mudaram de uma reprodução aquática ovípara ou larvípara (deposição de ovos ou larvas na água, respetivamente) para uma reprodução terrestre puerípara (parturição de juvenis terrestres), possivelmente em resposta à escassez de corpos aquáticos nos seus habitats para depositar a descendência. Esta maior independência da água pode ter envolvido mudanças substanciais na ecologia e evolução de populações pueríparas quando comparado com populações de anfíbios aquáticos. Por exemplo, pode-se esperar que anfíbios pueríparos dispersem por maiores distâncias devido à sua menor dependência de corpos de água para a reprodução.

Na presente tese doutoral, eu usei marcadores moleculares (maioritariamente microsatélites) para availar as implicações eco-evolutivas potenciais que resultaram de uma mudança de uma reprodução aquática para uma reprodução pueríparа terrestre em anfíbios, com especial destaque para a dispersão e o fluxo génico. Eu usei como modelo de estudo a salamandra-de-pintas-amarelas (*Salamandra salamandra*, Linnaeus 1758), que constitui um excecional e raro caso em que duas estratégias de reprodução co-ocorrem: (i) reprodução aquática larvípara (caracter ancestral), em que as fêmeas depositam larvas em corpos de água; e (ii) um modo de reprodução terrestre pueríparo, em que as fêmeas dão à luz juvenis terrestres metamorfoseados. O pueriparismo surgiu em *S. salamandra* durante o período do Plioceno-Pleistoceno na cordilheira Cantábrica (norte de Espanha), possivelmente, em resposta à escassez de água superficial em substratos cársticos calcários. Esta variação nas estratégias reprodutoras ao nível subespecífico permite fazer comparações robustas entre modos reprodutores, uma vez que esse tipo de comparações diminuem o efeito de um possível enviasamento causado por elevadas diferenças a nível fenotípico e ecológico commumente observadas em espécies muito divergentes a nível filogenético. Nesta tese, populações larvíparas de *S. s. gallaica* e populações pueríparas de *S. s. bernardezi*, localizadas no norte de Espanha, foram estudadas para abordar o meu objetivo principal.

O pueriparismo permitiu a sobrevivência de anfíbios em ambientes aonde a água é um recurso limitante (ex: substratos calcários, terrenos íngremes). No entanto, no capítulo 2, eu introduzo um caso de estudo que mostra perfeitamente que o pueriparismo também permite maiores taxas de sobrevivência num cenário de alterações contemporâneas da paisagem (urbanização). Em específico, eu analisei os padrões de variação genética em populações pueríparas e urbanas de *S. salamandra* na cidade histórica de Oviedo (Espanha). Estas populações encontram-se espalhadas pela cidade em pequenas parcelas de vegetação (ex: parques e jardins urbanos) e, algumas delas, têm persistido dentro dos limites da cidade por centenas de gerações. A sobrevivência a longo prazo destas populações só foi possível graças à sua reprodução pueríparа, uma vez que estas parcelas urbanas não têm água para o desenvolvimento de larvas. Análises genéticas revelaram que a maior parte das populações estudadas têm um tamanho populacional baixo ($Ne < 50$) e que estão altamente isoladas a nível genético, apesar de a diversidade genética ser relativamente alta. O pueriparismo, assim como outros mecanismos demográficos e genéticos, foram sugeridos como potenciais causas destes níveis de diversidade. Para além disto, a compreensão dos fatores que influenciam a deriva genética nas cidades é fundamental para prever a direção e a magnitude das alterações evolutivas nas espécies que habitam ambientes urbanos. Considerando isto, as populações de salamandras-de-pintas-amarelas analisadas em Oviedo constitutem um bom sistema para

examinar este tópico. Eu testei no total quatro variáveis independentes (tamanho da parcela, tempo desde isolamento, magnitude de *bottleneck* e tempo pós-*bottleneck*) e as análises de regressão demonstraram inequivocamente que o tamanho da parcela está positivamente associado com o *Ne* e, consequentemente, com a variação genética neutral em ambientes urbanos.

Os capítulos 3 e 4 foram dedicados ao estudo dos efeitos potenciais do pueriparismo na dispersão e conetividade genética. Dado que a dispersão e o fluxo génico estão intimamente associados com a distribuição de corpos de água para a reprodução em anfíbios, então eu hipotetizei que a evolução de uma reprodução terrestre pueríparа em salamandras-de-pintas-amarelas fosse acompanhada por mudanças nestes processos. No capítulo 3, eu usei métodos genéticos de autocorrelação espacial para avaliar se o pueriparismo causou diferenças significativas nos padrões de estrutura genética e dispersão a escalas locais (transetos de 1 km). Os resultados deste capítulo sugerem que os padrões de dispersão (*i.e.* comportamento de dispersão) são semelhantes entre os modos reprodutores e que os machos dispersam mais que as fêmeas em *S. salamandra*, embora dados adicionais sejam necessários para confirmar estes resultados. Além disto, dados recolhidos nos capítulos 3 e 4 demonstram que sistemas lóticos são largamente responsáveis por assimetrias na dispersão entre salamandras larvíparas e pueríparas. Análises de parentesco (capítulo 3) sugerem que dispersão mediada pela água pode promover eventos de longa dispersão durante a fase larvar aquática, podendo assim, aumentar as distâncias percorridas pelos indivíduos durante a sua vida. Para além disto, análises da genética da paisagem feitas no capítulo 4 demonstram inequivocamente que rios e ribeiras reduzem a conetividade genética apenas em populações pueríparas, muito provavelmente porque as salamandras pueríparas exibem um ciclo de vida totalmente terrestre. Este efeito não foi documentado em populações larvíparas, uma vez que indivíduos larvíparos provavelmente atravessam estes elementos aquáticos durante a fase larvar aquática. Finalmente, as análises da genética da paisagem feitas no capítulo 4 contribuiram com informação importante para a ecologia da paisagem desta espécie. Especificamente, estas análises revelaram que áreas agrícolas e, em menor grau, exposição ao vento e topografia, são importantes variáveis que explicam a diferenciação genética em populações larvíparas e pueríparas.

Em conclusão, esta tese doutoral contribuiu para uma melhor compreensão das implicações eco-evolutivas resultantes de uma mudança de uma estratégia aquática de reprodução (larviparismo) para uma estratégia terrestre (pueriparismo) em anfíbios. Para além disto, alguns tópicos pouco explorados sobre a ecologia e a evolução de *S. salamandra* foram também abordados nesta tese e os resultos obtidos podem ajudar futuros estudos focados

em aspectos ecológicos, evolutivos e de conservação relevantes para esta espécie e para outras também. Esta tese também aponta para futuras direções de investigação que podem eventualmente contribuir para um maior conhecimento dos efeitos ecológicos e evolutivos das transições nos modos reprodutores.

Palavras-chave: dispersão, estrutura genética, fluxo génico, genética da paisagem, genética de ambientes urbanos, larviparismo, microsatélites, *Ne*, população, pueriparismo, *Salamandra salamandra*, viviparismo.

Summary

The transition from an ancestral oviparous (egg-laying) to a derived viviparous (live-bearing) reproduction comprises a major vertebrate innovation that has occurred independently multiple times across vertebrates in response to strong selective pressures on offspring (*e.g.* predation and stressful environmental conditions). These changes in reproductive strategies caused profound phenotypic, ecological, and genetic alterations. Most studies examining the effects of shifts in reproductive modes have focused on the phenotypic and genetic alterations caused by the evolution of a derived reproductive mode, particularly, in reptiles. The effects of a novel reproductive mode on the ecology of individuals and, by extension, in the evolution of populations has received much less attention, although a few studies have explored some of the potential eco-evolutionary consequences underlying derived reproductive traits (*e.g.* higher colonization and survival rates in harsh environments, changes in phenotypic evolution and species diversification rates). One process that plays a crucial role in population dynamics and is intimately correlated with reproduction is dispersal (and gene flow). Hence, changes in reproductive biology and behaviour are expected to alter the way individuals disperse across the landscape, with potential consequences to successful reproduction (*e.g.* genetic connectivity), though this subject has been even more underexplored.

Transitions to a viviparous or pueriparous (the latter term is more accurate for amphibians) reproduction caused significant life-history alterations in amphibians, making them good systems in which to examine the eco-evolutionary effects of changes in reproductive modes. Most amphibians exhibit a biphasic life cycle in which an aquatic larval stage is followed by metamorphosis into terrestrial juveniles. However, some amphibians shifted from ancestral oviparous or larviparous aquatic reproduction (delivery of eggs or larvae in water, respectively) to a pueriparous terrestrial reproduction (parturition of terrestrial juveniles), possibly in response to a lack of suitable water bodies in their environments for depositing offspring. This greater independence from water may entail substantial changes in the ecology and evolution of pueriparous populations compared to their ancestral aquatic-breeding counterparts. For example, one can expect that pueriparous amphibians disperse farther across the landscape due to their lower dependence from water bodies suitable for breeding.

In the present thesis, I relied on molecular markers (mostly microsatellites) to evaluate some of the potential eco-evolutionary implications arising from the shift of an aquatic reproduction to a pueriparous terrestrial one in amphibians, with a special emphasis on dispersal and gene flow. I used as a model system the fire salamander (*Salamandra salamandra*, Linnaeus 1758), which constitutes an exceptional and rare case, with two distinct reproductive strategies co-

occurring: (i) an aquatic larviparous reproduction (the ancestral trait), in which females deliver larvae in water bodies; and (ii) a terrestrial pueriparous reproduction (derived trait), in which females deliver fully metamorphosed terrestrial juveniles. Pueriparity emerged in *S. salamandra* during the Pliocene-Pleistocene period in the Cantabrian mountains (northern Spain), possibly, in response to the lack of surface water in karstic limestone substrates. This variation in reproductive strategies within species allows robust comparisons between reproductive modes, as it decreases the potential effects of confounding factors, such as the high phenotypic and ecological dissimilarity commonly observed in distantly-related species. In this thesis, larviparous populations of *S. s. gallaica* and pueriparous populations of *S. s. bernardezi* located in northern Spain were studied to address the main goal.

Pueriparity enabled the survival of amphibians in natural water-limited environments (*e.g.* karstic limestone substrates, steep terrains), but in chapter 2, I present a case study which neatly shows this reproductive mode may also entail higher survival rates under a scenario of contemporary land cover changes (urbanized landscapes). Specifically, I assessed patterns of genetic variation in urban pueriparous populations of *S. salamandra* in the historical city of Oviedo (Spain). These populations inhabit small patches of vegetation (*e.g.* urban parks and gardens) scattered across the city, some of which have putatively persisted for hundreds of generations. This long-term persistence was only possible due to their pueriparous reproduction, as these patches lack surface water for the development of larvae. Genetic analyses revealed most studied populations are small ($Ne < 50$) and genetically isolated to a large extent, although genetic diversity is relatively elevated. Pueriparity, as well as other potential demographic and genetic mechanisms, were suggested as potential drivers of these diversity levels. Moreover, understanding the factors governing genetic drift in cities is key to better predict the direction and magnitude of evolutionary changes in urbanized landscapes. In this regard, the fire salamander populations studied in Oviedo also comprise a good system to examine this topic. I tested four predictors in total (patch size, time since isolation, bottleneck magnitude, and post-bottleneck time), and regression analyses clearly indicate patch size is positively associated with *Ne* and, consequently, with neutral genetic variation in urban settlements.

The following chapters 3 and 4 were dedicated to the study of the putative effects of pueriparity on dispersal and genetic connectivity. Given that dispersal and gene flow are intimately associated with the distribution of water bodies for breeding in amphibians, I expected the evolution of a terrestrial pueriparous reproduction in fire salamanders was accompanied by changes in these processes. In chapter 3, I employed a genetic spatial autocorrelation framework to evaluate whether pueriparity caused significant differences in

patterns of fine-scale genetic structure and dispersal at local scales (1-km transects) between reproductive modes and sexes. Results suggest that dispersal tendencies (*i.e.* dispersal behaviour) are similar between reproductive modes and that dispersal in *S. salamandra* is male-biased, although additional data is required to properly confirm these claims. Furthermore, data collected from chapters 3 and 4 demonstrate that lotic waters are largely responsible for dispersal asymmetries between larviparous and pueriparous salamanders. Parentage analyses (chapter 3) suggest water-borne dispersal (active or passive) may promote long-distance movements during the aquatic larval stage, thus potentially increasing the distances traveled by individuals during their life-time. Additionally, landscape genetic analyses performed in chapter 4 clearly showed lotic systems constrain genetic connectivity in pueriparous populations, probably because pueriparous salamanders exhibit a fully terrestrial life cycle. This effect was not documented in larviparous populations, as larviparous individuals likely transverse easily these features during the aquatic larval stage. Finally, landscape genetic analyses performed in chapter 4 contributed with valuable insights into the landscape ecology of this species. They revealed agricultural areas and, to a lesser extent, wind exposition and topography are important predictors of genetic differentiation in both larviparous and pueriparous populations.

In conclusion, the present doctoral thesis has contributed to a better understanding of the eco-evolutionary implications arising from the shift from an aquatic-breeding strategy (larviparity) to a terrestrial-breeding one (pueriparity) in amphibians. In addition to this, some overlooked aspects related to the ecology and evolution of *S. salamandra* were addressed and the results obtained here may help future ecological, evolutionary, and conservation research focused on this species and others. This thesis also opens exciting avenues for future research that can potentially contribute to greater knowledge of the ecological and evolutionary effects of transitions in reproductive modes.

Keywords: dispersal, gene flow, genetic structure, landscape genetics, larviparity, microsatellites, *Ne*, population, pueriparity, *Salamandra salamandra*, urban genetics, viviparity.

Contents

List of tables

Chapter 1

Chapter 2

Chapter 3

Chapter 4

Appendix A

Appendix B

Appendix C

Appendix D

List of figures

Chapter 1

Chapter 2

Chapter 3

Chapter 4

Appendix A

Appendix C

Appendix D

List of abbreviations

ABC – Approximate Bayesian Computation

AD – allele dropout

AFLP - amplified fragment length polymorphism

AIC – Akaike Information Criterion

AICc – Akaike Information Criterion corrected for small sample sizes

A_R – allelic richness

BCM - Bayesian clustering methods

CAI_AM - area-weighted mean of the core area index

CIs – confidence intervals

CLUMPY – clumpiness

Cyt b – cytochrome b gene

DAPC – discriminant analysis of principal components

DEM – digital elevation model

DTM – direct tracking methods

ECON_AM - area-weighted mean of the edge contrast index

ED – edge density

EVI – enhanced vegetation index

FA – false alleles

GDM - generalized dissimilarity modelling

GIS – geographic information system

GLM - generalised linear model

GLS – generalised least squares

GSA – genetic spatial autocorrelation

H_E – expected heterozygosity

H_O – observed heterozygosity

HWE – Hardy-Weinberg equilibrium

IBB – isolation-by-barrier

IBD – isolation-by-distance

IBE – isolation-by-environment

IBR – isolation-by-resistance

IW – inside walls (Oviedo)

Lat - latitude

LD – linkage disequilibrium

LE – linkage equilibrium

LMM – linear mixed models

Long – longitude

LSI - landscape shape index

MCMC – Markov chain Monte Carlo

MLPE - maximum-likelihood population effects

MLPP - mean logarithmic posterior probability

mtDNA – mitochondrial DNA

N_A – mean number of alleles per locus

NDWI - normalized difference water index

Ne – effective population size

NLM – neutral landscape model

Nm - number of immigrants entering a subpopulation each generation

nLSI – normalized landscape shape index

N_{PA} – number of individuals containing private alleles

OC – outside the city (Oviedo)

OW – outside walls (Oviedo)

P_A – number of private alleles

PAFRAC - perimeter-area fractal dimension

PCA – principal component analysis

PCR - polymerase chain reaction

Pgi - phosphoglucose isomerase gene

PI – Probability of Identity

PISibs – Probability of Identity accounting for the presence of relatives

PROX_CV - coefficient of variation of the proximity index

r – correlation coefficient

R – average relatedness

r_{auto} - autocorrelation coefficient

RAPD - randomly amplified polymorphic DNA

SA – sibship assignment

SE – standard error

SNP – single nucleotide polymorphism

SVL - snout-vent length

t^2 – t^2 heterogeneity test

TECI - total edge contrast index

TWI – topographic wetness index

VWC – vegetation water content

w_i - Akaike weight

w_+ - relative importance of each explanatory variable

WEI – wind exposition index

β – regression coefficient

μ - mutation rate

ω - Omega heterogeneity test

ω_{GROUPS} - Omega heterogeneity test among groups

Chapter 1

General introduction

1.1 – Evolution of viviparity and its eco-evolutionary implications

1.1.1 – Viviparity as a key innovation and its origin among vertebrates

The evolution of a trait that allow organisms to exploit new resources in ways previously inaccessible, with profound implications at ecological and evolutionary levels, is commonly referred to as "key innovation" (Losos 2010). Key innovations enable taxa to interact with the surrounding environment in a novel way, thus exposing them to selective pressures not experienced before and opening new avenues of evolutionary diversification (Losos 2010; Yoder *et al.* 2010). Examples of key innovations include the evolution of wings in birds and bats, pharyngeal jaws in labrid fishes, hairs and lactation in mammals, and the transition from an oviparous (egg-laying reproduction) to a viviparous (live-bearing) mode of reproduction (**Figure 1.1**; Losos 2010; Wagner and Lynch 2010; Sites *et al.* 2011). The latter is quite remarkable, as unlike other major vertebrate innovations (*e.g.* lactation, powered flight or endothermy), which arose independently on only a few occasions, changes in reproductive strategies have occurred multiple times in many vertebrate groups throughout their evolutionary histories (Blackburn 2015). The transition from oviparity to viviparity was undoubtedly the most common transition in reproductive modes in vertebrates, entailing profound morpho-physiological, life-history, behavioural, ecological and genetic changes, especially in females (see for example Stewart and Thompson 2003; Wagner and Lynch 2010; Pincheira-Donoso *et al.* 2013; van Dyke *et al.* 2014; Blackburn and Starck 2015; Lynch *et al.* 2015; Shine 2015; Wake 2015; Whittington *et al.* 2015; Helmstetter *et al.* 2016; Halliwell *et al.* 2017; Gao *et al.* 2019). In total, more than 150 independent evolutions of viviparity have been documented in vertebrates, though they emerged heterogeneously among clades (**Table 1.1**). Viviparity is most prevalent in squamate reptiles, in which more than 100 independent origins (ca. 20% of lizards and snakes) are accounted for (Sites *et al.* 2011; Feldman *et al.* 2015; Pyron 2015). At least eight independent origins of viviparity are also reported in amphibians, with viviparity being present in ca. six species of anurans (ca. 0.09%), 11 salamander species (ca. 1.6%; all within the Salamandridae family), and about 15% of caecilian species (Wake

2003; Buckley 2012; Blackburn 2015; Wake 2015). Most cartilaginous fishes and some species of bony fishes evolved viviparity at least on 23 occasions (Blackburn 2005; Blackburn 2015), while therian mammals are exclusively viviparous (*i.e.* a single origin). This reproductive trait did not emerge, however, in birds, crocodilians, chelonians, and agnathans (Blackburn 2015).

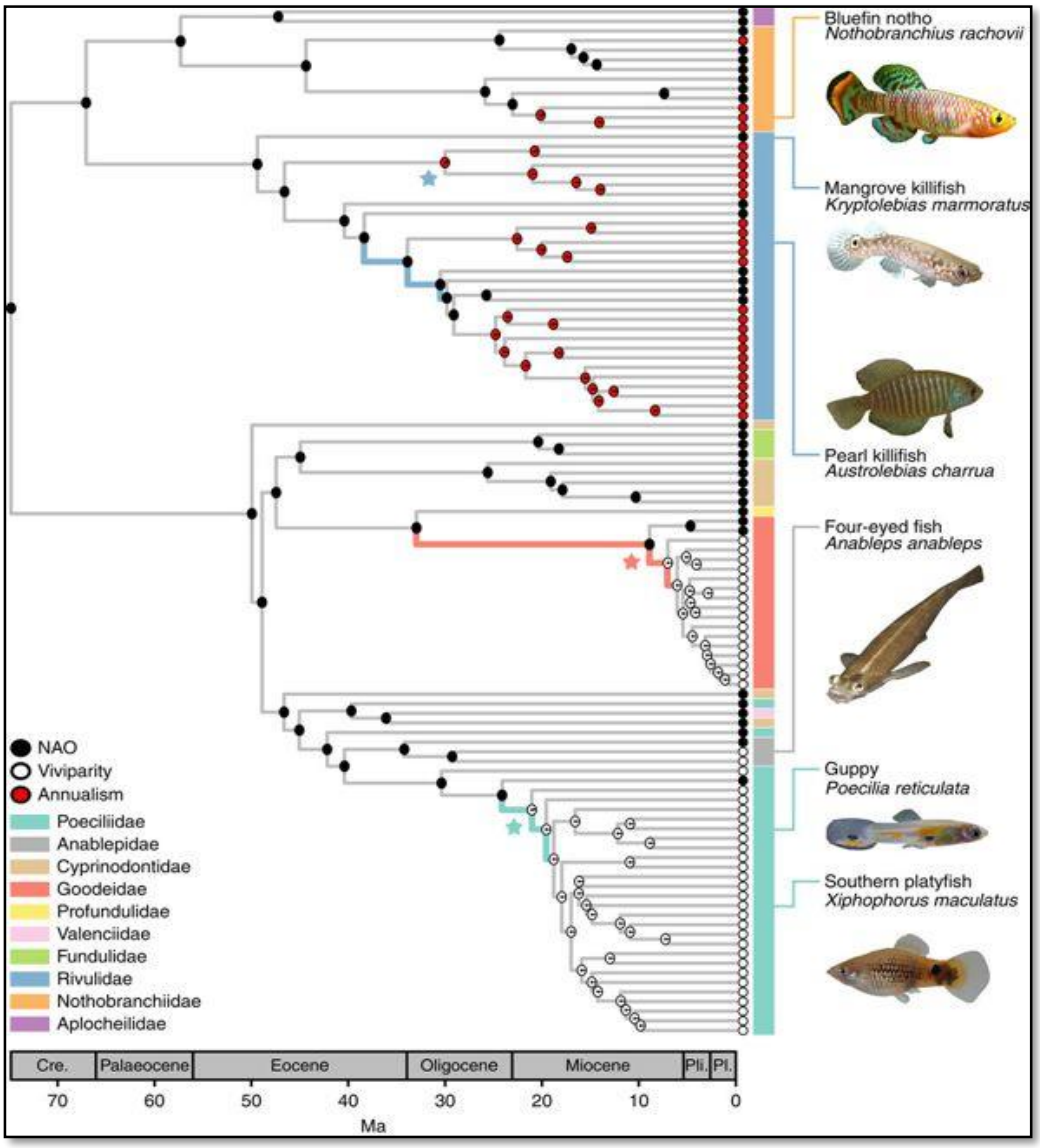

Fig. 1.1 Bayesian maximum clade credibility tree with ancestral reconstructed states of two key innovations in the Cyprinodontiformes order: viviparity (white dots in the tree branches) and annualism (red dots). Both traits are hypothesized to have enabled colonization of new environments, and possibly, to have affected diversification rates in this order. NAO - non-annual oviparous (black dots). Figure adapted from Helmstetter *et al.* (2016).

Table 1.1 Minimum number of independent evolutions of viviparity and percentage of known viviparous species per taxon. Adapted from Blackburn (2015).

Taxon	Origins of viviparity	% Viviparous
Squamata	115	20%
Extinct Reptilia	6	-
Mammalia	1	99%
Lissamphibia	8	1%
Teleostomi	13	2.5%
Chondrichthyes	9	55%
Placodermi	1	-
Total	153	

1.1.2 – Ecological factors driving the evolution of viviparity

Internal fertilization has been recognized as an indispensable pre-requisite for the evolution of viviparity in vertebrates, although other traits likely played a relevant role (*e.g.* hormones, pre-existing morpho-physiological conditions to retain eggs; see Wake 2004; Blackburn 2015). Additionally, in many viviparous species, the prolonged retention of embryos within females' reproductive tracts generally imposes more energetic costs (*e.g.* increased nutritional supply of embryos, physical burden of pregnancy, physiological constraints) than an egg-laying reproduction (Shine 1980; Wourms and Lombardi 1992; Blackburn 2015). Hence, the successful fixation of viviparity in a given taxon likely requires the fitness advantages entailed by a viviparous reproduction outweighs its higher inherent costs. Despite the importance of the pre-existing genetic pathways to successfully evolve viviparity (*e.g.* Murphy and Thompson 2011; Brandley *et al.* 2012; Whittington *et al.* 2015), changes in reproductive modes are primarily triggered in response to strong biotic and abiotic selective pressures on offspring (*e.g.* stressfull environments or predators). Because different vertebrate groups exhibit pronounced differences in their life-histories and ecologies, these selective pressures are expected to vary among vertebrate taxa.

1.1.2.1 – Therian mammals

All therian mammals are highly matrotrophic, *i.e.* substantial nutrition to developing embryos is provided by the mother through specialized structures, such as the placenta. Hence, they have been considered an excellent model to study the evolution of matrotrophy and placental complexity (Renfree *et al.* 2013; Lynch *et al.* 2015). However, the transition from oviparity to viviparity and the respective underlying ecological drivers cannot be investigated in this group, since this transition likely occurred one time (Blackburn 2015). It has been suggested the

evolution of viviparity in therian mammals is associated to optimal provisioning of nutrients to embryos (Blackburn 1999), although future research is needed to clarify this topic.

1.1.2.2 – Fishes

It has been suggested viviparity in fishes likely emerged in response to highly fluctuating environmental conditions and high predation rates upon eggs and larvae (Wourms and Lombardi 1992; Meyer and Lydeard 1993; Blackburn 1999). This is because viviparous fish females (and also females from other vertebrate groups) usually deliver few, but well-developed offspring (*e.g.* larger in size) compared to eggs or neonates of oviparous congeners. The more advanced developmental stage of newborns, together with the extended period of gestation within the mother in many viviparous fish species, confer greater protection not only from unstable environmental conditions, but also against predators (Wourms and Lombardi 1992). It has also been proposed that viviparity allows females to select more suitable habitats to deposit offspring and, thus, assure better conditions for the survival of newborns (Wourms and Lombardi 1992; Meyer and Lydeard 1993).

1.1.2.3 – Squamate reptiles

Besides therian mammals, squamate reptiles are the only extant amniotes known to have evolved viviparity. Squamate reptiles have been thoroughly studied to understand the evolution of viviparity from anatomical, physiological, ecological, and genetic perspectives, since this reproductive mode evolved independently multiple times in this group (*e.g.* Murphy and Thompson 2011; Sites *et al.* 2011; Pincheira-Donoso *et al.* 2013; Pyron and Burbrink 2014; Feldman *et al.* 2015; Pyron 2015; Ma *et al.* 2018; Gao *et al.* 2019). Several studies have demonstrated viviparity arose as an adaptation to low environmental temperatures, thus prompting researchers to formulate the “cold-climate hypothesis” (*e.g.* Pyron and Burbrink 2014; Ma *et al.* 2018; see also Fernández *et al.* 2017 for further considerations about this hypothesis). This hypothesis postulates that longer periods of embryo retention within the maternal organism were generally selected in cool and unstable climates to reduce egg mortality rates. This is because females can actively thermoregulate and assure optimal temperatures for the development of offspring, while eggs deposited in nests are exposed to greater fluctuations of the environmental temperature. Recently, Ma *et al.* (2018) performed a global test of this hypothesis in reptiles. The authors clearly showed viviparity is advantageous in cold climates, as it enabled viviparous reptiles to shorten development time and reduce energetic costs. This likely explains why a greater proportion of viviparous reptiles are found in cold regions compared to warm ones (**Figure 1.2**). Besides cold climates, hypoxia was also

suggested as potential driver of viviparity in the genus *Liolaemus*. Specifically, Pincheira-Donoso *et al.* (2017) proposed hypoxia at high elevations might have selected for a prolonged retention of embryos, once females can regulate and assure an optimal supply of oxygen to offspring. This hypothesis certainly merits further investigation to better understand the ecological drivers of viviparity in reptiles.

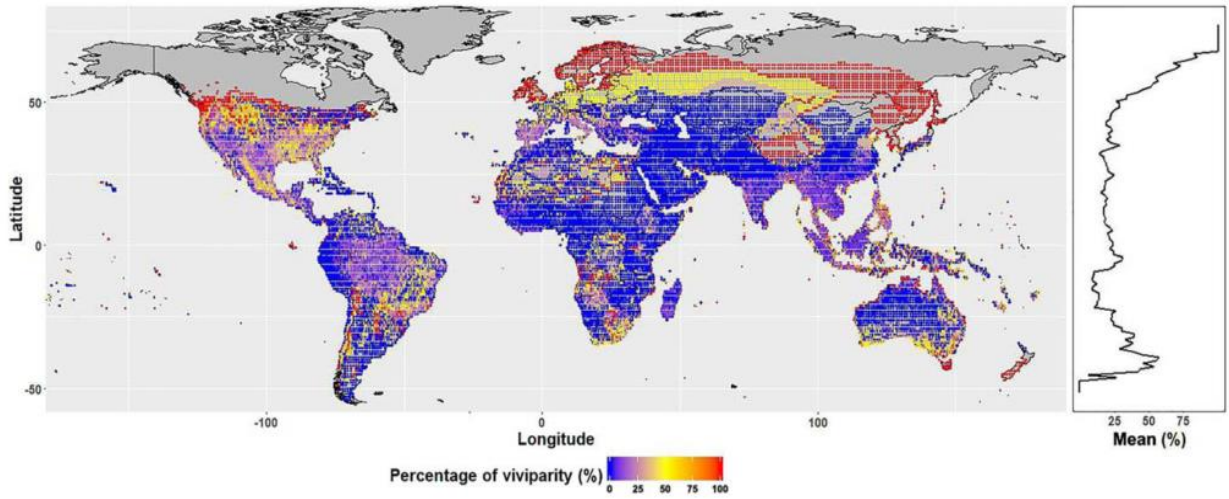

Fig. 1.2 Percentage of viviparous reptile species across the world. The proportion of viviparous species increases with increasing latitudes (red), which correspond to colder regions. Adapted from Ma *et al.* (2018).

1.1.2.4 – Amphibians

1.1.2.4.1 – Clarification of the terminologies used for amphibians in the present thesis

Amphibians are generally characterized by a biphasic life cycle, in which an aquatic larval stage is followed by metamorphosis into terrestrial juveniles (Wells 2007); however, they exhibit a huge diversity of reproductive modes (especially anurans), most of which involve different types of egg-laying strategies (Crump 2015). Due to their complex life cycle and numerous reproductive strategies, subcategories of oviparity and viviparity have been proposed to characterize the reproductive biology of amphibians. Because the study species of the present thesis is an amphibian (see section 1.4), clarifications concerning the terminologies used to describe amphibian reproductive biology are necessary.

The term “viviparity” was previously used in amphibians to acknowledge species in which females deliver fully-metamorphosed terrestrial juveniles (the aquatic larval stage is skipped). Conversely, species where females deliver eggs or pre-metamorphic aquatic larvae were broadly considered “oviparous” and “ovoviviparous”, respectively. Two subcategories, specific to amphibians, were proposed to characterize live-bearing in this group - larviparity and

pueriparity – which distinguish those species where females deliver pre-metamorphic aquatic larvae and terrestrial fully developed young, respectively (see Greven 2003 and Blackburn 2015). Hence, the independent origins of viviparity mentioned in section 1.1 for amphibians should be considered instead shifts to pueriparity, according to the recent nomenclature of reproductive strategies in this group; hereafter, the latter terms will be used consistently throughout the present thesis for amphibians.

Moreover, the terms “aquatic reproduction” and “terrestrial reproduction” are also used widely in the present thesis. These terms are not applied as synonyms of specific reproductive modes. Instead, they characterize the degree of dependence on water shown by species to complete their life cycle. Specifically, “aquatic reproduction” refers to aquatic-breeding strategies (*e.g.* oviparity, larviparity) that mandatorily require water for the development of offspring, while “terrestrial reproduction” encompasses terrestrial-breeding modes, such as pueriparity and direct-developing (deposition of eggs which hatch into miniature adults with no tadpole stage), in which offspring develop exclusively in terrestrial habitats.

1.1.2.4.2 – Ecological drivers of pueriparity in amphibians

Some amphibian species have evolved to a pueriparous reproduction from aquatic-breeding strategies (Liedtke *et al.* 2017; Kieren *et al.* 2018), thus involving drastic alterations on their life-history. In pueriparous amphibians the aquatic larval stage is skipped, with females delivering fully metamorphosed terrestrial juveniles (Wells 2007; Blackburn 2015). This remarkable modification has entailed a greater independence from water sources to survival and reproduction. Indeed, the evolution of terrestrial modes of reproduction in amphibians, including pueriparity and other terrestrial-breeding strategies (*e.g.* foam nesting, direct-developing), have been often associated to habitats where suitable water bodies (*e.g.* still-standing water) for the development of the progeny were historically and/or contemporaneously absent (Gomez-Mestre *et al.* 2012; Crump 2015; Velo-Antón et al. 2015; Jiménez-Robles *et al.* 2017; Lion *et al.* 2019). For example, in fire salamanders (family Salamandridae), it has been suggested both historical and contemporary lack of surface water were important selective agents for the evolution of pueriparity (García-París *et al.* 2003; Velo-Antón *et al.* 2007; Beukema *et al.* 2010). These observations led Velo-Antón *et al.* (2015) to formulate the “dry-climate hypothesis” to explain the origin of this reproductive mode in fire salamanders. Additionally, Liedtke *et al.* (2017) assessed the statistical relationship between continuous habitat measurements and life-history transitions of 79 species of African bufonids. They found that steep terrains, where water is fast flowing and likely unsuitable for the deposition of eggs/larvae, jointly with the absence of water bodies, are strong predictors of the

evolution of terrestrial-breeding strategies, including pueriparity (see also Goin and Goin 1962 and Lion *et al.* 2019). Other researchers have also posited that intense aquatic predation on eggs and larvae may have selected for a switch to terrestrial reproduction to reduce predation-driven mortality rates on the offspring (Haddad and Prado 2005; Gomez-Mestre *et al.* 2012).

1.1.3 – Eco-evolutionary implications of viviparity or pueriparity

The emergence of a viviparous or pueriparous (in amphibians) reproduction caused pronounced phenotypic changes in individuals (*e.g.* Buckley *et al.* 2007; Blackburn 2015; Wake 2015; Fernández *et al.* 2017), thus entailing potential changes in the ecology of organisms and, by extension, in the evolution of populations. However, this subject has received little attention. A proximate ecological outcome caused by viviparity/pueriparity was increased progeny survival rates compared to an ancestral reproductive mode under unfavourable ecological contexts, such as cool climates in reptiles, water-limited environments in amphibians, and high predation rates in fishes (see Wourms and Lombardi 1992; Liedtke *et al.* 2017; Ma *et al.* 2018). Consequently, individual fitness increased in viviparous and pueriparous taxa, thus enabling them to thrive in harsher environments and disperse to areas previously inaccessible (Pincheira-Donoso *et al.* 2013; Helmstetter *et al.* 2016; Ma *et al.* 2018). This subject has been thoroughly evaluated in reptiles. Specifically, several studies have shown that reptilian viviparity allowed colonization of northern latitudes and greater individual fitness compared to oviparous species in cool climates (*e.g.* Pincheira-Donoso *et al.* 2013; Pyron and Burbrink 2014; Yuan *et al.* 2016; Pincheira-Donoso *et al.* 2017; Ma *et al.* 2018; see also **Figure 1.2**). Some studies have also proposed in amphibians that pueriparity is a key trait enabling survival and long-term persistence of amphibian populations in water-limited environments. For instance, pueriparous amphibians have been found in areas exhibiting karstic limestone substrates where surface water is absent due to subterranean drainage (García-París *et al.* 2003; Beukema *et al.* 2010), islands where water bodies are scarce (Velo-Antón *et al.* 2012), steep terrains containing streams with fast flowing water (Liedtke *et al.* 2017; Lion *et al.* 2019), and urban settlements (Uotila *et al.* 2013; Álvarez *et al.* 2015). In fishes, it has not only been shown that viviparity is associated with lower egg and larval mortality rates when compared to oviparous species (Wourms and Lombardi 1992; Gunderson 1997), but also it has been suggested that it promotes colonization of new watersheds by a single pregnant female (Helmstetter *et al.* 2016).

A greater ability to colonize and thrive in harsher environments appears to have affected individuals and populations at evolutionary level, including the evolution of phenotypes and species diversification rates. For example, a recent study (Ledbetter and Bonett 2019)

demonstrated that terrestrial-breeding strategies in salamanders decreased the rate of hindlimb digit evolution, possible due to constrains in limb evolution imposed by a terrestrial plantigrade locomotion. In the lizard family Phrynosomatidae, Zúñiga-Vega *et al.* (2016) showed viviparity constrained life-history diversification (*e.g.* offspring size, age at maturity), though the exact cause could not be determined. Viviparity appears also to have facilitated the evolution of social grouping in reptiles, as supported by phylogenetic comparative analyses carried out by Halliwell *et al.* (2017). The authors advocated that live-bearing stimulates recurrent social interactions between parents and newborns; therefore, it is possible that the emergence of social groupings has been under constant selection, as the costs of parents tolerating juveniles are relatively low in reptiles (see Halliwell *et al.* 2017 and references therein). Finally, besides affecting evolutionary rates of phenotypes, Helmstetter *et al.* (2016) demonstrated that viviparity stimulated diversification rates in an order of freshwater fishes (Cyprinodontiformes; **Figure 1.1**). The authors argued that pregnant females carrying fertilized embryos can colonize geographically isolated watersheds and facilitate speciation in isolated freshwater habitats.

1.2 – Dispersal and the potential influence of changes in reproductive modes

The phenotypic and ecological modifications underlying the evolution of a novel reproductive mode (*e.g.* viviparity/pueriparity) may have also affected traits correlated with reproduction, such as dispersal-related processes (*e.g.* physical capacity for dispersal, dispersal behaviour, dispersal success rates). This is because the dispersal ecology of organisms is driven to a large extent by both reproductive biology and environmental conditions (Clobert *et al.* 2009; Bonte *et al.* 2012). Specifically, dispersal is a key mechanism for finding mates and breeding sites, thus governing to a large extent gene flow among populations (Bonte *et al.* 2012; Pittman *et al.* 2014; Cosgrove *et al.* 2018). However, individuals must adjust dispersal decisions and pathways in accordance with environmental conditions encountered during the dispersal process to increase reproductive success (Clobert *et al.* 2009; Bonte *et al.* 2012). Hence, the changes in reproductive biology and behaviour entailed by the evolution of a viviparous or pueriparous reproduction can potentially alter the way individuals interact with the surrounding environment (Shine 2015), which in turn may affect overall patterns of dispersal and gene flow.

1.2.1 – Dispersal: general overview

Movement, *i.e.* the spatial displacement of individuals across the landscape, has pervasive ecological and evolutionary implications across different levels of biological organization, influencing not only individual fitness, but also long-term persistence of populations, species' geographic ranges, and community composition and structure (Clobert *et al.* 2012; Baguette *et al.* 2013). Jeltsch *et al.* (2013) distinguished three main types of movement: foraging, migration, and dispersal. Each type of movement plays a specific role in the eco-evolutionary dynamics of populations and varies in respect to the spatio-temporal scale it operates (**Figure 1.3**). While foraging movements are usually performed on a regular basis at a local scale (home range) to acquire essential resources to survive (*e.g.* food, shelter; Jeltsch *et al.* 2013), in places where environmental conditions vary widely among seasons, individuals of many species undertake cyclical long-distance movements during weeks or months (migration) to track optimal ecological conditions (Cote *et al.* 2017b).

Dispersal is defined as the permanent movement of individuals away from their place of birth (natal dispersal) or among breeding sites (breeding dispersal) with potential consequences to successful reproduction (Matthysen 2012). It comprises a complex multi-causal process characterized by three stages: (1) departure of natal or breeding locations; (2) transfer (inter-patch movement); and (3) settlement into a novel breeding habitat (Bowler and Benton 2005; Clobert *et al.* 2009). The decision to disperse or not is based on whether the perceived benefits of leaving the natal habitat patch exceed the costs (energy, time, mortality risk) of moving to unfamiliar territories (Bonte *et al.* 2012). Traits directly involved in dispersal (*i.e.* dispersal-related traits), such as dispersal behaviour (emigration propensity, direction of movement, settlement choice) and the physical capacity for dispersal, are thus expected to be subjected to multiple selective pressures, so that they evolve in a way to maximize the benefits and reduce the costs inherent to dispersal (Bowler and Benton 2005; Duputié and Massol 2013).

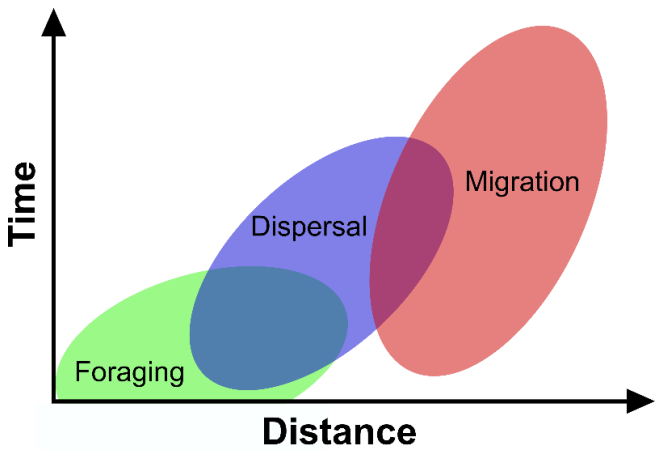

Fig. 1.3 A schematic overview of the spatio-temporal scales, in which the distinct types of movement operate. Adapted from Jeltsch *et al.* (2013).

1.2.2 – Role of dispersal in natural populations

Although occurring only once (in case of natal dispersal) or a few times (in case of breeding dispersal) in an individual's lifetime, dispersal plays a central role in the ecology and evolution of populations (Jeltsch *et al.* 2013; Burgess *et al.* 2016; Cayuela *et al.* 2018; Cosgrove *et al.* 2018). Successful dispersal is critical for organisms to find suitable sites to reproduce (*e.g.* water bodies in the case of amphibians), thus contributing primarily to gene flow (*i.e.* dispersal followed by successful reproduction) within and among populations (Ronce 2007).

Gene flow is critical for the long-term persistence and maintenance of the evolutionary potential of populations. This is because gene flow often promotes the arrival of new and beneficial alleles that boost standing genetic variation, thus potentially helping species adapting to changing environmental conditions (Aitken and Whitlock 2013; Baguette *et al.* 2013; Frankham 2015; Senner *et al.* 2018). Disruption of gene flow is usually associated with a decrease in genetic diversity and increase in genetic structure (or differentiation) between populations. These changes in the gene pool of populations may entail long-term negative consequences, including inbreeding depression and loss of standing adaptive genetic variation (Clark *et al.* 2010; Rivera-Ortíz *et al.* 2015; Richardson *et al.* 2016; Cosgrove *et al.* 2018; Pflüger *et al.* 2019). However, it should be noted that the extent to which interrupted gene flow affects genetic patterns of populations is dependent upon other factors, such as demography. For instance, populations exhibiting a large effective population size (*Ne*, number of individuals of an idealized population experiencing the same rate of inbreeding and genetic drift as the population under study) are less vulnerable to the long-term genetic effects of impeded gene flow (Epps and Keyghobadi 2015; Ellegren and Galtier 2016). Conversely, gene flow acquires even greater importance in populations exhibiting a small *Ne* and that have been isolated for many generations. In these populations, where genetic diversity is usually very low, genetic drift becomes a dominant evolutionary force shaping allele frequencies, often causing a pronounced decrease in genetic diversity, greater genetic structure (*i.e.* increase of genetic differentiation between populations), and also negative impacts on individual fitness (due to accumulation of deleterious mutations) and adaptive potential (Frankham 2005; Excoffier and Ray 2008; Hedrick and Garcia-Dorado 2016; Cosgrove *et al.* 2018). Reestablishment of gene flow among previously isolated and small-sized populations was shown to promote their genetic rescue and long-term viability (Frankham 2015). Despite its benefits, gene flow in some occasions can be detrimental, as it may contribute, for example, to arrival of maladapted alleles that reduce individual fitness (see Richardson *et al.* 2016 and references therein).

Dispersal is also key to population demography. It mediates the demographic rescue (increase in population size due to the arrival of immigrants) of small populations which may

help them cope against stochastic environmental fluctuations and reduce Allee effects (Rousset 2012). Dispersal also allows the colonization of unoccupied patches and regulates biotic interactions at intra- and inter-specific levels (*e.g.* alter levels of competition, avoidance of predators; Bowler and Benton 2005; Duputié and Massol 2013), though it may also be responsible for the spread of diseases (Richardson *et al.* 2016; Hemming-Schroeder *et al.* 2018). Additionally, species' ranges are shaped by dispersal to a large extent, as it comprises a mean for organisms to track optimal conditions and escape unsuitable environments (Travis *et al.* 2013).

1.2.3 – Factors driving dispersal

The extent to which selective pressures govern the evolution and expression of dispersal-related traits is largely dependent upon a complex interplay between individual's intrinsic traits (phenotype- or condition-dependent) and extrinsic factors (context-dependent), which ultimately determine whether or not dispersal occurs, and how far organisms travel across the landscape (Travis *et al.* 2012). While the internal state (phenotypes) of an individual enables dispersal from a physical perspective, the surrounding environment drives: (i) the decisions made by individuals at each stage of dispersal; (ii) dispersal success rates across the landscape; and (iii) the evolution of phenotypes directly or indirectly associated with it (Clobert *et al.* 2009; Cote *et al.* 2017a). This intricate relationship between phenotypes and context-dependent factors often leads to the emergence of patterns of covariation between dispersal and phenotypic traits. This correlation is commonly known as dispersal syndromes and recent studies have demonstrated they vary at both intra- and inter-specific levels (Stevens *et al.* 2010; Ronce and Clobert 2012; Palmer *et al.* 2014; Stevens *et al.* 2014). The accurate identification of dispersal syndromes, as well as the underlying factors responsible for their variation, is paramount not only to understand the ecology and evolution of populations, but also to assess their long-term persistence under a scenario of rapid landscape and climate changes, biotic invasions, and disease spread (*e.g.* Travis *et al.* 2013; Cote *et al.* 2017a; Pecl *et al.* 2017; Pflüger *et al.* 2019). However, it should be noted that decoupling the effects on dispersal of a single factor is not straightforward. The expression of dispersal-related traits results from interactions between intrinsic and extrinsic factors (**Figure 1.4**), and proper understanding of the mechanisms driving dispersal must be made in light of this intricate relationship.

1.2.3.1 – Intrinsic factors

1.2.3.1.1 – Phenotypic traits

A multitude of phenotypic traits (morphology, physiology, life-history, and behaviour) are tightly linked (or correlated) with dispersal-related traits, as they primarily determine if an organism is able to disperse at all (see Ronce and Clobert 2012 and references therein). It should be noted, however, that many phenotypic traits are determined to a large extent by the genetic architecture (genotypes) of individuals (**Figure 1.4**), thus implying dispersal has a strong genetic basis (see Baguette *et al.* 2015 and Saastamoinen *et al.* 2018 for more details). In addition to the genetic underpinning of dispersal, dispersal-related traits are also influenced by the interaction of two or more phenotypic traits (Clobert *et al.* 2009). For instance, dispersal propensity is intimately linked with behavioural syndromes (animal personalities), which in turn are partially governed by physiological (*e.g.* hormones) and life-history traits (*e.g.* age, social status; Cote *et al.* 2010; Ronce and Clobert 2012).

Both morphology and physiology play a major role in an individual's physical capacity for dispersal. One morphological trait that is usually positively correlated with locomotor performance is body size, as larger individuals are generally able to move longer distances at relatively low metabolic costs (Jenkins *et al.* 2007; Hein *et al.* 2012). Body condition (Bonte *et al.* 2012) and dispersal-enhancing anatomical features, such as the development of wings in some insect species (Zera and Denno 1997) and production of ballooning silk in spiders (De Meester and Bonte 2010), are also positively associated with greater dispersal capabilities. Moreover, physiology, and in particular, metabolism, have also been shown to affect dispersal capacity. For instance, Denton *et al.* (2017) showed that metabolic constraints arising from mitonuclear mismatches in unisexual *Ambystoma* salamanders hinder their dispersal capacity when compared to their sexual counterparts. Genetic studies performed in the Glanville fritillary butterfly (*Melitaea cinxia*) also showed that a single nucleotide polymorphism (SNP) in a gene encoding the glycolytic enzyme phosphoglucose isomerase (*Pgi*) was associated with greater flight metabolic and dispersal rates (Haag *et al.* 2005; Hanski *et al.* 2017). Dispersal behaviour is also partially governed by physiological mechanisms. For example, increased production of hormones (*e.g.* corticosterone, dopamine, serotonin) during particular life stages is known to affect personality and, by extension, dispersal behaviour (*e.g.* stimulate exploratory behaviour and/or higher dispersal activity; see Cote *et al.* 2010; Ronce and Clobert 2012).

Life-history traits (*e.g.* age, sex, fecundity, age at maturity, reproductive mode) in association with other phenotypic traits (*e.g.* behaviour) influence realized patterns of dispersal (Ronce and Clobert 2012). Two common life-history traits impacting dispersal are sex and age, which often lead to dispersal asymmetries among individuals (Bonte *et al.* 2012; Trochet *et al.*

2016). Individuals of one sex may, on average, move farther (sex-biased dispersal) due to a combination of unequal social (*e.g.* mating system) and ecological (*e.g.* competition for mates or resources) pressures acting upon morphological, physiological and behavioural traits of individuals from different genders (Trochet *et al.* 2016). Additionally, dispersal behaviour may change during an individual's lifetime. In many vertebrate species, subadults usually disperse farther and more frequently across sub-optimal habitats and anthropogenic barriers (*e.g.* roads) compared with adults, because they are compelled by their need to establish their own territories and reproduce (*e.g.* Semlitsch 2008; Carvalho *et al.* 2018).

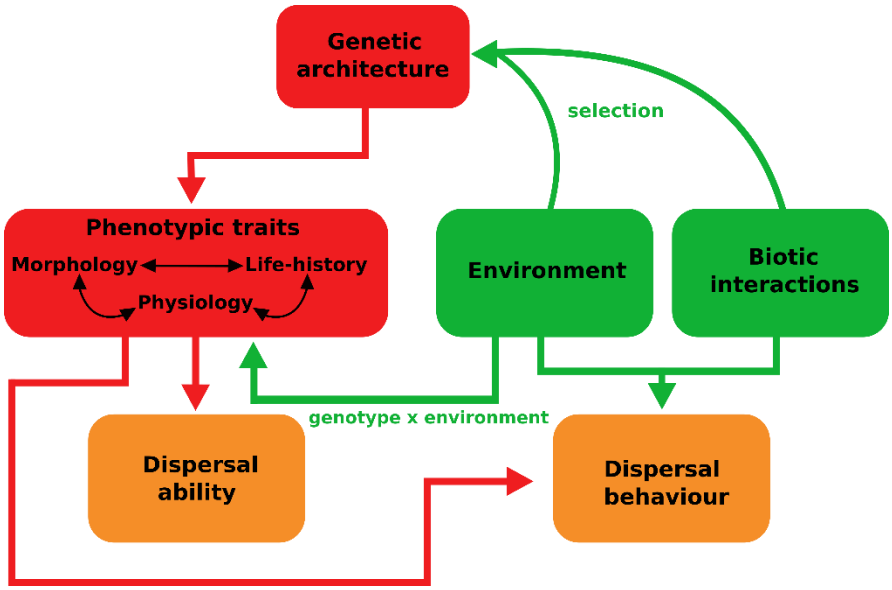

Fig. 1.4 Diagram of the intrinsic (red boxes) and extrinsic (green boxes) factors that influence the evolution and expression of dispersal-related traits (orange boxes). Phenotypic traits are primarily encoded by the genetic underpinning of an individual. Morpho-physiological and life-history traits interact (black arrows) and shape the dispersal ability and behaviour of organisms. However, external factors cause selective pressures (natural selection) that not only shape the evolution of phenotypic traits, but also affect the decisions (dispersal behaviour) made by organisms at each stage of dispersal. Finally, genotype-environment interactions at molecular level may modify phenotypes without promoting modifications in the underlying genotypes.

1.2.3.1.2 – Potential consequences to dispersal of the evolution of viviparity/pueriparity

I discussed some of the potential eco-evolutionary implications arising from the evolution of viviparity or pueriparity in section 1.1.3. Here, I provide a greater emphasis to the potential effects of transitions in reproductive modes on patterns of dispersal and gene flow, as two chapters of the present thesis are dedicated to this subject (see section 1.5). Given that species' reproductive biology is intimately linked with dispersal, alterations in reproductive strategies are expected to induce evolutionary changes in dispersal, with potential

consequences to genetic connectivity and the evolutionary dynamics (*e.g.* patterns of genetic structure) of populations. This subject has been, however, underexplored.

Only a few studies have contributed with some relevant insights. Viviparity was shown to negatively impact the dispersal ability of females during pregnancy compared to egg-laying congeners. This is because viviparous females of many species retain embryos for a longer period, thus incurring greater energetic costs due to the physical burden of carrying offspring for a longer period. This premise has been corroborated by a few experimental studies in viviparous reptiles and fishes, in which lower dispersal rates were recorded in pregnant females compared with oviparous females (*e.g.* Shine 1980; Shine 2015; Banet *et al.* 2016). Furthermore, viviparity often changes the way organisms interact with the surrounding environment, which in turn, may affect dispersal behaviour and dispersal success rates across landscapes. Dispersal behaviour and success in viviparous/pueriparous species is expected to be governed to a much lesser extent by the surrounding environment, because the shift to a viviparous reproduction entails a greater independence from habitat features required for successful reproduction (*e.g.* suitable nests for egg deposition in reptiles and water bodies for development of embryos and larvae in amphibians; see Russell *et al.* 2005; Semlitsch 2008; Shine 2015). Bearing this in mind, differences on dispersal behaviour were suggested as the main cause of higher seasonal road mortality rates in oviparous (but not viviparous) snakes (Bonnet *et al.* 1999). Specifically, the authors argued the observed high mortality rates of oviparous snakes were due to higher dispersal rates of oviparous females during the breeding season, which likely were compelled to cross roads more often to find nests (see also Shine 2015).

Amphibians are generally expected to have a very limited dispersal ability due to their small size and high dependence of humid environments to prevent desiccation (Hillman *et al.* 2014), which make them extremely vulnerable to rapid and pronounced environmental changes (Cushman 2006; Rivera-Ortíz *et al.* 2015). Similar to reptiles, dispersal in amphibians is to a large extent driven by the availability of specific landscape features, namely, freshwater habitats (*e.g.* streams, ponds; Russell *et al.* 2005; Semlitsch 2008; Pittman *et al.* 2014). After aestivation and/or hibernation periods, individuals move among aquatic breeding sites to mate and deposit eggs or larvae in water, so the latter can metamorphose into terrestrial juveniles (Semlitsch 2008; Pittman *et al.* 2014). Hence, the greater independence from water entailed by a terrestrial reproduction likely promoted significant changes in dispersal of pueriparous amphibians. The presence of pueriparous amphibians in harsh and water-limited environments (*e.g.* Álvarez *et al.* 2015; Liedtke *et al.* 2017), where survival of species with aquatic reproduction would not be possible, potentially suggests dispersal (and gene flow) are less

constrained by environmental factors; therefore, functional (genetic) connectivity among pueriparous populations may be higher compared to aquatic-breeding amphibians. Based on this premise, previous landscape studies have suggested that terrestrial reproduction (including pueriparity) in amphibians may promote higher connectivity in heterogeneous, fragmented landscapes, given their ability to thrive in water-limited environments (Measey *et al.* 2007; Sandberger-Loua *et al.* 2018). Nevertheless, because these studies did not compare patterns of connectivity with species exhibiting aquatic reproduction, inferences concerning the role of terrestrial reproduction on movement are very limited.

1.2.3.2 – Extrinsic factors

Biotic interactions (*e.g.* competition, predation) and environmental conditions (*e.g.* landscape composition and configuration, climate, and topography) govern each stage of dispersal to a large extent (**Figures 1.4 and 1.5**). They may not only affect the evolutionary trajectory of dispersal-related traits encoded genetically (*e.g.* by changing substantially allele frequencies; Phillips *et al.* 2006; Lowe and McPeek 2014; Williams *et al.* 2016; Saastamoinen *et al.* 2018), but also influence the association between specific genotypes and dispersal without incurring any changes in the underlying genetic mechanisms (*e.g.* genotype x environment interactions; Zera and Brisson 2012; Saastamoinen *et al.* 2018 and references therein). Extensive research, however, has shown that extrinsic factors affect predominantly dispersal success rates and the decisions (*i.e.* dispersal behaviour) employed by an organism under particular environmental contexts (**Figure 1.4**; Bowler and Benton 2005; Bonte *et al.* 2012; Baguette *et al.* 2013; Vasudev *et al.* 2015; Duputié and Massol 2013; Cote *et al.* 2017a; Zarnetske *et al.* 2017). Because my thesis is focused mainly on the latter, the present section mostly emphasizes the role of extrinsic factors on dispersal behaviour at each stage of dispersal.

1.2.3.2.1 – Biotic interactions

Provided that a capacity for kin recognition exists, the interaction between relatives may trigger dispersal as a mean to avoid kin competition and inbreeding (Bowler and Benton 2005; Bonte *et al.* 2012). Additionally, antagonistic interactions (*e.g.* intra- and inter-specific competition, predation, parasitism) can largely influence dispersal decisions (Bonte *et al.* 2012; Zarnetske *et al.* 2017). One important factor determining whether individuals emigrate from a resource patch is the density of conspecifics (density-dependent dispersal; Bowler and Benton 2005; Duputié and Massol 2013). Because both the density of conspecifics and availability of resources (food, shelter, breeding sites, mates) determine the resources available *per capita*,

intra-specific competition is expected to increase when population density is elevated, eventually forcing outcompeted individuals (usually subadults) to disperse (Bowler and Benton 2009; Rousset 2012). Likewise intra-specific competition, the presence of other species exerting antagonistic interactions (competition, predation) can also stimulate a higher dispersal propensity, and consequently, higher emigration rates (Bowler and Benton 2005; Bonte *et al.* 2012).

Biotic factors can also influence dispersal at later stages (transfer and settlement). Individuals dispersing throughout the matrix habitat (landscape surrounding resource patches that show sub-optimal or unsuitable environmental conditions for a given species) may compete and/or interact with other organisms, and thus, change dispersal tactics to minimize those interactions (Pita *et al.* 2007; Bonte *et al.* 2012; Driscoll *et al.* 2013). Finally, settlement choice in a given patch may be influenced by the presence of intra- and inter-specific antagonists, because an organism may gather extrinsic cues (*e.g.* visual, olfactory) from the surrounding environment to evaluate their presence and decide to settle or not (Bowler and Benton 2005; Clobert *et al.* 2009).

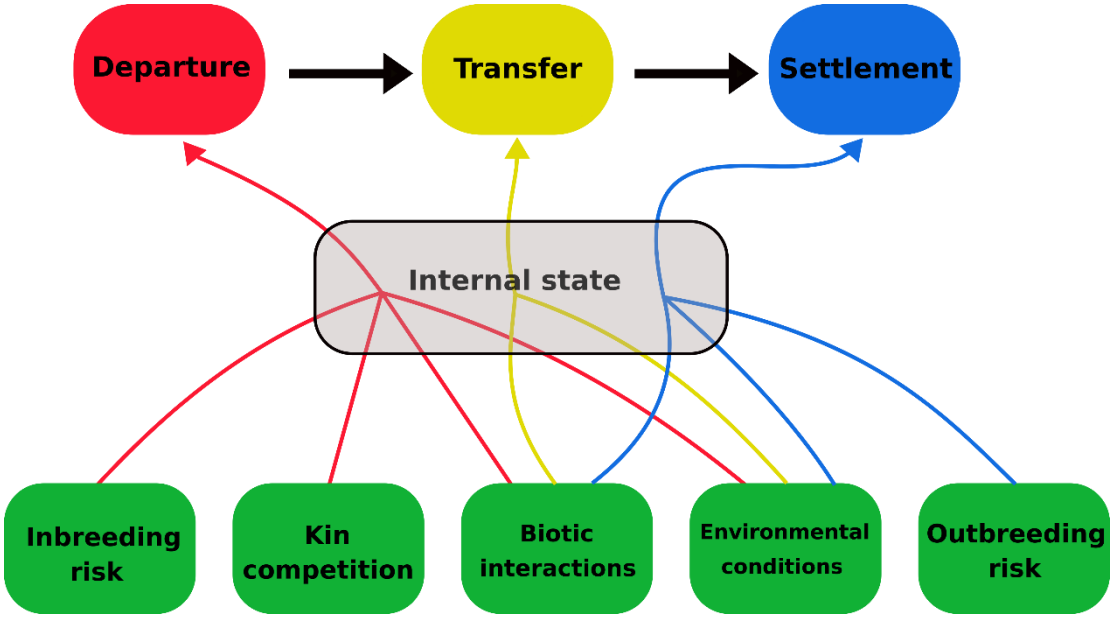

Fig. 1.5 Diagram showing the extrinsic factors (green boxes) affecting each stage of dispersal, as depicted by the coloured arrows. Each of these factors interacts always with the internal state of the individual in shaping realized dispersal patterns. Adapted from Clobert *et al.* (2009).

1.2.3.2.2 – Abiotic conditions

The stages of emigration and settlement are also largely influenced by patch's attributes (*e.g.* patch size, availability of resources, environmental conditions; Bowler and Benton 2005; Duputié and Massol 2013; Jackson and Fahrig 2016). Small-sized patches and/or with poor habitat quality (*e.g.* low amount of resources) present a lower carrying capacity, thus encouraging individuals to disperse or to find other settlement options (*i.e.* patches of lower quality are prone to receive fewer immigrants; Bowler and Benton 2005; Bonte *et al.* 2012; Duputié and Massol 2013; Pflüger and Balkenhol 2014; Jackson and Fahrig 2016).

A larger proportion of studies, however, have focused on the intermediate stage (transfer) of dispersal (see Pflüger and Balkenhol 2014). When an individual departs from a given resource patch, the quality and configuration of the matrix habitat is key to successful dispersal and gene flow (Baguette *et al.* 2013; Driscoll *et al.* 2013; Pflüger and Balkenhol 2014). The need to predict not only how specific matrix's features influence patterns of dispersal, but also the ecological and genetic responses induced by matrix's barrier effects, gave rise to the concept of landscape connectivity, *i.e.* a property characterizing the degree to which the landscape facilitates or hampers movement of an entity (individuals, seeds, genes) between resource patches (Taylor 1993). Shortly after, other related concepts, such as structural (physical arrangement of patches), functional (species' response to landscape's structure), and genetic (functional connectivity specific to genes) connectivity, along with new disciplines (*e.g.* landscape ecology and landscape genetics), emerged in the scientific literature, thus contributing for an improved understanding of the factors shaping population connectivity (see Manel *et al.* 2003; Fischer and Lindenmayer 2007; Baguette *et al.* 2013; Balkenhol *et al.* 2015; Vasudev *et al.* 2015; Saura *et al.* 2017; Cosgrove *et al.* 2018). Patterns of connectivity are expected to be relatively unaffected when the matrix is structurally similar to resource patches. However, in a world where anthropogenic activities have modified substantially the landscape, the matrix is in many cases a highly fragmented and heterogeneous mosaic of different land use types (Driscoll *et al.* 2013). These heterogeneous matrices often present harsh environmental conditions (*e.g.* lack of food and shelter, unfavourable microclimate conditions, high predatory rates) for many taxa, thus impeding dispersal and gene flow (Driscoll *et al.* 2013; Duputié and Massol 2013; Zarnetske *et al.* 2017). For example, landscape matrices containing a high proportion of agricultural and anthropogenic areas (*e.g.* roads, urban settlements) often impose significant barriers to movement (Riley *et al.* 2006; Clark *et al.* 2010; Driscoll *et al.* 2013; Jha 2015; LaPoint *et al.* 2015; Arntzen *et al.* 2017; Habel and Schmitt 2018). Furthermore, similarly to landscapes modified by anthropogenic activities, natural barriers (*e.g.* mountains, large rivers) can also constitute impassable physical barriers to

dispersal, as shown by studies reporting high levels of genetic differentiation between populations located in opposite sides of these natural features (*e.g.* Zalewski *et al.* 2009; Bartáková *et al.* 2015; Sánchez-Montes *et al.* 2018). Finally, in addition to physical barriers, physiological constraints imposed by climate may also change patterns of dispersal, particularly, under a scenario anthropogenic-driven climate change (Wasserman *et al.* 2012; Nuñez *et al.* 2013; Wiens 2016). For instance, as mean annual temperatures increase in many regions of the world, dispersal may be significantly hindered in heat-sensitive species (*e.g.* Castillo *et al.* 2014; Bi *et al.* 2019).

1.3 – Genetic data as a tool to study dispersal and gene flow

1.3.1 – Emergence of molecular markers in dispersal research

Traditionally, dispersal has been mainly studied through direct tracking methods (DTM), such as direct observation, mark-recapture protocols, and radio-telemetry (see Driscoll *et al.* 2014). The latter two methodologies allow accurately tracing the actual movement of organisms (including their dispersal trajectories and distances travelled), which impelled their wide application in movement ecology (*e.g.* Millspaugh and Marzluff 2001; Riley *et al.* 2006; Carvalho *et al.* 2018). However, obtaining large sample sizes (number of individuals tracked) and long-term movement data with DTM is challenging due to their inherent financial and logistical (equipment and human resources) constraints. As a result, DTM were generally applied in short-term studies, focused on a few individuals, and were restricted to small areas (see Millspaugh and Marzluff 2001; Zeller *et al.* 2012; Cayuela *et al.* 2018). The emergence of GPS/satellite-tracking and accelerometers enabled an increase in sample size, detailed tracking of dispersal pathways, and expansion of study areas (Kays *et al.* 2015; Gurarie *et al.* 2017), though the costs and logistics underlying these methods are still substantial (Thomas *et al.* 2011).

Because dispersal is the primary mechanism driving gene flow (successful breeding), patterns of genetic variation can act as a reliable proxy to indirectly study dispersal in many occasions (Broquet and Petit 2009; Zeller *et al.* 2012; Baguette *et al.* 2013). Indeed, molecular markers can be a more tractable tool to obtain dispersal information under many circumstances. For example, genetic data is generally more cost-effective in providing relevant dispersal data at large scales and for rare and elusive organisms that are difficult to track (*e.g.* non-invasive sampling; Beja-Pereira *et al.* 2009). Additionally, unlike DTM, molecular markers allow inferring the evolutionary consequences of dispersal on genetic variation, as they enable collecting data on effective dispersal (*i.e.* gene flow; Spear *et al.* 2010; Zeller *et al.* 2012; Driscoll *et al.* 2014; Carvalho *et al.* 2018).

1.3.2 – Considerations about using genetic data in dispersal research

Understanding not only what type of dispersal information can be inferred from genetic data, but also the inherent distinctions between measuring gene flow and movement is key to conveniently use molecular markers (**Table 1.2**). First, molecular markers provide little information on the ecological and behavioural aspects of dispersal compared to DTM, as the latter enable recording the trajectories and decisions made during dispersal with much greater detail (Zeller *et al.* 2012; Cayuela *et al.* 2018). Second, although dispersal and gene flow are often correlated (Spear *et al.* 2010; Wang and Shaffer 2017), direct tracking of animals and gene flow estimates involve necessarily distinct spatio-temporal scales. While DTM allow documenting the actual physical presence of an individual at a given location and period, patterns of genetic variation among populations represent the long-term average of effective dispersal over multiple generations (Broquet and Petit 2009; Spear *et al.* 2010). This implies that genes may reach locations separated by distances greater than a single organism can travel during its lifetime since genes are transferred across intermediate populations over time. Hence, areas not connected directly by single generation dispersal events may still experience high rates of gene flow. It should be noted, however, that some genetic methods can also provide limited data on non-effective dispersal (see section 1.3.4). Third, the opposite pattern can also occur, *i.e.* immigrants can disperse among locations, but due to environmental, behavioural, and social constraints, they may fail to reproduce and contribute to the gene pool of a given population. For instance, natural selection against immigrants is an environmentally-driven factor that may limit gene flow, as immigrants poorly adapted to the local environmental conditions of a patch may not be able to establish and reproduce (Nosil *et al.* 2005; Wang and Bradburd 2014). Additionally, the reproduction of newly arrived immigrants to a particular area or social group may be hindered by dominant or resident individuals in highly territorial species (Riley *et al.* 2006; Handley and Perrin 2007; Carvalho *et al.* 2018). Lastly, there is a disconnect between measured genetic patterns (*e.g.* gene flow, genetic structure) and the eco-evolutionary processes responsible for them, a process commonly known as time lag (Landguth *et al.* 2010; Epps and Keyghobadi 2015). In other words, the influence of external perturbations (*e.g.* population bottlenecks, habitat loss and fragmentation) on population genetic parameters may be detectable only some/many generations later when populations reach the mutation-drift equilibrium. Accordingly, one should bear in mind that estimated gene flow rates correspond to past patterns of effective dispersal rather than contemporary ones, although the temporal scale of the measured genetic patterns depends also on the molecular markers being used (Zellmer and Knowles 2009; Epps *et al.* 2013; see also Wang 2010).

Moreover, the magnitude of time lags varies in function of intrinsic and extrinsic factors to populations, such as *Ne*, dispersal ability, landscape connectivity changes, generation time, among others (reviewed in Epps and Keyghobadi 2015). Small-sized populations of species with high dispersal abilities and low generation time are expected to exhibit shorter time lags.

Table 1.2 Main differences concerning the type of dispersal information provided by DTM and genetic data.

DTM	Genetic data
-High-resolution dispersal data (movement trajectories and behavioural decisions);	-Some genetic methods (*e.g.* assignment and parentage analyses) may yield qualitative and indirect non-effective dispersal data;
-Does not provide data about effective dispersal (gene flow);	-Allows estimating gene flow rates. These estimates reflect short- and long-distance effective dispersal of several individuals over many generations;
-Enables determining with high precision the phenotypic and ecological factors influencing dispersal, but does not offer hints concerning the evolutionary consequences of dispersal;	-Allows inferring the role of phenotypes and landscape barriers to dispersal with lower detail than DTM, however, it provides information on the genetic (evolutionary) consequences of dispersal;
-Generally costly to track many individuals. Besides, DTM are usually applied at local scales for short-term, but recent DTM have been progressively circumventing these issues;	-Easily applied to both local and regional scales at relatively low costs of genotyping many individuals
-Document actual physical movement.	-There is a time lag associated with gene flow estimates, *i.e.* gene flow measures reflect long-term effective dispersal rather than the present levels of gene flow.

1.3.3 – Microsatellites: a marker of choice in dispersal research

Since the 1990s, a multitude of nuclear genetic markers (*e.g.* randomly amplified polymorphic DNA [RAPDs]; amplified fragment length polymorphism [AFLPs]; *e.g.* Hadrys *et al.* 1992; Scataglini *et al.* 2000) were used to infer dispersal from patterns of genetic structure, but the low information content of these markers rendered their applicability (Schlötterer 2004). Microsatellites are tandem repeats of 1–6 nucleotides in length scattered throughout the nuclear genomes of most taxa, which unlike RAPDs and AFLPs, are multi-allelic and co-dominant (heterozygotes can be distinguished from homozygotes) markers that usually exhibit elevated levels of polymorphism due to high mutation rates (ranging from 10^{-6} to 10^{-2}; Selkoe and Toonen 2006; Putman and Carbone 2014). Because microsatellites are polymorphic, fast-evolving and neutrally inherited loci, they comprise powerful tools to investigate contemporary evolutionary processes at fine-scale (*i.e.* within the last tens to hundreds of generations),

including dispersal, its evolutionary consequences to population dynamics and the effects of landscape connectivity on gene flow and genetic structure (**Figure 1.6**; Manel and Holderegger 2013; Driscoll *et al.* 2014; Putman and Carbone 2014; Allendorf 2017).

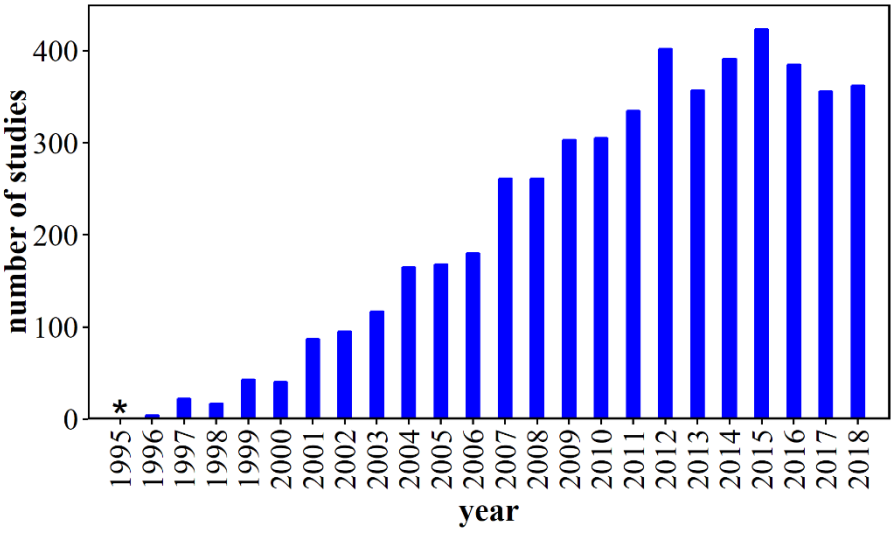

Fig. 1.6 Histogram showing the number of research papers citing microsatellites in dispersal research. This data was obtained from Web of Science by using the "advanced search" option and the following search string "TS = (microsatellite* AND dispersal)" for each year since 1990. Only in 1995 and subsequent years, there were studies matching this search (only one study in 1995 was found, as denoted by the asterisk).

1.3.4 – Genetic methods to examine dispersal patterns

Genetic methods employing microsatellite multilocus genotype data can be useful to estimate gene flow rates or to provide fine-scale qualitative and quantitative information on non-effective dispersal (Waits and Storfer 2015). Specifically, microsatellites were used successfully: (1) to determine the influence of phenotypic variation on dispersal patterns (*e.g.* Cushman and Lewis 2010; Banks and Peakall 2012; Burkhart *et al.* 2017; Grant and Liebgold 2017; Sánchez-Montes *et al.* 2018); (2) to estimate historical and contemporary gene flow rates among highly isolated populations (Velo-Antón *et al.* 2013; Duryea *et al.* 2015); and (3) to examine the effects of landscape (both anthropogenic and natural) barriers and heterogeneity on contemporary functional genetic connectivity (*e.g.* Zalewski *et al.* 2009; Cushman and Lewis 2010; Velo-Antón *et al.* 2013; Waits and Storfer 2015; Noguerales *et al.* 2016; Carvalho *et al.* 2018; Sánchez-Montes *et al.* 2018). Understanding which methods are suitable to address specific hypotheses, as well as their underlying limitations, is crucial for maximizing the usefulness of microsatellites in dispersal research (Cayuela *et al.* 2018). Though multiple methodologies were developed to infer dispersal and gene flow, I will focus on those able to incorporate microsatellites, and that have found extensive applicability in the

genetics of dispersal, because microsatellites were mostly employed in the present thesis. A total of four methodological groups are outlined: (1) *F* statistics; (2) coalescence-based methods; (3) assignment methods; and (4) analysis of spatial patterns of genetic distances.

1.3.4.1 – F statistics

Sewall Wright proposed that F_{ST} (summary statistic quantifying differences in allelic frequencies among populations; see Meirmans and Hedrick 2011 and Whitlock 2011) could be derived from the number of immigrants entering a subpopulation each generation (*Nm*, which is the product between *Ne* of each population and the migration rates [*m*] among populations) through a simple equation based on the island model of population structure (Wright 1931; Wright 1943):

$$F_{ST} = \frac{1}{4Nm + 1}$$

Thus, solving this equation in function of *Nm*:

$$Nm = \frac{F_{ST} - 1}{4F_{ST}}$$

would provide the effective number of immigrants given that F_{ST} was known. It should be noted the migration rates incorporated in this equation correspond to dispersal rates and not the ecological process (*i.e.* cyclic migrations) described in section 1.1.

Initial estimates of dispersal from genotypic data relied on these indirect measures (see Neigel 1997 and references therein). Gene flow is often negatively correlated with genetic structure, and thus, these measures can be used to infer qualitatively the on-going levels of gene flow between populations (Whitlock and McCauley 1999; but see also Richardson *et al.* 2016). However, because the island model underlying this equation makes a large number of unrealistic assumptions (*e.g.* infinite number of populations, no mutation and selection, migration-drift equilibrium; see Whitlock and McCauley 1999), the utility of this metric is very limited in dispersal research. Nonetheless, F_{ST} (and other genetic distance metrics) are useful descriptive statistics of genetic structure that can be complemented with other approaches.

1.3.4.2 – Coalescent-based methods

Several methods based on coalescent theory are able to estimate long-term gene flow rates (among other demographic parameters) from microsatellites, such as the maximum-likelihood

estimators implemented in software MIGRATE (it has also incorporated a Bayesian estimator; Beerli and Felsenstein 2001; Beerli 2009) and IMa2 (isolation-with-migration model; **Figure 1.7**; Nielsen and Wakeley 2001; Hey and Nielsen 2007). However, obtaining accurate estimates with these methods using only microsatellites is challenging due to computational and convergence issues, sensitivity to violation of model assumptions, and microsatellite high polymorphism and complex mutational patterns (Hey and Nielsen 2007; Beerli 2009; Pinho and Hey 2010; Epps *et al.* 2013; Putman and Carbone 2014; Hey *et al.* 2015). This may help explain why microsatellites have found little use with these methods.

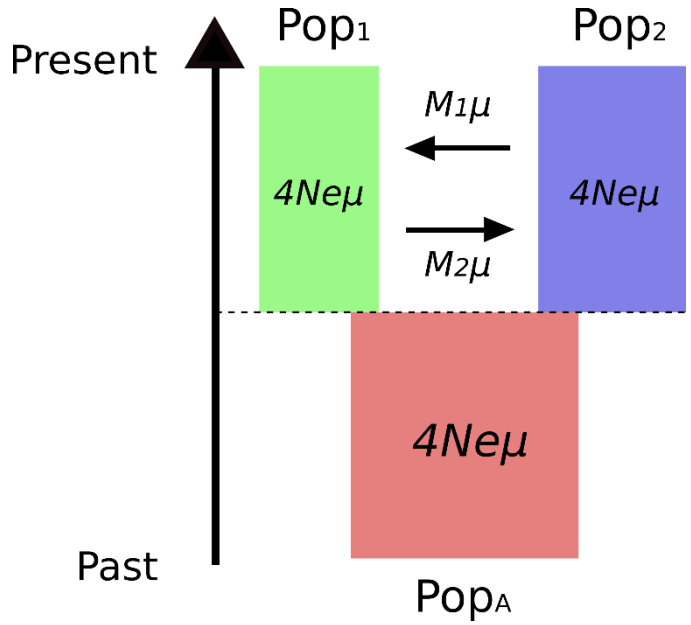

Fig. 1.7 Schematic overview of the isolation-with-migration model implemented in software IMa. The model assumes an ancestral population (Pop_A) splits into two descendant populations (Pop_1 and Pop_2). Each population exhibits a *Ne* value scaled by the mutation rate (μ). Migration rates scaled by μ ($M_1\mu$ and $M_2\mu$) represent the movement of genes as time moves forward. Gene flow is assumed to be constant following population splitting. Adapted from Pinho and Hey (2010).

1.3.4.3 – Assignment methods

Assignment methods comprise a group of statistical approaches that rely on multilocus genetic data to ascertain population genetic membership of individuals (reviewed in Manel *et al.* 2005; Broquet and Petit 2009). Here, I highlight two major groups of assignment methodologies: (i) Bayesian clustering methods (BCM); and (ii) kinship analysis.

1.3.4.3.1 – Bayesian clustering methods

The growth of Bayesian statistics in population genetics (Beaumont and Rannala 2004) prompted the development of BCM (*e.g.* STRUCTURE, TESS, BAYESASS) that are commonly used to ascertain population genetic membership of individuals (Pritchard *et al.* 2000; Wilson and Rannala 2003; Manel *et al.* 2005; Jombart *et al.* 2010; Caye *et al.* 2016). In general, BCM apply Markov chain Monte Carlo (MCMC) iterative algorithms to calculate the

posterior assignment probabilities of each individual from the observed multilocus genotype data (**Figure 1.8A**). Therefore, they enable clustering individuals into discrete genetic demes without *a priori* knowledge of population boundaries, comprise an efficient way to visualize population admixture, and in the case of BAYESASS, allows the calculation of non-effective immigration rates (Manel *et al.* 2005; Broquet and Petit 2009). Their efficiency is greater when population genetic divergence is high and the number of unsampled populations is low (Faubet *et al.* 2007; Broquet and Petit 2009). For instance, they are particularly effective in detecting abrupt genetic discontinuities caused by major landscape barriers to movement (*e.g.* roads, Riley *et al.* 2006; Blair *et al.* 2012; Carvalho *et al.* 2018; rivers or mountains, Zalewski *et al.* 2009; Sánchez-Montes *et al.* 2018). However, in complex and heterogeneous landscapes, where genetic structure is better characterized by continuous gradients or clines, BCM are prone to spatial autocorrelation and tend to overestimate genetic structure (Frantz *et al.* 2009; Schwartz and McKelvey 2009; Meirmans 2012), though other factors, such as sampling strategy and number of markers also contribute to their overall accuracy (Schwartz and McKelvey 2009; Meirmans 2012; Rodríguez-Ramilo and Wang 2012; Wang 2017). Nonetheless, in landscape connectivity studies, BCM have been a useful exploratory tool to examine patterns of genetic structure, thus acting as a good complement to other spatially-explicit methods (*e.g.* Velo-Antón *et al.* 2013; Noguerales *et al.* 2016; Gutiérrez-Rodríguez *et al.* 2017).

1.3.4.3.2 – Kinship analysis

Kinship analysis comprises a group of statistical techniques where familial relationships (*e.g.* parent-offspring, full-siblings, half-siblings) are assigned between two or more individuals (**Figure 1.8B**). The development of highly polymorphic markers, such as microsatellites or the use of a large number of SNPs have allowed performing parentage analyses with greater accuracy (Kane and King 2009; Jones *et al.* 2010; Christie 2013). In dispersal research, parentage analysis has been applied to detect putative anthropogenic barriers to dispersal (Sawaya *et al.* 2014; Carvalho *et al.* 2018), investigate marine metapopulation connectivity (Saenz-Agudelo *et al.* 2009; Christie *et al.* 2017), and to understand how phenotypic variation affects patterns of dispersal (Proctor *et al.* 2004; Hall *et al.* 2009; Waser and Hadfield 2011; Moore *et al.* 2014). They provide a much finer resolution in assignments compared with BCM, though the number of assignments is generally lower because much more genetic information (*e.g.* number of samples and sampling coverage) are needed to solve accurately pedigree configurations (Kane and King 2009). They also perform better than BCM under scenarios of low genetic divergence, although Christie *et al.* (2017) showed that both have limited power to

quantify migration rates. Currently, the most popular kinship analysis relying on microsatellites is the program COLONY due to its robust full-pedigree likelihood algorithm, high versatility concerning input parameters (*e.g.* inclusion of genotyping errors, mating system, ploidy, inclusion of known familial relationships), and ability to calculate *Ne* (Jones and Wang 2010; Wang 2016).

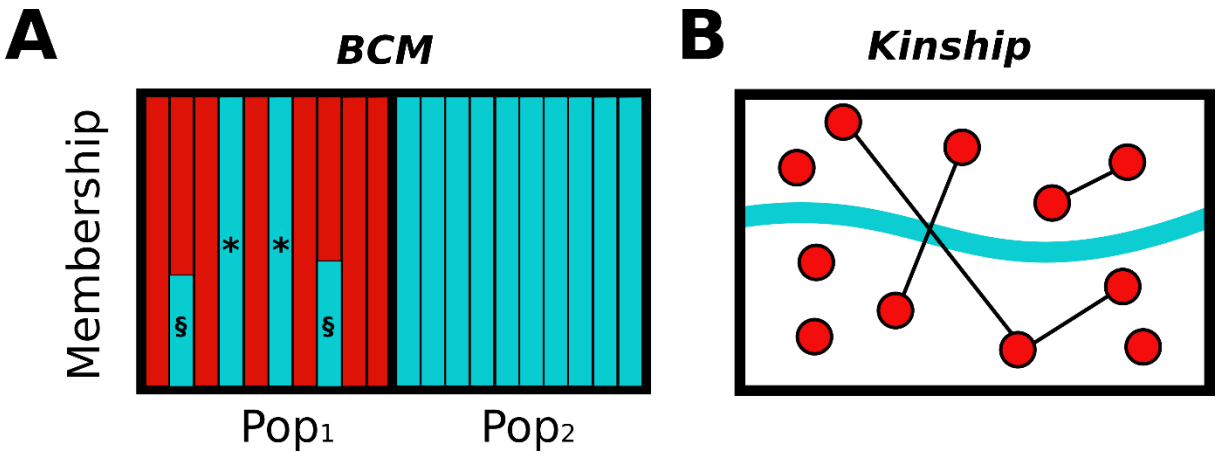

Fig. 1.8 Overview of the output provided by: (A) STRUCTURE (the most widely used BCM); and (B) kinship analysis; (A) STRUCTURE-like plot depicting the genetic membership of sampled individuals belonging to two putative populations (Pop_1 and Pop_2). Each bar corresponds to a sampled individual and populations are separated by a thick black line. Two individuals in Pop_1 were identified as potential immigrants from Pop_2 (individuals marked with asterisks), while two other individuals (denoted by symbol "§") exhibit genetic ancestry from both populations; (B) Landscape containing individuals (red circles), in which some of them share familial relationships (black lines; *e.g.* parent-offspring or full-sibling relations). Parentage analysis can be used to assess if a landscape barrier (blue polygon; *e.g.* road or river) hinders dispersal. In this illustration, the existence of related individuals on different sides of the putative barrier indicates that the considered barrier is permeable to dispersal.

1.3.4.4 – Analysis of spatial patterns of genetic distances

Statistical analyses of spatial patterns of genetic distances among individuals or populations have comprised a powerful framework to uncover dispersal and gene flow patterns across the landscape. Here, I will focus on two commonly used analytical frameworks: (i) the genetic spatial autocorrelation (GSA) framework introduced by Smouse and Peakall (1999) and implemented in software GenAlEx (Peakall and Smouse 2012); and (ii) the statistical association (correlation or regression) between ecological distances (calculated from environmental variables and/or geographic distances) and genetic distances among sampled individuals or populations, a framework commonly used in landscape genetics studies (Manel *et al.* 2003).

1.3.4.4.1 – Genetic spatial autocorrelation

GSA includes a distance-based approach that uses pairwise genetic and Euclidean geographic distance matrices as input to estimate fine-scale genetic structure across space. Geographic distances between pairs of individuals must be binned into distance classes and an autocorrelation coefficient (r_{auto}; bounded by [-1,1]) representing the genetic similarity between pairs of individuals is computed for each distance class, with results being summarized in a correlogram (Smouse and Peakall, 1999). Subsequent statistical tests allow testing if r_{auto} values are significantly different from zero and if they are significantly different among populations for a particular distance class (Smouse and Peakall, 1999; Smouse *et al.* 2008). Distance classes displaying positive r_{auto} estimates indicate that pairs of individuals within that class are genetically more similar. Positive r_{auto} values for shortest distance classes indicate that individuals are philopatric, while for farther distance classes, it may suggest dispersal to a specific range of distances (**Figure 1.9**). GSA has been used mostly to test for sex-biased dispersal (*e.g.* Banks and Peakall 2012; Blyton *et al.* 2015), although few studies have employed GSA to assess the influence of a particular phenotypic trait on dispersal patterns (*e.g.* colouration in salamanders; Grant and Liebgold 2017). Moreover, to obtain accurate results, a large number of samples must be obtained per population. Also, choosing an adequate number of distance classes to build correlograms is not always straightforward, though knowledge on movement ecology of a given species enables making more informed decisions regarding this parameter (Banks and Peakall 2012).

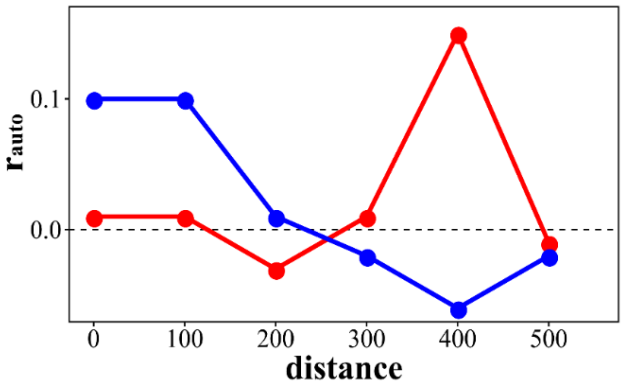

Fig. 1.9 A simplified correlogram showing r_{auto} values across 100-m distance intervals. Each coloured line may correspond to individuals from different groups or populations. For illustrative purposes, one may assume that the red and blue lines correspond to males and females, respectively. Under this scenario, the correlogram would indicate that females were philopatric (highest r_{auto} values were estimated for the shortest distance classes), while males comprised the dispersing sex, as many related individuals were found at on average 400 m apart.

1.3.4.4.2 – Landscape genetics

The rapid landscape and climate changes driven by anthropogenic activities have been having a profound impact on species' population connectivity, thus threatening their long-term persistence (Fischer and Lindenmayer 2007; Baguette *et al.* 2013; Haddad *et al.* 2015; Rivera-Ortíz *et al.* 2015; Pecl *et al.* 2017). The need to assess and predict the impact of human-

induced environmental changes in wildlife, together with recent technological advances in molecular and computational resources, stimulated researchers to combine tools from population genetics and spatial ecology over the last three decades (Manel *et al.* 2003; Balkenhol *et al.* 2015). Manel *et al.* (2003) formally defined the field of "landscape genetics" as an interdisciplinary field integrating population genetics and landscape ecology, among others (**Figure 1.10**). Since then, much conceptual and analytical work has been done to develop this discipline (see for example Storfer *et al.* 2010; Manel and Holderegger 2013; Hall and Beissinger 2014; Dyer 2015a; Dyer 2015b; DiLeo and Wagner 2016; Richardson *et al.* 2016; Shirk *et al.* 2018; Peterson *et al.* 2019). Here, I follow the definition of landscape genetics provided by Balkenhol *et al.* (2015), who defined it as "*research that combines population genetics, landscape ecology, and spatial analytical techniques to explicitly quantify the effects of landscape composition, configuration, and matrix quality on microevolutionary processes, such as gene flow, drift, and selection, using neutral and adaptive genetic data*". In the present thesis, I consider that the analytical landscape genetics framework involves three main steps: (1) study design; (2) quantification of both environmental and genetic variation among individuals or populations; and (3) the statistical association between genetic variation and environmental heterogeneity (**Figure 1.11**). Each step must be adjusted in function of the objectives and the hypotheses being tested (Hall and Beissinger 2014).

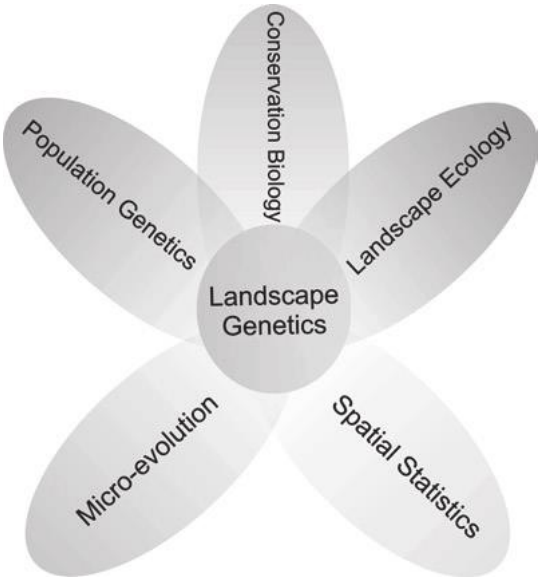

Fig. 1.10 A landscape genetics framework integrates a broad range of fields. Highly technical skills from these fields (*e.g.* GIS/remote-sensing, population genetic analyses, ecological niche modeling, landscape metrics) are necessary to perform robust analyses. Landscape genetic approaches, and their respective output, should be discussed between researchers and managers to contribute not only to a greater understanding of the interaction between species and the environment, but also for species conservation. Retrieved from Murphy and Evans (2011).

First, to delineate a proper study design in landscape genetics, one should make many decisions concerning: (i) the spatio-temporal scale, which should match the biology and ecology of the focal species (*e.g.* inclusion of past and contemporary relevant environmental variables, the study's spatial extent should match the scale of dispersal of the focal species;

Zellmer and Knowles 2009; Anderson *et al.* 2010; Galpern and Manseau 2013; Zhang *et al.* 2016); (ii) the sampling scheme (*e.g.* individual- *vs.* population-based sampling, number of landscape replicates, number of samples and their spatial distribution; Schwartz and McKelvey 2009; Short Bull *et al.* 2011; Landguth *et al.* 2012; Oyler-McCance *et al.* 2013; Hall and Beissinger 2014; Hand *et al.* 2016); and (iii) number of markers and the marker's content (polymorphism), because a higher number of highly polymorphic loci (and samples) increases statistical power (Hale *et al.* 2012; Landguth *et al.* 2012; Hall and Beissinger 2014). It should be noted, however, that these decisions are also highly dependent on logistical conditions (*e.g.* costs, available human resources, inaccessibility to certain areas); therefore, a trade-off between optimal sampling design and logistics must be taken into consideration to obtain the best possible results.

Second, after performing sampling, researchers must generate spatial and genetic data that will be later statistically associated. Several analytical methods are available to assess the effects of landscape on gene flow (see Hall and Beissinger 2014). Matrix modelling, *i.e.* correlation or regression between a response matrix (usually pairwise genetic distances) and one or more predictor matrices (ecological distances), has been the most widely applied statistical approach in landscape genetics (Zeller *et al.* 2016; Shirk *et al.* 2018); therefore, in this paragraph, I will focus on the generation of genetic and ecological distance matrices. In landscape genetics studies, microsatellites have been widely used to calculate genetic distance matrices due to their high level of polymorphism and fast rates of evolution, which make them ideal to study the effects of recent environmental changes on neutral genetic variation (Storfer *et al.* 2010; Wang 2010; Waits and Storfer 2015). Genetic distance matrices may comprise either population- (*e.g.* F_{ST}) or individual-based (*e.g.* proportion of shared alleles, D_{PS}) distance measures (see Hall and Beissinger 2014; Shirk *et al.* 2017). Moreover, matrices of ecological distances are computed from environmental data (*e.g.* temperature, land cover) stored in file formats commonly applied in GIS (*e.g.* raster files). These ecological matrices are used to formulate and test hypotheses concerning how particular environmental variables affect gene flow. There are four broad hypotheses (or models) that are usually tested within a landscape genetics framework: (i) the isolation-by-distance (IBD) model, which assumes gene flow decreases linearly with increasing geographic distances (Wright 1943; Orsini *et al.* 2013); (ii) the isolation-by-barrier (IBB) model, which is used to test explicitly the effects of specific discrete landscape features (*e.g.* roads, rivers) on genetic differentiation (Cushman *et al.* 2006; Prunier *et al.* 2014); (iii) the isolation-by-resistance (IBR) model, which reflects more accurately compared to the IBD model, how landscape configuration, heterogeneity, and quality influence patterns of gene flow (Cushman *et al.* 2006; McRae 2006;

McRae and Beier 2007); and (iv) the isolation-by-environment (IBE) model, which assesses how environmental dissimilarity among sites affect gene flow, regardless of the geographic distance (or landscape complexity) separating them (*e.g.* natural and sexual selection against immigrants may hinder reproduction of immigrants due to reduce fitness; Wang *et al.* 2013; Wang and Bradburd 2014). Both IBD and IBB matrices can be calculated in a straightforward way. For the former, the geographic coordinates (or a "flat" raster with all cell values equal to one) of sampling localities are used to calculate a pairwise geographic distance matrix (*e.g.* Cushman *et al.* 2006; Velo-Antón *et al.* 2013; Antunes *et al.* 2018), while for the latter, individuals sampled in the same side of a barrier are coded with "0" and individuals located in opposite sides are coded with "1" in a distance matrix (*e.g.* Prunier *et al.* 2014). To calculate a IBE model, a principal component analysis (PCA) can be applied to a set of environmental layers and the IBE matrix is estimated from the Euclidean distances between localities plotted on the resulting principal component axes (Wang 2013; Noguerales *et al.* 2016; Antunes *et al.* 2018). To calculate IBR matrices, resistance surfaces (univariate or multivariate raster layers describing quantitatively the cost or permeability of the landscape to movement/gene flow) must be generated, and from these, pairwise cost-weighted distances must be derived. Unlike IBD and IBE models, the IBR matrices require more procedures to be estimated. Specifically, two analytical steps must be carried out: (i) parameterization of resistance surfaces; and (ii) computation of cost-weighted distances between focal nodes (*e.g.* habitat patches, individuals, populations) within a resistance surface. The first step requires the assignment of resistance (cost) values to each cell (this procedure is often called "parameterization" of resistance surfaces; see Spear *et al.* 2010; Zeller *et al.* 2012; Zeller *et al.* 2018). This task is challenging because quantifying the exact magnitude of the effects of each environmental variable on gene flow is not free of bias and not well understood for the vast majority of the species. Parameterization of resistance surfaces can be accomplished through different approaches. First, costs may be assigned based on researcher's knowledge of the focal species (*i.e.* expert opinion; Cushman *et al.* 2006; Castillo *et al.* 2014; Dudaniec *et al.* 2016; Cleary *et al.* 2017). Parameterization based on expert opinion can be applied easily but is often arbitrary and inaccurate (Spear *et al.* 2010; Zeller *et al.* 2012). Second, resistance costs can be derived from habitat suitability layers estimated using non-genetic field data, such as occurrence records, dispersal data collected from DTM or species distribution modelling (Stevens *et al.* 2006; Velo-Antón *et al.* 2013; Keeley *et al.* 2017; Zeller *et al.* 2018). This empirical-based parameterization approach is based on the assumption that movement and gene flow are correlated, although in some occasions that may not be true (Spear *et al.* 2010; Keeley *et al.* 2017). Finally, optimization algorithms, which perform an exhaustive search of the parameter space

(resistance values) to identify the resistance surfaces that have the greatest statistical fit with the observed genetic data, have shown promise (Shirk *et al.* 2010; Peterman 2018). However, it should be noted that in some occasions the fittest surface may still be a poor descriptor of true landscape resistance depending on the genetic information content and chosen variables (Graves *et al.* 2013). Following parameterization of resistance surfaces, pairwise cost-weighted distance matrices can be computed using different methods, although the most popular are: (i) least-cost modelling and derived approaches, which in general seek to identify a single optimal route (*i.e.* a sequence of cells in which the cumulative cost is lowest) between two focal nodes (Adriaensen *et al.* 2003; Etherington 2016); and (ii) current flow (or circuit-based) modeling, which analogous to electricity and its properties of a random walk in an electric circuit, estimate resistance as the probability of a random individual travelling through the cells that connect nodes (McRae 2006; Pelletier *et al.* 2014). Their usefulness under particular scenarios is largely determined by many aspects, such as the spatial scale, available computational resources, the objectives of the study, and the biology and ecology of the target species (see Spear *et al.* 2010; Kool *et al.* 2013; Panzacchi *et al.* 2016). Nevertheless, current flow has shown to be quite versatile, as its ability to account for multiple pathways and estimate averaged cumulative resistance between nodes allows capturing more realistically gene flow patterns in many circumstances (McRae and Beier 2007; McRae *et al.* 2008). See for instance Kool *et al.* (2013), Etherington *et al.* (2016), Rayfield *et al.* (2016), and Campos (2018) for further considerations about the potential applications and limitation of these methods, as well other available algorithms to estimate pairwise cost-weighted distances from resistance surfaces.

Lastly, the statistical association between pairwise genetic and ecological distance matrices allows the identification of the environmental drivers of gene flow. Most landscape genetic studies have applied Mantel (correlation between two distance matrices [one genetic and one ecological]; Mantel 1967) or partial Mantel tests (correlation between two distance matrices while controlling the effect of a third ecological distance matrix; Smouse *et al.* 1987) to assess the strength of correlation between genetic and ecological distances (Manel and Holderegger 2013; Zeller *et al.* 2016). However, over the last years, several simulation studies have been pointing out some statistical issues inherent to these tests, namely, high rates of type-I errors, low predictive power, and high sensitivity to violation of the independence and linearity assumptions (see Guillot and Rousset 2013; Zeller *et al.* 2016). Accordingly, other more sophisticated methods have been developed and applied in landscape genetics, such as multiple matrix regression with randomization (MMRR), which basically extends the Mantel test to a multiple regression framework (Wang 2013), ordination techniques (Kierepka and

Latch 2014), structural equation modelling (Wang *et al.* 2013), linear mixed effects models (LMM; Clarke *et al.* 2002; van Strien *et al.* 2012), gravity models (Murphy *et al.* 2010; Robertson *et al.* 2018), Bayesian inference (Bradburd *et al.* 2013; Botta *et al.* 2015), and generalized dissimilarity modelling (GDM; Ferrier *et al.* 2007; Micheletti and Storfer 2017). Some of them have shown great promise in landscape genetics model selection. For instance, LMM with maximum-likelihood population effects allows accounting for the non-independence between pairwise observations through the inclusion of random effects and showed great performance in landscape genetics (Shirk *et al.* 2018), while GDM comprises a statistical technique capable of modeling non-linear relationships between response and predictor matrices. The singly constrained gravity models comprise an interesting network-based approach that integrates spatial proximity between sites, patches' structural characteristics (*e.g.* patch quality) attracting immigrants, and the resistance of intervening habitat between sites to gene flow (Murphy *et al.* 2010). Finally, Bayesian models have been useful to quantify and disentangle the relative effects of geography and the environment on genetic differentiation (Bradburd *et al.* 2013; Botta *et al.* 2015).

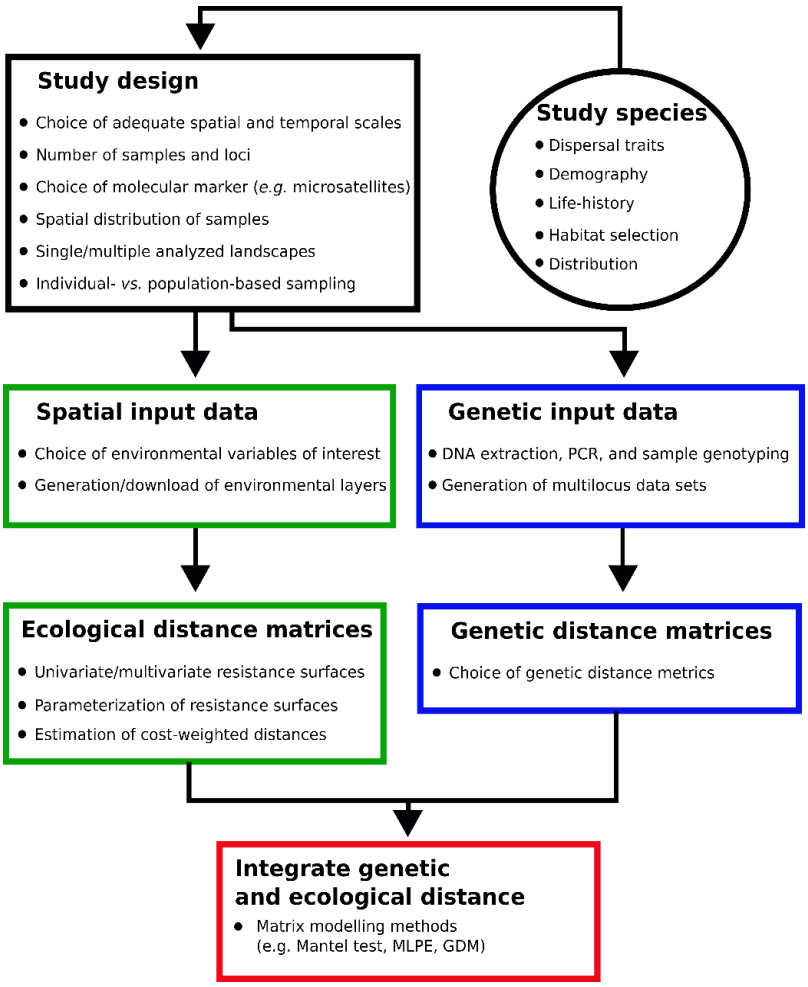

Fig. 1.11 A simplified landscape genetics framework focused on matrix modeling approaches. This framework involves: (1) study design (black box), which is partially dependent upon the biology and ecology of the target species (black oval); (2) calculation of genetic distance matrices (blue boxes); (3) calculation of matrices of ecological distances (green boxes); and (4) statistical association between ecological and genetic distance matrices (red box). Adapted from Hall and Beissinger (2014).

1.4 – The fire salamander (*Salamandra salamandra*)

1.4.1 – Pueriparity in the family Salamandridae

The fire salamander (*Salamandra salamandra*, Linnaeus 1758) belongs to the family Salamandridae which includes a total of 21 genera and 121 species (AmphibiaWeb 2018). This family is divided into two major groups, newts (about 100 species) and true salamanders (includes *Salamandra*, *Chioglossa*, *Mertensiella,* and *Lyciasalamandra*; ca. 20 species). Pueriparity in urodeles arose only in this family, from which a total of 11 species exhibit pueriparity, including all 7 *Lyciasalamandra* species (all strictly pueriparous) and four (out of six) *Salamandra* species (**Figure 1.12**; Buckley 2012; Kieren *et al.* 2018). In the latter genus, the alpine fire salamanders *S. atra* and *S. lanzai* are strictly pueriparous, whereas the remaining four species (*S. salamandra*, *S. algira*, *S. infraimmaculata,* and *S. corsica*) are acknowledged as larviparous (Buckley 2012). However, some populations of *S. salamandra* and *S. algira* also evolved pueriparity, comprising rare cases among amphibians exhibiting both aquatic and terrestrial reproduction within the same species (García-París *et al.* 2003; Beukema *et al.* 2010; Velo-Antón *et al.* 2015; Dinis and Velo-Antón 2017).

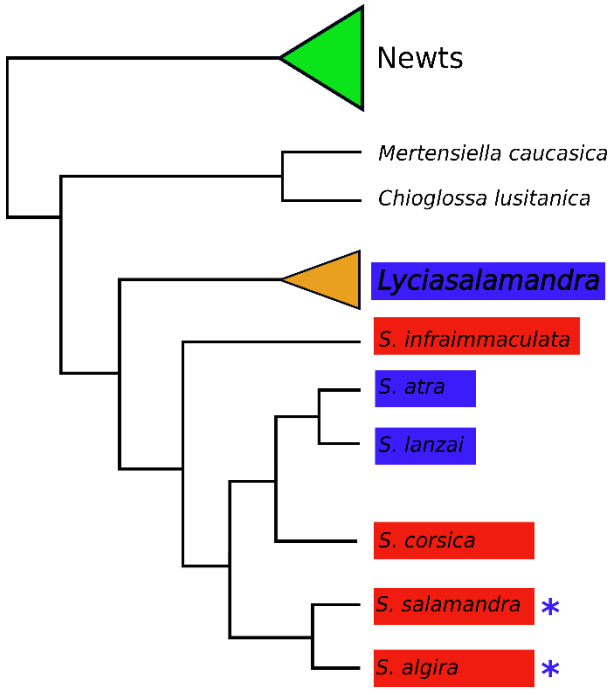

Fig. 1.12 Simplified phylogenetic tree of the family Salamandridae based on data from Zhang *et al.* (2008). The clade "Newts" includes ca. 100 species of highly aquatic organisms. Among the clade "true salamanders" (ca. 20 species), phylogenetic relationships are also represented with especial emphasis in the *Salamandra* genus (six species in total; see Rodríguez *et al.* 2017). Species/groups highlighted in blue are pueriparous (all *Lyciasalamandra* species, *S. atra*, and *S. lanzai*), while *Salamandra* species highlighted in red are larviparous. Blue asterisks in *S. salamandra* and *S. algira* indicate pueriparity arose on few populations, although both being mostly larviparous throughout their distribution range.

1.4.2 - Distribution range, subspecies, and evolution of pueriparity in *Salamandra salamandra*

Salamandra salamandra is widely distributed in the western Palearctic region, being distributed from the southern Iberian Peninsula to eastern Europe, including the Balkan Peninsula, southern Poland and western corner of Ukraine (**Figure 1.13**; Kuzmin *et al.* 2009; Sillero *et al.* 2014). A total of 13 subspecies are currently recognized (see Joger and Steinfartz 1995; Steinfartz *et al.* 2000; Petrov 2007; Velo-Antón and Buckley 2015; Beukema *et al.* 2016a), although the taxonomy of some subspecies is still debated due to the lack of diagnostic characters and nuclear markers supporting their subspecific status. It is clear, however, most subspecies are endemic to the Iberian Peninsula: *S. s. gallaica*, *S. s. bejarae*, *S. s. crespoi*, *S. s. morenica*, *S. s. longirostris*, *S. s. almanzoris*, *S. s. bernardezi*, *S. s. fastuosa* and *S. s. terrestris* (the latter is also present in central Europe; Velo-Antón and Buckley 2015; Beukema *et al.* 2016a; Pereira *et al.* 2016; **Figure 1.14**). Indeed, the remarkable phenotypic variation (body size and shape, colouration, reproductive modes; Beukema *et al*. 2016b) and genetic differentiation found across Iberian populations at inter- and intra-subspecific levels makes this species both polytypic and polymorphic. Much of this phenotypic and genetic divergence is likely due to the complex biogeographic history of the Iberian Peninsula (Steinfartz *et al.* 2000; García-París *et al.* 2003; Velo-Antón *et al.* 2007; Reis *et al.* 2011; Vences *et al.* 2014; Velo-Antón and Buckley 2015; Velo-Antón *et al.* 2015; Beukema *et al.* 2016a; Pereira *et al.* 2016). Specifically, during the Quaternary (Pleistocene), strong climatic oscillations, together with the topographic and geological heterogeneity of this region, caused cyclic range contractions and expansions of *S. salamandra* populations, thus promoting allopatric divergence at phenotypic and genetic levels among populations isolated in glacial refugia (*e.g.* García-París *et al*. 2003; Velo-Antón *et al.* 2007; Antunes *et al.* 2018).

Salamandra salamandra constitutes an exceptional and rare case, with two distinct reproductive strategies co-occurring: larviparity and pueriparity (**Figure 1.13**). Throughout most of its range, *S. salamandra* females are larviparous (the ancestral trait). However, during the Pliocene-Pleistocene period in the Cantabrian mountains (northern Spain), environmental-driven pressures (possibly the lack of surface water in karstic limestone substrates) have been suggested as the main driver of the evolution of pueriparity in the subspecies *S. s. bernardezi* (García-París *et al.* 2003). Subsequent interglacial cycles characterized by more favourable climate promoted the spread of this trait throughout its range, later introgressing eastwards with *S. s. fastuosa*. Pueriparity was also reported in two insular land-bridge populations of *S. s. gallaica* located in the islands of Ons and San Martiño, which are part of the Galician Atlantic

Islands National Park (north-western Spain; **Figure 1.13**; Velo-Antón *et al.* 2007, Velo-Antón *et al.* 2012). Genetic studies have shown pueriparity in these islands emerged independently since these insular pueriparous populations do not form a monophyletic group with the remaining pueriparous populations from Northern Spain (Velo-Antón *et al.* 2007). Additionally, these studies have proposed this independent origin of pueriparity likely occurred much more recently and within a short amount of time after the formation of these islands (<8,000 ya), probably, due to lack of surface water in these islands in the recent past (Velo-Antón *et al.* 2007, Velo-Antón *et al.* 2012; Lourenço *et al.* 2018).

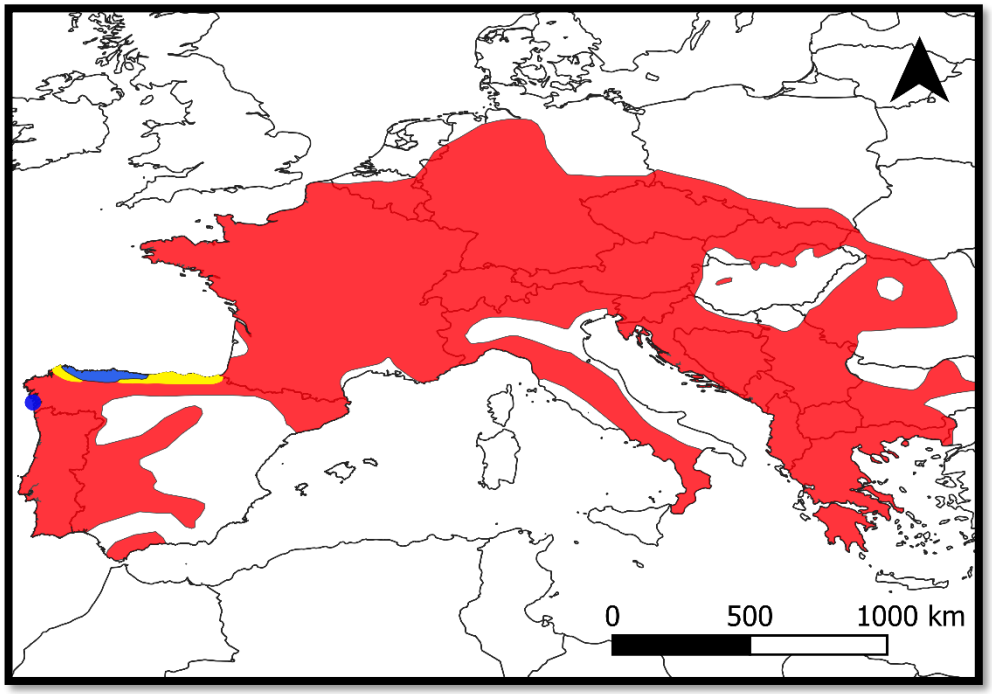

Fig. 1.13 Distribution range of *S. salamandra*. Throughout most of its range, *S. salamandra* females are larviparous (red), while pueriparity is restricted to a small area in northern Spain (blue). The yellowed areas illustrate roughly the contact zones between pueriparous and larviparous populations, in which, preliminary data has shown that there is substantial phenotypic and genetic admixture. A second independent origin of pueriparity was also detected in two insular populations located in the islands of Ons and San Martiño in the Spanish north-western coast (highlighted by a blue circle).

1.4.3 – *Salamandra salamandra* as a model system

1.4.3.1 – Studied subspecies and considerations on sampling design

The main objective of the present thesis is to contribute to a better understanding of the eco-evolutionary implications underlying the shift from an aquatic reproduction to a terrestrial one in amphibians, using *S. salamandra* as a case study. Comparative studies integrating multiple species with marked differences in a trait of interest (*e.g.* life-history) can be a valuable approach to investigate how specific phenotypes influence the species-landscape interaction

(*e.g.* patterns of gene flow; Richardson 2012; Sánchez-Montes *et al.* 2018). However, when relying on distantly related species, inferences gathered from these studies may be limited. This is because these species often present high phenotypic and ecological dissimilarity, which may make difficult to isolate and disentangle the effects of a single trait in ecological and evolutionary processes. This potential source of bias can be reduced when comparing subspecies (or closely related species) because phenotypic and ecological dissimilarity are usually lower compared to distantly related species (*e.g.* Garcia *et al.* 2017; Hendrix *et al.* 2017).

Although several subspecies are recognized in *S. salamandra*, the present thesis is focused only on two Iberian subspecies that were sampled in the north-western part of Iberian Peninsula: (i) *S. s. gallaica*; and (ii) *S. s. bernardezi* (**Figures 1.13 and 1.14**). The subspecies *S. s. gallaica* exhibits larviparity in mainland populations, whereas *S. s. bernardezi* exhibits pueriparous reproduction (Velo-Antón *et al.* 2015). To perform robust comparisons between reproductive modes in both subspecies, several considerations were taken into account. First, the distribution range of *S. s. gallaica* is wider, as it encompasses Atlantic and Mediterranean ecosystems, while *S. s. bernardezi* is restricted to Atlantic ecosystems in north Spain (**Figure 1.14**; Velo-Antón and Buckley 2015). Because environmental factors may affect patterns of dispersal and gene flow, we restricted sampling of both subspecies to northwestern Spain to ensure more valid comparisons, as the climate (Atlantic influence) and the type of native vegetation (*e.g.* predominance of deciduous forests of *Quercus* spp.) are similar across this region (Amigo *et al.* 2017). Second, in the present thesis, genetic studies were performed not only at both individual and population levels, but also at local and regional scales. Some methodologies employed in those studies (*e.g.* spatial autocorrelation) require the inclusion of several samples to be relatively accurate (Banks and Peakall 2012; Landguth *et al.* 2012). The north-western Iberia contains a fair amount of suitable humid habitats for fire salamanders, which probably promote the high population abundances observed in this region (Velo-Antón and Buckley 2015; Lourenço, personal observation). This makes the acquisition of a large number of tissue samples a considerably easier task when compared to *S. algira* populations or southern subspecies (including southern populations of *S. s. gallaica*). In fact, collecting a large number of samples in southern Iberia is challenging, as population sizes are likely smaller due to the drier conditions and low availability of aquatic breeding sites (see for example Antunes *et al.* 2018). Third, it is also more feasible to sample adult individuals in northern populations. Previous genetic studies performed in southern amphibian populations have partially relied on tissue samples collected from larvae, probably, because is harder to find adult individuals (*e.g.* Recuero *et al.* 2007; Antunes *et al.* 2018). Larvae are often spatially

clustered and there is an increased likelihood of sampling relatives. This may be a potential source of bias, as the inclusion of related individuals may introduce significant biases in population and landscape genetic analyses (Goldberg and Waits 2010; Rodríguez-Ramilo and Wang 2012; Sánchez-Montes *et al.* 2017; Wang 2018); therefore, sampling areas where a large number of adult individuals can be sampled are preferable. Fourth, the insular pueriparous populations of *S. s. gallaica* were not included in this thesis due to their independent origin of pueriparity (Velo-Antón *et al.* 2007), and population-specific characteristics (isolated populations, low genetic diversity, and differentiated behaviour; Velo-Antón *et al.* 2012; Velo-Antón and Cordero-Rivera 2017; Lourenço *et al.* 2018). Lastly, both subspecies share a contact zone in this region, where substantial genetic and phenotypic admixture takes place (Galán 2007; Velo-Antón *et al.* 2017). Hence, I did not include populations from this hybrid zone to avoid confounding genetic effects (see **Figure 1.13**).

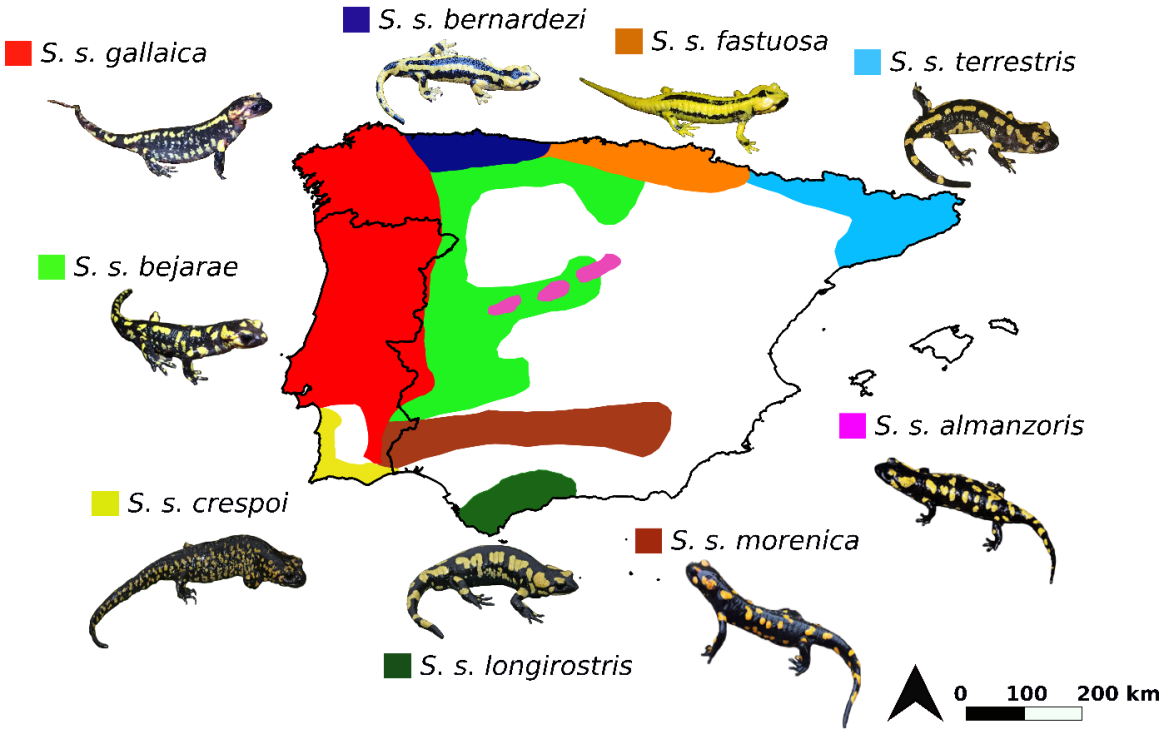

Fig. 1.14 Approximate distribution of the nine recognized *S. salamandra* subspecies in the Iberian Peninsula. Distribution data was based on previous studies (Reis *et al.* 2011; Velo-Antón and Buckley 2015; Pereira *et al.* 2016). Animals in the figure were edited from photographs taken by Guillermo Velo-Antón and Jeroen Speybroeck (source: http://www.fieldherpforum.com/forum/viewtopic.php?f=2&t=9660).

1.4.3.2 – Why Salamandra algira was not included in this thesis?

In amphibians, as mentioned above, intra-specific variation of aquatic (larviparity) and terrestrial (pueriparity) reproduction is extremely rare. Certainly, our knowledge about the eco-evolutionary implications of a terrestrial pueriparous reproduction in amphibians would benefit from studies focusing on larviparous and pueriparous populations of both species. *Salamandra salamandra* is widely distributed in Europe and presents high population densities in some regions (*e.g.* northern-western Spain), which makes sampling a large number of adult individuals an easier task (*e.g.* Velo-Antón *et al.* 2015; Lourenço *et al.* 2018). However, unlike *S. salamandra*, *S. algira* exhibits a heavily fragmented distribution in North Africa (Morocco and Algeria) due to the arid conditions of this region (Escoriza *et al.* 2006; Dinis *et al.* 2019). Hence, this species is mostly restricted to mountain ranges where the availability of humid habitats with dense vegetation or rock crevices and surface water for reproduction is greater (Dinis and Velo-Antón 2017; Dinis *et al.* 2019). This patchy distribution, together with its limited ecological tolerance in North Africa, makes the task of finding and sampling a large number (hundreds) of adult individuals unfeasible.

1.4.4 – Phenotypic and ecological characterization of both studied subspecies

1.4.4.1 – Morphology and life-history

At the morphological level, both *S. s. gallaica* and *S. s. bernardezi* exhibit great intra- and inter-subspecific variation in patterns of colouration throughout their distribution (**Figure 1.15**). However, in general, *S. s. gallaica* shows a dorsal dark colouration with yellow blotched patterns and often with red spots (Guiberteau *et al.* 2012; Velo-Antón and Buckley 2015; Alarcón-Ríos *et al.* 2019), while *S. s. bernardezi* exhibits a dorsal dark colouration with varying patterns of yellow stripes (Beukema *et al.* 2016a). Besides body colouration, both subspecies differ in some morphometric attributes, most remarkably, in body size. While the snout-vent length (SVL) in *S. s. gallaica* usually varies between 120-200 mm (up to 250 mm), *S. s. bernardezi* individuals are smaller, with some individuals reaching up to 180 mm in SVL (Velo-Antón and Buckley 2015; Velo-Antón *et al.* 2015). Sexual dimorphism is not marked in this species despite females appearing to be slightly larger than males (García-París *et al.* 2004; Cordero-Rivera *et al.* 2007; Alarcón-Ríos *et al.* 2017).

In both subspecies, the breeding season and gestation months are highly variable depending on environmental pressures. Nevertheless, in lowland populations inhabiting the focal region (north-western Spain), the breeding season is generally in Autumn, followed by a second peak in the Spring (Velo-Antón and Buckley 2015). After collecting male's sperm (see

details about reproduction in Arnold 1987), females store it in internal receptive organs (spermathecae) up to several months to fecund unfertilized eggs within the oviduct. Additionally, females from both subspecies can store sperm from more than one male (Caspers *et al.* 2014; Velo-Antón unpublished data); therefore, multiple males can contribute genetically to a single clutch of newborns, though about 70% of the progeny is sired by a single male (usually the first male that copulates with the female; Caspers *et al.* 2014). Larviparous females can deliver up to 90 (on average 30-40) larvae in water bodies (*e.g.* streams, ponds) after a gestation period of 80-90 days, while pueriparous females deliver 1-35 fully metamorphosed terrestrial juveniles after the same gestation period (Buckley *et al.* 2007; Velo-Antón *et al.* 2015). Ontogenetic processes are responsible for the early metamorphosis of juveniles within pueriparous females, despite the equal gestation periods. Remarkably, heterochronic events (*i.e.* changes in the relative timing of ontogenetic events; *e.g.* earlier hatch of embryos within the oviduct), jointly with a remarkable accelerated growth of cephalic structures that enable an intrauterine cannibalistic behaviour of siblings, allow embryos to acquire additional nutrients and thus, grow rapidly and complete metamorphosis still inside the mother (see details in Buckley *et al.* 2007). Furthermore, in larviparous populations, after larvae being released into water, they feed for a few months (ca. 1-5 months) until attaining metamorphosis, although the larval stage may extend for more than one year in environments with low temperatures and scarce food resources (*e.g.* montane habitats; Alcobendas and Castanet 2000; Velo-Antón and Buckley 2015). Juveniles from both pueriparous and larviparous populations reach sexual maturity (generation time) at 4-5 years (Alcobendas and Castanet 2000). See **Table 1.3** for a summary of the major phenotypic and life-history differences between both *S. s. gallaica* and *S. s. bernardezi.*

1.4.4.2 – Activity and habitat use

Fire salamanders of both subspecies exhibit nocturnal activity, with the exception of the diurnal insular pueriparous population from San Martiño island (north-western Galician, Spain; Velo-Antón and Cordero-Rivera 2017). During the day, they hide in underground burrows, underneath rocks, walls or fallen logs, while at night, given appropriate environmental conditions (*i.e.* high humidity [90-100%] combined with mild temperatures [5º-18ºC]), fire salamanders become ground active and search for prey (usually small invertebrates) and mates during the breeding season (Velo-Antón and Buckley 2015; Catenazzi 2016). During colder and warmer months, individuals usually hibernate and aestivate, respectively, although months of inactivity vary with latitude and altitude.

Unlike adult newts, who spend most of their life cycle in a diverse range of freshwater systems, adult individuals of *Salamandra salamandra* are terrestrial, with females returning to water only to deliver larvae (in case of larviparous populations, including *S. s. gallaica* ones; **Figure 1.15**; Velo-Antón *et al.* 2015). Densities of individuals of both subspecies are usually high in moist and shaded environments, particularly, in deciduous forests with nearby streams and ponds, where levels of humidity are elevated and larviparous females can give birth to the aquatic larvae (Ficetola *et al.* 2012; Velo-Antón and Buckley 2015). However, they can also be found in a wide range of terrestrial habitats, such as native coniferous forests, scrublands, and even pine (*Pinus* spp.) and eucalyptus (*Eucalyptus* spp.) plantations with the soil covered extensively by shrubs (**Table 1.3**; Velo-Antón and Buckley 2015). This species is generally absent in agricultural (*e.g.* pastures, crops and plantations) and urban areas, though due to their great independence from water, pueriparous populations can also inhabit water-limited and harsh environments, such as small gardens and urban parks (Álvarez *et al.* 2015; Iglesias-Carrasco *et al.* 2017) and islands (Velo-Antón *et al.* 2012; Lourenço *et al.* 2018).

Table 1.3 Summary of some remarkable morphological, ecological, and life-history differences between the studied subspecies.

Feature	*S. s. gallaica*	*S.s. bernardezi*
Reproductive mode	Larviparity	Pueriparity
Offspring	Up 90 larvae	1-35 metamorphosed juveniles
Dependent on water to complete life cycle?	Yes	No
Colouration	Variable, but usually dark colouration with yellow blotched patterns and red spots. Reddish, greyish and melaninc morphs can also be found	Variable, but usually dark colouration with yellow stripes. Brownish, yellowish and melanic morphs can also be found.
Adult body size	Up to 250 mm	Up to 180 mm
Habitat use	Preferably in moist and deciduous woodlands with water bodies nearby for females giving birth to larvae, although they can be found in shrublands, and *Eucalyptus* and *Pinus* plantations	Preferably in deciduous woodlands, although it can be found in shrublands, *Eucalyptus* and *Pinus* plantations, and water-limited environments, such as urban parks.

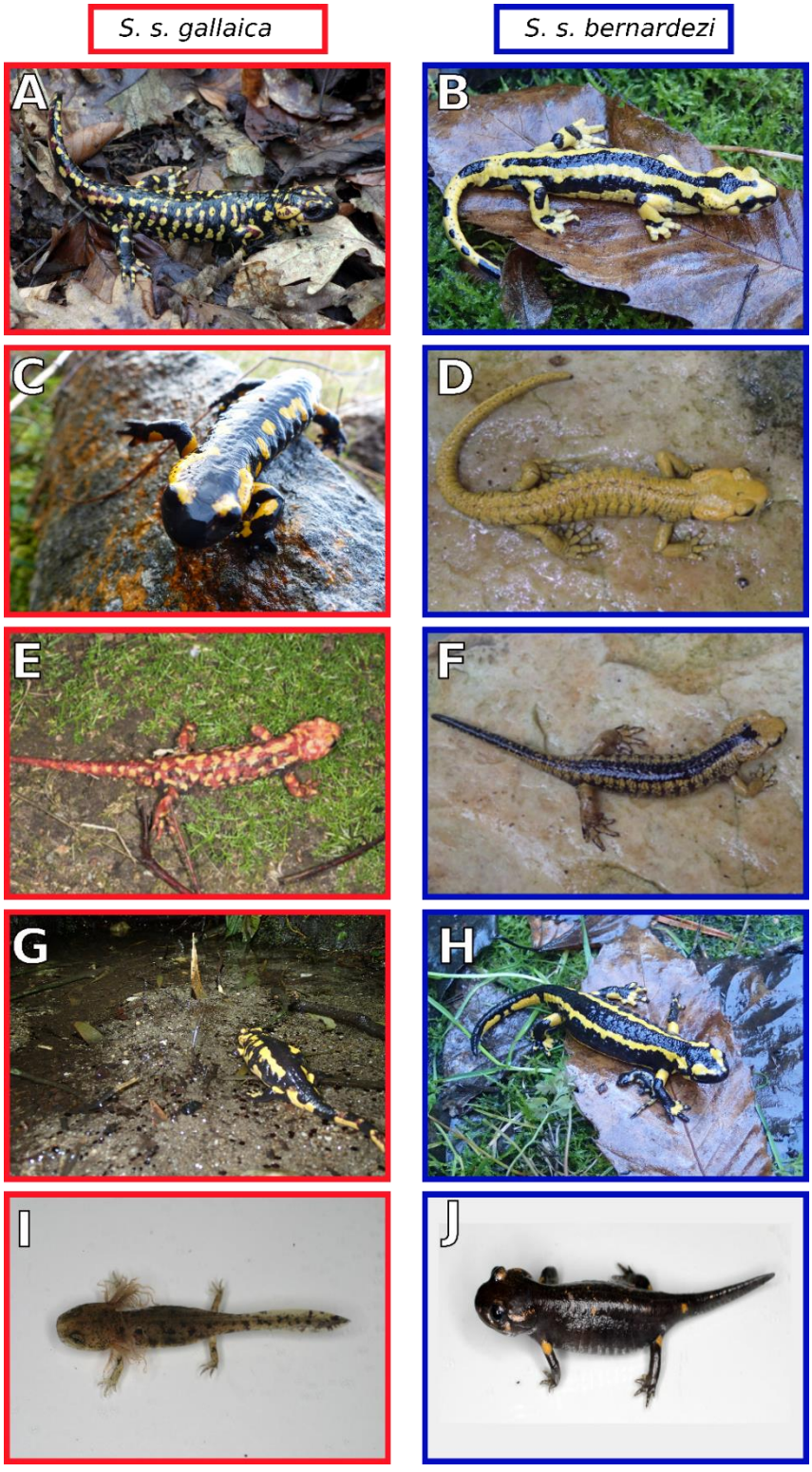

Fig. 1.15 These photos show some of the phenotypic variation found in both subspecies (panels A, C, and E for *S. s. gallaica* and panels B, D, and F for S. s. bernardezi). Females of *S. s. gallaica* must go to water bodies (e.g. ponds, streams) to deliver larvae (panels G and I), whereas females of *S. s. bernardezi* deliver fully metamorphosed terrestrial juveniles (panels H and J). Photo credits: Guillermo Velo-Antón and Bernardo Antunes.

1.4.4.3 – Dispersal ecology

Ecological studies examining dispersal in *S. salamandra* are scarce, particularly, in pueriparous populations. Fire salamanders are relatively sedentary and territorial (average home range size is ca. 6000 m^2; Schulte *et al.* 2007; Hendrix *et al.* 2017), although they can disperse much farther than other salamander species, such as lungless plethodontid salamanders (typically < 60 m; reviewed in Smith and Green 2005). Previous mark-recapture studies in larviparous populations have shown most individuals moved up to 200 m (Rebelo and Leclair 2003; Schulte *et al.* 2007), while a few individuals were recorded to disperse up to 500 m (Schulte *et al.* 2007; Hendrix *et al.* 2017). This distance threshold (500 m) seems the scale at which most (larviparous) salamanders move, as corroborated by spatial autocorrelation analyses in a larviparous population studied in Italy (Ficetola *et al.* 2012). Additionally, fire salamanders moving more than 500 m were recorded by Hendrix *et al.* (2017) in the Kottenforst (Germany). This population of fire salamanders has been the target of several studies due to a set of behavioural and genetic differences existing between two subpopulations, in which females of each subpopulation have adapted to deliver larvae either in ponds or streams (see for example Steinfartz *et al.* 2007; Caspers and Steinfartz 2011; Bletz *et al.* 2016). By using mark-recapture techniques and telemetry to compare movement patterns between both larviparous subpopulations, Hendrix *et al.* (2017) found that very few pond-adapted individuals carried out long-distance movements up to 1.9 km, while stream-adapted individuals did not move beyond 500 m. Besides terrestrial movement, in larviparous populations, passive water-borne dispersal (due to strong water discharges after heavy rain) along the stream during the larval stage may also promote long-distance dispersal events (Thiesmeier and Schuhmacher 1990; Reinhardt *et al.* 2018), although maximum water-borne dispersal distances and rates are poorly known. Moreover, so far there is no conclusive evidence of sex-biased dispersal in this species. While Schulte *et al.* (2007) did not observe sex-specific differences in movement patterns in *S. s. terrestris*, few studies have suggested male-biased dispersal as a potential driver of the mito-nuclear discordances observed in *S. salamandra* across different regions and different subspecies (northern Spain, García-París *et al.* 2003; central Spain, Pereira *et al.* 2016). Additionally, Helfer *et al.* (2012) used ecological and molecular methods to confirm male-biased dispersal in a *Salamandra* alpine species (*S. atra*).

1.5 – Structure and objectives of the thesis

The main objective of the present doctoral dissertation is to contribute to a better understanding of the ecological consequences (long-term persistence in stressful environments, patterns of dispersal) and, by extension, of the population evolutionary implications (gene flow and genetic connectivity) of a transition from an ancestral reproductive strategy (aquatic larviparous reproduction) to a derived one (terrestrial pueriparous reproduction) in amphibians, using fire salamanders (*S. salamandra*) as a case study. To accomplish this task, a comparative framework using two *S. salamandra* subspecies (*S. s. gallaica* and *S. s. bernardezi*) with different reproductive strategies (larviparity and pueriparity) will be employed. Such comparison at intra-specific level may contribute with valuable information to increase our knowledge about this subject.

This thesis is subdivided in six chapters. Chapter 1 consists of a general introduction to subjects relevant to the following chapters, such as:

- evolution of viviparity in vertebrates, with a especial emphasis in amphibians;
- the potential eco-evolutionary consequences underlying the evolution of viviparity (and pueriparity in amphibians);
- definition of dispersal, description of the factors governing it, and the potential effects of changes in reproductive modes in patterns of dispersal and gene flow;
- use of molecular markers in dispersal research;
- description of relevant phenotypic, ecological, and evolutionary aspects of the study species (*Salamandra salamandra*) and why it is a good model system to examine the main goal of the present thesis.

I studied urban pueriparous populations of *S. s. bernardezi* inhabiting small parks and gardens in the city of Oviedo (northern Spain) in chapter 2. Pueriparity has putatively enabled the long-term persistence of these populations in Oviedo. These populations in Oviedo constitute an excellent model for research in urban genetics, as their particularities enable me to examine the influence of time, demography, and population-specific traits on neutral genetic variation in urbanized contexts. Three objectives were addressed:

- to estimate and compare patterns of genetic diversity and genetic structure in urban and rural populations;
- to estimate historical and contemporary *Ne* of urban populations;

- to quantify the contributions of population-specific traits, including demographic history, time since isolation and patch attributes to genetic differentiation and diversity.

This chapter was published in a SCI journal:

- Lourenço A, Álvarez D, Wang IJ, Velo-Antón G (2017) Trapped within the city: integrating demography, time since isolation and population-specific traits to assess the genetic effects of urbanization. *Molecular Ecology*, **26**, 1498–1514.

In chapter 3, I used a GSA framework to estime patterns of fine-scale genetic structure and, thus, infer and compare patterns of dispersal larviparous and pueriparous fire salamanders. This study was performed at a local scale (1-km transects) and in sites showing favourable environmental conditions for fire salamanders. Two objectives were addressed:

- to compare patterns of fine-scale genetic structure and indirectly, of dispersal, between individuals exhibiting distinct reproductive modes (larviparity or pueriparity);
- to examine sex-specific differences in dispersal between males and females.

This chapter was published in a SCI journal:

- Lourenço A, Antunes B, Wang IJ, Velo-Antón G (2018) Fine-scale genetic structure in a salamander with two reproductive modes: does reproductive mode affect dispersal? *Evolutionary Ecology*, **32**, 699-732.

In chapter 4, I employed a comparative landscape genetics framework to compare patterns of genetic connectivity between larviparous and pueriparous populations sampled in two analogous landscape plots. Two objectives were addressed:

- to characterize and evaluate differences in patterns of genetic diversity and structure between pueriparous and larviparous populations;
- to identify the environmental variables governing genetic connectivity in populations exhibiting different reproductive strategies.

This chapter was published in a SCI journal:

Lourenço A, Gonçalves J, Carvalho F, Wang IJ, Velo-Antón G (2019) Comparative landscape genetics reveals the evolution of viviparity reduces genetic connectivity in fire salamanders. *Molecular Ecology*, **28**, 4573–4591.

The results obtained in chapters 2-4 are summarized in a general discussion (chapter 5). In chapter 5, I also discuss how these findings contribute to a better understanding of the eco-evolutionary implications arising from transitions in reproductive modes, ending this chapter by highlighting future avenues of research in this topic. Finally, chapter 6 displays all supplementary information associated with Chapters 2-4. I have also included a paper (Álvarez *et al.* 2015) co-authored by me to complement chapter 2 (Appendix D).

1.6 - References

Adriaensen F, Chardon JP, De Blust G *et al.* (2003) The application of “least-cost” modelling as a functional landscape model. *Landscape and Urban Planning*, **64**, 233–247.

Aitken SN, Whitlock MC (2013) Assisted gene flow to facilitate local adaptation to climate change. *Annual Review of Ecology, Evolution, and Systematics*, **44**, 367-388.

Alarcón-Ríos L, Nicieza AG, Kaliontzopoulou A, Buckley D, Velo-Antón G (2019) Evolutionary history and not heterochronic modifications associated with viviparity drive head shape differentiation in a reproductive polymorphic species, *Salamandra salamandra*. *Evolutionary Biology*. doi: https://doi.org/10.1007/s11692-019-09489-3

Alarcón-Ríos L, Velo-Antón G, Kaliontzopoulou A (2017) A non-invasive geometric morphometrics method for exploring variation in dorsal head shape in urodeles: sexual dimorphism and geographic variation in *Salamandra salamandra*. *Journal of Morphology*, **278**, 475–485.

Alcobendas M, Castanet J (2000) Bone growth plasticity among populations of *Salamandra salamandra*: interactions between internal and external factors. *Herpetologica*, **56**, 14–26.

Allendorf FW (2017) Genetics and the conservation of natural populations: allozymes to genomes. *Molecular Ecology*, **26**, 420–430.

Álvarez D, Lourenço A, Oro D, Velo-Antón G (2015) Assessment of census (*N*) and effective population size (*Ne*) reveals consistency of *Ne* single-sample estimators and a high *Ne*/*N* ratio in an urban and isolated population of fire salamanders. *Conservation Genetics Resources*, **7**, 705–712.

Amigo J, Rodríguez-Guitián MA, Honrado JJP, Alves P (2017) The lowlands and midlands of northwestern Atlantic Iberia. In: *The vegetation of the Iberian Peninsula, vol 1* (ed. Loidi J), pp 191-250. Springer, Switzerland.

AmphibiaWeb (2018) Information on amphibian biology and conservation. Berkeley, California: AmphibiaWeb. Available: https://amphibiaweb.org/ (accessed 04-06-2018).

Anderson CD, Epperson BK, Fortin MJ *et al.* (2010) Considering spatial and temporal scale in landscape-genetic studies of gene flow. *Molecular Ecology*, **19**, 3565–3575.

Antunes B, Lourenço A, Caeiro-Dias G *et al.* (2018) Combining phylogeography and landscape genetics to infer the evolutionary history of a short-range Mediterranean relict, *Salamandra salamandra longirostris*. *Conservation Genetics*, **19**, 1411–1424.

Arnold SJ (1987) The comparative ethology of courtship in salamandrid salamanders. 1. *Salamandra and Chioglossa*. *Ethology*, **74**, 133-145.

Arntzen JW, Abrahams C, Meilink WRM, Iosif R, Zuiderwijk A (2017) Amphibian decline, pond loss and reduced population connectivity under agricultural intensification over a 38 year period. *Biodiversity and Conservation*, **26**, 1411–1430.

Baguette M, Blanchet S, Legrand D, Stevens VM, Turlure C (2013) Individual dispersal, landscape connectivity and ecological networks. *Biological Reviews*, **88**, 310–326.

Baguette M, Legrand D, Stevens VM (2015) An individual-centered framework for unravelling genotype-phenotype interactions. *Trends in Ecology and* Evolution, **30**, 709-710.

Balkenhol N, Cushman S, Storfer A, Waits L (2015) Introduction to landscape genetics – concepts, methods, applications. In: *Landscape genetics: concepts, methods, applications* (eds Balkenhol N, Cushman S, Storfer A, Waits L), pp 1-8. John Wiley & Sons Ltd, United Kingdom.

Banet AI, Svendsen JC, Eng KJ, Reznick DN (2016) Linking reproduction, locomotion, and habitat use in the Trinidadian guppy (*Poecilia reticulata*). *Oecologia*, **181**, 87–96.

Banks SC, Peakall R (2012) Genetic spatial autocorrelation can readily detect sex-biased dispersal. *Molecular* Ecology, **21**, 2092–2105.

Bartáková V, Reichard M, Blažek R, Polačik M, Bryja J (2015) Terrestrial fishes: rivers are barriers to gene flow in annual fishes from the African savanna. *Journal of Biogeography*, **42**, 1832-1844.

Beaumont MA, Rannala B (2004) The Bayesian revolution in genetics. *Nature Reviews Genetics*, **5**, 251–261.

Beerli P (2009) How to use MIGRATE or why are Markov chain Monte Carlo programs difficult to use? In: *Population genetics for animal conservation* (eds Bertorelle G, Bruford MW, Hauffe HC, Rizzoli A, Vernesi C), pp 42-79. Cambridge Univeristy Press, Cambridge.

Beerli P, Felsenstein J (2001) Maximum likelihood estimation of a migration matrix and effective population sizes in n subpopulations by using a coalescent approach. *Proceedings of the National Academy of Sciences*, **98**, 4563–4568.

Beja-Pereira A, Oliveira R, Alves PC, Schwartz MK, Luikart G (2009) Advancing ecological understandings through technological transformations in noninvasive genetics. *Molecular Ecology Resources*, **9**, 1279–1301.

Beukema W, De Pous P, Donaire D, Escoriza D, Gogaerts S, Toxopeus AG, de Bie CAJM, Roca J, Carranza S (2010) Biogeography and contemporary climatic differentiation among Moroccan *Salamandra algira*. *Biological Journal of the Linnean Society*, **101**, 626–641.

Beukema W, Nicieza AG, Lourenço A, Velo-Antón G (2016a) Colour polymorphism in *Salamandra salamandra* (Amphibia: Urodela), revealed by a lack of genetic and environmental differentiation between distinct phenotypes. *Journal of Zoological Systematics and Evolutionary Research*, **54**, 127–136.

Beukema W, Speybroeck J, Velo-Antón G (2016b) *Salamandra*. *Current Biology*, **26**, R696–R697.

Bi K, Linderoth T, Singhal S *et al.* (2019) Temporal genomic contrasts reveal rapid evolutionary responses in an alpine mammal during recent climate change. *PLoS Genetics*, **15**, e1008119.

Blackburn DG (1999). Viviparity and oviparity: evolution and reproductive strategies. In: *Encyclopedia of Reproduction Vol. 4* (eds Knobil TE, Neill JD), pp. 994-1003. London Academic Press.

Blackburn DG (2005) Evolutionary origins of viviparity in fishes. In: *Viviparous fishes* (eds Grier J and Uribe MC), pp. 287-301. New Life Publications, Homestead, Florida.

Blackburn DG (2015) Evolution of vertebrate viviparity and specializations for fetal nutrition: a quantitative and qualitative analysis. *Journal of Morphology*, **276**, 961–990.

Blackburn DG, Starck JM (2015) Morphological specializations for fetal maintenance in viviparous vertebrates: an introduction and historical retrospective. *Journal of Morphology*, **276**, E1-E16.

Blair C, Weigel DE, Balazik M *et al.* (2012) A simulation-based evaluation of methods for inferring linear barriers to gene flow. *Molecular Ecology Resources*, **12**, 822–833.

Bletz MC, Goedbloed DJ, Sanchez E *et al.* (2016) Amphibian gut microbiota shifts differentially in community structure but converges on habitat-specific predicted functions. *Nature Communications*, **7**, 13699.

Blyton MDJ, Banks SC, Peakall R (2015) The effect of sex-biased dispersal on opposite-sexed spatial genetic structure and inbreeding risk. *Molecular Ecology*, **24**, 1681–1695.

Bonnet X, Naulleau G, Shine R (1999) The dangers of leaving home: dispersal and mortality in snakes. *Biological Conservation*, **89**, 39–50.

Bonte D, van Dyck H, Bullock JM *et al.* (2012) Costs of dispersal. *Biological Reviews*, **87**, 290–312.

Botta F, Eriksen C, Fontaine MC, Guillot G (2015) Enhanced computational methods for quantifying the effect of geographic and environmental isolation on genetic differentiation. *Methods in Ecology and Evolution*, **6**, 1270–1277.

Bowler DE, Benton TG (2005) Causes and consequences of animal dispersal strategies: relating individual behaviour to spatial dynamics *Biological Reviews*, **80**, 205–225.

Bowler DE, Benton TG (2009) Variation in dispersal mortality and dispersal propensity among individuals: the effects of age, sex and resource availability. *Journal of Animal Ecology,* **78**, 1234-1241.

Bradburd GS, Ralph PL, Coop GM (2013) Disentangling the effects of geographic and ecological isolation on genetic differentiation. *Evolution*, **67**, 3258–3273.

Brandley MC, Young RL, Warren DL, Thompson MB, Wagner GP (2012) Uterine gene expression in the live-bearing lizard, *Chalcides ocellatus*, reveals convergence of squamate reptile and mammalian pregnancy mechanisms. *Genome Biology and Evolution*, **4**, 394–411.

Broquet T, Petit EJ (2009) Molecular estimation of dispersal for ecology and population genetics. *Annual Review of Ecology, Evolution, and Systematics*, **40**, 193–216.

Buckley D (2012) Evolution of viviparity in salamanders (Amphibia, Caudata). In: *eLS*. Wiley, Chichester. doi:10.1002/9780470015902.a0022851

Buckley D, Alcobendas M, García-París M, Wake MH (2007) Heterochrony, cannibalism, and the evolution of viviparity in *Salamandra salamandra*. *Evolution and Development*, **9**, 105–115.

Burgess SC, Baskett ML, Grosberg RK, Morgan SG, Strathmann RR (2016) When is dispersal for dispersal? Unifying marine and terrestrial perspectives. *Biological Reviews*, **91**, 867–882.

Burkhart JJ, Peterman WE, Brocato ER *et al.* (2017) The influence of breeding phenology on the genetic structure of four pond-breeding salamanders. *Ecology and Evolution*, **7**, 4670–4681.

Campos JC (2018) *Landscape connectivity and remote sensing applications for assessing biodiversity patterns in desert environments* (Doctoral dissertation). Retrieved from Repositório Aberto da Universidade do Porto (Accession No. 101569262).

Carvalho F, Lourenço A, Carvalho R, Alves PC, Mira A, Beja P (2018) The effects of a motorway on movement behaviour and gene flow in a forest carnivore: joint evidence from road mortality, radio tracking and genetics. *Landscape and Urban Planning*, **178**, 217–227.

Caspers BA, Krause ET, Hendrix R *et al.* (2014) The more the better - polyandry and genetic similarity are positively linked to reproductive success in a natural population of terrestrial salamanders (*Salamandra salamandra*). *Molecular Ecology*, **23**, 239–250.

Caspers BA, Steinfartz S (2011) Preference for the other sex: olfactory sex recognition in terrestrial fire salamanders (*Salamandra salamandra*). *Amphibia-Reptilia*, **32**, 503–508.

Castillo JA, Epps CW, Davis AR, Cushman SA (2014) Landscape effects on gene flow for a climate-sensitive montane species, the American pika. *Molecular Ecology*, **23**, 843–856.

Catenazzi A (2016) Ecological implications of metabolic compensation at low temperatures in salamanders. *PeerJ*, **4**, e2072.

Caye K, Deist TM, Martins H, Michel O, François O (2016) TESS3: fast inference of spatial population structure and genome scans for selection. *Molecular Ecology Resources*, **16**, 540–548.

Cayuela H, Rougemont Q, Prunier JG *et al.* (2018) Demographic and genetic approaches to study dispersal in wild animal populations: A methodological review. *Molecular Ecology*, **27**, 3976–4010.

Christie MR (2013) Bayesian parentage analysis reliably controls the number of false assignments in natural populations. *Molecular Ecology*, **22**, 5731–5737.

Christie MR, Meirmans PG, Gaggiotti OE, Toonen RJ, White C (2017) Disentangling the relative merits and disadvantages of parentage analysis and assignment tests for inferring population connectivity. *ICES Journal of Marine Science*, **74**, 1749–1762.

Clark RW, Brown WS, Stechert R, Zamudio KR (2010) Roads, interrupted dispersal, and genetic diversity in timber rattlesnakes. *Conservation Biology*, **24**, 1059–1069.

Clarke RT, Rothery P, Raybould AF (2002) Confidence limits for regression relationships between distance matrices: estimating gene flow with distance. *Journal of Agricultural, Biological, and Environmental Statistics*, **7**, 361–372.

Cleary KA, Waits LP, Finegan B (2017) Comparative landscape genetics of two frugivorous bats in a biological corridor undergoing agricultural intensification. *Molecular Ecology*, **26**, 4603–4617.

Clobert J, Baguette M, Benton TG, Bullock JM (2012) *Dispersal ecology and evolution.* Oxford University Press, Oxford.

Clobert J, Le Galliard JF, Cote J, Meylan S, Massot M (2009) Informed dispersal, heterogeneity in animal dispersal syndromes and the dynamics of spatially structured populations. *Ecology Letters*, **12**, 197–209.

Cordero-Rivera A, Velo-Antón G, Galán P (2007) Ecology of amphibians in small coastal Holocene islands: local adaptations and the effect of exotic tree plantations. *Munibe*, **25**, 94–103.

Cosgrove AJ, McWhorter TJ, Maron M (2018) Consequences of impediments to animal movements at different scales: a conceptual framework and review. *Diversity and Distributions*, **24**, 448–459.

Cote J, Bestion E, Jacob S, Travis J, Legrand D, Baguette M (2017a) Evolution of dispersal strategies and dispersal syndromes in fragmented landscapes. *Ecography*, **40**, 56–73.

Cote J, Bocedi G, Debeffe L *et al.* (2017b) Behavioural synchronization of large-scale animal movements – disperse alone, but migrate together? *Biological Reviews*, **92**, 1275–1296.

Cote J, Clobert J, Brodin T, Fogarty S, Sih A (2010) Personality-dependent dispersal: characterization, ontogeny and consequences for spatially structured populations. *Philosophical Transactions of the Royal Society B: Biological Sciences*, **365**, 4065-4076.

Crump ML (2015) Anuran reproductive modes: evolving perspectives. *Journal of Herpetology*, **49**, 1–16.

Cushman SA (2006) Effects of habitat loss and fragmentation on amphibians: a review and prospectus. *Biological Conservation*, **128**, 231-240.

Cushman SA, Lewis JS (2010) Movement behavior explains genetic differentiation in American black bears. *Landscape Ecology*, **25**, 1613–1625.

Cushman SA, McKelvey KS, Hayden J, Schwartz MK (2006) Gene flow in complex landscapes: testing multiple hypotheses with causal modeling. *The American Naturalist*, **168**, 486–499.

De Meester N, Bonte D (2010) Information use and density-dependent emigration in an agrobiont spider. *Behavioral Ecology*, **21**, 992–998.

Denton RD, Greenwald KR, Gibbs HL (2017) Locomotor endurance predicts differences in realized dispersal between sympatric sexual and unisexual salamanders. *Functional Ecology*, **31**, 915–926.

DiLeo MF, Wagner HH (2016) A landscape ecologist's agenda for landscape genetics. *Current Landscape Ecology Reports*, **1**, 115-126.

Dinis M, Merabet K, Martínez-freiría F *et al.* (2019) Allopatric diversification and evolutionary melting pot in a North African Palearctic relict: the biogeographic history of *Salamandra algira*. *Molecular Phylogenetics and Evolution*, **130**, 81–91.

Dinis M, Velo-Antón G (2017) How little do we know about the reproductive mode in the north African salamander, *Salamandra algira*? Pueriparity in divergent mitochondrial lineages of *S. a. tingitana*. *Amphibia-Reptilia*, **38**, 540–546.

Driscoll DA, Banks SC, Barton PS *et al.* (2014) The trajectory of dispersal research in conservation biology. Systematic review. *PLoS ONE*, **9**, e95053.

Driscoll DA, Banks SC, Barton PS, Lindenmayer DB, Smith AL (2013) Conceptual domain of the matrix in fragmented landscapes. *Trends in Ecology and Evolution*, **28**, 605–613.

Dudaniec RY, Worthington Wilmer J, Hanson JO, Warren M, Bell S, Rhodes JR (2016) Dealing with uncertainty in landscape genetic resistance models: A case of three co-occurring marsupials. *Molecular Ecology*, **25**, 470–486.

Duputié A, Massol F (2013) An empiricist's guide to theoretical predictions on the evolution of dispersal. *Interface Focus*, **3**, 20130028.

Duryea MC, Zamudio KR, Brasileiro CA (2015) Vicariance and marine migration in continental island populations of a frog endemic to the Atlantic Coastal forest. *Heredity*, **115**, 225–234.

Dyer RJ (2015a) Is there such a thing as landscape genetics? *Molecular Ecology*, **24**, 3518–3528.

Dyer RJ (2015b) Population graphs and landscape Genetics. *Annual Review of Ecology, Evolution, and Systematics*, **46**, 327–342.

Ellegren H, Galtier N (2016) Determinants of genetic diversity. *Nature Reviews Genetics*, **17**, 422-433.

Epps CW, Keyghobadi N (2015) Landscape genetics in a changing world: disentangling historical and contemporary influences and inferring change. *Molecular Ecology*, **24**, 6021–6040.

Epps CW, Wasser SK, Keim JL, Mutayoba BM, Brashares JS (2013) Quantifying past and present connectivity illuminates a rapidly changing landscape for the African elephant. *Molecular Ecology*, **22**, 1574–1588.

Escoriza D, Comas MM, Donaire D, Carranza S (2006) Rediscovery of *Salamandra algira* Bedriaga, 1833 from the Beni Snassen massif (Morocco) and phylogenetic relationships of North African *Salamandra*. *Amphibia-Reptilia*, **27**, 448-455.

Etherington TR (2016) Least-cost modelling and landscape ecology: concepts, applications, and opportunities. *Current Landscape Ecology Reports*, **1**, 40–53.

Excoffier L, Ray N (2008) Surfing during population expansions promotes genetic revolutions and structuration. *Trends in Ecology and Evolution*, **23**, 347-351.

Fahrig L (2007) Non-optimal animal movement in human-altered landscapes. *Functional Ecology*, **21**, 1003–1015.

Faubet P, Waples R, Gaggiotti OE (2007) Evaluating the performance of a multilocus Bayesian method for the estimation of migration rates. *Molecular Ecology*, **16**, 1149–1166.

Feldman A, Bauer AM, Castro-Herrera F *et al.* (2015) The geography of snake reproductive mode: a global analysis of the evolution of snake viviparity. *Global Ecology and Biogeography*, **24**, 1433–1442.

Fernández JB, Kubisch EL, Ibargüengoytía NR (2017) Viviparity advantages in the lizard *Liolaemus sarmientoi* from the end of the world. *Evolutionary Biology*, **44**, 325–338.

Ferrier S, Manion G, Elith J, Richardson K (2007) Using generalized dissimilarity modelling to analyse and predict patterns of beta diversity in regional biodiversity assessment. *Diversity and Distributions*, **13**, 252–264.

Ficetola GF, Manenti R, De Bernardi F, Padoa-Schioppa E (2012) Can patterns of spatial autocorrelation reveal population processes? An analysis with the fire salamander. *Ecography*, **35**, 693–703.

Fischer J, Lindenmayer DB (2007) Landscape modification and habitat fragmentation: a synthesis. *Global Ecology and Biogeography*, **16**, 265–280.

Frankham R (2005) Genetics and extinction. *Biological Conservation*, **126**, 131–140.

Frankham R (2015) Genetic rescue of small inbred populations: meta-analysis reveals large and consistent benefits of gene flow. *Molecular Ecology*, **24**, 2610–2618.

Frantz AC, Cellina S, Krier A, Schley L, Burke T (2009) Using spatial Bayesian methods to determine the genetic structure of a continuously distributed population: clusters or isolation by distance? *Journal of Applied Ecology*, **46**, 493–505.

Galán P (2007) Viviparismo y distribución de *Salamandra salamandra bernardezi* en el norte de Galicia. *Boletín de la Asociación Herpetológica Española*, **18**, 44–49.

Galpern P, Manseau M (2013) Finding the functional grain: comparing methods for scaling resistance surfaces. *Landscape Ecology*, **28**, 1269–1281.

Gao W, Sun Y-B, Zhou W-W *et al.* (2019) Genomic and transcriptomic investigations of the evolutionary transition from oviparity to viviparity. *Proceedings of the National Academy of Sciences*, **116**, 3646–3655.

Garcia VOS, Ivy C, Fu J (2017) Syntopic frogs reveal different patterns of interaction with the landscape: a comparative landscape genetic study of *Pelophylax nigromaculatus* and *Fejervarya limnocharis* from central China. *Ecology and Evolution*, **7**, 9294–9306.

García-París M, Alcobendas M, Buckley D, Wake D (2003) Dispersal of viviparity across contact zones in Iberian populations of Fire salamanders (*Salamandra*) inferred from discordance of genetic and morphological traits. *Evolution*, **57**, 129–143.

García-París M, Montori A, Herrero P (2004) *Fauna Ibérica. Vol. 24. Amphibia, Lissamphibia*. Museo Nacional de Ciencias Naturales y Consejo Superior de Investigaciones Científicas, Madrid.

Goin OB, Goin CJ (1962) Amphibian eggs and the montane environment. *Evolution*, **16**, 364–371.

Goldberg CS, Waits LP (2010) Quantification and reduction of bias from sampling larvae to infer population and landscape genetic structure. *Molecular Ecology Resources*, **10**, 304-313.

Gomez-Mestre I, Pyron RA, Wiens JJ (2012) Phylogenetic analyses reveal unexpected patterns in the evolution of reproductive modes in frogs. *Evolution*, **66**, 3687–3700.

Grant AH, Liebgold EB (2017) Color-biased dispersal inferred by fine-scale genetic spatial autocorrelation in a color polymorphic salamander. *Journal of* Heredity, **108**, 588–593.

Graves TA, Beier P, Royle JA (2013) Current approaches using genetic distances produce poor estimates of landscape resistance to interindividual dispersal. *Molecular Ecology*, **22**, 3888–3903.

Greven H (2003) Larviparity and pueriparity. In: *Reproductive Biology and Phylogeny of Urodela* (eds. Jamieson BGM, Sever DM), pp 447-475. Science Publishers. Enfield, NH, USA.

Guiberteau DF, Váquez Graña R, López JE (2012) Variabilidad de patrones y pigmentación en *Salamandra salamandra galaica*. *Butlletí de la Societat Catalana d'Herpetologia*, **20**, 115-120.

Guillot G, Rousset F (2013) Dismantling the Mantel tests. *Methods in Ecology and Evolution*, **4**, 336–344.

Gunderson DR (1997) Trade-off between reproductive effort and adult survival in oviparous and viviparous fishes. *Canadian Journal of Fisheries and Aquatic Sciences*, **54**, 990–998.

Gurarie E, Fleming CH, Fagan WF, Laidre KL, Hernández-Pliego J, Ovaskainen O (2017) Correlated velocity models as a fundamental unit of animal movement: synthesis and applications. *Movement Ecology*, **5**, 13.

Gutiérrez-Rodríguez J, Gonçalves J, Civantos E, Martínez-Solano I (2017) Comparative landscape genetics of pond-breeding amphibians in Mediterranean temporal wetlands: the positive role of structural heterogeneity in promoting gene flow. *Molecular Ecology*, **26**, 5407–5420.

Haag CR, Saastamoinen M, Marden JH, Hanski I (2005) A candidate locus for variation in dispersal rate in a butterfly metapopulation. *Proceedings of the Royal Society B*, **272**, 2449–2456.

Habel JC, Schmitt T (2018) Vanishing of the common species: empty habitats and the role of genetic diversity. *Biological Conservation*, **218**, 211-216.

Haddad CFB, Prado CPA (2005) Reproductive modes in frogs and their unexpected diversity in the Atlantic Forest of Brazil. *BioScience*, **55**, 207.

Haddad NM, Brudvig LA, Clobert J *et al.* (2015) Habitat fragmentation and its lasting impact on Earth's ecosystems. *Science Advances*, **1**, e1500052.

Hadrys H, Balick M, Schierwater B (1992) Applications of random amplified polymorphic DNA (RAPD) in molecular ecology. *Molecular Ecology*, **1**, 55-63.

Hale ML, Burg TM, Steeves, TE (2012) Sampling for microsatellite-based population genetic studies: 25 to 30 individuals per population is enough to accurately estimate allele frequencies. *PloS ONE*, **7**, e45170.

Hall LA, Beissinger SR (2014) A practical toolbox for design and analysis of landscape genetics studies. *Landscape Ecology*, **29**, 1487–1504.

Hall LA, Palsbøll PJ, Beissinger SR *et al.* (2009). Characterizing dispersal patterns in a threatened seabird with limited genetic structure. *Molecular Ecology*, **18**, 5074-5085.

Halliwell B, Uller T, Holland BR, While GM (2017) Live bearing promotes the evolution of sociality in reptiles. *Nature Communications*, **8**, 2030.

Hand BK, Muhlfeld CC, Wade AA *et al.* (2016) Climate variables explain neutral and adaptive variation within salmonid metapopulations: the importance of replication in landscape genetics. *Molecular Ecology*, **25**, 689–705.

Handley LJL, Perrin N (2007) Advances in our understanding of mammalian sex-biased dispersal. *Molecular Ecology*, **16**, 1559–1578.

Hanski I, Schulz T, Wong SC, Ahola V, Ruokolainen A, Ojanen SP (2017) Ecological and genetic basis of metapopulation persistence of the Glanville fritillary butterfly in fragmented landscapes. *Nature Communications*, **8**, 14504.

Hedrick PW, Garcia-Dorado A (2016) Understanding inbreeding depression, purging, and genetic rescue. *Trends in Ecology and Evolution*, **31**, 940-952.

Hein AM, Hou C, Gillooly JF (2012) Energetic and biomechanical constraints on animal migration distance. *Ecology Letters*, **15**, 104-110.

Helfer V, Broquet T, Fumagalli L (2012) Sex-specific estimates of dispersal show female philopatry and male dispersal in a promiscuous amphibian, the alpine salamander (*Salamandra atra*). *Molecular Ecology*, **21**, 4706–4720.

Helmstetter AJ, Papadopulos AST, Igea J, van Dooren TJM, Leroi AM, Savolainen V (2016) Viviparity stimulates diversification in an order of fish. *Nature Communications*, **7**, 11271.

Hemming-Schroeder E, Lo E, Salazar C, Puente S, Yan G (2018) Landscape genetics: A toolbox for studying vector-borne diseases. *Frontiers in Ecology and Evolution*, **6**, 21.

Hendrix R, Schmidt BR, Schaub M, Krause ET, Steinfartz S (2017) Differentiation of movement behaviour in an adaptively diverging salamander population. *Molecular Ecology*, **26**, 6400–6413.

Hey J, Chung Y, Sethuraman A (2015) On the occurrence of false positives in tests of migration under an isolation with migration model. *Molecular Ecology*, **24**, 5078–5083.

Hey J, Nielsen R (2007) Integration within the Felsenstein equation for improved Markov chain Monte Carlo methods in population genetics. *Proceedings of the National Academy of Sciences*, **104**, 2785–2790.

Hillman SS, Drewes RC, Hedrick MS, Hancock TV (2014) Physiological vagility: correlations with dispersal and population genetic structure of amphibians. *Physiological and Biochemical Zoology*, **87**, 105–112.

Iglesias-Carrasco M, Martín J, Cabido C (2017) Urban habitats can affect body size and body condition but not immune response in amphibians. *Urban Ecosystems*, **20**, 1331–1338.

Jackson ND, Fahrig L (2016) Habitat amount, not habitat configuration, best predicts population genetic structure in fragmented landscapes. *Landscape Ecology*, **31**, 951–968.

Jeltsch F, Bonte D, Reineking B *et al.* (2013) Integrating movement ecology with biodiversity. *Movement Ecology*, **1**, 6.

Jenkins DG, Brescacin CR, Duxbury CV *et al.* (2007) Does size matter for dispersal distance? *Global Ecology and Biogeography*, **16**, 415–425.

Jha S (2015) Contemporary human-altered landscapes and oceanic barriers reduce bumble bee gene flow. *Molecular Ecology*, **24**, 993-1006.

Jiménez-Robles O, Guayasamin JM, Ron SR, De la Riva I (2017) Reproductive traits associated with species turnover of amphibians in Amazonia and its Andean slopes. *Ecology and Evolution*, **7**, 2489–2500.

Joger U, Steinfartz S (1995) Protein electrophoretic data on taxonomic problems in East Mediterranean *Salamandra* (Urodela: Salamandridae). In: *Scientia Herpetologica* (eds Llorente GA, Montori A, Santos X, Carretero MA), pp. 33-36. Barcelona.

Jombart T, Devillard S, Balloux F (2010) Discriminant analysis of principal components: a new method for the analysis of genetically structured populations. *BMC Genetics*, **11**, 94.

Jones AG, Small CM, Paczolt KA, Ratterman NL (2010) A practical guide to methods of parentage analysis. *Molecular Ecology Resources*, **10**, 6–30.

Jones OR, Wang J (2010) COLONY: A program for parentage and sibship inference from multilocus genotype data. *Molecular Ecology Resources*, **10**, 551–555.

Kane NC, King MG (2009) Using parentage analysis to examine gene flow and spatial genetic structure. *Molecular Ecology*, **18**, 1551–1552.

Kays R, Crofoot MC, Jetz W, Wikelski M (2015) Terrestrial animal tracking as an eye on life and planet. *Science*, **348**, aaa2478.

Keeley ATH, Beier P, Keeley BW, Fagan ME (2017) Habitat suitability is a poor proxy for landscape connectivity during dispersal and mating movements. *Landscape and Urban Planning*, **161**, 90–102.

Kieren S, Sparreboom M, Hochkirch A, Veith M (2018) A biogeographic and ecological perspective to the evolution of reproductive behaviour in the family Salamandridae. *Molecular Phylogenetics and Evolution*, **121**, 98–109.

Kierepka EM, Latch EK (2014) Performance of partial statistics in individual-based landscape genetics. *Molecular Ecology Resources*, **15**, 512–525.

Kool JT, Moilanen A, Treml EA (2013) Population connectivity: recent advances and new perspectives. *Landscape Ecology*, **28**, 165–185.

Kuzmin S, Papenfuss T, Sparreboom M *et al.* (2009). *Salamandra salamandra*. In: *The IUCN Red List of Threatened Species 2009*.

LaPoint S, Balkenhol N, Hale J, Sadler J, van der Ree R (2015) Ecological connectivity research in urban areas. *Functional Ecology*, **29**, 868–878.

Landguth EL, Cushman SA, Schwartz MK, McKelvey KS, Murphy M, Luikart G (2010) Quantifying the lag time to detect barriers in landscape genetics. *Molecular Ecology*, **19**, 4179–4191.

Landguth EL, Fedy BC, Oyler-McCance SJ *et al.* (2012) Effects of sample size, number of markers, and allelic richness on the detection of spatial genetic pattern. *Molecular Ecology Resources*, **12**, 276–284.

Ledbetter NM, Bonett RM (2019) Terrestriality constrains salamander limb diversification: implications for the evolution of pentadactyly. *Journal of Evolutionary Biology*. https://doi.org/10.1111/jeb.13444

Liedtke HC, Müller H, Hafner J, Penner J, Gower DJ, Mazuch T, Rödel M-O, Loader SP (2017) Terrestrial reproduction as an adaptation to steep terrain in African toads. *Proceedings of the Royal Society* B, **284**, 20162598.

Lion MB, Mazzochini GG, Garda AA *et al.* (2019) Global patterns of terrestriality in amphibian reproduction. *Global Ecology and Biogeography*, **28**, 744–756.

Losos JB (2010) Adaptive Radiation, ecological opportunity, and evolutionary determinism. *The American Naturalist*, **175**, 623–639.

Lowe WH, McPeek MA (2014) Is dispersal neutral? *Trends in Ecology and Evolution*, **29**, 444–450.

Lourenço A, Sequeira F, Buckley D, Velo-Antón G (2018) Role of colonization history and species-specific traits on contemporary genetic variation of two salamander species in a Holocene island-mainland system. *Journal of Biogeography*, **45**, 1054–1066.

Lynch VJ, Nnamani MC, Kapusta A *et al.* (2015) Ancient transposable elements transformed the uterine regulatory landscape and transcriptome during the evolution of mammalian pregnancy. *Cell Reports*, **10**, 551–562.

Ma L, Buckley LB, Huey RB, Du W-G (2018) A global test of the cold-climate hypothesis for the evolution of viviparity of squamate reptiles. *Global Ecology and Biogeography*, **27**, 679–689.

Manel S, Gaggiotti OE, Waples RS (2005). Assignment methods: matching biological questions with appropriate techniques. *Trends in Ecology and Evolution*, **20**, 136-142.

Manel S, Holderegger R (2013) Ten years of landscape genetics. *Trends in Ecology and Evolution*, **28**, 614–621.

Manel S, Schwartz MK, Luikart G, Taberlet P (2003) Landscape genetics: combining landscape ecology and population genetics. *Trends in Ecology and Evolution*, **18**, 189–197.

Mantel N (1967) The detection of disease clustering and a generalized regression approach. *Cancer Research*, **27**, 209–220.

Matthysen E (2012) Multicausality of dispersal: a review. In: *Dispersal ecology and evolution* (eds Clobert J, Baguette J, Benton TG, Bullock JM), pp. 3-40. Oxford University Press, Oxford.

McRae BH (2006) Isolation by resistance. *Evolution*, **60**, 1551–1561.

McRae BH, Beier P (2007) Circuit theory predicts gene flow in plant and animal populations. *Proceedings of the National Academy of Sciences*, **104**, 19885–19890.

McRae BH, Dickson BG, Keitt TH, Shah VB (2008). Using circuit theory to model connectivity in ecology, evolution, and conservation. *Ecology*, **89**, 2712-2724.

Measey GJ, Galbusera P, Breyne P, Matthysen E (2007) Gene flow in a direct-developing, leaf litter frog between isolated mountains in the Taita Hills, Kenya. *Conservation Genetics*, **8**, 1177–1188.

Meirmans PG (2012) The trouble with isolation by distance. *Molecular Ecology*, **21**, 2839–2846.

Meirmans PG, Hedrick PW (2011) Assessing population structure: F_{ST} and related measures. *Molecular Ecology Resources*, **11**, 5–18.

Meyer A, Lydeard C (1993) The evolution of copulatory organs, internal fertilization, placentae and viviparity in killifishes (Cyprinodontiformes) inferred from a DNA phylogeny of the tyrosine kinase gene *X-src*. *Proceedings of Royal Society London B*, **254**, 153–162.

Micheletti SJ, Storfer A (2017) An approach for identifying cryptic barriers to gene flow that limit species' geographic ranges. *Molecular Ecology*, **26**, 490–504.

Millspaugh JJ, Marzluff JM (2001) *Radio tracking and animal populations*. Academic Press, Washington.

Moore JA, Draheim HM, Etter D, Winterstein S, Scribner KT (2014) Application of large-scale parentage analysis for investigating natal dispersal in highly vagile vertebrates: a case study of American black bears (*Ursus americanus*). *PLoS ONE*, **9**, e91168.

Murphy MA, Dezzani R, Pilliod DS, Storfer A (2010). Landscape genetics of high mountain frog metapopulations. *Molecular Ecology*, **19**, 3634–3649.

Murphy MA, Evans JS (2011) Genetic patterns as a function of landscape process: applications of neutral genetic markers for predictive modeling in landscape ecology. In: *Predictive species and habitat modeling in Landscape Ecology* (eds Drew CA, Wiersma Y, Huettmann F), pp 161-188. Springer, New York, NY.

Murphy BF, Thompson MB (2011) A review of the evolution of viviparity in squamate reptiles: The past, present and future role of molecular biology and genomics. *Journal of Comparative Physiology B: Biochemical, Systemic, and Environmental Physiology*, **181**, 575–594.

Neigel JE (1997) A comparison of alternative strategies for estimating gene flow from genetic markers. *Annual Review in Ecology and Systematics*, **28**, 105-128.

Nielsen R, Wakeley J (2001) Distinguishing migration from isolation: a Markov chain Monte Carlo approach. *Genetics*, **158**, 885-896.

Noguerales V, Cordero PJ, Ortego J (2016) Hierarchical genetic structure shaped by topography in a narrow-endemic montane grasshopper. *BMC Evolutionary Biology*, **16**, 96.

Nosil P, Vines TH, Funk DJ (2005) Reproductive isolation by natural selection against immigrants from divergent habitats. *Evolution*, **59**, 705–719.

Nuñez TA, Lawler JJ, McRae BH *et al.* (2013) Connectivity planning to address climate change. *Conservation Biology*, **27**, 407-416.

Orsini L, Vanoverbeke J, Swillen I, Mergeay J, De Meester L (2013) Drivers of population genetic differentiation in the wild: isolation by dispersal limitation, isolation by adaptation and isolation by colonization. *Molecular Ecology*, **22**, 5983–5999.

Oyler-McCance SJ, Fedy BC, Landguth EL (2013) Sample design effects in landscape genetics. *Conservation Genetics*, **14**, 275–285.

Palmer SCF, Coulon A, Travis JM (2014) Inter-individual variability in dispersal behaviours impacts connectivity estimates. *Oikos*, **123**, 923–932.

Panzacchi M, Van Moorter B, Strand O *et al.* (2016) Predicting the continuum between corridors and barriers to animal movements using Step Selection Functions and Randomized Shortest Paths. *Journal of Animal* Ecology, **85**, 32-42.

Peakall R, Smouse PE (2012) GenAlEx 6.5: genetic analysis in Excel. Population genetic software for teaching and research – an update. *Bioinformatics*, **28**, 2537–2539.

Pecl GT, Araújo MB, Bell J *et al.* (2017) Biodiversity redistribution under climate change: impacts on ecosystems and human well-being. *Science*, **355**, eaai9214.

Pelletier D, Clark M, Anderson MG, Rayfield B, Wulder MA, Cardille JA (2014) Applying circuit theory for corridor expansion and management at regional scales: tiling, pinch points, and omnidirectional connectivity. *PLoS ONE*, **9**, e84135.

Pereira RJ, Martínez-Solano I, Buckley D (2016) Hybridization during altitudinal range shifts: nuclear introgression leads to extensive cyto-nuclear discordance in the fire salamander. *Molecular Ecology*, **25**, 1551–1565.

Peterman WE (2018) ResistanceGA: An R package for the optimization of resistance surfaces using genetic algorithms. *Methods in Ecology and Evolution*, **9**, 1638–1647.

Peterson EE, Hanks EM, Hooten MB, Ver Hoef JM, Fortin M-J (2019) Spatially-structured statistical network models for landscape genetics. *Ecological Monographs*, **89**, e01355.

Petrov BP (2007) Amphibians and reptiles of Bulgaria: fauna, vertical distribution, zoogeography, and conservation. In: *Biogeography and Ecology of Bulgaria* (eds Fet V, Popov A), pp. 85-107. Springer, Dordrecht.

Pflüger FJ, Balkenhol N (2014) A plea for simultaneously considering matrix quality and local environmental conditions when analysing landscape impacts on effective dispersal. *Molecular Ecology*, **23**, 2146–2156.

Pflüger FJ, Signer J, Balkenhol N (2019) Habitat loss causes non-linear genetic erosion in specialist species. *Global Ecology and Conservation*, *17*(1), e00507.

Phillips BL, Brown GP, Webb JK, Shine R (2006) Invasion and the evolution of speed in toads. *Nature*, **439**, 803.

Pincheira-Donoso D, Jara M, Reaney A, García-Roa R, Saldarriaga-Córdoba M, Hodgson DJ (2017) Hypoxia and hypothermia as rival agents of selection driving the evolution of viviparity in lizards. *Global Ecology and Biogeography*, **26**, 1238–1246.

Pincheira-Donoso D, Tregenza T, Witt MJ, Hodgson DJ (2013) The evolution of viviparity opens opportunities for lizard radiation but drives it into a climatic cul-de-sac. *Global Ecology and Biogeography*, **22**, 857–867.

Pinho C, Hey J (2010) Divergence with gene flow: models and data. *Annual Review of Ecology, Evolution, and Systematics*, **41**, 215–230.

Pita R, Beja P, Mira A (2007) Spatial population structure of the Cabrera vole in Mediterranean farmland: the relative role of patch and matrix effects. *Biological Conservation*, **134**, 383–392.

Pittman SE, Osbourn MS, Semlitsch RD (2014) Movement ecology of amphibians: a missing component for understanding population declines. *Biological Conservation*, **169**, 44–53.

Pritchard JK, Stephens M, Donnelly P (2000) Inference of population structure using multilocus genotype data. *Genetics*, **155**, 945–959.

Proctor MF, McLellan BN, Strobeck C, Barclay RMR (2004) Gender-specific dispersal distances of grizzly bears estimated by genetic analysis. *Canadian Journal of Zoology*, **82**, 1108–1118.

Prunier JG, Kaufmann B, Léna JP, Fenet S, Pompanon F, Joly P (2014) A 40-year-old divided highway does not prevent gene flow in the alpine newt *Ichthyosaura alpestris*. *Conservation Genetics*, **15**, 453–468.

Putman AI, Carbone I (2014) Challenges in analysis and interpretation of microsatellite data for population genetic studies. *Ecology and Evolution*, **4**, 4399–4428.

Pyron RA (2015) Advancing perspectives on parity-mode evolution. *Journal of Experimental Zoology Part B: Molecular and Developmental Evolution*, **324**, 562–563.

Pyron RA, Burbrink FT (2014) Early origin of viviparity and multiple reversions to oviparity in squamate reptiles. *Ecology Letters*, **17**, 13–21.

Rayfield B, Pelletier D, Dumitru M, Cardille JA, Gonzalez A (2016) Multipurpose habitat networks for short-range and long-range connectivity: a new method combining graph and circuit connectivity. *Methods in Ecology and Evolution*, **7**, 222–231.

Rebelo R, Leclair MH (2003) Site tenacity in the terrestrial salamandrid *Salamandra salamandra*. *Journal of Herpetology*, **37**, 440–445.

Recuero E, Iraola A, Rubio X, Machordom A, García-París M (2007) Mitochondrial differentiation and biogeography of *Hyla meridionalis* (Anura: Hylidae): an unusual phylogeographical pattern. *Journal of Biogeography*, **34**, 1207-1219.

Reinhardt T, Bauldauf L, Ilić M, Fink P (2018) Cast away: drift as the main determinant for larval survival in western fire salamanders (*Salamandra salamandra*) in headwater streams. *Journal of Zoology*, **306**, 171-179.

Reis DM, Cunha RL, Patrão C, Rebelo R, Castilho R (2011) *Salamandra salamandra* (Amphibia: Caudata: Salamandridae) in Portugal: not all black and yellow. *Genetica*, **139**, 1095–1105.

Renfree MB, Suzuki S, Kaneko-Ishino T (2013) The origin and evolution of genomic imprinting and viviparity in mammals. *Philosophical Transactions of the Royal Society B*, **368**, 20120151.

Richardson JL (2012) Divergent landscape effects on population connectivity in two co-occurring amphibian species. *Molecular Ecology*, **21**, 4437–4451.

Richardson JL, Brady SP, Wang IJ, Spear SF (2016) Navigating the pitfalls and promise of landscape genetics. *Molecular Ecology*, **25**, 849–863.

Riley SPD, Pollinger JP, Sauvajot RM, York EC, Bromley C, Fuller TK,Wayne RK (2006) A southern California freeway is a physical and social barrier to gene flow in carnivores. *Molecular Ecology*, **15**, 1733–1741.

Rivera-Ortíz F, Aguilar R, Arizmendi MDC, Quesada-Avendaño M, Oyama K (2015) Habitat fragmentation and genetic variability of tetrapod populations. *Animal Conservation*, **18**, 249–258.

Robertson JM, Murphy MA, Pearl CA *et al.* (2018) Regional variation in drivers of connectivity for two frog species (*Rana pretiosa* and *R. luteiventris*) from the U.S. Pacific Northwest. *Molecular Ecology*, **27**, 3242–3256.

Rodríguez-Ramilo ST, Wang J (2012) The effect of close relatives on unsupervised Bayesian clustering algorithms in population genetic structure analysis. *Molecular Ecology Resources*, **12**, 873–884.

Rodríguez A, Burgon JD, Lyra M *et al.* (2017) Inferring the shallow phylogeny of true salamanders (*Salamandra*) by multiple phylogenomic approaches. *Molecular Phylogenetics and Evolution*, **115**, 16–26.

Ronce O (2007) How does it feel to be like a rolling stone ? *Ten questions about dispersal evolution. Annual Review of Ecology Evolution and Systematics*, **38**, 231–253.

Ronce O, Clobert J (2012) Dispersal syndromes. In: *Dispersal ecology and evolution* (eds Clobert J, Baguette J, Benton TG, Bullock JM), pp. 119-138. Oxford University Press, Oxford.

Rousset F (2012) Demographic consequences of the selective forces controlling density-dependent dispersal. In: *Dispersal ecology and evolution* (eds Clobert J, Baguette J, Benton TG, Bullock JM), pp. 266-279. Oxford University Press, Oxford.

Russell AP, Bauer AM, Johnson MK (2005) Migration in amphibians and reptiles: an overview of patterns and orientation mechanisms in relation to life history strategies. In: *Migration of organisms* (ed Elewa AMT), pp. 151-203. Springer-Verlag, Berlin Heidelberg.

Saastamoinen M, Bocedi G, Cote J *et al.* (2018) Genetics of dispersal. *Biological Reviews*, **93,** 574-599.

Saenz-Agudelo P, Jones G, Thorrold S, Planes S (2009) Estimating connectivity in marine populations: an empirical evaluation of assignment tests and parentage analysis under different gene flow scenarios. *Molecular Ecology*, **18**, 1765–1776.

Sánchez-Montes G, Ariño AH, Vizmanos JL, Wang J, Martínez-Solano I (2017) Effects of sample size and full sibs on genetic diversity characterization: a case study of three syntopic Iberian pond-breeding amphibians. *Journal of Heredity*, **108**, 535–543.

Sánchez-Montes G, Wang J, Ariño AH, Martínez-Solano I (2018) Mountains as barriers to gene flow in amphibians: quantifying the differential effect of a major mountain ridge on the genetic structure of four sympatric species with different life history traits. *Journal of Biogeography*, **45**, 318–331.

Sandberger-Loua L, Rödel M-O, Feldhaar H (2018) Gene-flow in the clouds: landscape genetics of a viviparous, montane grassland toad in the tropics. *Conservation Genetics*, **19**, 169–180.

Saura S, Bastin L, Battistella L, Mandrici A, Dubois G (2017) Protected areas in the world's ecoregions: How well connected are they? *Ecological Indicators*, **76**, 144–158.

Sawaya MA, Kalinowski ST, Clevenger AP (2014) Genetic connectivity for two bear species at wildlife crossing structures in Banff National Park. *Proceedings of the Royal Society B: Biological Sciences*, **281**, 20131705.

Scataglini MA, Confalonieri VA, Lanteri AA (2000) Dispersal of the cotton boll weevil (Coleoptera: Curculionidae) in South America: evidence of RAPD analysis. *Genetica*, **108**, 127-136.

Schlötterer C (2004) The evolution of molecular markers — just a matter of fashion? *Nature Reviews Genetics*, **5**, 63.

Schulte U, Küsters D, Steinfartz S (2007) A PIT tag based analysis of annual movement patterns of adult fire salamanders (*Salamandra salamandra*) in a Middle European habitat. *Amphibia-Reptilia*, **28**, 531–536.

Schwartz MK, McKelvey KS (2009) Why sampling scheme matters: the effect of sampling scheme on landscape genetic results. *Conservation Genetics*, **10**, 441–452.

Selkoe KA, Toonen RJ (2006) Microsatellites for ecologists: a practical guide to using and evaluating microsatellite markers. *Ecology Letters*, **9**, 615–629.

Semlitsch RD (2008) Differentiating migration and dispersal processes for pond-breeding amphibians. *Journal of Wildlife Management*, **72**, 260–267.

Senner NR, Stager M, Cheviron ZA (2018) Spatial and temporal heterogeneity in climate change limits species' dispersal capabilities and adaptive potential. *Ecography*, **41**, 1428–1440.

Shine R (1980) “Costs” of reproduction in reptiles. *Oecologia*, **46,** 92–100.

Shine R (2015) The evolution of oviparity in squamate reptiles: an adaptationist perspective. *Journal of Experimental Zoology Part B: Molecular and Developmental Evolution*, **324**, 487–492.

Shirk AJ, Landguth EL, Cushman SA (2017) A comparison of individual-based genetic distance metrics for landscape genetics. *Molecular Ecology Resources*, **29**, 1487-1504.

Shirk AJ, Landguth EL, Cushman SA (2018) A comparison of regression methods for model selection in individual-based landscape genetic analysis. *Molecular Ecology Resources*, **18**, 55–67.

Shirk AJ, Wallin DO, Cushman SA, Rice CG, Warheit KI (2010) Inferring landscape effects on gene flow: a new model selection framework. *Molecular Ecology*, **19**, 3603–3619.

Short Bull RA, Cushman SA, Mace R *et al.* (2011) Why replication is important in landscape genetics: American black bear in the Rocky Mountains. *Molecular Ecology*, **20**, 1092–1107.

Sillero N, Campos J, Bonardi A *et al.* (2014) Updated distribution and biogeography of amphibians and reptiles of Europe. *Amphibia-Reptilia*, **35**, 1-31.

Sites JW, Reeder TW, Wiens JJ (2011) Phylogenetic insights on evolutionary novelties in lizards and snakes: sex, birth, bodies, niches, and venom. *Annual Review of Ecology, Evolution, and Systematics*, **42**, 227–244.

Smith MA, Green DM (2005) Dispersal and the metapopulation in amphibian and paradigm ecology are all amphibian conservation: populations metapopulations? *Ecography*, **28**, 110–128.

Smouse PE, Long JC, Sokal RR (1986) Multiple regression and correlation extensions of the Mantel test of matrix correspondence. *Systematic Zoology*, **35**, 627-632.

Smouse PE, Peakall R (1999) Spatial autocorrelation analysis of individual multiallele and multilocus genetic structure. *Heredity*, **82**, 561-573.

Smouse PE, Peakall R, Gonzales E (2008) A heterogeneity test for fine-scale genetic structure. *Molecular Ecology*, **17**, 3389–3400.

Spear SF, Balkenhol N, Fortin MJ, McRae BH, Scribner K (2010) Use of resistance surfaces for landscape genetic studies: considerations for parameterization and analysis. *Molecular Ecology*, **19**, 3576–3591.

Steinfartz S, Veith M, Tautz D (2000) Mitochondrial sequence analysis of *Salamandra* taxa suggests old splits of major lineages and postglacial recolonizations of Central Europe from distinct source populations of *Salamandra salamandra*. *Molecular Ecology*, **9**, 397–410.

Steinfartz S, Weitere M, Tautz D (2007) Tracing the first step to speciation: ecological and genetic differentiation of a salamander population in a small forest. *Molecular Ecology*, **16**, 4550–4561.

Stevens VM, Pavoine S, Baguette M (2010) Variation within and between closely related species uncovers high intra-specific variability in dispersal. *PLoS ONE*, **5**, e11123.

Stevens VM, Verkenne C, Vandewoestijne S, Wesselingh RA, Baguette M (2006) Gene flow and functional connectivity in the natterjack toad. *Molecular Ecology*, **15**, 2333–2344.

Stevens VM, Whitmee S, Le Galliard JF *et al.* (2014) A comparative analysis of dispersal syndromes in terrestrial and semi-terrestrial animals. *Ecology Letters*, **17**, 1039–1052.

Stewart JR, Thompson MB (2003) Evolutionary transformations of the fetal membranes of viviparous reptiles: a case study of two lineages. *Journal of Experimental Zoology Part A: Comparative Experimental Biology*, **299**, 13-32.

Storfer A, Murphy MA, Spear SF, Holderegger R, Waits LP (2010) Landscape genetics: where are we now? *Molecular Ecology*, **19**, 3496–3514.

Taylor PD, Fahrig L, Henein K, Merriam G (1993) Connectivity is a vital element of landscape structure. *Oikos*, **68**, 571-573.

Thiesmeier B, Schuhmacher H (1990) Causes of larval drift of the fire salamander, *Salamandra salamandra terrestris*, and its effects on population dynamics. *Oecologia*, **82**, 259–263.

Thomas B, Holland JD, Minot EO (2011) Wildlife tracking technology options and cost considerations. *Wildlife Research*, **38**, 653-663.

Travis JMJ, Delgado M, Bocedi G *et al.* (2013) Dispersal and species response to climate change. *Oikos*, **122**, 1532–1540.

Travis JMJ, Mustin K, Bartoń KA *et al.* (2012) Modelling dispersal: An eco-evolutionary framework incorporating emigration, movement, settlement behaviour and the multiple costs involved. *Methods in Ecology and Evolution*, **3**, 628–641.

Trochet A, Courtois EA, Stevens VM *et al.* (2016) Evolution of sex-biased dispersal. *The Quarterly Review of Biology*, **91**, 297–320.

Uotila E, Crespo-Diaz A, Sanz-Azkue I, Rubio X (2013) Variation in the reproductive strategies of *Salamandra salamandra* (Linnaeus, 1758) populations in the province of Gipuzkoa (Basque Country). *Munibe*, **61**, 91–101.

van Dyke JU, Brandley MC, Thompson MB (2014) The evolution of viviparity: molecular and genomic data from squamate reptiles advance understanding of live birth in amniotes. *Reproduction*, **147**, R15–R26.

van Strien MJ, Keller D, Holderegger R (2012) A new analytical approach to landscape genetic modelling: least-cost transect analysis and linear mixed models. *Molecular Ecology*, **21**, 4010–4023.

Vasudev D, Fletcher RJ, Goswami VR, Krishnadas M (2015) From dispersal constraints to landscape connectivity: lessons from species distribution modeling. *Ecography*, **38**, 967–978.

Velo-Antón G, Buckley D (2015) Salamandra común – *Salamandra salamandra*. *In: Enciclopedia Virtual de los Vertebrados Españoles* (eds Carrascal LM, Salvador A). Museo Nacional de Ciencias Naturales, Madrid. http://www.vertebradosibericos.org

Velo-Antón G, Cordero-Rivera A (2017) Ethological and phenotypic divergence in insular fire salamanders: diurnal activity mediated by predation? *Acta Ethologica*, **20**, 243–253.

Velo-Antón G, García-París M, Galón P, Cordero Rivera A (2007) The evolution of viviparity in holocene islands: ecological adaptation versus phylogenetic descent along the transition from aquatic to terrestrial environments. *Journal of Zoological Systematics and Evolutionary Research*, **45**, 345–352.

Velo-Antón G, Lourenço A, Galán P, Nicieza A, Tarroso P (2017). Understanding hybrid zones between divergent phenotypic and genetic populations of fire salamanders. *19th European Congress of Herpetology (SEH)*. Salzburg, Austria (19th – 22th September 2017). Oral presentation

Velo-Antón G, Parra JL, Parra-Olea G, Zamudio KR (2013) Tracking climate change in a dispersal-limited species: reduced spatial and genetic connectivity in a montane salamander. *Molecular Ecology*, **22**, 3261–3278.

Velo-Antón G, Santos X, Sanmartín-Villar I, Cordero-Rivera A, Buckley D (2015) Intraspecific variation in clutch size and maternal investment in pueriparous and larviparous *Salamandra salamandra* females. *Evolutionary Ecology*, **29**, 185–204.

Velo-Antón G, Zamudio KR, Cordero-Rivera A (2012) Genetic drift and rapid evolution of viviparity in insular fire salamanders (*Salamandra salamandra*). *Heredity*, **108**, 410–418.

Vences M, Sanchez E, Hauswaldt JS *et al.* (2014) Nuclear and mitochondrial multilocus phylogeny and survey of alkaloid content in true salamanders of the genus *Salamandra* (Salamandridae). *Molecular Phylogenetics and Evolution*, **73**, 208–216.

Wagner GP, Lynch VJ (2010) Evolutionary novelties. *Current Biology*, **20**, R48-R52.

Wake MH (2003) Reproductive modes, ontogenies, and the evolution of body forms. *Animal Biology*, **53**, 209–223.

Wake MH (2004) Environmental effects, embryonization, and the evolution of viviparity. In: *Environment, development, and evolution: towards a synthesis* (eds Hall BK, Pearson RD, Müller GB), pp 151-170. Massachusetts Institute of Technology, Cambridge.

Wake MH (2015) Fetal adaptations for viviparity in amphibians. *Journal of Morphology*, **276**, 941–960.

Waits LP, Storfer A (2015) Basics of population genetics: quantifying neutral and adaptive genetic variation for landscape genetic studies. In: *Landscape genetics: concepts, methods, applications* (eds Balkenhol N, Cushman S, Storfer A, Waits L), pp 35-57. John Wiley & Sons Ltd, United Kingdom.

Wang IJ (2010) Recognizing the temporal distinctions between landscape genetics and phylogeography. *Molecular Ecology*, **19**, 2605–2608.

Wang IJ (2013) Examining the full effects of landscape heterogeneity on spatial genetic variation: a multiple matrix regression approach for quantifying geographic and ecological isolation. *Evolution*, **67**, 3403–3411.

Wang IJ, Bradburd GS (2014) Isolation by environment. *Molecular Ecology*, **23**, 5649–5662.

Wang IJ, Glor RE, Losos JB (2013) Quantifying the roles of ecology and geography in spatial genetic divergence. *Ecology Letters*, **16**, 175–182.

Wang IJ, Shaffer HB (2017) Population genetic and field ecological analyses return similar estimates of dispersal over space and time in an endangered amphibian. *Evolutionary Applications*, **10**, 630–639.

Wang J (2016) A comparison of single-sample estimators of effective population sizes from genetic marker data. *Molecular Ecology*, **25**, 4692–4711.

Wang J (2017) The computer program structure for assigning individuals to populations: easy to use but easier to misuse. *Molecular Ecology Resources*, **17**, 981–990.

Wang J (2018) Effects of sampling close relatives on some elementary population genetics analyses. *Molecular Ecology Resources*, **18**, 41–54.

Waser PM, Hadfield JD (2011) How much can parentage analyses tell us about precapture dispersal? *Molecular Ecology*, **20**, 1277–1288.

Wasserman TN, Cushman SA, Shirk AS, Landguth EL, Littell JS (2012) Simulating the effects of climate change on population connectivity of American marten (*Martes americana*) in the northern Rocky Mountains, USA. *Landscape Ecology*, **27**, 211–225.

Wells KD (2007) *The ecology and behavior of amphibians*. The University of Chicago Press, Chicago.

Whittington CM, Griffith OW, Qi W, Thompson MB, Wilson AB (2015) Seahorse brood pouch transcriptome reveals common genes associated with vertebrate pregnancy. *Molecular Biology and Evolution*, **32**, 3114–3131.

Whitlock MC (2011) G'_{ST} and D do not replace F_{ST}. *Molecular Ecology*, **20**, 1083–1091.

Whitlock MC, Mccauley DE (1999) Indirect measures of gene flow and migration: $F_{ST} \neq 1/(4Nm+1)$. *Heredity*, **82**, 117-125.

Wiens JJ (2016) Climate-related local extinctions are already widespread among plant and animal species. *PLoS Biology*, **14**, e2001104.

Williams JL, Kendall BE, Levine JM (2016) Rapid evolution accelerates plant population spread in fragmented experimental landscapes. *Science*, **353**, 482–485.

Wilson GA, Rannala B (2003) Bayesian inference of recent migration rates using multilocus genotypes. *Genetics*, **163**, 1177-1191.

Wourms JP, Lombardi J (1992) Reflections on the evolution of piscine viviparity. *American Zoologist*, **32**, 276–293.

Wright S (1931) Evolution in Mendelian populations. *Genetics*, 16, 97–159.

Wright S (1943) Isolation by distance. *Genetics*, **28**, 114–138.

Yoder JB, Clancey E, Des Roches S *et al.* (2010) Ecological opportunity and the origin of adaptive radiations. *Journal of Evolutionary Biology*, **23**, 1581–1596.

Yuan FL, Pickett EJ, Bonebrake TC (2016) Cooler performance breadth in a viviparous skink relative to its oviparous congener. *Journal of Thermal Biology*, **61**, 106–114.

Zalewski A, Piertney SB, Zalewska H, Lambin X (2009) Landscape barriers reduce gene flow in an invasive carnivore: geographical and local genetic structure of American mink in Scotland. *Molecular Ecology*, **18**, 1601-1615.

Zarnetske PL, Baiser B, Strecker A, Record S, Belmaker J, Tuanmu MN (2017) The interplay between landscape structure and biotic interactions. *Current Landscape Ecology Reports*, **2**, 12–29.

Zeller KA, Creech TG, Millette KL *et al.* (2016) Using simulations to evaluate Mantel-based methods for assessing landscape resistance to gene flow. *Ecology and Evolution*, **6**, 4115–4128.

Zeller KA, Jennings MK, Vickers TW, Ernest HB, Cushman SA, Boyce WM (2018) Are all data types and connectivity models created equal? Validating common connectivity approaches with dispersal data. *Diversity and Distributions*, **24**, 868–879.

Zeller KA, McGarigal K, Whiteley AR (2012) Estimating landscape resistance to movement: a review. *Landscape Ecology*, **27**, 777–797.

Zellmer AJ, Knowles LL (2009) Disentangling the effects of historic *vs.* contemporary landscape structure on population genetic divergence. *Molecular Ecology*, **18**, 3593–3602.

Zera AJ, Brisson JA (2012) Quantitative, physiological, and molecular genetics of dispersal/migration. In: *Dispersal ecology and evolution* (eds Clobert J, Baguette J, Benton TG, Bullock JM), pp. 63–82. Oxford University Press, Oxford.

Zera AJ, Denno RF (1997) Physiology and ecology of dispersal polymorphism in insects. *Annual Review of Entomology*, **42**, 207-230.

Zhang P, Papenfuss TJ, Wake MH, Qu L, Wake DB (2008) Phylogeny and biogeography of the family Salamandridae (Amphibia: Caudata) inferred from complete mitochondrial genomes. *Molecular Phylogenetics and Evolution*, **49**, 586–597.

Zhang Y-H, Wang IJ, Comes HP, Peng H, Qiu Y-X (2016) Contributions of historical and contemporary geographic and environmental factors to phylogeographic structure in a Tertiary relict species, *Emmenopterys henryi* (Rubiaceae). *Scientific Reports*, **6**, 24041.

Zúñiga-Vega JJ, Fuentes-G JA, Ossip-Drahos AG, Martins EP (2016) Repeated evolution of viviparity in phrynosomatid lizards constrained interspecific diversification in some life-history traits. *Biology Letters*, **12**, 20160653.

Chapter 2

Population genetics of urban pueriparous populations

Paper I

Trapped within the city: integrating demography, time since isolation and population-specific traits to assess the genetic effects of urbanization.

André Lourenço[1,2], David Álvarez[3], Ian J. Wang[4] and Guillermo Velo-Antón[2]

Article published in *Molecular Ecology*, 2017, **26**, 1498-1514. doi: 10.1111/mec.14019

[1] Departamento de Biologia da Faculdade de Ciências da Universidade do Porto, Rua Campo Alegre, 4169-007 Porto, Portugal.

[2] CIBIO/InBIO, Centro de Investigacao em Biodiversidade e Recursos Genéticos da Universidade do Porto, Instituto de Ciências Agrárias de Vairão, Rua Padre Armando Quintas 7, 4485-661 Vairão, Portugal

[3] Ecology Unit, Department of Organisms and Systems Biology, University of Oviedo, C/ Catedrático Rodrigo Uría, 33071 Oviedo, Spain

[4] Department of Environmental Science, Policy and Management, University of California, 130 Mulford Hall #3114, Berkeley, CA 94705 USA

2.1 – Abstract

Urbanization is a severe form of habitat fragmentation that can cause many species to be locally extirpated and many others to become trapped and isolated within an urban matrix. The role of drift in reducing genetic diversity and increasing genetic differentiation is well recognized in urban populations. However, explicit incorporation and analysis of the demographic and temporal factors promoting drift in urban environments are poorly studied. Here, we genotyped 15 microsatellites in 320 fire salamanders from the historical city of Oviedo (Est. 8th century) to assess the effects of time since isolation, demographic history (historical effective population size; *Ne*) and patch size on genetic diversity, population structure and contemporary *Ne*. Our results indicate that urban populations of fire salamanders are highly differentiated, most likely due to the recent *Ne* declines, as calculated in coalescence analyses, concomitant with the urban development of Oviedo. However, urbanization only caused a small loss of genetic diversity. Regression modelling showed that patch size was positively associated with contemporary *Ne*, while we found only moderate support for the effects of demographic history when excluding populations with unresolved history. This highlights the interplay between different factors in determining current genetic diversity and structure. Overall, the results of our study on urban populations of fire salamanders provide some of the very first insights into the mechanisms affecting changes in genetic diversity and population differentiation via drift in urban environments, a crucial subject in a world where increasing urbanization is forecasted.

Keywords: demography, genetic drift, genetic isolation, microsatellite, population effective size, *Salamandra salamandra*.

2.2 – Introduction

Identifying the mechanisms underlying patterns of genetic diversity and structure arising from habitat loss and fragmentation continues to be a major target of ecological and evolutionary studies of natural populations (*e.g.* Weckworth *et al.* 2013; Rivera-Ortíz *et al.* 2015; Richardson *et al.* 2016). Among the many causes of habitat fragmentation, urbanization is regarded as one of the most rapid and pervasive drivers of landscape change, causing isolation and local extirpations of populations in numerous vulnerable species (McKinney 2006). Nevertheless, some species with small home range requirements are able to persist in urban environments (*e.g.* Noël and Lapointe 2010; Munshi-South 2012; Yamamoto *et al.* 2013; Rodriguez-Martínez *et al.* 2014; Beninde *et al.* 2016). These urban dwellers inhabiting high-contrast edge areas are usually confined within small remnant patches of vegetation (*e.g.* city

parks) surrounded by an impervious matrix of buildings and roads. Under this scenario of genetic isolation (*i.e.* reduced or absent gene flow) and small population size, genetic drift becomes a dominant force shaping allele frequencies, leading to a decrease in genetic diversity and an increase in genetic differentiation (Frankham 2005).

Recent empirical research in urban areas has shown indeed that urbanization significantly limits functional connectivity (gene flow) among urban populations, which, coupled with the stronger effects of drift in small populations, substantially increases genetic differentiation (Delaney *et al.* 2010; Munshi-South and Kharchenko 2010; Munshi-South *et al.* 2013; Munshi-South *et al.* 2016). Moreover, using genomic approaches, Munshi-South *et al.* (2016) found that urban populations of the white-footed mouse (*Peromyscus leucopus*) in New York City exhibit lower genome-wide variation compared with rural populations (see also Gortat *et al.* 2015), corroborating the deleterious effects of drift on genetic diversity in urban populations. However, despite the excellent work that has recently been performed on urban populations, we currently know little about the historical and population-specific factors that influence how the effects of drift are expressed in urban populations.

Two factors predominate in determining how strong the effects of drift are in isolated populations: (i) time since isolation and (ii) long-term (historical) and contemporary effective population size (*Ne*; Frankham 2005; Ellegren and Galtier 2016). The former determines how long drift acts without the homogenizing force of gene flow, such that populations isolated for longer periods bear more effects from drift (Frankham 2005). For the latter, phenomena such as founder effects or bottlenecks cause a pronounced decline in *Ne* from the ancestral population, reducing genome-wide allelic diversity. This reduction of allelic diversity is accompanied by increased genetic divergence as the effect of drift becomes stronger in small populations (Segelbacher *et al.* 2014; Spurgin *et al.* 2014; Ellegren and Galtier 2016). To our knowledge, while a handful of studies on urban populations have examined evidence of past bottlenecks (*e.g.* Noël and Lapointe 2010; Munshi-South and Nagy 2014), no urban genetics studies have incorporated quantitative estimates of contemporary *Ne* to characterize the genetic effects of urbanization. Additionally, the effects of time since isolation were only considered as a predictor of genetic diversity and differentiation in two studies (Delaney *et al.* 2010; Munshi-South and Nagy 2014), though both showed contrasting results, illustrating the difficulties in accurately quantifying its effects.

To investigate the combined roles of demographic and temporal effects on genetic diversity and population structure in urban systems, we studied urban populations of fire salamanders (*Salamandra salamandra*, Linnaeus 1758) in the historical city of Oviedo (Spain). *Salamandra salamandra* is mostly larviparous (parturition of aquatic larvae) throughout its wide distribution

range in Europe, but it has evolved to pueriparity (parturition of fully developed terrestrial juveniles) during the Pliocene–Pleistocene in northern Spain (including Oviedo; García-París *et al.* 2003) and during the Holocene in two off-shore islands of NW Spain (Velo-Antón *et al.* 2007; Velo-Antón *et al.* 2012). This remarkable reproductive shift entails greater independence from surface water as the aquatic larval stage is removed (Velo-Antón *et al.* 2015), allowing *S. salamandra* to cope with the harsh conditions of an urban environment. We sampled 12 populations within Oviedo and four outside the city to fulfil three main objectives: (i) to estimate and compare patterns of genetic diversity and genetic structure in urban and rural populations; (ii) to estimate historical and contemporary *Ne* of urban populations; and (iii) to quantify the contributions of population-specific traits, including demographic history, time since isolation and patch attributes to genetic differentiation and diversity.

Oviedo and *S. salamandra* comprise an excellent model for research on urban genetics for four key reasons. First, the nearly impervious urban matrix and low dispersal capability exhibited by fire salamanders (Schulte *et al.* 2007) generate an expectation that these populations have been isolated for many generations. Second, Oviedo contains populations with very low total census sizes (Álvarez *et al.* 2015) confined within small and discrete patches, making it straightforward to obtain representative demographic data and measure relevant variables known to be related to genetic variation (*e.g.* patch size; see Wang *et al.* 2014; Jackson and Fahrig 2016). Third, the availability of historical documents and maps of Oviedo depicting the period when particular buildings were constructed provides a clear means of estimating when urban populations became isolated within the city. Lastly, populations became isolated during distinct time frames (some more than 1000 years ago), and consequently, the short- and long-term effects of isolation can both be assessed. In our analysis, we test three main hypotheses: (i) urban populations exhibit higher genetic divergence and reduced diversity compared with rural populations; (ii) on patch–matrix landscapes such as urban environments, patch size is a strong predictor of contemporary *Ne* and, consequently, of the strength of contemporary drift (Ellegren and Galtier 2016); and (iii) urban populations which experienced an older decline and which were isolated for longer periods show greater genetic differentiation and reduced genetic diversity due to long-term effects of small *Ne*.

2.3 – Materials and methods

2.3.1 – Study area and sampling

Our study was carried out in Oviedo (Spain; latitude: 43.36; longitude: -5.85), a historical city founded during the late 8th century (González García 1984). Two walls surrounding the city

were constructed, the first in 768 AD and the second about 500 years later, enclosing mostly ecclesiastic buildings in a total area of approximately 0.11 km^2. Fire salamander populations within the wall perimeters became isolated during this period not only due to these walls, but also within these ecclesiastic buildings that comprise small closed systems surrounded by additional walls. Over time, Oviedo continued to expand beyond the outer walls and other populations became isolated as the city encompassed them (**Figure 2.1**). Localities inside (IW) and outside historical walls (OW) that were *a priori* known or suspected fire salamander habitats were inspected during rainy nights from November 2013 until November 2014. We collected 256 tail or toe clip samples from mostly adult individuals in urban parks, small gardens and ecclesiastic buildings (**Figure 2.1; Figure A1 in Appendix A**), covering a total of 12 urban patches (**Figure 2.2; Table A1 and Supplementary Text A1 in Appendix A**). Additionally, we sampled 64 adult individuals from four rural localities outside Oviedo (OC) to examine how urbanization affected genetic variation (**Figure A2 in Appendix A**). These four localities are located in forested patches and edge areas in contact with meadows, although the surroundings of Oviedo are heavily fragmented. Hence, sampling localities holding large areas of suitable habitat near the city was impossible. The sex of each sampled individual was recorded and all samples were stored in 100% ethanol.

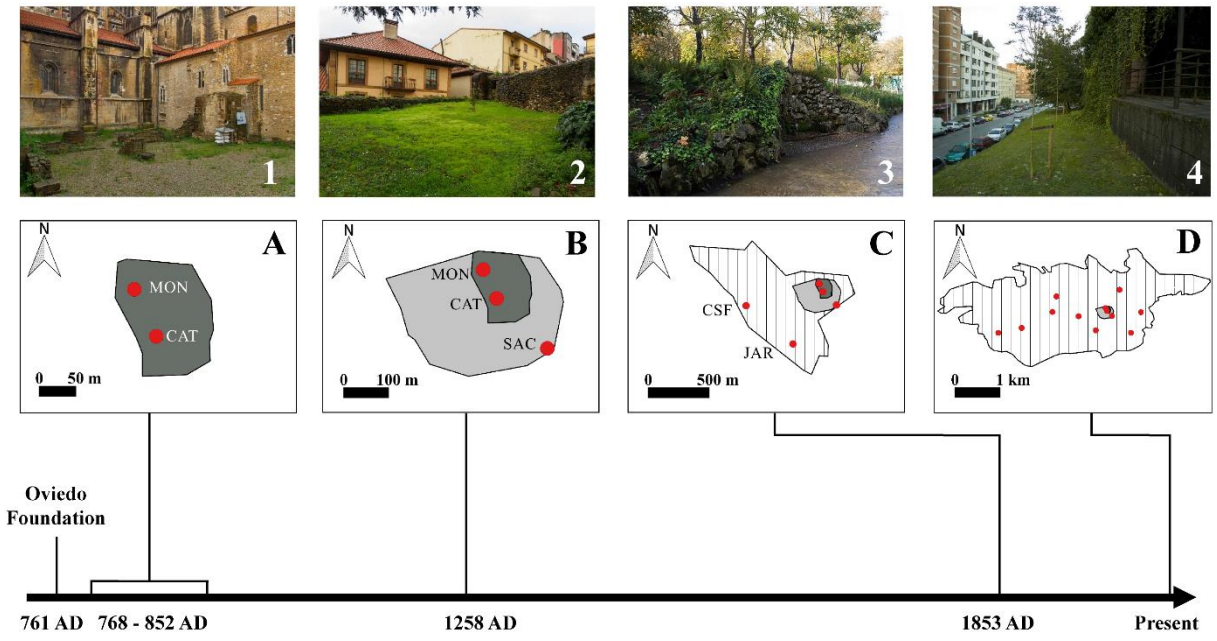

Fig. 2.1 Reconstruction of the fire salamanders' population history in Oviedo across time. Dark grey and light grey polygons correspond to the area within inner and outer walls, respectively, while dashed polygons represent the Oviedo's urban matrix. Sampled populations are illustrated by red points. (A) Erection of walls which trapped populations CAT (photograph 1) and MON; (B) construction of a second wall further isolated population SAC (photograph 2) from outer wall's perimeter; (C) urbanization surrounding wall's perimeter isolates populations CSF (photograph 3) and JAR; (D) Oviedo experiences a major urbanization within a short time frame where several populations became progressively isolated (including population FC – photograph 4).

2.3.2 – Laboratory procedures and genotyping

Genomic DNA was extracted using Genomic DNA Tissue Kit (EasySpin), following the manufacturer's protocol. Quantity and quality of extracted products were verified in a 0.8% agarose gel. A total of 15 microsatellites (Steinfartz *et al.* 2004; Hendrix *et al.* 2010) distributed in five optimized multiplexes were amplified through polymerase chain reactions (PCR; **Table A2 in Appendix A**), following the conditions described in Álvarez *et al.* (2015; see this paper in **Appendix D**). PCR products were visualized on a 2% agarose gel and subsequently run on an ABI3130XL capillary sequencer (Applied Biosystems). Allele scoring was performed in GENEMAPPER 4.0 (Applied Biosystems). To evaluate genotyping errors, a second independent amplification of about 10% (n = 34) of our data set was conducted. Allele dropout and false allele rates were estimated using 10 000 iterations in PEDANT 1.0 (Johnson and Haydon 2007). Frequencies of null alleles were calculated in INEST 2.0 (Chybicki and Burczyk 2009) using the individual inbreeding model (200,000 iterations thinned every 100 iterations and a burn-in of 10%).

2.3.3 – Population genetics analyses

Deviations from Hardy–Weinberg equilibrium (HWE) and linkage equilibrium (LE) were assessed in GENEPOP 4.2 (Rousset 2008; dememorization = 10,000, batch length = 10,000, batch number = 5,000). The false discovery rate (Benjamini and Hochberg 1995) was applied to correct p-values from HWE and LE multiple exact tests. GENALEX 6.5 (Peakall and Smouse 2012) was employed to calculate observed (H_O) and expected heterozygosities (H_E), mean alleles per marker (N_A), number of private alleles (P_A) and number of individuals containing private alleles in a sampled locality (N_{PA}). Average relatedness (R) was calculated using the triadic likelihood estimator implemented in COANCESTRY, including R estimates accounting for inbreeding and genotyping errors (we included error frequencies obtained in INEST and PEDANT; Wang 2011). Finally, allelic richness (A_R) corrected for the smallest locality's sample size in our data set was estimated using the R package *diveRsity* (Keenan *et al.* 2013).

2.3.4 – Contemporary *Ne*

We estimated contemporary *Ne* using two genetic single-sample estimators: (i) the linkage disequilibrium method (LD; Waples 2006) as implemented in NEESTIMATOR 2.01 (Do *et al.* 2014); and (ii) the sibship assignment method (SA; Wang 2009) in COLONY2 (Jones and Wang 2010). We obtained *Ne* estimates and jackknife 95% confidence intervals (CIs) for each sampled locality with the LD method by assuming random mating. Our mean sample size (n =

20) is lower than 25, and thus, the frequency to screen out rare alleles (P_{CRIT}) was set within the following interval: $1/(2n) \leq P_{CRIT} \leq 1/n$ (Waples and Do 2010). We chose a value, P_{CRIT} = 0.04, on the conservative side of this range. For the SA method, we used the sex of individuals to split samples into candidate mothers and fathers. No *a priori* information concerning known parents was used. Individuals categorized as subadults, for which we could not determine the sex, were allocated only to the offspring sample. Given that fire salamanders reach sexual maturity at 4 years (Alcobendas and Castanet 2000) and live for more than 20 years (Rebelo and Caetano 1995), we also included individuals from the candidate parent samples in the pool of candidate offspring samples because our adult samples may have encompassed multiple generations. Common to all analyses, we implemented the full-likelihood method, high-likelihood precision, medium run length and random mating under scenarios of polygamy for both sexes. To assess whether inbreeding and genotyping errors (estimated in PEDANT and INEST) influenced *Ne* estimation, we performed analyses under different combination of these parameters to check for congruence. Three independent runs (with different seed values) were conducted for each combination of parameters and *Ne* values among runs were averaged. Thus, in total, 12 runs per sampled locality were performed. Both methods assume that samples belong to the same cohort, but fire salamanders are iteroparous animals with overlapping generations. However, although the exact *Ne* estimates should be interpreted with some caution (Waples *et al.* 2014), we argue that these calculations are still useful for providing approximate population sizes and for comparing relative population sizes across populations.

2.3.5 – Demographic history

We used the VarEff method implemented in the R package *VarEff* (Nikolic and Chevalet 2014) to calculate historical *Ne*, which we used as a proxy for demographic history. This method employs an approximate likelihood Markov chain Monte Carlo (MCMC) approach that relies on motif distance frequencies between alleles to estimate variation in *Ne* over time. Loci SST-A6-I and Sal3 were discarded from this analysis because they exhibited irregular motif repeat length, and consequently, VarEff analyses were performed with 13 loci. Locus SalE5 was also excluded for population MIL because it was monomorphic. We performed trial runs with varying parameters to adjust parameter values. In the final run, we set the estimated mutation rate to 0.00127 (as estimated in eastern tiger salamanders; Bulut *et al.* 2009) for all loci, using a two-phased mutation model with a proportion of 0.22 for multistep mutations (Peery *et al.* 2012). The parameter JMAX (number of changes in past *Ne*) had little effects on the results, with small values generating slightly steeper curves in demographic trajectories. Accordingly, following recommendations from Nikolic and Chevalet (2014), we set a low value

of JMAX = 4 (maximum of four changes in past *Ne*). The prior for past *Ne* was set by applying the formula Θ1/(4μ) (Nikolic and Chevalet 2014), while the prior for the number of generations since population origin was set to 500 generations to encompass Oviedo's founding period (equivalent to 2000 years based on a generation time of 4 years; Alcobendas and Castanet 2000). Variance of both priors was set to two and the coefficient of correlation between *Ne* in successive time intervals was 0.5 (a correlation of 0 would indicate that *Ne* at time t+ 1 would be independent of *Ne* at time t). Finally, we set 10,000 batches with a length of 10, thinned every 200 batches to avoid autocorrelation in the MCMC chain. The first 10,000 batches were discarded as part of the burn-in period (see all input parameters in **Table A3 in Appendix A**). To reconstruct demographic trajectories, we post-processed the output of VarEff to calculate the median of *Ne* for ten generation intervals (50 intervals in total given that population origin was set to 500 generations ago). In addition, we calculated two metrics from VarEff to characterize long-term *Ne* patterns: (i) the magnitude (MG) of *Ne* decline and (ii) post-bottleneck time (POST). These metrics are summarized in **Table 2.1**.

Table 2.1 Descriptions for explanatory variables used in regression models. Logarithmic transformation and standardization were used prior to regression analyses for all variables.

Predictor	Data type	Description	Transformation	Mean (range)
Time since isolation	Integer	Number of generations in which a population is hypothetically isolated (generation = 4 years).	Logarithmic	80.5 (6-310)
Patch size	Integer	Patch size (m^2) of sampled localities.	Logarithmic	2847.9 (155-8698)
Magnitude	Continuous	Variable characterizing bottleneck severity according to VarEff output. It expresses the average decrease of *Ne* per ten generations when a bottleneck started. We devised this metric by using a simple formula: $$magnitude = \frac{N1 - N2}{\Delta G}$$ in which N1 is the *Ne* before the population experienced a bottleneck and N2 corresponds to *Ne* after it stabilized to numbers identical to contemporary *Ne*. ΔG is the elapsed number of generations between N1 and N2. Therefore, bottlenecks with greater *Ne* decreases within a small number of generations will have a larger magnitude.	Logarithmic	522.2 (101.9-1516.0)
Post-bottleneck time	Integer	Number of generations elapsed since the beginning of a pronounced *Ne* decline until the present.	Logarithmic	136.7 (30-490)

2.3.6 – Analyses of genetic isolation

We inferred population genetic structure for the 16 sampled localities in STRUCTURE 2.3.4 (Pritchard *et al.* 2000). Analyses were run using the admixture model with correlated allele frequencies. No informative priors regarding population origin were used. Ten independent runs were carried out for a number of clusters (K) ranging from 1 to 20. For each run, we set a burn-in period of 5×10^4 iterations followed by 5×10^5 MCMC iterations. The output generated from multiple independent runs across each K was summarized and graphically represented using the main pipeline implemented in software CLUMPAK with default advanced options (Kopelman *et al.* 2015). The optimal value of K was selected based on two different criteria: (i) the K exhibiting the highest mean logarithmic posterior probability (MLPP; Pritchard *et al.* 2000) and (ii) the K displaying the largest value of ΔK (Evanno *et al.* 2005).

The R package *diveRsity* was used to calculate, between sampled localities, two measures of genetic differentiation and respective 95% CIs, computed through 1000 bootstrap replicates: (1) pairwise F_{ST} (Weir and Cockerham's 1984), and (2) pairwise Jost´s D_{EST} (Jost 2008). We considered pairwise estimates as significant when 95% CIs did not overlap zero, as recommended by Keenan *et al.* (2013).

Contemporary immigration rates and respective 95% CIs were estimated using a Bayesian approach implemented in BAYESASS 3.0 (Wilson and Rannala 2003). This MCMC method calculates the posterior mean of migration rates based on the posterior probabilities of individual migrant ancestry and it performs well when there is high genetic differentiation between populations ($F_{ST} > 0.05$; Faubet *et al.* 2007). We set a total of 1.5×10^7 iterations with a burn-in of 1×10^6 steps and a sampling frequency of 1,000 iterations for each run. We followed the software's guidelines to adjust the MCMC mixing parameters for allele frequencies (ΔA), inbreeding (ΔF) and migration rates (ΔM). Three separate runs with different seed values were conducted. Convergence was assessed in TRACER 1.6 (Rambaut *et al.* 2014) by comparing mean log-probabilities among runs and inspecting whether the total log-likelihood achieved stationarity. If results converged, immigration rates were averaged among runs. Migration rates were identified as significant if 95% CIs did not overlap zero.

2.3.7 – Statistical analyses

We first tested for significant differences in seven metrics descriptive of genetic diversity (A_R, R, H_O), differentiation (mean proportion of cluster membership; DIFF) and contemporary *Ne* (Ne_SA, Ne_LD and Ne_mean) among the sampled locality groups (IW vs OW vs OC). The variable "DIFF" for each locality was extracted by averaging the correspondent proportion of cluster membership among individuals at that locality in the ten runs conducted in

STRUCTURE for the most supported K. The three *Ne* metrics were obtained independently from the two approaches we used to estimate *Ne* (Ne_LD and Ne_SA) and from the average of *Ne* point estimates between both methods (Ne_mean). Statistical differences were assessed using a non-parametric Kruskall-Wallis test.

We used regression analysis to investigate the influence of time since isolation, demographic history and patch size on the same seven population genetic metrics of genetic variation and contemporary *Ne* (response variables). Specifically, we tested four explanatory variables: (1) time since isolation (in generations; TI); (2) patch size (m^2; PS) where a population occurs; (3) bottleneck magnitude (MG) calculated from VarEff output to assess if the strength of a bottleneck affected contemporary genetic parameters; and (4) post-bottleneck time (in generations; POST) as calculated in VarEff to evaluate the long-term genetic effects of a pronounced decline of *Ne* in these urban populations. Given the small sample size (n = 12 urban populations), we kept the models as simple as possible to avoid overfitting. Regression analyses were performed for each response variable using a set of six models comprising all possible combinations of two predictors (*i.e.* TI+PS; TI+MG; TI+POST; PS+MG; PS+POST; MG+POST). Prior to regression analyses, logarithmic transformations were applied to predictors to reduce the influence of extreme observations. All predictors were standardized to allow direct comparisons between individual regression coefficients in each model (Schielzeth 2010). Pairwise correlations among explanatory variables revealed that they were not significantly correlated ($r < 0.7$), and thus we retained all of them in the regression analyses. Although the identification and calculation of the effect sizes of the single most important explanatory variable was not possible because we did not test a full model including all predictors, fitting these models was still valuable for qualitatively identifying the significant predictors for each response variable.

To choose the most suitable regression analysis for each of the response variables analysed, we checked whether the assumptions of normality and homogeneity of variances were violated by following recommendations provided by Zuur *et al.* (2009) (**Supplementary Text A2 in Appendix A**). We used three distinct methods to estimate the parameters for different models: (1) a multiple linear regression using ordinary least squares estimates for models with normally distributed residuals and with predictors displaying homogeneous variances; (2) a generalised least squares method for models with normally distributed residuals and heterogeneous variances in predictors; and (3) a negative binomial generalized linear model for models violating the assumptions of normality and presenting a large variance in residuals (see also **Table A4 in Appendix A**). Afterwards, we used an information-theoretic approach (Burnham and Anderson 2002) to identify the set of predictor variables that should

be retained in each of the six candidate models being tested for each response variable. All possible combinations of the candidate model's predictors were assessed (*i.e.* three nested models in which two contained just one predictor and one model with two predictors). A null model (intercept-only model) without explanatory variables was also included. Models were ranked according to their Akaike weight (w_i), a metric that can be interpreted as the probability of a particular model being the best from a candidate model set. If a single model had a wi > 0.95, we identified that model as the best, otherwise ($w_i < 0.95$) we produced a 95% confidence set by including models until the cumulative w_i exceeded 0.95. In the latter case, unconditional regression coefficients and standard errors (SE), as well the relative importance of each explanatory variable (w_+; cumulative sum of each model's w_i where a given variable was included) were calculated through model averaging to reduce model uncertainty (Grueber *et al.* 2011). We identified a particular predictor as biologically important when the predictor met two criteria in all of the independent candidate models in which it was included: (1) high values of w_+; and (2) unconditional 95% CIs estimates that did not overlap zero.

Finally, we repeated the full set of regression analyses after excluding one of the oldest populations, CAT, because it exhibited signs of recent admixture (see section 3.4.4). Recent admixture can counteract the long-term effects of isolation and *Ne* decline on genetic variation (Jangjoo *et al.* 2016; Furman *et al.* 2016) and therefore, accurate testing of the effects of population history predictors in genetic diversity and structure may be compromised in regression modelling. All statistical analyses described in this section were carried out in R software (R Development Core Team 2015). Generalised least squares were carried out using the R package *nlme* (Pinheiro *et al.* 2015), whereas the negative binomial generalized linear models were performed using R package *MASS* (Venables and Ripley 2002). Predictor standardization and the information criterion testing were conducted using the R package *MuMIn* (Barton 2016).

2.4 – Results

2.4.1 – Marker validation and genetic diversity

Overall, we found no evidence of allele dropout or false alleles, except for locus SST-C3 which revealed a small dropout rate of 0.032. Six markers showed high mean null allele frequencies (see Discussion), two of which (SST-C3 and SalE06) also showed deviations from HWE (heterozygote deficit) in several populations, although there was no evidence of LD (**Table A5 in Appendix A**). Markers displaying deviations from HWE may provide spurious conclusions; therefore, we excluded these two markers and repeated all analyses to compare results between 13 vs 15 microsatellites.

All but two populations contained private alleles and four exhibited a high number of individuals with private alleles (N_{PA}: 9 - 16). Genetic diversity was high overall (H_O > 0.588), although populations CSF and MIL (OW) and MON (IW) displayed a lower allelic richness (A_R < 4.4) and number of alleles (N_A < 5.2) than most populations (**Table 2.2**). These three populations also exhibited the highest relatedness levels (R > 0.220; **Table 2.2**). When calculating relatedness in COANCESTRY, including potential genotyping errors had negligible effects, whereas inbreeding resulted in a mean increase in R of 0.059 (**Table A6 in Appendix A**). Genetic diversity statistics based on 13 vs. 15 loci were similar (**Table A7 in Appendix A**). The only exception was A_R which presented smaller values with 13 loci, although A_R estimates were correlated between 13 vs 15 loci (r = 0.69).

Table 2.2 Standard population (Pop) genetic statistics from the 16 studied populations of fire salamanders: N – number of samples collected; Location – the population's relative location in the city (OC – outside city; OW – within city but outside walls; IW – inside historical walls); N_A – mean number of alleles; P_A – number of private alleles; N_{PA} – number of individuals with private alleles; H_O – observed heterozygosity; H_E – expected heterozygosity; A_R – allelic richness; R – mean relatedness and respective 95% CIs (in parentheses) without accounting for inbreeding and genotyping errors.

Pop	Location	N	N_A	P_A	N_{PA}	H_O	H_E	A_R	R
FC	OW	30	8.3	7	12	0.678	0.756	6.27	0.094 (0.020 – 0.315)
PT	OW	20	7.4	5	5	0.680	0.749	5.81	0.099 (0.013 – 0.375)
CSF	OW	18	5.2	3	3	0.635	0.669	4.40	0.220 (0.077 – 0.484)
TEN	OW	20	6.9	1	1	0.737	0.751	5.72	0.125 (0.029 – 0.369)
ARC	OW	20	6.8	2	7	0.658	0.711	5.54	0.136 (0.026 – 0.383)
JAR	OW	21	7.1	0	0	0.641	0.712	5.26	0.129 (0.017 – 0.413)
OTE	OW	21	7.0	3	4	0.721	0.745	5.54	0.137 (0.041 – 0.383)
IND	OW	19	6.4	0	0	0.638	0.720	5.22	0.130 (0.037 – 0.412)
MIL	OW	20	4.6	1	1	0.658	0.645	4.10	0.265 (0.119 – 0.522)
SAC	IW	19	6.4	4	9	0.680	0.728	5.44	0.123 (0.028 – 0.366)
CAT	IW	24	7.3	4	4	0.663	0.727	5.79	0.116 (0.034 – 0.347)
MON	IW	24	4.7	3	16	0.619	0.642	3.92	0.288 (0.118 – 0.563)
LIL	OC	19	8.4	5	3	0.730	0.774	6.48	0.076 (0.014 – 0.305)
VIL	OC	17	6.8	3	10	0.693	0.700	5.66	0.183 (0.047 – 0.420)
BEN	OC	15	7.5	1	1	0.726	0.766	6.10	0.075 (0.005 – 0.324)
TIN	OC	13	6.4	5	7	0.654	0.722	5.56	0.187 (0.064 – 0.397)

2.4.2 – Contemporary *Ne*

The LD and SA methods yielded small *Ne* estimates (LD: mean = 81.2, range = 8-632; SA: mean = 50.4, range = 22-140; **Table 2.3**). The results of both approaches were moderately correlated (r = 0.57), with three OW populations (MIL, CSF and OTE) and two IW populations (MON and CAT) exhibiting the lowest *Ne* (*Ne* ≤ 15 and *Ne* ≤ 31 for LD and SA analyses, respectively). Both methods consistently identified the largest populations (PT, JAR and three OC populations; *Ne* ≥ 58), though the LD method failed to deliver precise estimates for BEN and VIL. Different models in COLONY2 provided very similar results, regardless of the model used (r > 0.97), with identical results in the case of including inbreeding or a slight decrease in

Ne when accounting for potential genotyping errors (**Table A8 in Appendix A**). Thus, we discuss only estimates provided by the COLONY2 standard models. Differences in *Ne* estimates based on 13 loci were very small, although the LD method detected a large but much lower *Ne* (*Ne* = 127; **Table A9 in Appendix A**) for population JAR compared with the one obtained when employing 15 loci (*Ne* = 632).

Table 2.3 *Ne* estimates based on two methods (Linkage Disequilibrium, LD; Sibship Assignment, SA) and their mean (*Ne* mean) with respective 95% CIs in parenthesis. The results of the SA analysis were generated with a model excluding inbreeding and genotyping errors. Inf - infinite

Population	*Ne* LD	*Ne* SA	*Ne* mean
FC	33 (25 - 48)	59 (37 - 106)	46 (31 – 77)
PT	192 (35 - Inf)	58 (33 - 144)	126 (34 – Inf)
CSF	13 (8 - 23)	23 (12 - 51)	18 (10 – 37)
TEN	25 (17 - 40)	36 (20 - 72)	30 (18 – 56)
ARC	99 (40 - Inf)	40 (23 - 79)	70 (31 – Inf)
JAR	632 (50 - Inf)	65 (36 - 164)	348 (43 – Inf)
OTE	15 (10 - 23)	27 (14 - 55)	21 (12 – 39)
IND	23 (15 - 42)	34 (19 - 72)	28 (17 – 57)
MIL	8 (5 - 12)	22 (12 - 46)	15 (8 – 29)
SAC	31 (20 - 58)	38 (21 - 81)	34 (20 – 69)
CAT	12 (10 - 16)	31 (18 - 60)	22 (14 – 38)
MON	10 (6 - 15)	26 (15 - 56)	18 (10 – 35)
LIL	29 (20 - 49)	68 (36 - 193)	48 (28 – 121)
VIL	Inf (236 - Inf)	109 (53 - 1001)	Inf (144 – Inf)
BEN	Inf (77 - Inf)	140 (54 - Inf)	Inf (66 – Inf)
TIN	16 (11 - 24)	31 (15 - 152)	24 (13 – 88)

2.4.3 – Demographic history

VarEff identified pronounced and recent *Ne* declines (congruent with the historical development of Oviedo) for all populations except population TIN (**Figure 2.3**). Estimates of MG indicated a mean decrease of *Ne* = 522.2 (range = 102 - 1516) per 10 generations, with populations PT, ARC and OTE putatively experiencing stronger declines (**Figure 2.3; Table A10 in Appendix A**). Additionally, *Ne* declines in IW populations started earlier and thus, these populations have higher estimates of POST (overall mean = 136.7; range = 30 – 490; **Figure 2.3; Table A10 in Appendix A**). Identical demographic trends were obtained when using 11 loci (**Figure A3 in Appendix A**). The magnitude (mean = 443.1; range 1.2 – 1895.5) and post-bottleneck time (mean = 162.7; range 40 – 490) values were also fairly similar, except in populations FC, ARC, MIL, LIL and BEN (**Table A10 in Appendix A**).

2.4.4 – Analyses of genetic isolation

Results from STRUCTURE depicted clear patterns of genetic structure in most populations. The best supported numbers of clusters were K=16 and K=17 following the ΔK and the MLPP

approaches, respectively (**Figures A4-A5 in Appendix A**). Both scenarios showed a stronger genetic structure in populations MIL, MON, SAC (the latter two located IW) and VIL and TIN (both located OC). A higher number of clusters (K=17) supported by the MLPP method compared with sampled populations (n=16) arose from four individuals with unknown genetic ancestry in population CAT. Running STRUCTURE with 13 loci provided similar patterns. However, though the MLPP approach produced the same best K (K=17, including the same four individuals with unknown genetic ancestry), the ΔK method yielded a different one (K=5) (**Figure 2.2; Figure A6 in Appendix A**). Considering this congruence in the MLPP approach, we used the individual cluster membership values obtained with K=17 to calculate DIFF for regression analyses.

Pairwise estimates of genetic differentiation were typically high, ranging from 0.039 (the westernmost population pair FC/PT) to 0.206 (MON/VIL) for F_{ST} and 0.053 (FC/PT) to 0.498 (VIL/TIN) for D_{EST} (**Table 2.4**). All pairwise comparisons for both metrics were significant except for D_{EST} for population pair FC/PT (lower bound of 95% CIs = -0.002). Populations CSF, MON and MIL along with two non-urban populations (TIN and VIL), presented the highest mean values of pairwise differentiation. Pairwise values calculated based on 13 loci were similar, although some were not significant (**Table A11 in Appendix A**).

The three replicate runs in BAYESASS generated very similar mean log-probabilities and the MCMC chain achieved stationarity (**Figure A7 in Appendix A**), supporting convergence among runs. Contemporary migration rates were very low with an average pairwise immigration rate about of 1.2%. Only four population pairs yielded significant immigration rates, namely PT (9.5% and 8.8% immigrant ancestry from FC and IND, respectively), BEN (10.8% immigrant ancestry from TEN) and LIL (7.6% immigrant ancestry from IND). Since the assumption of HWE is relaxed in BAYESASS, we did not perform this analysis with 13 locus subset.

2.4.5 – Regression analyses

Kruskal-Wallis tests did not show significant differences for the tested variables among the three groups of populations (IW vs OW vs OC). A Wilcoxon sign rank test comparing urban (*IW* + *OW*) vs non-urban (*OC*) populations showed that differences in A_R (W = 9; p = 0.078) and Ne_SA (W = 7.5; p = 0.052) approached statistical significance. There was indeed a tendency for higher A_R and *Ne* (mean ± SD) in OC populations (A_R = 6.0 ± 0.4; Ne_SA = 87.0 ± 47.6) compared to IW + OW populations (A_R = 5.2 ± 0.7; Ne_SA = 38.2 ± 14.7). Because the LD method provided infinite estimates in two *OC* populations, we could not perform these tests for Ne_LD and Ne_mean due to the small sample size of the remaining *OC* group.

Nevertheless, Wilcoxon sign rank tests were performed to compare IW vs OW populations for Ne_LD and Ne_mean, but none were statistically significant. When using 13 loci, Wilcoxon sign rank tests approached significance for Ne_SA and H_O ($p < 0.09$). A_R also showed significant differences (W=0; $p = 0.004$) between OC ($A_R = 4.6 \pm 0.2$) and IW + OW groups ($A_R = 3.6 \pm 0.4$).

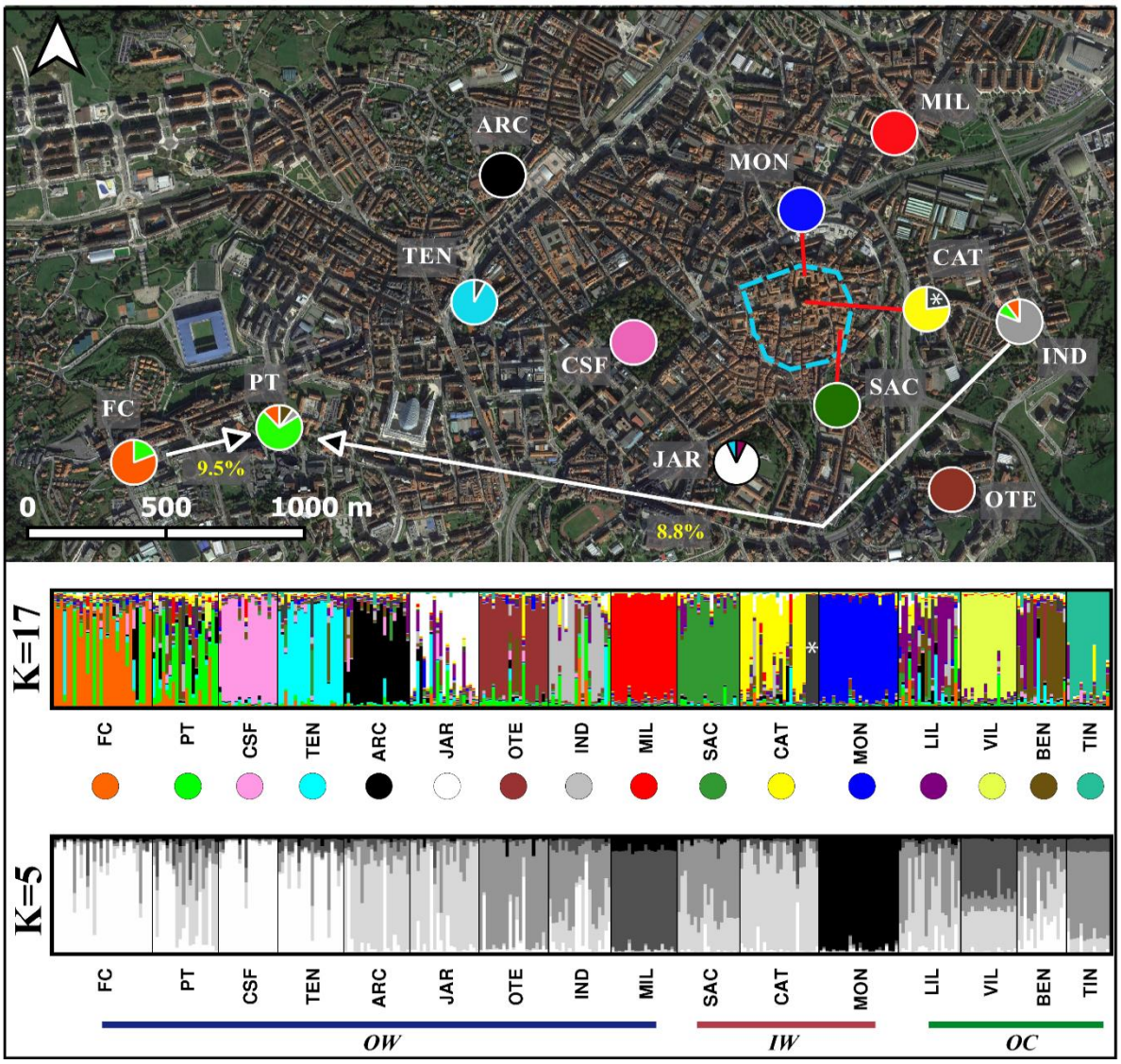

Fig. 2.2 Aerial photograph of Oviedo illustrating the sampling locations of urban populations (OW and IW). The two STRUCTURE barplots positioned below the aerial photograph represent the optimal number of clusters (K) according to the MLPP approach (K = 17) and the ΔK method (K = 5) using the 13 loci in HWE. Populations located outside Oviedo (OC) are not shown on the map (see also **Figure A2 in Appendix A**). The pie charts in the map represent the population cluster membership obtained with STRUCTURE for K = 17 (*i.e.* the top barplot). The position of pie charts corresponds to the location of sampled localities except in populations located in the inner wall perimeter (dashed blue line). Each pie chart is labelled with the respective population codes. Coloured circles below the barplot for K = 17 represent the main genetic membership for each studied population. Directions (arrows) and rates of gene flow (yellow numbers) are also illustrated among urban populations. The white asterisk in population CAT denotes individuals exhibiting a genetic membership not shared with other sampled populations.

Table 2.4 Matrix of pairwise genetic differentiation between populations calculated from 13 loci. Below and above the diagonal are pairwise F_{ST} and Jost's D_{EST}, respectively. All pairwise values are significant except pairwise D_{EST} in population pair FC/PT (in bold).

	FC	PT	CSF	TEN	ARC	JAR	OTE	IND	MIL	SAC	CAT	MON	LIL	VIL	BEN	TIN
FC	0	**0.053**	0.251	0.142	0.135	0.240	0.171	0.156	0.325	0.236	0.212	0.313	0.199	0.333	0.159	0.426
PT	0.039	0	0.261	0.182	0.099	0.196	0.185	0.132	0.352	0.195	0.135	0.346	0.161	0.286	0.144	0.437
CSF	0.095	0.112	0	0.252	0.308	0.254	0.237	0.210	0.395	0.334	0.312	0.398	0.203	0.398	0.205	0.492
TEN	0.067	0.074	0.102	0	0.183	0.157	0.172	0.170	0.326	0.210	0.185	0.262	0.144	0.272	0.165	0.270
ARC	0.080	0.063	0.133	0.094	0	0.182	0.211	0.183	0.278	0.178	0.146	0.408	0.102	0.273	0.156	0.410
JAR	0.084	0.081	0.118	0.077	0.087	0	0.253	0.237	0.326	0.233	0.169	0.363	0.135	0.253	0.182	0.374
OTE	0.063	0.062	0.103	0.071	0.088	0.089	0	0.179	0.357	0.213	0.228	0.306	0.209	0.380	0.166	0.326
IND	0.071	0.055	0.106	0.073	0.089	0.089	0.071	0	0.362	0.193	0.131	0.412	0.143	0.301	0.215	0.361
MIL	0.121	0.127	0.177	0.139	0.130	0.147	0.137	0.146	0	0.296	0.267	0.326	0.362	0.291	0.382	0.462
SAC	0.083	0.061	0.122	0.089	0.085	0.090	0.073	0.083	0.127	0	0.147	0.389	0.123	0.337	0.265	0.441
CAT	0.075	0.064	0.133	0.078	0.074	0.068	0.078	0.075	0.105	0.069	0	0.370	0.166	0.246	0.198	0.363
MON	0.125	0.142	0.193	0.138	0.176	0.167	0.139	0.172	0.185	0.158	0.153	0	0.341	0.445	0.353	0.452
LIL	0.067	0.066	0.095	0.066	0.059	0.060	0.068	0.057	0.124	0.048	0.062	0.138	0	0.231	0.119	0.313
VIL	0.107	0.120	0.171	0.130	0.124	0.127	0.133	0.135	0.151	0.125	0.125	0.207	0.088	0	0.361	0.498
BEN	0.051	0.047	0.095	0.057	0.079	0.072	0.070	0.073	0.137	0.082	0.079	0.146	0.053	0.113	0	0.334
TIN	0.123	0.139	0.172	0.110	0.145	0.124	0.113	0.126	0.196	0.147	0.134	0.192	0.102	0.179	0.094	0

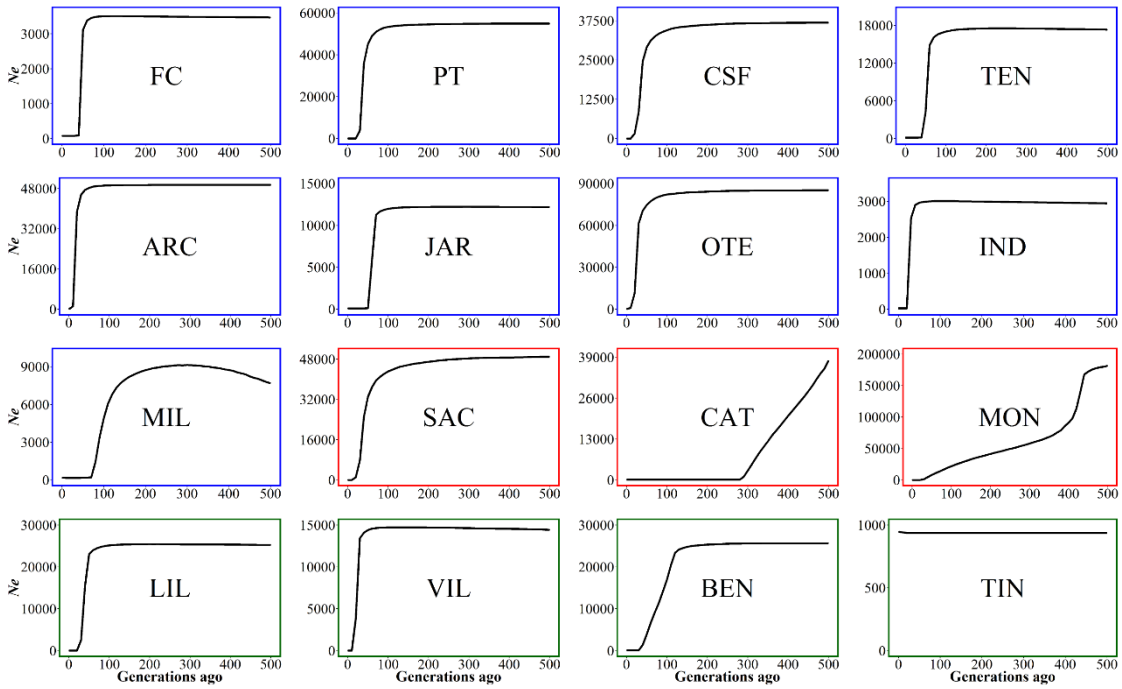

Fig. 2.3 *Ne* trajectories from present (0) to 500 generations ago for the 16 populations analysed in VarEff. Different colours in plots' borders represent the relative location of the population (blue – OW; red – IW; green – OC). Note that the y-axis (*Ne*) has a different scale in each plot.

For response variables characterizing genetic diversity and differentiation (A_R, R, H_O, and DIFF), no regression model was significantly better than the null model (**Table A12 in Appendix A**). PS was positively associated with contemporary *Ne* (namely Ne_LD and Ne_mean; **Table A13 in Appendix A**), exhibiting high importance (range w_+ = 0.70 – 0.89) and 95% CIs that did not overlap zero (**Table 2.5**). POST was negatively associated with Ne_LD, except in models containing PS, and thus, we identified PS as the only meaningful predictor of contemporary *Ne*. There was also minor evidence of a negative association of TI with A_R, with only one model showing 95% CIs that did not overlap zero. All model results are provided in **Tables A14 and A15 in Appendix A**. Regression models based on variables estimated with 13 loci provided similar results with PS exhibiting a positive relationship with Ne_LD and Ne_mean (**Table A16 in Appendix A**).

When excluding population CAT, which showed evidence of potential admixture, in addition to strong support for the influence of PS on contemporary *Ne*, POST also showed a significant negative relationship with A_R (range w_+ = 0.59 – 0.72; 95% CIs = [-0.907, -0.031]) and a positive association with DIFF (range w_+ = 0.64 – 0.68; 95% CIs = [0.004, 0.158]) (**Table A17 in Appendix A**). This statistical significance exhibited by POST with both metrics did not hold when testing a dataset based on 13 loci and without CAT.

Table 2.5 Regression modelling results for models exhibiting higher support than the null model and containing significant associations between response variables and a predictor (underlined). Regression parameters were obtained by model averaging for each response variable. The following regression parameters are represented: regression coefficients (β), standard errors (SE), 95% CIs of β and variable relative importance (w_+). Intercept (null model) estimates are not shown. Predictor variables used were time since isolation (TI), patch size (PS), bottleneck magnitude (MG) and post-bottleneck time (POST). Response variables shown: *Ne* obtained with LD approached (Ne_LD) and averaged *Ne* (Ne_mean).

Model	β	SE	95%CI	w_+
Ne_LD ~ TI+PS				
PS	1.049	0.264	(0.590, 1.516)	0.84
Ne_LD ~ PS+MG				
PS	1.080	0.334	(0.553, 1.644)	0.89
Ne_LD ~ PS+POST				
PS	1.021	0.250	(0.574, 1.468)	0.70
Ne_mean ~ TI+PS				
TI	-0.028	0.105	(-0.684, 0.255)	0.13
PS	0.707	0.210	(0.239, 1.176)	1.00
Ne_mean ~ PS+MG				
PS	0.712	0.216	(0.230, 1.194)	1.00
MG	-0.125	0.256	(-0.704, 0.454)	0.09
Ne_mean ~ PS+POST				
PS	0.703	0.208	(0.238, 1.168)	1.00
POST	-0.069	0.161	(-0.772, 0.135)	0.22

2.5 – Discussion

Identifying the processes driving changes in genetic variation during urbanization is crucial for understanding contemporary evolution and for conservation practices. Here, we examined a well-characterized urban population system and used an extensive analytical framework to study the effects of urbanization on genetic diversity, differentiation and contemporary *Ne*. Coalescence analyses demonstrated the drastic effects of urbanization on historical *Ne*, contributing to an increase in genetic differentiation (likely occurring in tens to a few hundreds of generations). Furthermore, the incorporation of demographic history, time since isolation and patch data in a regression modelling framework revealed that patch size was paramount in determining contemporary *Ne* and, by extension, influencing genetic drift in shaping contemporary genetic diversity and differentiation. The evidence for the roles of demographic history and time since isolation was mixed – both had little importance in regression models including all 16 populations, but demographic history had a significant relationship with allelic richness and population differentiation in models that excluded a IW population (CAT) showing signs of recent admixture. Hence, this study highlights the complex interplay between

demography, time and habitat in shaping current patterns of genetic variation. It comprises one of the very few empirical studies conducted in urban environments that explicitly incorporates these factors to show how urbanization affects genetic variation.

2.5.1 – Do urban populations exhibit high genetic differentiation, reduced genetic diversity and small *Ne*?

Contrary to our expectations, we did not find that urban populations of fire salamanders exhibited lower genetic diversity than rural populations. Although Ne_SA and A_R were lower in urban (IW + OW) compared with rural (OW) populations, these differences were not statistically significant. Overall, the urban populations studied here exhibit low effective population sizes, but given the environmental context (*i.e.* small-sized patches and high anthropogenic disturbance), the estimated *Ne* values are higher than expected. Studies performed in urban amphibian populations lack quantitative demographic data, preventing us from inferring if the demographic patterns seen here are similar to other urban dwellers. Interestingly, though, *Ne* exhibited by Oviedo's populations are comparable to effective sizes observed in metapopulation systems of pond-breeding amphibians outside of urban environments (*e.g.* Beebee 2009; Wang *et al.* 2011; Wang 2012; Roth and Jehle 2016). On the other hand, *Ne* in most populations is below recommended thresholds proposed in the literature to avoid inbreeding depression (*Ne* > 50 in Jamieson and Allendorf 2012; *Ne* > 100 in Frankham *et al.* 2014), making them potentially vulnerable to deleterious effects of genetic drift (Frankham 2005). Whether this small *Ne* coupled with the high relatedness levels is negatively reflected in individual fitness remains unknown. Previous studies conducted in lizards and frogs found higher fluctuating asymmetry in urban populations comparatively to their rural counterparts (*e.g.* Lazić *et al.* 2013; Eterovick *et al.* 2016), although the causes of higher fluctuating asymmetry were attributed to factors other than inbreeding.

The low *Ne* and high relatedness levels reported here together with the high genetic diversity in Oviedo appear conflicting. A previous study (Álvarez *et al.* 2015) conducted in population FC (IW) revealed unexpectedly high genetic diversity despite the small number of individuals confined within a small patch (248 m^2). We confirmed this pattern by expanding sampling throughout Oviedo. Overall, genetic diversity metrics (mean H_O = 0.667; mean A_R = 5.25) were relatively high across sampled urban sites. This suggests that they were not substantially affected by urbanization, despite being slightly lower than in rural populations; similar diversity values were also found in natural mainland populations of fire salamanders in Galician populations (NW Spain; Velo-Antón *et al.* 2012). Genetic studies performed in urban environments with distinct urban-dwelling amphibian species reported lower mean values of

diversity for the moor frog (*Rana arvalis*; Arens *et al.* 2007) and in plethodontid salamanders (Noël and Lapointe 2010; Munshi-South *et al.* 2013), while in the wood frog (*Lithobates sylvaticus*; Furman *et al.* 2016) diversity levels were very similar to those observed in our study. In Oviedo, fire salamander populations are putatively isolated to a greater extent than these species (see below), making the observed genetic diversity even more surprising. Álvarez *et al.* (2015) suggested that the availability of shelter and food resources during subterranean activity may constitute key factors for the survival of these populations. During sampling, we did indeed observe that crevices and holes in walls and other structures are abundant and used as a refuge by fire salamanders, possibly reducing mortality and maintaining *Ne* in high enough values to promote relatively high levels of diversity. Additionally, Álvarez *et al.* (2015) found very high *Ne*/*N* ratios (>0.50; see Palstra and Fraser 2012) which suggest the existence of mechanisms of genetic compensation. For instance, the ability of females to store sperm from multiple males (Caspers *et al.* 2014) and deliver offspring with multiple paternity in a single parturition event may increase the reproductive success of males in such a small area, possibly boosting *Ne* and genetic diversity.

Multiple lines of evidence demonstrated very high genetic differentiation between populations of fire salamanders in Oviedo, despite being isolated for only tens to a few hundred generations and separated by only several hundred metres (*e.g.* CAT/MON are only 93 m apart). BAYESASS found no evidence of contemporary gene flow between all but four pairs of populations, possibly due to the urban matrix coupled with the low dispersal capability of fire salamanders (Schulte *et al.* 2007; Ficetola *et al.* 2012). Estimates of pairwise F_{ST} (global F_{ST} = 0.103 for IW and OW populations) for many population pairs are also high, almost comparable to those in insular populations of fire salamanders, which putatively have been isolated for much longer (VeloAntón *et al.* 2012). Other studies in urban-dwelling amphibians have found a global F_{ST} that varies considerably across different systems, being much lower in moor frogs (Furman *et al.* 2016) and in the red-backed salamander (*Plethodon cinereus*) on Montréal Island (Noël and Lapointe 2010) but quite high in the stream-dwelling northern dusky salamander (*Desmognathus fuscus*) in New York, where population extirpation and degradation of streams likely led to a marked decrease in genetic diversity as well.

Although we detected very little contemporary gene flow in our study system, populations FC and PT exhibited moderate gene flow and low pairwise F_{ST}. These populations are separated by 500 m in the western corner of Oviedo. This area is more recent and less urbanized compared with the central area of the city, containing some green spaces (*e.g.* parks) between FC and PT that may be acting as stepping stones in promoting genetic connectivity (**Figure 2.2**). Given the short time over which these populations have been

isolated, we cannot exclude the possibility that admixture observed here may constitute an artefact of historical gene flow rather than reflecting contemporary genetic connectivity. Historical migration may also explain why gene flow estimates in three population pairs, involving IW and OC populations, were high. Given the low dispersal capability of fire salamanders and the nearly impervious urban matrix, recent gene flow between urban and rural populations is very unlikely.

Obtaining accurate estimates of the optimal number of clusters (K) is challenging because complex patterns of genetic structure may arise due to the combination of species life-history traits, population-specific demography and historical processes. Meirmans (2015) suggested that the interpretation of distinct valid (sub)optimal K values may be more informative to better understand the actual genetic structure than just looking at a single K value. In this study, the ΔK (K = 5 and K = 16) and the MLPP (K = 17) approaches yielded different optimal K. While K = 5 may reflect the uppermost hierarchical structure in our study system (Evanno *et al.* 2005), a high number of independent genetic units (K = 16/17) is also plausible considering our results (*i.e.* high pairwise differentiation, absence of gene flow and population small *Ne*). Interestingly, K = 17 raises the possibility of immigration to Oviedo's cathedral (CAT), as shown by the assignment of four individuals to a unique unsampled genetic cluster, in spite of being putatively isolated for more than 1000 years by the cathedral's walls. Intentional or accidental human-mediated translocations to population CAT within the last tens of generations cannot be ruled out. During the Spanish civil revolution (1930s), the cathedral's walls were destroyed, remaining unrepaired for about 10 years. During this period, it is possible that CAT received immigrants from other unsampled IW populations such as one adjacent in the cathedral's graveyard.

2.5.2 – What are the influences of patch size, demographic history and time since isolation on genetic variation and contemporary demography?

Our regression modelling revealed that patch size is an important driver of effective population size in urban populations. A larger patch of suitable habitat houses greater availability of food resources and shelter, increasing the population size that can be sustained (*e.g.* Jackson and Fahrig 2016). Hence, it is not surprising that OC populations exhibited larger *Ne* compared to populations located in Oviedo (IW + OW). This is one of the first empirical studies to quantitatively show the relationship between patch size and *Ne*, and our results are consistent with others that have found similar associations in other amphibians (*e.g.* Wang *et al.* 2011). Because it is intimately linked with genetic drift, *Ne* can influence patterns of genetic differentiation (Weckworth *et al.* 2013; Ellegren and Gautier 2016). Our results are consistent

with this in some urban populations (*e.g.* population JAR), in which larger *Ne* was associated with lower genetic differentiation (**Tables 2.4 and 2.5**) compared to others isolated for similar lengths of time. On the other hand, some populations with very low *Ne* (*e.g.* population CSF) exhibited genetic diversity and differentiation similar to populations isolated for much longer such as IW populations (see below).

The other two factors we studied are related to population history: (1) demographic history (historical *Ne*) and (2) time since isolation. In line with our expectations, we found evidence for pronounced declines in *Ne* across our study system. Considering the history of these urban populations, the estimated dates of these declines (fairly recent) are concomitant with the construction and increasing urbanization of Oviedo. Additionally, we also identified, as hypothesized, older declines in IW populations, which are putatively the oldest urban populations. The existence of bottlenecks, as supported by VarEff, may explain why null allele frequencies were high for some loci. Dabrowski *et al.* (2014) recently demonstrated a high false detection rate of null alleles positively correlated with the occurrence of bottlenecks. Although INEST (which we used to detect null alleles) was not tested in that study, the large variance in null allele frequencies for our loci (SD > 0.10) points to stochastic effects in genetic composition caused by bottlenecks rather than consistent failure of allele scoring due to null alleles.

Despite the role of past declines in contemporary *Ne*, the influence of demographic history on genetic diversity and structure, as tested through regression modelling in our study, is not as clear as in other studies (*e.g.* Spurgin *et al.* 2014; Gonzalez Quevedo *et al.* 2015; Funk *et al.* 2016; Vandergast *et al.* 2016). Both variables derived from VarEff (MG and POST) had low relative importance. We also did not find significant differences in genetic variation between populations putatively isolated longer. To the best of our knowledge, empirical evidence explicitly demonstrating a link between time since isolation and genetic structure in urban environments is scarce (see Delaney *et al.* 2010), although previous studies highlighted a negative association between island age (proxy for time since isolation) and genetic diversity (Hurston *et al.* 2009; Wang *et al.* 2014).

Lack of statistical support for the roles of demographic history (MG and POST) and time since isolation may have three explanations, not mutually exclusive. First, although VarEff managed to correctly identify population demographic trends, we cannot discount the possibility that MG and POST may be quantitatively imprecise since VarEff was developed recently and has not been thoroughly tested. Second, the time-lag (number of generations to reach mutation-drift equilibrium after major demographic events) may be insufficient to generate significant changes in genetic patterns in populations affected by urbanization more

recently (see Peery *et al.* 2012; Epps and Keyghobadi 2015). This may be most prominent in populations displaying a large *Ne* (*e.g.* ARC and JAR), which is associated with an increase in time-lag to detect these effects (Epps and Keyghobadi 2015). Third, if there was indeed effective migration of individuals from other unsampled populations to CAT, long-term deleterious effects of isolation and demographic bottlenecks may have been ameliorated (Jangjoo *et al.* 2016; but see also Richardson *et al.* 2016). Therefore, population CAT potentially deviated from the assumption that it has been isolated for more than 1000 years, preventing us from adequately testing the role of long-term isolation and demographic history in genetic variation. In a statistical analysis with a relatively small sample size (n=12), a single population deviating from initial assumptions may have a large weight on modelled results. By removing CAT from statistical analyses, we found that post-bottleneck time had a significant negative relationship with allelic richness and a significant positive relationship with genetic differentiation. This suggests that populations experiencing older *Ne* declines in Oviedo (and which not have experienced recent gene flow) have lower diversity and increased structure, once they have been subject to the detrimental pressures of increasing urban development for a greater number of generations (Epps and Keyghobadi 2015). Time since isolation remained non-significant after removing CAT, suggesting that post-bottleneck time has greater importance in determining population genetic parameters. This statistical support for post-bottleneck time did not hold in a dataset of 13 loci, and thus, these results should be interpreted with caution. Sampling more populations and unravelling the demographic history of population CAT will be crucial to assessing the influence of both factors in contemporary genetic variation.

2.6 – Conclusions

More and more species exist outside of protected areas, subjecting them to threats from land use change, habitat fragmentation, and urbanization. Our study highlights the complex interplay between time since isolation, demographic history and population-specific traits in shaping neutral genetic variation (genetic diversity and differentiation) and contemporary demographic patterns (contemporary *Ne*) in populations experiencing severe habitat fragmentation via processes like urbanization. Only recently has empirical information on population genetic patterns in urban dwelling species been gathered, and more studies of urban landscape genetics are needed to better understand how urbanization affects biodiversity at the population level. The increasing availability of genomic tools has also increasingly allowed researchers to examine the effects of urbanization in adaptive genetic variation (Harris *et al.* 2015; Harris and Munshi-South 2016), which continues to be critical for understanding how species adapt to urban landscapes. In a world where continued growth in

urbanization is predicted (Seto *et al.* 2012), studies focused on both neutral and adaptive genetic variation in urban dwelling species will be fundamental in helping us understand and predict the effects of urbanization in the future.

2.7 – Acknowledgments

We are grateful to Community of the Monasterio de San Pelayo and to Benito Gallego for allowing the access to the Monastery and Cathedral's courtyard. We thank also to Jacobo Blanco and Tomás Cortizo for providing old maps and documents about Oviedo. This work was funded by FEDER funds through the Operational Programme for Competitiveness Factors — COMPETE and by National Funds through FCT - Foundation for Science and Technology under the PTDC/BIA-EVF/3036/2012 and FCOMP- 01-0124-FEDER-028325. GVA and AL are supported by FCT (IF/ 01425/2014 and PD/BD/106060/2015, respectively).

2.8 – References

Alcobendas M, Castanet J (2000) Bone growth plasticity among populations of *Salamandra salamandra*: interactions between internal and external factors. *Herpetologica*, **56**, 14–26.

Álvarez D, Lourenço A, Oro D, Velo-Antón G (2015) Assessment of census (*N*) and effective population size (*Ne*) reveals consistency of *Ne* single-sample estimators and a high *Ne*/*N* ratio in an urban and isolated population of fire salamanders. *Conservation Genetics Resources*, **7**, 705–712.

Arens P, van der Sluis T, van't Westende, Vosman B, Vos CC, Smulders MJM (2007) Genetic population differentiation and connectivity among fragmented Moor frog (*Rana arvalis*) populations in The Netherlands. *Landscape Ecology*, **19**, 504-511.

Barton K (2016) MuMIn: multi-model inference. R package version 1.15.6

Beebee TJC (2009) A comparison of single-sample effective size estimators using empirical toad (*Bufo calamita*) population data: Genetic compensation and population size-genetic diversity correlations. *Molecular Ecology*, **18**, 4790–4797.

Beninde J, Feldmeier S, Werner M *et al.* (2016) Cityscape genetics: structural vs. functional connectivity of an urban lizard population. *Molecular Ecology*, **25**, 4984–5000.

Benjamini Y, Hochberg Y (1995) Controlling the false discovery rate: a practical and powerful approach to multiple testing. *Journal of the Royal Statistical Society. Series B.*, **57**, 289–300.

Bulut Z, McCormick CR, Gopurenko D, Williams RN, Bos DH, DeWoody JA (2009) Microsatellite mutation rates in the eastern tiger salamander (*Ambystoma tigrinum tigrinum*) differ 10-fold across loci. *Genetica*, **136**, 501-504.

Burnham K, Anderson D (2002) *Model selection and multimodel inference – a practical information-theoretic approach*. Springer-Verlag, New York.

Caspers BA, Krause ET, Hendrix R *et al.* (2014) The more the better - polyandry and genetic similarity are positively linked to reproductive success in a natural population of terrestrial salamanders (*Salamandra salamandra*). *Molecular Ecology*, **23**, 239–250.

Chybicki IJ, Burczyk J (2009) Simultaneous estimation of null alleles and inbreeding coefficients. *The Journal of Heredity*, **100**, 106–113.

Dabrowski MJ, Pilot M, Kruczyk M, Zmihorski M, Umer HM, Gliwicz J (2014) Reliability assessment of null allele detection: Inconsistencies between and within different methods. *Molecular Ecology Resources*, **14**, 361–373.

Delaney KS, Riley SPD, Fisher RN (2010) A rapid, strong, and convergent genetic response to urban habitat fragmentation in four divergent and widespread vertebrates. *PLoS ONE*, **5**, e12767.

Do C, Waples RS, Peel D, MacBeth GM, Tillett BJ, Ovenden JR (2014) NeEstimator v2: re-implementation of software for the estimation of contemporary effective population size (*Ne*) from genetic data. *Molecular Ecology Resources*, **14**, 209–214.

Ellegren H, Galtier N (2016) Determinants of genetic diversity. *Nature Reviews Genetics*, **17**, 422-433.

Epps CW, Keyghobadi N (2015) Landscape genetics in a changing world: disentangling historical and contemporary influences and inferring change. *Molecular Ecology*, **24**, 6021–6040.

Eterovick PC, Sloss BL, Scalzo JAM, Alford RA (2016) Isolated frogs in a crowded world: Effects of human-caused habitat loss on frog heterozygosity and fluctuating asymmetry. *Biological Conservation*, **195**, 52–59.

Evanno G, Regnaut S, Goudet J (2005) Detecting the number of clusters of individuals using the software STRUCTURE: a simulation study. *Molecular Ecology*, **14**, 2611 – 2620.

Faubet P, Waples RS, Gaggiotti OE (2007) Evaluating the performance of a multilocus Bayesian method for the estimation of migration rates. *Molecular Ecology*, **16**, 1149-1166.

Ficetola GF, Manenti R, De Bernardi F, Padoa-Schioppa E (2012) Can patterns of spatial autocorrelation reveal population processes? An analysis with the fire salamander. *Ecography*, **35**, 693–703.

Frankham R (2005) Genetics and extinction. *Biological Conservation*, **126**, 131–140.

Frankham R, Bradshaw CJ, Brook BW (2014) Genetics in conservation management: Revised recommendations for the 50/500 rules, Red List criteria and population viability analyses. *Biological Conservation*, **170**, 56–63.

Funk WC, Lovich RE, Hohenlohe PA *et al.* (2016) Adaptive divergence despite strong genetic drift: Genomic analysis of the evolutionary mechanisms causing genetic differentiation in the island fox (*Urocyon littoralis*). *Molecular Ecology*, **25**, 2176–2194.

Furman BLS, Scheffers BR, Taylor M, Davis C, Paszkowski CA (2016) Limited genetic structure in a wood frog (*Lithobates sylvaticus*) population in an urban landscape inhabiting natural and constructed wetlands. *Conservation Genetics*, **17**, 19–30.

García-París M, Alcobendas M, Buckley D, Wake D (2003) Dispersal of viviparity across contact zones in Iberian populations of Fire salamanders (*Salamandra*) inferred from discordance of genetic and morphological traits. *Evolution*, **57**, 129–143.

González García VJ (1984) *El Oviedo antiguo y medieval (Estudio histórico-arqueológico sobre los orígenes y la formación de la ciudad)*. Colección Sancta Ovetensis: Principado Asturias, nº VIII. Ayuntamiento de Oviedo.

Gonzalez-Quevedo C, Spurgin LG, Illera JC, Richardson DS (2015) Drift, not selection, shapes toll-like receptor variation among oceanic island populations. *Molecular Ecology*, **24**, 5852–5863.

Gortat T, Rutkowski R, Gryczyńska A, Pieniążek A, Kozakiewicz A, Kozakiewicz M (2015) Anthropopressure gradients and the population genetic structure of *Apodemus agrarius*. *Conservation Genetics*, **16**, 649–659.

Grueber CE, Nakagawa S, Laws RJ, Jamieson IG (2011) Multimodel inference in ecology and evolution: challenges and solutions. *Journal of Evolutionary Biology*, **24**, 699–711.

Harris SE, O'Neill RJ, Munshi-South J (2015) Transcriptome resources for the white-footed mouse (*Peromyscus leucopus*): new genomic tools for investigating ecologically divergent urban and rural populations. *Molecular Ecology Resources*, **15**, 382-394.

Harris SE, Munshi-South J (2016) Scans for positive selection reveal candidate genes and local adaptation of *Peromyscus leucopus* populations to urbanization. *bioRxiv*, doi: 10.1101/038141.

Hendrix R, Schmidt BR, Schaub M, Krause ET, Steinfartz S (2017) Differentiation of movement behaviour in an adaptively diverging salamander population. *Molecular Ecology*, **26**, 6400–6413.

Hendrix R, Hauswaldt JS, Veith M, Steinfartz S (2010) Strong correlation between cross-amplification success and genetic distance across all members of 'True salamanders'

(Amphibia: Salamandridae) revealed by *Salamandra salamandra*-specific microsatellite loci. *Molecular Ecology Resources*, **10**, 1038–1047.

Hurston H, Voith L, Bonanno J *et al.* (2009) Effects of fragmentation on genetic diversity in island populations of the Aegean wall lizard *Podarcis erhardii* (Lacertidae, Reptilia). *Molecular Phylogenetics and Evolution*, **52**, 395–405.

Jackson ND, Fahrig L (2016) Habitat amount, not habitat configuration, best predicts population genetic structure in fragmented landscapes. *Landscape Ecology*, **31**, 951-968.

Jamieson IG, Allendorf FW (2012) How does the 50/500 rule apply to MVPs? *Trends in Ecology and Evolution*, **27**, 578–84.

Jangjoo M, Matter SF, Roland J, Keyghobadi N (2016) Connectivity rescues genetic diversity after a demographic bottleneck in a butterfly population network. *Proceedings of the National Academy of Sciences*, **113**, 10914–10919.

Johnson PCD, Haydon DT (2007) Maximum-likelihood estimation of allelic dropout and false allele error rates from microsatellite genotypes in the absence of reference data. *Genetics*, **175**, 827–842.

Jones O, Wang J (2010) COLONY: a program for parentage and sibship inference from multilocus genotype data. *Molecular Ecology Resources*, **10**, 551–555.

Jost L (2008) G_{ST} and its relatives do not measure differentiation. *Molecular Ecology*, **17**, 4015–4026.

Keenan K, McGinnity P, Cross TF, Crozier WW, Prodöhl PA (2013) diveRsity: an R package for the estimation of population genetics parameters and their associated errors. *Methods in Ecology and Evolution*, **4**, 782-788.

Kopelman NM, Mayzel J, Jakobsson M, Rosenberg NA, Mayrose I (2015) CLUMPAK: a program for identifying clustering modes and packaging population structure inferences across K. *Molecular Ecology Resources*, **15**, 1179-1191.

Lazić MM, Kaliontzopoulou A, Carretero MA, Crnobrnja-Isailović J (2013) Lizards from urban areas are more asymmetric: using fluctuating asymmetry to evaluate environmental disturbance. *PLoS ONE*, **8**, e84190.

McKinney ML (2006) Urbanization as a major cause of biotic homogenization. *Biological Conservation*, **127**, 247–260.

Meirmans PG (2015) Seven common mistakes in population genetics and how to avoid them. *Molecular Ecology*, **24**, 3223–3231.

Munshi-South J (2012) Urban landscape genetics: canopy cover predicts gene flow between white-footed mouse (*Peromyscus leucopus*) populations in New York City. *Molecular Ecology*, **21**, 1360–1378.

Munshi-South J, Kharchenko K (2010) Rapid, pervasive genetic differentiation of urban white-footed mouse (*Peromyscus leucopus*) populations in New York City. *Molecular Ecology*, **19**, 4242–4254.

Munshi-South J, Nagy C (2014) Urban park characteristics, genetic variation, and historical demography of white-footed mouse (*Peromyscus leucopus*) populations in New York City. *PeerJ*, **2**, e310.

Munshi-South J, Zak Y, Pehek E (2013) Conservation genetics of extremely isolated urban populations of the northern dusky salamander (*Desmognathus fuscus*) in New York City. *PeerJ*, **1**, e64.

Munshi-South J, Zolnik CP, Harris SE (2016) Population genomics of the Anthropocene: urbanization is negatively associated with genome-wide variation in white-footed mouse populations. *Evolutionary Applications*, **9**, 546–564.

Nikolic N, Chevalet C (2014) Detecting past changes of effective population size. *Evolutionary Applications*, **7**, 663–681.

Noël S, Lapointe FJ (2010) Urban conservation genetics: study of a terrestrial salamander in the city. *Biological Conservation*, **143**, 2823–2831.

Palstra FP, Fraser DJ (2012) Effective/census population size ratio estimation: a compendium and appraisal. *Ecology and Evolution*, **2**, 2357–2365.

Peakall R, Smouse PE (2012) GenAlEx 6.5: genetic analysis in Excel. Population genetic software for teaching and research – an update. *Bioinformatics*, **28**, 2537-2539.

Peery MZ, Kirby R, Reid BN *et al.* (2012) Reliability of genetic bottleneck tests for detecting recent population declines. *Molecular Ecology*, **21**, 3403–3418.

Pinheiro J, Bates D, DebRoy S, Sarkar D, R Development Core Team (2015) nlme: linear and nonlinear mixed effects models. R package version 3.1-122.

Pritchard JK, Stephens M, Donnelly P (2000) Inference of population structure using multilocus genotype data. *Genetics*, **155**, 945–959.

R Development Core Team (2015) R: a language and environment for statistical computing. R Foundation for Statistical Computing, Vienna, Austria.

Rebelo R, Caetano MH (1995) Use of the skeletochronological method for ecodemographical studies on *Salamandra salamandra gallaica* from Portugal. In: *Scientia Herpetologica* (eds Llorente GA, Montori A, Santos X, Carretero MA), pp. 135-140. Barcelona

Rambaut A, Suchard MA, Xie D, Drummond AJ (2014) Tracer v1.6. Available from http://beast.bio.ed.ac.uk/Tracer

Richardson JL, Brady SP, Wang IJ, Spear SF (2016) Navigating the pitfalls and promise of landscape genetics. *Molecular Ecology*, **25**, 849–863.

Rivera-Ortíz F, Aguilar R, Arizmendi MDC, Quesada-Avendaño M, Oyama K (2015) Habitat fragmentation and genetic variability of tetrapod populations. *Animal Conservation*, **18**, 249–258.

Rodriguez-Martínez S, Carrete M, Roques S, Rebolo-Ifrán N, Tella JL (2014) High urban breeding densities do not disrupt genetic monogamy in a bird species. *PLoS ONE*, **9**, e91314.

Roth S, Jehle R (2016) High genetic diversity of common toad (*Bufo bufo*) populations under strong natural fragmentation on a Northern archipelago. *Ecology and Evolution*, **6**, 1626–1636.

Rousset F (2008) GENEPOP'007: a complete re-implementation of the GENEPOP software for Windows and Linux. *Molecular Ecology Resources*, **8**, 103-106.

Schielzeth H (2010) Simple means to improve the interpretability of regression coefficients. *Methods in Ecology and Evolution*, **1**, 103–113.

Schulte U, Küsters D, Steinfartz S (2007) A PIT tag based analysis of annual movement patterns of adult fire salamanders (*Salamandra salamandra*) in a Middle European habitat. *Amphibia-Reptilia*, **28**, 531–536.

Segelbacher G, Strand TM, Quintela M *et al.* (2014) Analyses of historical and current populations of black grouse in Central Europe reveal strong effects of genetic drift and loss of genetic diversity. *Conservation Genetics*, **15**, 1183–1195.

Seto KC, Güneralp B, Hutyra LR (2012) Global forecasts of urban expansion to 2030 and direct impacts on biodiversity and carbon pools. *Proceedings of the National Academy of Sciences of the United States of America*, **109**, 16083–16088.

Spurgin LG, Illera JC, Jorgensen TH, Dawson DA, Richardson DS (2014) Genetic and phenotypic divergence in an island bird: isolation by distance, by colonization or by adaptation? *Molecular Ecology*, **23**, 1028–1039.

Steinfartz S, Kuesters D, Tautz D (2004) Isolation and characterization of polymorphic tetranucleotide microsatellite loci in the fire salamander *Salamandra salamandra* (Amphibia: Caudata). *Molecular Ecology Notes*, **4**, 626–628.

Vandergast AG, Wood DA, Thompson AR, Fisher M, Barrows CW, Grant TJ (2016) Drifting to oblivion? Rapid genetic differentiation in an endangered lizard following habitat fragmentation and drought. *Diversity and Distributions*, **22**, 344–357.

Velo-Antón G, García-París M, Galón P, Cordero Rivera A (2007) The evolution of viviparity in holocene islands: ecological adaptation versus phylogenetic descent along the transition from aquatic to terrestrial environments. *Journal of Zoological Systematics and Evolutionary Research*, **45**, 345–352.

Velo-Antón G, Santos X, Sanmartín-Villar I, Cordero-Rivera A, Buckley D (2015) Intraspecific variation in clutch size and maternal investment in pueriparous and larviparous *Salamandra salamandra* females. *Evolutionary Ecology*, **29**, 185–204.

Velo-Antón G, Zamudio KR, Cordero-Rivera A (2012) Genetic drift and rapid evolution of viviparity in insular fire salamanders (*Salamandra salamandra*). *Heredity*, **108**, 410–418.

Venables WN, Ripley BD (2002) *Modern applied statistics with S*. Springer, New York.

Wang IJ (2012) Environmental and topographic variables shape genetic structure and effective population sizes in the endangered Yosemite toad. *Diversity and Distributions*, **18**, 1033–1041.

Wang IJ, Johnson JR, Johnson BB, Shaffer HB (2011) Effective population size is strongly correlated with breeding pond size in the endangered California tiger salamander, *Ambystoma californiense*. *Conservation Genetics*, **12**, 911–920.

Wang J (2009) A new method for estimating effective population sizes from a single sample of multilocus genotypes. *Molecular Ecology*, **18**, 2148–2164.

Wang J (2011) Coancestry: A program for simulating, estimating and analysing relatedness and inbreeding coefficients. *Molecular Ecology Resources*, **11**, 141–145.

Wang S, Zhu W, Gao X *et al.* (2014) Population size and time since island isolation determine genetic diversity loss in insular frog populations. *Molecular Ecology*, **23**, 637–648.

Waples RS (2006) A bias correction for estimates of effective population size based on linkage disequilibrium at unlinked gene loci. *Conservation Genetics*, **7**, 167–184.

Waples RS, Antao T, Luikart G (2014) Effects of overlapping generations on linkage disequilibrium estimates of effective population size. *Genetics*, **197**, 769–780.

Waples RS, Do C (2010) Linkage disequilibrium estimates of contemporary Ne using highly variable genetic markers: a largely untapped resource for applied conservation and evolution. *Evolutionary Applications*, **3**, 244–262.

Weckworth B V, Musiani M, Decesare NJ, McDevitt AD, Hebblewhite M, Mariani S (2013) Preferred habitat and effective population size drive landscape genetic patterns in an endangered species. *Proceedings of the Royal Society B*, **280**, 20131756.

Weir BS, Cockerham CC (1984) Estimating F-statistics for the analysis of population structure. *Evolution*, **38**, 1358-1370.

Wilson GA, Rannala B (2003) Bayesian inference of recent migration rates using multilocus genotypes. *Genetics*, **163**, 1177-1191.

Yamamoto J, Uchida K, Takami Y (2013) Colonization and persistence of urban ant populations as revealed by joint estimation of kinship and population genetic parameters. *Journal of Heredity*, **104**, 639–648.

Zuur AF, Ieno EN, Walker NJ, Saveliev AA, Smith GM (2009) *Mixed effects models and extensions in ecology*. Springer, New York.

Chapter 3

Differences in dispersal between reproductive modes

Paper II

Fine-scale genetic structure in a salamander with two reproductive modes: does reproductive mode affect dispersal?

André Lourenço[1,2], Bernardo Antunes[1,2], Ian J. Wang[3] and Guillermo Velo-Antón[2]

Article published in *Evolutionary Ecology*, 2018, **32**, 699-732. doi: 10.1007/s10682-018-9957-0

[1] Departamento de Biologia da Faculdade de Ciências da Universidade do Porto, Rua Campo Alegre, 4169-007 Porto, Portugal.

[2] CIBIO/InBIO, Centro de Investigacao em Biodiversidade e Recursos Genéticos da Universidade do Porto, Instituto de Ciências Agrárias de Vairão, Rua Padre Armando Quintas 7, 4485-661 Vairão, Portugal

[3] Department of Environmental Science, Policy and Management, University of California, 130 Mulford Hall #3114, Berkeley, CA 94705 USA

3.1 – Abstract

Reproduction is intimately linked with dispersal, but the effects of changes in reproductive strategies on dispersal have received little attention. Such changes have occurred in many taxonomic groups, resulting in profound alterations in life-history. In amphibians, many species shifted from oviparous/larviparous aquatic reproduction (deposition of eggs or pre-metamorphic larvae in water) to pueriparous terrestrial reproduction (parturition of terrestrial juveniles). The latter provides greater independence from water by skipping the aquatic larval stage; however, the eco-evolutionary implications of this evolutionary step have been underexplored, largely because reproductive modes rarely vary at the intraspecific level, preventing meaningful comparisons. We studied the effects of a transition to pueriparity on dispersal and fine-scale genetic structure in the fire salamander (*Salamandra salamandra*), a species exhibiting two co-occurring reproductive modes: larviparity and pueriparity. We performed genetic analyses (parentage and genetic spatial autocorrelation) using 11 microsatellite loci to compare dispersal and fine-scale genetic structure in three larviparous and three pueriparous populations (354 individuals in total). We did not find significant differences between reproductive modes, but in some larviparous populations movement patterns may be influenced by site-specific features (type of water bodies), possibly due to passive water-borne dispersal of larvae along streams. Additionally, females (especially larviparous ones) appeared to be more philopatric, while males showed greater variation in dispersal distances. This study also points to future avenues of research to better understand the eco-evolutionary implications of changes in reproductive modes in amphibians.

Keywords: dispersal, larviparity, pueriparity, transition in reproductive mode, *Salamandra salamandra*, spatial autocorrelation.

3.2 – Introduction

Dispersal influences many ecological (*e.g.* tracking optimal conditions), demographic (*e.g.* regulating population density), and evolutionary (*e.g.* gene flow) processes, contributing to the long-term persistence of populations (Bowler and Benton 2005; Cosgrove *et al.* 2018). Dispersal is a trait with multi-causality, governed by a complex interplay between intrinsic (phenotype-dependent) and extrinsic (environment-dependent) factors (Clobert *et al.* 2009; Ousterhout and Semlitsch 2018), which often promote high variability in dispersal-related traits (*e.g.* physical capacity for dispersal and movement behaviour) not only among but also within species (Stevens *et al.* 2010). The effects of environmental variation (including landscape

composition and configuration, climate, and topography) between patches on animal movement have been shown to influence patterns of dispersal to a large extent (*e.g.* Velo-Antón *et al.* 2013; Wang 2013; Ousterhout and Semlitsch 2018). Besides extrinsic factors, a multitude of intrinsic traits (*e.g.* body size, age, sex, physiology, behaviour and genetic) are known to covary with dispersal-related traits (Ronce and Clobert 2012; Saastamoinen *et al.* 2018). In particular, sex is commonly associated with differences in dispersal in various taxa, with individuals of one sex usually moving farther due to unequal social (*e.g.* mating system) and/or ecological (*e.g.* competition for mates or resources) pressures acting upon them (Trochet *et al.* 2016).

Because dispersal is the primary mechanism driving gene flow, dispersal-related traits and other co-evolving traits are often intimately linked with reproductive biology, evolving in a way to increase fitness and reproductive success (Bowler and Benton 2005; Bonte *et al.* 2012). Hence, species that have undergone transitions in reproductive modes may have also experienced evolutionary changes in dispersal-related traits, but this topic has remained largely underexplored. A transition from an egg-laying reproductive mode to a live-bearing (viviparous) one has occurred more than 150 times in a wide array of vertebrates (mostly in reptiles and, to a lesser extent, in amphibians; reviewed in Blackburn 2015), entailing profound morphological, physiological, life-history, behavioural, ecological, and genetic changes, especially in females (*e.g.* Buckley *et al.* 2007; van Dyke *et al.* 2014; Shine 2015; Helmstetter *et al.* 2016; Halliwell *et al.* 2017). Previous work has shown that a transition to viviparity may affect dispersal capacity. For instance, in reptiles and fishes, viviparous females incur greater energetic costs and, consequently, have lower dispersal abilities due to the physical burden of carrying offspring for a longer period compared to egg-laying congeners (see Shine 1980; Shine 2015; Banet *et al.* 2016). Additionally, dispersal behaviour in these examples is expected to be governed to a much lesser extent by the surrounding environment, because the shift in reproductive mode (*e.g.* live-bearing) entailed a greater independence from habitat features required for successful reproduction (*e.g.* suitable nests for egg deposition in reptiles and water bodies for development of embryos and larvae in amphibians; see Russell *et al.* 2005; Shine 2015). This subject, in particular, has received very little attention, although a couple of studies on reptiles have suggested that low availability of nesting sites promotes longer movements of oviparous, compared to viviparous females, because they must seek suitable sites for egg deposition (see Shine 2015).

In the three amphibian orders, there are examples of species shifting from ancestral oviparous or larviparous aquatic reproduction (delivery of eggs or larvae in water, respectively) to pueriparous terrestrial reproduction (parturition of terrestrial juveniles; Blackburn 2015),

possibly triggered by the lack of surface water in drier environments, as proposed by Velo-Antón *et al.* (2015) in *Salamandra*. The larval stage in pueriparous amphibians is absent, conferring a fully terrestrial lifestyle and total independence from water when depositing offspring. Given that the dispersal ecology of aquatic-breeding amphibians is intrinsically linked to the distribution and availability of water sources for reproduction (Russell *et al.* 2005; Semlitsch 2008), a shift from aquatic reproduction to terrestrial is expected to bring changes in dispersal behaviour. Specifically, terrestrial modes of reproduction putatively allow individuals to expand home ranges and colonize new areas to exploit more resources without relying on proximity to suitable water bodies (Liedtke *et al.* 2017; Lourenço *et al.* 2017). Based on this premise, previous landscape studies have suggested that terrestrial reproduction in amphibians may promote higher connectivity in heterogeneous, fragmented landscapes, given their ability to thrive in water-limited environments (direct-developer Dwarf squeaker frog, *Arthroleptis xenodactyloides*, Measey *et al.* 2007; pueriparous Nimba toad, *Nimbaphrynoides occidentalis*, Sandberger-Loua *et al.* 2018). Conversely, the lungless plethodontid salamanders (Plethodontidae), in which most species exhibit terrestrial reproduction (direct-developing), have very limited dispersal capacity (typically < 60 m; reviewed in Smith and Green 2005) and significant genetic differentiation over fine spatial scales mostly due to their high susceptibility to desiccation (*e.g. Batrachoseps attenuates*, Martínez-Solano *et al.* 2007; *Plethodon albagula*, Peterman *et al.* 2014).

Previous studies, however, have not included direct comparisons between aquatic and terrestrial breeding amphibians with similar traits and inhabiting analogous landscape contexts and, therefore, do not provide strong inferences about the effects of terrestrial reproduction on dispersal. Studies including species with multiple reproductive modes (aquatic vs. terrestrial reproduction) at the intraspecific level are crucial for performing comparative analyses that provide quantitative assessments of the effects of reproductive mode on dispersal. Such systems can reduce the potential bias arising from comparisons between closely related species, in which confounding factors such as differences in other phenotypic traits and the environments they inhabit may prevent robust conclusions. However, variation in reproductive modes within species is rare (Blackburn *et al.* 2015; Velo-Antón *et al.* 2015).

In amphibians, intraspecific variation in reproductive strategies involving live-bearing has been reported in only two sister urodele species, the fire salamander (*Salamandra salamandra*, Linnaeus 1758; Velo-Antón *et al.* 2015) and the North-African fire salamander (*S. algira*, Bedriaga 1883; Dinis and Velo-Antón 2017). To better understand the influence of terrestrial reproduction on movement, we used *S. salamandra* as a model system. Two distinct reproductive strategies co-occur in *S. salamandra*: larviparity, in which females deliver up to

ca. 90 larvae in water bodies (*e.g.* streams and ponds) after a gestation period of approximately 90 days; and pueriparity, in which females deliver ca. 1-35 fully metamorphosed terrestrial juveniles after the same gestation period (Buckley *et al.* 2007; Velo-Antón *et al.* 2015). Throughout most of its range, *S. salamandra* females are larviparous (the ancestral trait), but pueriparity is present in three Iberian subspecies (*S. s. bernardezi*, *S. s. fastuosa* and *S. s. gallaica*; Velo-Antón *et al.* 2015). While pueriparity in *S. s. bernardezi* likely arose during the Pleistocene in the Cantabrian Mountains (north of Spain), later introgressing eastwards with *S. s. fastuosa* populations during subsequent cycles of warm and cold climates (García-París *et al.* 2003), pueriparity in *S. s. gallaica* originated independently in only two insular populations of northwestern Spain (Velo-Antón *et al.* 2007, 2012). Moreover, not only because shifts in reproductive strategies can cause greater changes in the biology and ecology of females, but also because sex itself is a major factor influencing dispersal within species, testing for sex-biased dispersal in *S. salamandra* may contribute additional insights into the role of terrestrial reproduction on dispersal and its evolutionary consequences. Whether there are sex-specific differences in dispersal in *S. salamandra* is unclear. While Schulte *et al.* (2007) did not observe sex-specific differences in movement patterns in *S. s. terrestris*, several studies suggested male-biased dispersal as a potential driver of the mito-nuclear discordances observed in *S. salamandra* across different regions and different subspecies (northern Spain, García-París *et al.* 2003; central Spain, Pereira *et al.* 2016). Moreover, Helfer *et al.* (2012) used ecological and molecular methods to confirm male-biased dispersal in an alpine *Salamandra* species (*S. atra*).

Here, we use multilocus nuclear genetic data (microsatellites) to compare dispersal and fine-scale genetic structure between larviparous and pueriparous populations in *S. salamandra*. We hypothesize that (H1) pueriparous females will exhibit higher genetic similarity at greater distances (genetic autocorrelation), due to dispersal behaviour promoting longer dispersal movements, compared to larviparous females. This pattern is expected to arise due to greater dependency on proximity to water for delivery of larvae in larviparous females. Furthermore, given the mito-nuclear discordances found across the range of *S. salamandra*, likely due to male-biased dispersal, together with available evidence of such mechanism in other *Salamandra* species, we expect (H2) that males move farther than females.

3.3 – Materials and methods

3.3.1 – Study area and sampling

Our study focused on two *S. salamandra* Iberian subspecies – *S. s. gallaica and S. s. bernardezi* – co-distributed across the western Iberian Peninsula (**Figure 3.1**). The subspecies *S. s. gallaica* exhibits exclusively larviparity in mainland populations, whereas *S. s. bernardezi*

exhibits pueriparous reproduction (Velo-Antón and Buckley 2015). The two known pueriparous insular populations of *S. s. gallaica* were not included in this study due to their specific characteristics (isolated populations, low genetic diversity, and differentiated behaviour; Velo-Antón *et al.* 2012; Velo-Antón and Cordero-Rivera 2017). The environmental niche of *S. s. gallaica* (which includes Mediterranean and Atlantic ecosystems) is wider than in *S. s. bernardezi* (only occurring in Atlantic ecosystems; Velo-Antón and Buckley 2015). Because environmental variation may influence patterns of dispersal (Cosgrove *et al.* 2018), we restricted sampling of *S. s. gallaica* to northwestern Spain, where climate (Atlantic influence) and vegetation (*e.g.* predominance of deciduous forests of Quercus spp.) are similar to the Cantabrian region (Amigo *et al.* 2017). Both subspecies also share a contact zone in this region (**Figure 3.1**), where substantial genetic and phenotypic admixture takes place (Galán 2007; Velo-Antón unpublished data), and thus we did not include populations from this hybrid zone.

We sampled during rainy nights in the months of April and November of 2016-2017, coinciding with the periods of highest activity of adult salamanders in northern Spain. We collected a total of 354 toe clip samples from individual adults (180 males and 174 females) in six localities (three per reproductive mode), with a sample size per locality of 53-67 (**Figure 3.1; Table 3.1**). The impact of this procedure on the animals is expected to be minimal, as fire salamanders are capable of regenerating limbs within a few weeks (see Blaustein *et al.* 2018). The sampled localities exhibit favourable habitat conditions for *S. salamandra* at the local scale, comprising humid deciduous woodlands (*e.g. Quercus* spp. and *Fagus* spp.) with a high availability of shelter (*e.g.* fallen logs and rocks; Velo-Antón and Buckley 2015). In most localities, adjacent streams (ca. < 1 m width) and rivers (ca. 10-30 m width) were present, the only exception being the locality of SGAL_Larv, in which a small stream is located more than 200 m away from the sampled site. We chose to sample in putative good quality habitat to avoid the presence of unsuitable habitat or anthropogenic features that could potentially disrupt standard dispersal ecology in this species, thus assuring a continuous distribution of individuals. In each locality, we sampled individuals along a ca. 1-km long transect. This length was deemed adequate based on previous long-term (≥ 2 years) mark-recapture studies that showed dispersal distances less than 500 m for most individuals of *S. salamandra* (Rebelo and Leclair 2003; Schulte *et al.* 2007; Hendrix *et al.* 2017). We also attempted to sample individuals on the same side of the stream or river to avoid potential barrier effects to dispersal. This condition was not met in the localities of PEGA_Larv and VILL_Puer, in which 19 and 18 salamanders, respectively, were sampled on the opposite side of the stream along one stretch of the transect due to steep terrain and/or very dense vegetation. These individuals were still kept for downstream analyses because (1) in both localities, the opposite sides of the streams

were connected by small (ca. 1.5-m long) wood bridges, which we observed many fire salamanders crossing (AL and GVA personal observations), and (2) kinship analyses carried out in COLONY showed that many pairs of relatives comprised individuals sampled on opposite sides of these streams (seven out of ten in PEGA_Larv and four out of 20 in VILL_Puer; see **Figure 3.2**). Additionally, we sexed all individuals through inspection of the cloaca (Velo-Antón and Buckley 2015) and recorded their locations with a handheld GPS. A roughly even number of males and females were sampled in each locality to prevent biases in spatial autocorrelation analyses arising from uneven sample sizes, though we avoided clustering samples from the same sex to have adequate representations along the transects of both sexes (**Figure 3.2**). Because some localities were sampled during multiple nights, we carried out two procedures to avoid resampling previously captured individuals. First, we inspected toes from all encountered individuals. Second, in some localities, samples were collected seven months apart (*e.g.* April and November of 2016). Because fire salamanders are capable of regenerating their toes, we used the option Multilocus Matches implemented in GENALEX 6.5 (Peakall and Smouse 2012) to check for genotype matches.

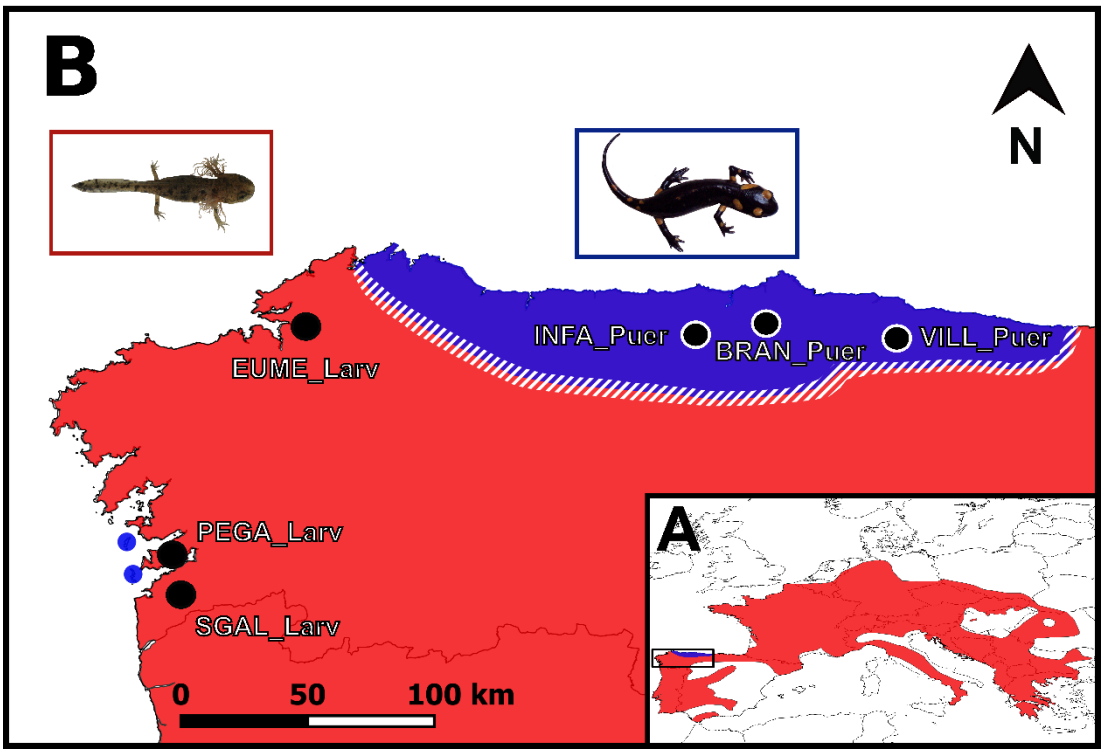

Fig. 3.1 Study area. (A) Distribution of *Salamandra salamandra* in Europe, with larviparous and pueriparous populations highlighted in red and blue, respectively. (B) Sampled localities and respective acronyms illustrated in our study area. The two blue dots in the northwestern coast of Spain correspond to the two pueriparous insular populations of *S. s. gallaica* not included in this study (see main text). The white dashed polygon illustrates roughly the contact zone between larviparous and pueriparous populations.

Table 3.1 Population genetic statistics from the studied localities. The name of each population (Pop) depicts the associated reproductive mode (Larv – larviparity; Puer – pueriparity). Latitude (Lat) and longitude (Long) coordinates are also displayed, along with a brief description of the surrounding habitat in each locality (Hab; D – deciduous forest; M – mixed coniferous and deciduous forests; S – adjacent stream of width < 1 m; R – adjacent river of width ca. 10-30 m). Genetic diversity statistics are: n – number of samples collected; nm – number of sampled males; nf – number of sampled females; MA – minimum number of allele mismatches among individuals; N_A – mean number of alleles per locus; H_O – observed heterozygosity; H_E – expected heterozygosity; A_R – allelic richness; F - population mean inbreeding coefficient; R – population average relatedness.

Pop	Lat	Long	Hab	n	nm	nf	M_A	N_A	H_O	H_E	A_R	F	R
PEGA_Larv	42.32	-8.72	D-S	55	30	25	4	12.18	0.78	0.79	11.07	0.01	0.03
EUME_Larv	43.41	-8.08	D-R	53	26	27	6	9.27	0.65	0.72	8.19	0.02	0.05
SGAL_Larv	42.13	-8.68	M	56	26	30	6	12.73	0.77	0.80	11.15	0.03	0.03
INFA_Puer	43.36	-6.26	D-R	61	32	29	5	12.82	0.76	0.82	11.60	0.02	0.03
BRAN_Puer	43.41	-5.92	D-R	62	30	32	4	11.55	0.76	0.81	10.52	0.04	0.04
VILL_Puer	43.34	-5.30	D-S	67	36	31	7	11.91	0.78	0.84	11.10	0.02	0.04

3.3.2 – Laboratory procedures and genotyping

Genomic DNA was extracted from fresh tissue using the Genomic DNA Tissue Kit (EasySpin), following the manufacturer's protocol. The quantity and quality of extracted products were assessed in a 0.8% agarose gel. A total of 14 microsatellites (Steinfartz *et al.* 2004; Hendrix *et al.* 2010), distributed in four optimized multiplexes (panels Ssal1, Ssal2, Ssal3 and Ssal4), were amplified through polymerase chain reactions (PCR; see **Supplementary Text B1** for PCR conditions and **Table B1 in Appendix B** for multiplex details). PCR products were verified on a 2% agarose gel and run on an ABI3130XL capillary sequencer (Applied Biosystems). Alleles were scored in GENEMAPPER 4.0 (Applied Biosystems; see **Supplementary Text B1** for more details concerning allele scoring).

3.3.3 – Population genetic analyses

We tested whether microsatellite loci deviated from Hardy–Weinberg equilibrium (HWE) and linkage equilibrium (LE) by performing exact tests in GENEPOP 4.2 (Rousset 2008; dememorization = 5000, batch length = 10000, batch number = 1000). We applied the false discovery rate (Benjamini and Hochberg 1995) to correct p-values from HWE and LE multiple exact tests. Because the inclusion of related individuals may introduce significant biases in these tests (Sánchez-Montes *et al.* 2017), we excluded individuals sharing familial relationships from these analyses (see Parentage analyses, below). The presence of null alleles was investigated in INEST 2.0 (Chybicki and Burczyk 2009) with a total of 200 000 iterations, thinned every 200 iterations and with a burn-in of 10% for the individual inbreeding model.

We estimated the mean number of alleles per locality (N_A), observed (H_O) and expected heterozygosity (H_E), and allelic richness (A_R) with the R (R Development Core Team 2017)

package diveRsity (Keenan *et al.* 2013). The A_R metric was corrected for the smallest locality's sample size in our data set (n = 53). Population mean inbreeding coefficient (F) was calculated in INEST 2.0, while population average relatedness (R) was estimated using the triadic likelihood estimator implemented in COANCESTRY (Wang 2011).

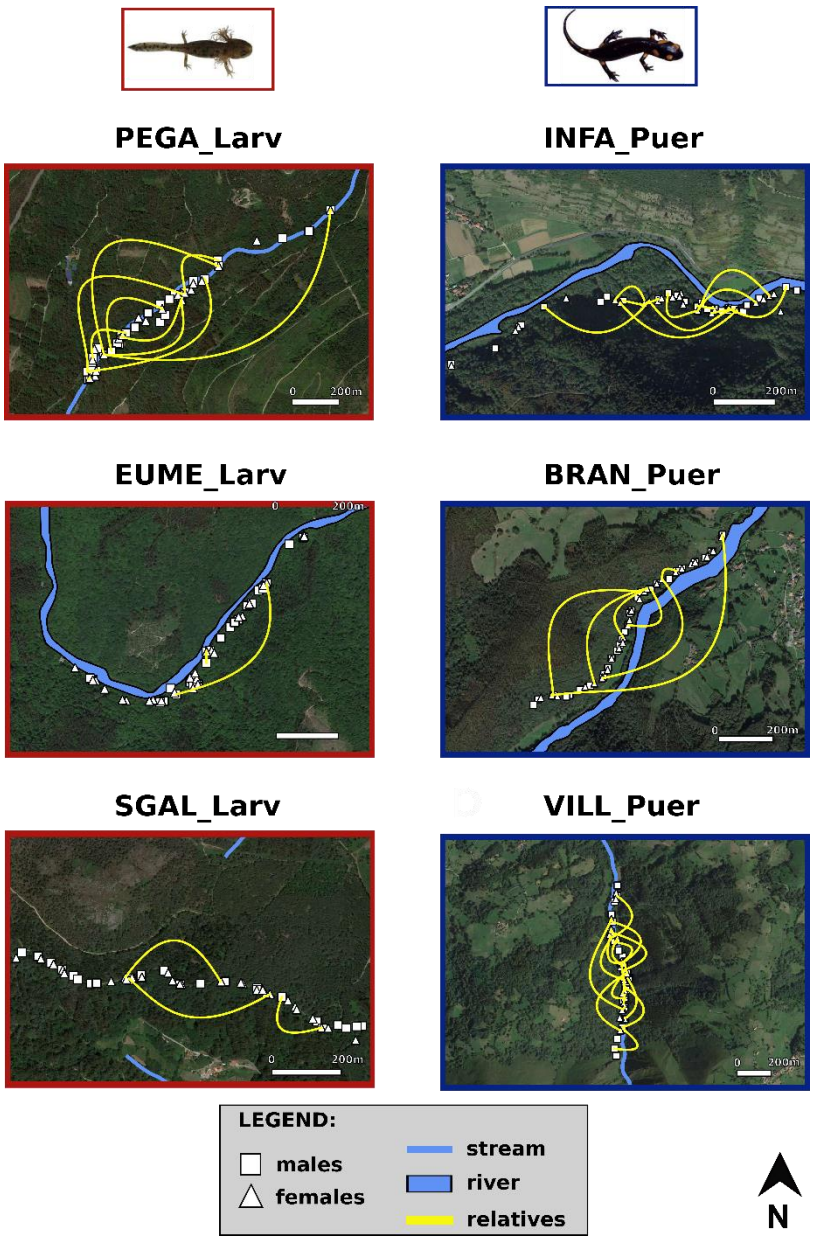

Fig. 3.2 Aerial photographs of sampled localities. Each panel illustrates the spatial distribution of males and females along with their kinship relationships identified in COLONY (posterior probability ≥ 0.80). Water bodies (large rivers and streams) are also displayed. Left and right panels correspond to localities in which the reproductive mode of females is larviparity (PEGA_Larv, EUME_Larv, and SGAL_Larv) and pueriparity (INFA_Puer, BRAN_Puer, and VILL_Puer), respectively.

3.3.4 – Comparing patterns of dispersal between reproductive modes and sexes

Long-term radio tracking and mark-recapture approaches have provided important tools to measure dispersal in *S. salamandra* populations (*e.g.* Rebelo and Leclair 2003; Schulte *et al.* 2007; Schmidt *et al.* 2014; Hendrix *et al.* 2017). Although these methods provide detailed dispersal and demographic data (*e.g.* survival rates), they are generally time-consuming and usually restricted to single populations. Molecular data alone have been found to be consistent with radio-tracking and mark-recapture estimates in amphibians and shown to be reliable for examining dispersal (Liebgold *et al.* 2011; Banks and Peakall 2012; Wang and Shaffer 2017), while enabling the simultaneous study of multiple populations with lower sampling effort.

We employed a genetic spatial autocorrelation approach (Smouse and Peakall 1999), as implemented in GENALEX 6.5 (option Spatial) to examine the influence of reproductive mode and sex on fine-scale genetic structure and, thus, infer dispersal from these genetic patterns (Peakall *et al.* 2003; Banks and Peakall 2012). This method has been applied widely to infer variation in patterns of dispersal between sexes based on genetic structure (Banks and Peakall 2012), including in the direct-developing red-back salamander (*Plethodon cinereus*), in which it was shown consistent with mark-recapture estimates of dispersal (Liebgold *et al.* 2011). Additionally, genetic spatial autocorrelation was successfully used to infer variation in dispersal between groups with another phenotypic trait, body colouration, in *Plethodon cinereus* (Grant and Liebgold 2017), further demonstrating its utility for our study. This multivariate distance-based method uses pairs of genetic and geographic distance matrices as input and calculates an autocorrelation coefficient (r_{auto}; bounded by [-1,1]) as a measure of genetic similarity between pairs of individuals for each distance class, with results summarized in a correlogram. Distance classes displaying positive r_{auto} values indicate that pairs of individuals within that class are more genetically similar than average. If positive values are found within the shortest distance classes, it may indicate that individuals are philopatric to their natal areas, while positive r_{auto} values at farther distance classes may indicate dispersal of many related individuals over a specific range of distances.

We first built two multilocus data sets per sampled locality (12 in total): one for males and one for females. Pairwise between-individual matrices of Euclidean geographic distances and genetic distances were calculated for each multilocus data set (option *Distance*), except for the locality of EUME_Larv. The path of the stream in this locality did not allow for sampling along a straight transect, so we calculated stream-distances between individuals rather than Euclidean distances (**Figure 3.2**; see details in **Supplementary Text B2**). To test whether reproductive mode (H1) and sex (H2) influence fine-scale genetic structure (and dispersal), we

generated four “combined” correlograms comparing patterns of genetic structure between the following subsamples: (1) larviparous males vs. pueriparous males; (2) larviparous females vs. pueriparous females; (3) larviparous males vs. larviparous females; and (4) pueriparous males vs. pueriparous females (see below). We used the option *Multiple Pop Subsets* to generate these “combined” correlograms in which an overall r_{auto} value is estimated for each distance class based on the individual r_{auto} estimates of each population included in the subsample (*e.g.* the overall r_{auto} values for the subsample “larviparous males” are calculated from r_{auto} estimates obtained from males sampled at PEGA_Larv, EUME_Larv, and SGAL_Larv; see Peakall *et al.* 2003 and Banks and Peakall 2012 for more details about this method). Additionally, because patterns of genetic structure may vary significantly among sampled localities, we generated six additional within-locality correlograms comparing males vs. females to provide complementary insights into the effects of reproductive mode and sex on dispersal. The latter six correlograms were computed using the option *Multiple Pops* (i.e. males and females were treated as separate “populations”; Banks and Peakall 2012). We estimated overall r_{auto} values for the “combined” correlograms at eight distance classes for a total length of 1 km in each subsample (100-m classes up to 700 m, and a distance class of 701-1000 m). The size and number of distance classes were chosen based on the dispersal ecology of *S. salamandra* (Schulte *et al.* 2007; Hendrix *et al.* 2017) and as a trade-off between resolution and sample size in each class (i.e. number of pairs of individuals binned into each class). We decided to pool all pairs separated by >700 m in one class (701-1000 m) due to small sample sizes. Also because of small sample sizes, within-locality correlograms were computed only for six distance classes in each sex (0-100 m, 101-200 m, 201-300 m, 301-500 m, 501-700 m, and 701-1000 m). Lastly, in some localities, very few pairs of individuals were separated by a distance greater than 1000 m. We decided to exclude these observations from these analyses, not only to avoid estimating r_{auto} values based on low sample sizes for distance classes >1000 m but also to make correlograms directly comparable.

We first assessed patterns of fine-scale genetic structure at both global (i.e. whole correlogram) and individual distance class levels. These analyses were performed to quantify the degree of genetic structure of the groups being compared (i.e. subsamples in the case of “combined” correlograms, and males and females in the case of within-locality correlograms). To test for deviations from the null hypothesis of no genetic structure (i.e. a “flat” correlogram) for each group at the global scale, we employed the heterogeneity Omega test (ω; Smouse *et al.* 2008). Estimates of ω, as well as other heterogeneity tests (see below), were regarded as significant at $p < 0.01$, as recommended by Banks and Peakall (2012). Additionally, we performed 9999 permutations of the data to generate a null distribution of no spatial genetic

structure (*i.e.* $r_{auto} = 0$) for each distance class. The r_{auto} values estimated from our multilocus data for each distance class were then compared to this null distribution with a one-tailed t-test ($p < 0.05$), allowing us to determine whether r_{auto} values were significantly higher or lower than expected by chance. The 95% confidence intervals (CIs) of each r_{auto} value were computed through 10 000 bootstrap resamplings.

Additional statistical tests were carried out to test explicitly our two hypotheses. For the "combined" correlograms, to test for general differences in fine-scale genetic structure (and infer dispersal differences) between reproductive modes (H1; larviparous males vs. pueriparous males and larviparous females vs. pueriparous females), we employed the heterogeneity Omega group test (ω_{GROUPS}; $p < 0.01$; Smouse *et al.* 2008) to assess global differences in r_{auto} patterns among subsamples and the heterogeneity t^2 test ($p < 0.01$; Smouse *et al.* 2008) to quantify differences in r_{auto} values for each distance class. To test for differences in dispersal between sexes at distance class and global scales (H2; larviparous males vs. larviparous females and pueriparous males vs. pueriparous females), these same heterogeneity tests were also used.

For within-locality correlograms, we compared r_{auto} patterns between each pair of sampled localities at global and distance class levels to test our hypothesis that pueriparous females will disperse farther, on average, than larviparous females (H1). We expected that pairwise comparisons involving the sampled localities with different reproductive modes will exhibit greater differences in r_{auto}. These pairwise comparisons were restricted to individuals of the same sex (i.e. males vs. males and females vs. females from different sites; total of 15 comparisons per sex). Pairwise heterogeneity Omega group tests (ω_{GROUPS}; $p < 0.01$; Smouse *et al.* 2008) were employed to assess global differences in r_{auto} patterns among pairs of localities, whereas differences in r_{auto} values for each distance class were assessed through pairwise heterogeneity t^2 tests ($p < 0.01$; Smouse *et al.* 2008). Finally, to test our hypothesis that males disperse farther than females (H2), we performed the same heterogeneity tests, but comparisons of r_{auto} values between males and females were performed only within each sampled locality to avoid potential bias arising from environmental variation between localities.

3.3.5 – Parentage analyses

For each sampled locality, we performed parentage analyses using COLONY 2.0.6.1 (Jones and Wang 2010) to identify putative pairs of relatives and evaluate the spatial distribution of related individuals. COLONY requires the input of three subsamples: (i) putative fathers; (ii) putative mothers; and (iii) putative offspring. *Salamandra salamandra* is an iteroparous species, meaning that multiple cohorts coexist contemporaneously. Because

precise age determination in the field was unfeasible and because fire salamanders are known to live for more than 20 years (Rebelo and Caetano 1995), our data set may contain parent-offspring pairs even though our sampling was restricted to adult salamanders. Accordingly, males and females were distributed in the candidate father and mother samples, respectively, and all individuals were pooled in the candidate offspring sample. The inclusion of individuals both in parent and offspring subsamples decreases the statistical power of this method to identify relatives, although COLONY has been shown to perform satisfactorily under these conditions (Wang and Santure 2009). A total of three runs per sampled locality with different seed numbers were performed. In each run, we set the full-likelihood method, with high likelihood precision and long run length under a scenario of polygamy for both sexes. Sibship scaling was deactivated, and no *a priori* information regarding known parents was provided. We identified pairs of individuals as related if they exhibited a posterior probability higher than 0.8 in at least two runs. This probability threshold is lower than those employed in previous studies (*e.g.* 0.95; Richards-Zawacki *et al.* 2012; Carvalho *et al.* 2018). However, we were not interested in determining the exact familial relationships (*e.g.* parent-offspring, full-siblings or half-siblings) but rather in identifying the most related pairs of individuals within our sample (hereafter “relatives”). To assess the spatial distribution of relatives, we calculated the proportion of relatives separated across three distance intervals: (i) ≤ 200 m (most individuals [ca. 80-90%] move < 200 m; Schulte *et al.* 2007; Hendrix *et al.* 2017); (ii) 201-500 m (the scale at which some individuals disperse among breeding localities; Ficetola *et al.* 2012); and (iii) > 500 m (rare long-distance dispersal events; Ficetola *et al.* 2012; Hendrix *et al.* 2017). Finally, we calculated the Probability of Identity (PI) in GENALEX, which is the probability that two individuals drawn at random from a given population share identical genotypes at all loci, to assess the power of our multilocus data for discriminating individuals. The PI when accounting for the presence of relatives (PISibs) was also estimated.

3.4 – Results

3.4.1 – Population genetic analyses

All sampled individuals in a transect exhibited a minimum of four to seven allele mismatches with each other (**Table 3.1**). Therefore, we concluded that no genotyped salamander comprised a recapture, and all individuals were kept for downstream analyses. Three loci showed consistent deviations from HWE (heterozygote deficits) and clear evidence for null alleles, one (SalE2) in all larviparous populations and two (SST-C3 and SalE06) in all pueriparous populations. We excluded these three loci, and all downstream analyses were performed with the remaining 11 loci. There was

no evidence for deviations from LE. Both larviparous and pueriparous groups showed similar and very high levels of genetic diversity (range N_A: 9.27 – 12.82; range H_O: 0.65 – 0.78; range H_E: 0.72 – 0.84; A_R: 8.19 – 11.60), while inbreeding (range F: 0.01-0.04) and relatedness (range R: 0.03-0.05) were both very low (**Table 3.1**).

3.4.2 – Comparison of dispersal patterns between reproductive modes and sexes

At the global level, both larviparous (ω = 38.4, $p < 0.01$; **Figure 3.3B** and **Figure 3.4A**) and pueriparous females (ω = 44.3, $p < 0.01$; **Figure 3.3B** and **Figure 3.4B**) exhibited significant positive genetic structure according to the heterogeneity ω test, while analyses within each sampled locality showed that only females in two larviparous populations (PEGA_Larv, ω = 30.9, $p < 0.01$; EUME_Larv, ω = 30.9, $p < 0.01$) and males from one larviparous population (SGAL_Larv, ω = 31.9, $p < 0.01$) exhibited strong genetic structure (**Figure 3.5**). At the distance class level, significant genetic structure was found at 0-100 m for larviparous females ($r_{auto} = 0.020$, $p = 0.02$) and at 501-600 m for both larviparous ($r_{auto} = 0.024$, $p = 0.03$) and pueriparous females ($r_{auto} = 0.034$, $p < 0.01$) in "combined" correlograms (**Figure 3.3**; **Tables B2-B5 in Appendix B**). Analyses within each sampled locality revealed strong genetic structure only for a total of four distance classes (two in females for distances ≤ 200 m and two in males for distances ≥ 300 m; **Figure 3.5** and **Tables B6-B7 in Appendix B**).

The heterogeneity ω_{GROUPS} tests performed in the "combined" correlograms did not show significant differences between neither reproductive modes nor sexes at the global level (**Table B8 in Appendix B**). We also did not find significant differences in genetic structure between reproductive modes at the distance class level (**Table B9 in Appendix B**). However, between sexes, we found that larviparous females showed a much higher genetic similarity than larviparous males at a distance class of 100 m ($t^2 = 7.03$, $p < 0.01$; see **Figure 3.4** and **Table B9 in Appendix B**). Although pueriparous females exhibiting also a higher r_{auto} than pueriparous males at 100 m, this difference was not statistically significant.

Pairwise comparisons involving within-locality correlograms revealed no significant differences between reproductive modes at both the global (**Tables B10-B11 in Appendix B**) and distance class levels (**Tables B12-B13 in Appendix B**). Only the larviparous population pair PEGA_Larv/EUME_Larv showed significant differences in r_{auto} at a distance of 101-200 m ($t^2 = 6.95$, $p < 0.01$; **Table B14 in Appendix B**). We also did not find statistical support for sex-biased dispersal within any locality. Nevertheless, for distances up to 100 m, females always exhibited higher r_{auto} values than males, and for the 701-1000 m distance class, males and females in most study sites

exhibited non-significant positive and negative r_{auto}, respectively. One exception is that females in SGAL_Larv showed a non-significant positive r_{auto} at 701-1000 m.

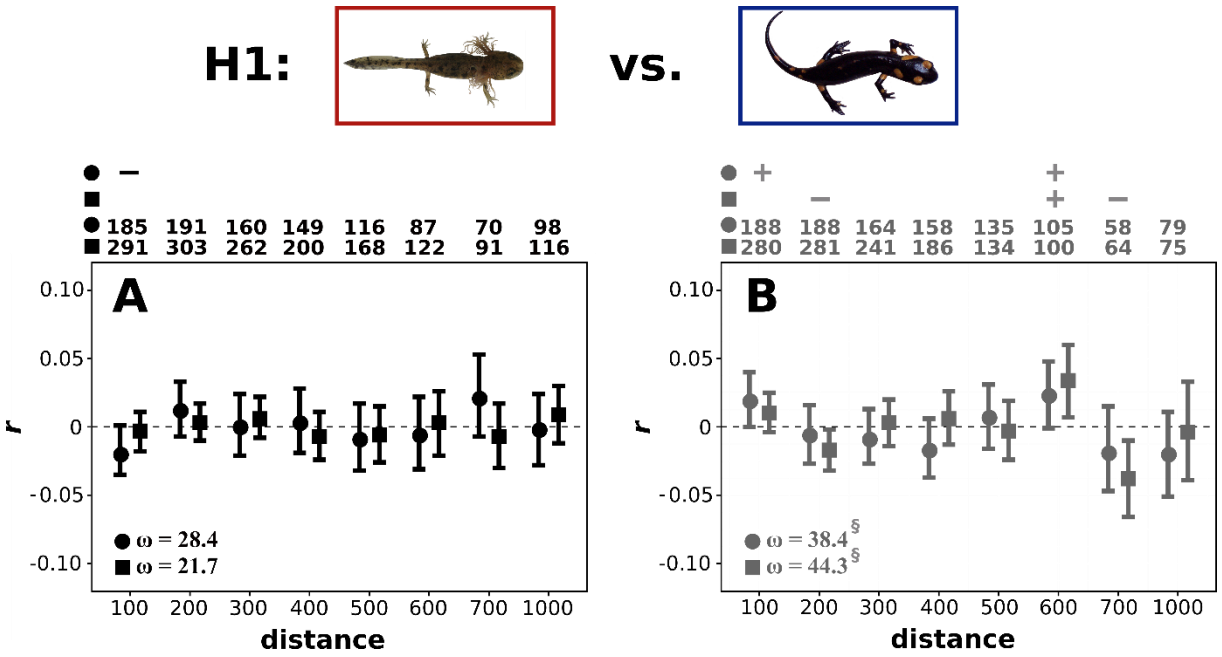

Fig. 3.3 "Combined" correlograms of the autocorrelation coefficient, r_{auto}, comparing the following subsamples: (A) larviparous males (black circles) vs. pueriparous males (black squares); and (B) larviparous females (grey circles) vs. pueriparous females (grey squares). These correlograms were generated to test explicitly our hypothesis of differences in genetic structure between reproductive modes (H1). Omega (ω) statistics at the whole correlogram (global) level are shown for each analysed subsample, and significant ω values ($p < 0.01$) are denoted by the symbol (§). The numbers above the plot indicate the number of pairs analysed per subsample (represented by the symbols at left of these numbers) for each distance class. The symbols "+" and "-" denote distance classes for which r_{auto} values are significantly higher or lower than zero (dashed line; $p < 0.05$), respectively, based on one-tailed tests for a particular subsample (represented by the symbols at left).

3.4.3 – Parentage analyses

COLONY identified a total of 54 pairs of relatives (**Figure 3.2; Table 3.2**). The number of pairs of relatives identified per locality varied between two (EUME_Larv) and 20 (VILL_Puer). The minimum (8.3 m) and maximum (1162.8 m) distances between relatives were both recorded in PEGA_Larv. Overall, the frequency of pairs of relatives was higher in pueriparous populations up to 200 m, whereas larviparous and pueriparous populations showed similar frequencies for distances of 201-500 m (**Figure 3.6; Table 3.2**). At distances > 500 m, larviparous populations showed a higher proportion of relatives compared to pueriparous populations (**Figure 3.6**). The population of Pega_LARV, in which four pairs of relatives were identified more than 500 m apart, primarily accounted for this pattern (**Table 3.2**). Both PI (range: 1.8×10^{-16} – 1.6×10^{-11}) and PISibs (range: 6.4×10^{-6} – 6.3×10^{-5}) were very low.

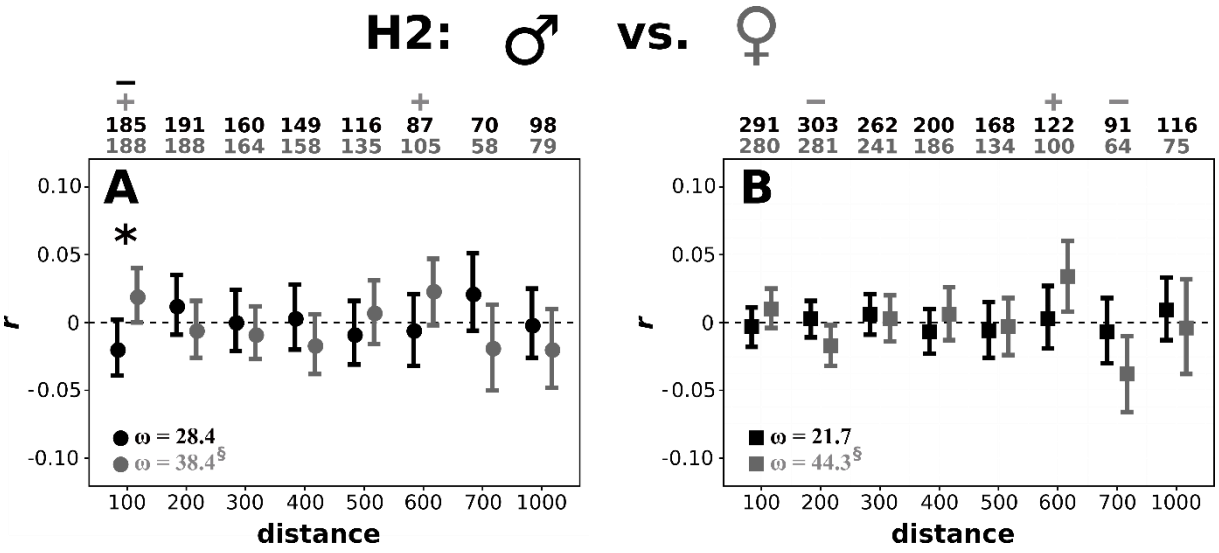

Fig. 3.4 "Combined" correlograms of the autocorrelation coefficient, r_{auto}, comparing the following subsamples: (A) larviparous males (black circles) vs. larviparous females (grey circles); and (B) pueriparous males (black squares) vs. pueriparous females (grey squares). These correlograms were generated to test explicitly our hypothesis of differences in genetic structure between sexes (H2). Omega (ω) statistics at the whole correlogram (global) level are shown for each analysed subsample, and significant ω values (p < 0.01) are denoted by the symbol (§). The numbers above the plot indicate the number of pairs of males (black) and females (grey) analysed for each distance class. The symbols "+" and "-" (males, black; females, grey) denote distance classes for which r_{auto} values are significantly higher or lower than zero (dashed line; p < 0.05), respectively, based on one-tailed tests. Black asterisks denote distance classes for which r_{auto} values between analysed subsamples are significantly different (p < 0.01) according to t^2 tests.

3.5 – Discussion

3.5.1 – Do pueriparous females disperse farther than larviparous ones?

Here, we took advantage of one of the very few species exhibiting both aquatic and terrestrial reproduction to perform comparisons between reproductive modes and infer their effects on dispersal based on patterns of genetic structure. Contrary to our predictions, we did not find significant differences in patterns of genetic structure (and therefore dispersal) between larviparous and pueriparous females (or males) at fine spatial scales. Previous studies on pueriparous and direct-developing amphibians indicated that terrestrial reproduction allows individuals to survive, disperse, and reproduce in a wider range of sub-optimal habitats due to higher independence from surface water compared to species with aquatic reproduction (Gibbs 1998; Marsh *et al.* 2004; Liedtke *et al.* 2017; Lourenço *et al.* 2017). This greater independence from water potentially promotes higher genetic connectivity in heterogeneous and fragmented landscapes at the population level (Measey *et al.* 2007; Sandberger-Loua *et al.* 2018). For instance, based on allozyme data sets and patterns of isolation-by-distance, Tilley (2016) observed higher genetic divergence between populations of aquatic-breeding salamanders (*Desmognathus*) compared to those of

direct-developing lungless salamanders (*Plethodon*), suggesting this pattern could be due to the higher dependence of *Desmognathus* salamanders on aquatic breeding habitats (headwaters of streams).

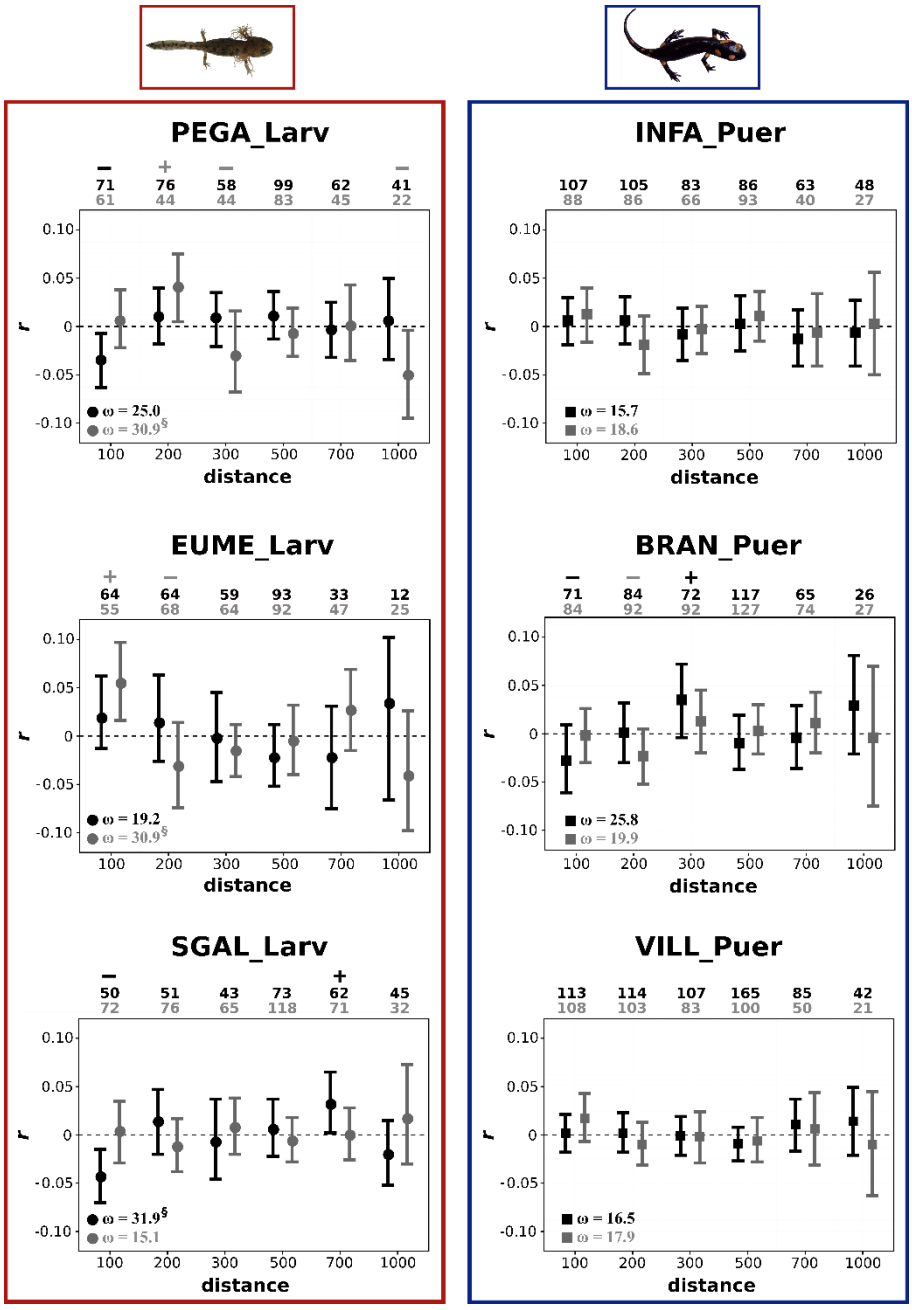

Fig. 3.5 Correlograms of the autocorrelation coefficient, r_{auto}, comparing males (larviparous, black circles; pueriparous, black squares) and females (larviparous, grey circles; pueriparous, grey squares) sampled in larviparous (left panel; PEGA_Larv, EUME_Larv, and SGAL_Larv) and pueriparous populations (right panel; INFA_Puer, BRAN_Puer, and VILL_Puer). Omega (ω) statistics at the whole correlogram (global) level are shown for each analysed population, and significant ω values ($p < 0.01$) are denoted by the symbol (§). The numbers above the plot indicate the number of pairs of males (black) and females (grey) analysed for each distance class. The symbols "+" and "-" (males, black; females, grey) denote distance classes for which r_{auto} values are significantly higher or lower than zero (dashed line; $p < 0.05$) based on one-tailed tests, respectively.

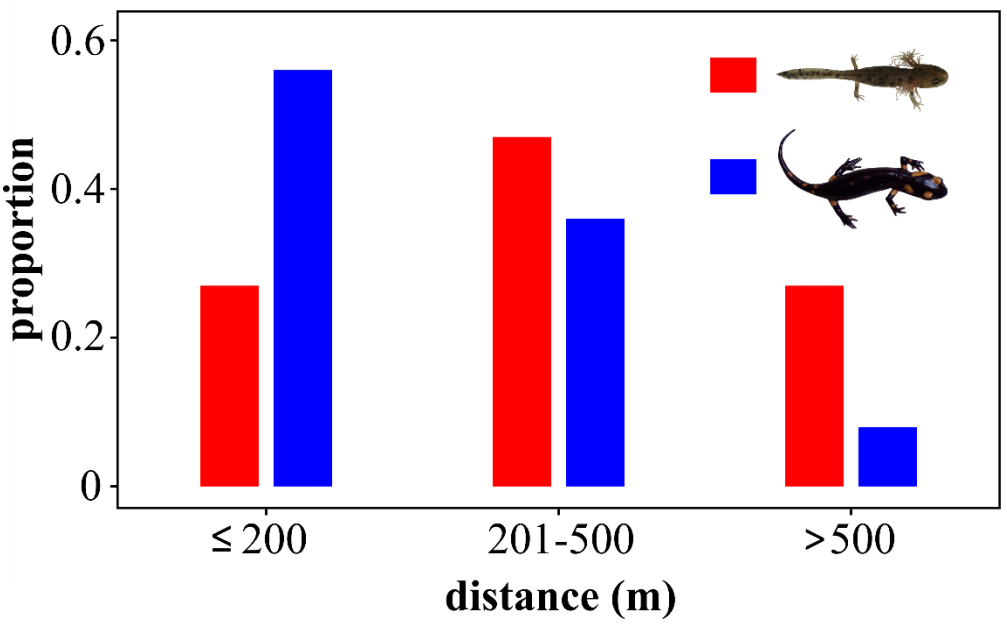

Fig. 3.6 Proportion of pairs of relatives identified in COLONY from larviparous (red) and pueriparous (blue) populations of *Salamandra salamandra* across three distance classes (200 m, 201-500 m, and >500 m).

Table 3.2 Summary statistics of kinship relationships identified in COLONY for each population (Pop). The following statistics are displayed: N_kin (number of pairs of relatives identified), and Range (distance range between pairs of relatives identified in a population). The number and proportion (p; within square brackets) of pairs of relatives found within 3 distance classes (≤ 200, 201-500, and > 500) are also displayed.

Pop	N_kin	Range (m)	≤ 200 [p]	201-500 [p]	> 500 [p]
PEGA_Larv	10	8.3 – 1162.8	2 [0.20]	4 [0.40]	4 [0.40]
EUME_Larv	2	9.9 – 465.7	1 [0.50]	1 [0.50]	-
SGAL_Larv	3	145.8 – 410.1	1 [0.33]	2 [0.67]	-
INFA_Puer	12	55.6 – 377.8	8 [0.67]	4 [0.33]	-
BRAN_Puer	7	61.0 – 873.5	2 [0.29]	3 [0.42]	2 [0.29]
VILL_Puer	20	9.0 – 579.8	12 [0.6]	7 [0.35]	1 [0.05]

Environmental conditions are a major driver of differentiation in dispersal strategies within species due to divergent selective pressures acting on individuals with different traits (Bowler and Benton 2005; Cote *et al.* 2017). Selection for dispersal will often occur if the benefits of emigrating outweigh those of remaining in the natal patch (Ousterhout and Semlitsch 2018). Within *S. salamandra*, Hendrix *et al.* (2017) used mark-recapture techniques and telemetry to compare movement patterns between two larviparous subpopulations of *S. salamandra*, in which individuals of each subpopulation deliver larvae either in ponds or streams. The authors found that individuals reproducing in ponds dispersed farther and exhibited higher variation in dispersal distances than salamanders reproducing in streams, possibly to cope with the spatio-temporal availability of pond habitats. In our study system, the potential benefits of terrestrial breeding for dispersal and

population connectivity in heterogeneous and fragmented habitats may not be expressed, at least in *S. salamandra*, at small spatial scales and in regions with largely intact, suitable habitats. *In situ* observations of the habitat (mostly deciduous forests), together with high observed population density and genetic diversity, suggest that our study sites contained favourable conditions for survival and reproduction in both larviparous and pueriparous populations. These conditions may have resulted in similar dispersal tendencies between larviparous and pueriparous salamanders, as the key resource (water) that may be responsible for any dispersal asymmetry between reproductive modes is not a limiting factor in our study sites (except possibly in SGAL_Larv; see below). Because the lineages of pueriparous *S. salamandra* are both relatively recent, we also cannot rule out the possibility that they retained ancestral dispersal traits; essentially, the shift in reproductive mode might not have been followed by a behavioural adaptation to the derived pueriparous condition in *S. s. bernardezi*, though dispersal-related traits can show low conservation at the intraspecific level (Stevens *et al.* 2010). Moreover, although *S. salamandra* comprises a good model to test our hypotheses because it has multiple reproductive modes, there are potentially important differences between larviparous and pueriparous fire salamanders. Specifically, larviparous *S. s. gallaica* individuals are generally larger (body size up to 250 mm) than *S. s. bernardezi* individuals (body size up to 180 mm; Velo-Antón and Buckley 2015; Velo-Antón *et al.* 2015), and previous studies have shown larger salamanders usually show higher dispersal capacity (Bennett *et al.* 1989; but see also Denton *et al.* 2017). Hence, if pueriparity and larger body size (found in larviparous populations) both lead to greater dispersal distances, then we may not observe differences between different reproductive modes. Complementing our genetic analyses with mark-recapture or radio tracking data at our study sites may help clarify these results.

Despite the lack of major differences in dispersal and fine-scale genetic structure between larviparous and pueriparous salamanders according to genetic spatial autocorrelation, parentage analyses in larviparous salamanders at the PEGA_Larv locality revealed a disproportionately higher number of pairs of relatives farther apart (> 500 m) compared to the other populations (**Figure 3.6; Table 3.2**). This may suggest that water-borne long-distance dispersal (active or passive due to strong discharges after heavy rain) along the stream during the larval stage may have contributed to these patterns, as reported previously in larvae of *S. salamandra* (Thiesmeier and Schuhmacher 1990; Reinhardt *et al.* 2018). Water-borne dispersal is unlikely to occur in large rivers similar to the one located in EUME_Larv, as its strong current and drifting objects probably causes high mortality rates due to physical damage, thus preventing successful dispersal (see Segev and Blaustein 2014). Additionally, we cannot entirely discount rare long-distance movements undertaken by adults over single or multiple generations in explaining the patterns obtained in PEGA_Larv. Hendrix *et al.* (2017) found that stream-adapted individuals did not move beyond 500 m, while 90% of the studied

pond-adapted salamanders moved up to 700 m, with a few pond-adapted individuals performing long-distance movements up to 1.9 km possibly driven by the limited availability of ponds in their study area, as hypothesized by the authors. However, we find those types of movements unlikely in our study, because (1) many ecological studies in adult larviparous fire salamanders have systematically reported small home ranges and dispersal distances below 500 m in suitable environments (Schulte *et al.* 2007; Ficetola *et al.* 2012; Schmidt *et al.* 2014), and (2) if long-distance movements of adults were common, then we would expect to observe similar patterns in other studied larviparous populations.

Interestingly, unlike the other larviparous and pueriparous populations, females in SGAL_Larv showed a relatively elevated relatedness for a distance of > 700 m (**Figure 3.5**). This contrasting pattern may be related to the lack of nearby aquatic systems along this transect (**Figure 3.2**). Dispersal behaviour, particularly in female amphibians, is often driven by the availability of breeding resources (water bodies) within their perceptual range (Russell *et al.* 2005; Semlitsch 2008; Wang *et al.* 2012). For instance, Wang *et al.* (2012) showed that female-biased dispersal in a frog was favoured in islands containing a lower density of breeding sites compared to those with abundant reproductive resources. The lower abundance of nearby water bodies in SGAL_Larv potentially prompted females to adjust their dispersal behaviour, increasing dispersal distances to increase the likelihood of encountering water bodies to deposit larvae. Increasing the number of sampled larviparous populations at varying distances from aquatic systems (both streams and rivers), as well as incorporating field ecological approaches (*e.g.* mark-recapture or telemetry) is crucial to providing further insights on how salamanders navigate these landscapes.

3.5.2 – Do males disperse farther than females?

Larviparous females had significantly higher relatedness than larviparous males at a distance class of < 100 m, suggesting females exhibit more philopatric behaviour. Additionally, the higher (although non-significant) r_{auto} values of females compared to males at < 100 m in both “combined” (**Figure 3.4B**) and within-locality (**Figure 3.5**) correlograms also seem to support a marked philopatric behaviour of females. However, the underlying causes cannot be determined from our data, though Helfer *et al.* (2012) have suggested that philopatry in *S. atra* females may be driven by resource-defence mechanisms. Additionally, many pueriparous and larviparous females moved long distances, up to ca. 500-600 m (**Figure 3.3B**). In high-quality environments, there is a trade-off between resource availability and competition among individuals that governs the probability of dispersal (*e.g.* Bowler and Benton 2005; Liebgold *et al.* 2011). For some females, it is possible that very high intraspecific competition forced them to disperse. Indeed, a distance of 500-600 m has been observed directly (movement data, Schulte *et al.* 2007; stream-adapted fire salamanders in

Hendrix *et al.* 2017) and indirectly (ecological spatial autocorrelation analyses; Ficetola *et al.* 2012) as the maximum dispersal distance for many fire salamander individuals, with occasional long-distance movements (pond-adapted fire salamanders; Hendrix *et al.* 2017). On the other hand, males often exhibited higher, though not statistically significant, genetic relatedness compared to females at 700-1000 m, with the exception of females in SGAL_Larv. This may suggest that males in the studied localities exhibit greater variation in dispersal distances than females, partially supporting the male-biased dispersal hypothesis proposed by biogeographic studies to justify the mito-nuclear discordances found throughout the distribution of this species (García-París *et al.* 2003; Pereira *et al.* 2016). Nevertheless, longer transects with a higher number of sampled individuals across more sites are needed to confirm this and further elucidate the underlying drivers of dispersal in males and females in this system.

3.6 – Conclusions

To our knowledge, empirical studies addressing the eco-evolutionary implications of shifts in reproductive modes for dispersal and fine-scale genetic structure are scarce. Our study, which focused on fire salamander populations exhibiting contrasting reproductive strategies (aquatic vs. terrestrial reproduction), revealed no obvious differences in movement patterns between reproductive modes across the studied landscapes, which were largely composed of contiguous suitable habitat. However, our results raise the possibility that the intrinsic dispersal behaviour of larviparous salamanders may be associated with site-specific landscape features (i.e. abundance and type of water bodies), which under particular environmental contexts may translate to marked differences in dispersal-related traits compared to pueriparous salamanders, although further work is needed to validate this hypothesis. Female fire salamanders (especially larviparous ones) also appeared more philopatric than males, although patterns of dispersal in females deserve further investigation under scenarios with low water body availability. This study also provides avenues for future research on the outcomes of shifts in reproductive modes in amphibians. Specifically, *S. salamandra* comprises a good system to explicitly test the hypothesis that pueriparous amphibians should show higher population connectivity than larviparous populations in fragmented landscapes. Additionally, the association between larval and adult dispersal ecology and water dependence in larviparous populations requires further investigation, which will help to elucidate how the spatiotemporal availability of aquatic breeding resources contributes to patterns of sex-biased dispersal and regional connectivity in this species.

3.7 – Acknowledgments

We thank B. Correia, M. Dinis, M. Henrique, P. Pereira, and P. Alves for help during field work, and S. Lopes for laboratory assistance. We also thank Dr. Rod Peakall, Dr. Peter Smouse, and Dr. Jinliang Wang for their advice on statistical analyses. Fieldwork for obtaining tissue samples was done with the corresponding permits from the regional administrations (Xunta de Galicia, Ref. 410/2015; Gobierno del Principado de Asturias, Ref. 2016/001092). Sampling procedures were carried out following the Guidelines for Use of Live Amphibians and Reptiles in Field and Laboratory Research, 2nd Edition, revised by the Herpetological Animal Care and Use Committee (HACC) of the American Society of Ichthyologists and Herpetologists, 2004. Lab work was supported by FEDER funds through the Operational Programme for Competitiveness Factors – COMPETE (FCOMP-01-0124-FEDER-028325 and POCI-01-0145-FEDER-006821); and by National Funds through FCT – Foundation for Science and Technology (PTDC/BIA-EVF/3036/2012). Field work was supported by a Student Grant Scheme granted by the British Herpetological Society (2016-12-01). GVA and AL are supported by FCT (IF/01425/2014 and PD/BD/106060/2015, respectively). The authors declare no conflicts of interest. We thank the editor in chief Dr. Matthew Symonds, the associate editors and three anonymous referees for constructive comments on earlier versions of the manuscript.

3.8 – References

Amigo J, Rodríguez-Guitián MA, Honrado JJP, Alves P (2017) The lowlands and midlands of northwestern Atlantic Iberia. *In*: Loidi J (ed) *The vegetation of the Iberian Peninsula Volume 1*. Springer, Switzerland, pp. 191-250.

Banet AI, Svendsen JC, Eng KJ, Reznick DN (2016) Linking reproduction, locomotion, and habitat use in the Trinidadian guppy (*Poecilia reticulata*). *Oecologia*, **181**, 87–96.

Banks SC, Peakall R (2012) Genetic spatial autocorrelation can readily detect sex-biased dispersal. Molecular Ecology, **21**, 2092–2105.

Benjamini Y, Hochberg Y (1995) Controlling the false discovery rate: a practical and powerful approach to multiple testing. *Journal of the Royal Statistical Society B*, **57**, 289–300.

Bennett A, Garland T, Else P (1989) Individual correlation of morphology, muscle mechanics, and locomotion in a salamander. *American Journal of Physiology*, **256**, R1200–R1208.

Blackburn DG (2015) Evolution of vertebrate viviparity and specializations for fetal nutrition: a quantitative and qualitative analysis. *Journal of Morphology*, **276**, 961–990.

Blaustein L, Segev O, Rovelli V *et al.* (2018) Compassionate approaches for the conservation and protection of fire salamanders. *Israel Journal of Ecology and Evolution*. doi: 10.1163/22244662-06303001

Bonte D, van Dyck H, Bullock JM, *et al.* (2012) Costs of dispersal. *Biological Reviews*, **87**, 290–312.

Bowler DE, Benton TG (2005) Causes and consequences of animal dispersal strategies: relating individual behaviour to spatial dynamics. *Biological Reviews*, **80**, 205–225.

Buckley D, Alcobendas M, García-París M, Wake MH (2007) Heterochrony, cannibalism, and the evolution of viviparity in *Salamandra salamandra*. *Evolution and Development*, **9**, 105–115.

Carvalho F, Lourenço A, Carvalho R, Alves PC, Mira A, Beja P (2018) The effects of a motorway on movement behaviour and gene flow in a forest carnivore: joint evidence from road mortality, radio tracking and genetics. *Landscape Urban Planning*, **178**, 217–227.

Chybicki IJ, Burczyk J (2009) Simultaneous estimation of null alleles and inbreeding coefficients. *Journal of Heredity*, **100**, 106–113.

Clobert J, Le Galliard JF, Cote J, Meylan S, Massot M (2009) Informed dispersal, heterogeneity in animal dispersal syndromes and the dynamics of spatially structured populations. *Ecology Letters*, **12**, 197–209.

Cosgrove AJ, McWhorter TJ, Maron M (2018) Consequences of impediments to animal movements at different scales: a conceptual framework and review. *Diversity and Distributions*, **24**, 448–459.

Cote J, Bestion E, Jacob S, Travis J, Legrand D, Baguette M (2017) Evolution of dispersal strategies and dispersal syndromes in fragmented landscapes. *Ecography*, **40**, 56–73.

Denton RD, Greenwald KR, Gibbs HL (2017) Locomotor endurance predicts differences in realized dispersal between sympatric sexual and unisexual salamanders. *Functional Ecology*, **31**, 915–926.

Dinis M, Velo-Antón G (2017) How little do we know about the reproductive mode in the north African salamander, *Salamandra algira*? Pueriparity in divergent mitochondrial lineages of *S. a. tingitana*. *Amphibia-Reptilia*, **38**, 540–546.

Ficetola GF, Manenti R, De Bernardi F, Padoa-Schioppa E (2012) Can patterns of spatial autocorrelation reveal population processes? An analysis with the fire salamander. *Ecography*, **35**, 693–703.

Galán P (2007) Viviparismo y distribución de *Salamandra salamandra bernardezi* en el norte de Galicia. *Boletín de la Asociación Herpetológica Española*, **18**, 44–49.

García-París M, Alcobendas M, Buckley D, Wake D (2003) Dispersal of viviparity across contact zones in Iberian populations of Fire salamanders (*Salamandra*) inferred from discordance of genetic and morphological traits. *Evolution*, **57**, 129–143.

Gibbs JP (1998) Distribution of woodland amphibians along a forest fragmentation gradient. *Landscape Ecology*, **13**, 263–268.

Grant AH, Liebgold EB (2017) Color-biased dispersal inferred by fine-scale genetic spatial autocorrelation in a color polymorphic salamander. *Journal of Heredity*, **108**, 588–593.

Halliwell B, Uller T, Holland BR, While GM (2017) Live bearing promotes the evolution of sociality in reptiles. *Nature Communications*, **8**, 2030.

Helfer V, Broquet T, Fumagalli L (2012) Sex-specific estimates of dispersal show female philopatry and male dispersal in a promiscuous amphibian, the alpine salamander (*Salamandra atra*). *Molecular Ecology*, **21**, 4706–4720.

Helmstetter AJ, Papadopulos AST, Igea J, Van Dooren TJM, Leroi AM, Savolainen V (2016) Viviparity stimulates diversification in an order of fish. *Nature Communications*, **7**, 11271.

Hendrix R, Hauswaldt JS, Veith M, Steinfartz S (2010) Strong correlation between cross-amplification success and genetic distance across all members of 'True salamanders' (Amphibia: Salamandridae) revealed by *Salamandra salamandra*-specific microsatellite loci. *Molecular Ecology Resources*, **10**, 1038–1047.

Hendrix R, Schmidt BR, Schaub M, Krause ET, Steinfartz S (2017). Differentiation of movement behaviour in an adaptively diverging salamander population. *Molecular Ecology*, **26**, 6400–6413.

Jones O, Wang J (2010) COLONY: a program for parentage and sibship inference from multilocus genotype data. *Molecular Ecology Resources*, **10**, 551–555.

Keenan K, McGinnity P, Cross TF, Crozier WW, Prodöhl PA (2013) diveRsity: an R package for the estimation of population genetics parameters and their associated errors. *Methods in Ecology and Evolution*, **4**, 782–788.

Liebgold EB, Brodie ED, Cabe PR (2011) Female philopatry and male-biased dispersal in a direct-developing salamander, *Plethodon cinereus*. *Molecular Ecology*, **20**, 249–257.

Liedtke HC, Müller H, Hafner J *et al.* (2017) Terrestrial reproduction as an adaptation to steep terrain in African toads. *Proceedings of the Royal Society B*, **284**, 20162598.

Lourenço A, Álvarez D, Wang IJ, Velo-Antón G (2017) Trapped within the city: integrating demography, time since isolation and population-specific traits to assess the genetic effects of urbanization. *Molecular Ecology*, **26**, 1498–1514.

Marsh DM, Thakur KA, Bulka KC, Clarke LB (2004) Dispersal and colonization through open fields by a terrestrial, woodland salamander. *Ecology*, **85**, 3396–3405.

Martínez-Solano I, Jockusch EL, Wake DB (2007) Extreme population subdivision throughout a continuous range: phylogeography of *Batrachoseps attenuatus* (Caudata: Plethodontidae) in western North America. *Molecular Ecology*, **16**, 4335–4355.

Measey GJ, Galbusera P, Breyne P, Matthysen E (2007) Gene flow in a direct-developing, leaf litter frog between isolated mountains in the Taita Hills, Kenya. *Conservation Genetics*, **8**, 1177–1188.

Ousterhout BH, Semlitsch RD (2018) Effects of conditionally expressed phenotypes and environment on amphibian dispersal in nature. *Oikos*, **127**, 1142-1151.

Peakall R, Ruibal M, Lindenmayer DB (2003) Spatial autocorrelation analysis offers new insights into gene flow in the Australian bush rat, *Rattus Fuscipes*. *Evolution*, **57**, 1182–1195.

Peakall R, Smouse PE (2012) GenAlEx 6.5: genetic analysis in Excel. Population genetic software for teaching and research – an update. *Bioinformatics*, **28**, 2537–2539.

Pereira RJ, Martínez-Solano I, Buckley D (2016) Hybridization during altitudinal range shifts: nuclear introgression leads to extensive cyto-nuclear discordance in the fire salamander. *Molecular Ecology*, **25**, 1551–1565.

Peterman WE, Connette GM, Semlitsch RD, Eggert LS (2014) Ecological resistance surfaces predict fine-scale genetic differentiation in a terrestrial woodland salamander. *Molecular Ecology*, **23**, 2402–2413.

R Development Core Team (2017) R: A language and environment for statistical computing. R Foundation for Statistical Computing, Vienna, Austria. https://www.R-project.org/

Rebelo R, Caetano MH (1995) Use of the skeletochronological method for ecodemographical studies on Salamandra salamandra gallaica from Portugal. *In*: Llorente GA, Montori A, Santos X, Carretero MA (eds) *Scientia Herpetologica: papers submitted from the 7th Ordinary General Meeting of Societas Europaea Herpetologica*, Barcelona, September 1993. Asociación Herpetológica Española, Barcelona, pp 135-140.

Rebelo R, Leclair MH (2003) Site tenacity in the terrestrial salamandrid *Salamandra salamandra*. *Journal of Herpetology*, **37**, 440–445.

Reinhardt T, Bauldauf L, Ilić M, Fink P (2018) Cast away: drift as the main determinant for larval survival in western fire salamanders (*Salamandra salamandra*) in headwater streams. *Journal of Zoology*, **306**, 171-179.

Richards-Zawacki CL, Wang IJ, Summers K (2012) Mate choice and the genetic basis for colour variation in a polymorphic dart frog: inferences from a wild pedigree. *Molecular Ecology*, **21**, 3879-3892.

Ronce O, Clobert J (2012) Dispersal syndromes. *In*: Clobert J, Baguette J, Benton TG, Bullock JM (eds) *Dispersal ecology and evolution*. Oxford University Press, Oxford, pp. 119-138.

Rousset F (2008) GENEPOP'007: a complete re-implementation of the GENEPOP software for Windows and Linux. *Molecular Ecology Resources*, **8**, 103–106.

Russell AP, Bauer AM, Johnson MK (2005) Migration in amphibians and reptiles: an overview of patterns and orientation mechanisms in relation to life history strategies. *In*: Elewa AMT (ed) *Migration of organisms*. Springer-Verlag, Berlin Heidelberg, pp. 151-203.

Saastamoinen M, Bocedi G, Cote J, *et al.* (2018) Genetics of dispersal. *Biological Reviews*, **93**, 574-599.

Sánchez-Montes G, Ariño AH, Vizmanos JL, Wang J, Martínez-Solano I (2017) Effects of sample size and full sibs on genetic diversity characterization: a case study of three syntopic Iberian pond-breeding amphibians. *Journal of Heredity*, **108**, 535–543.

Sandberger-Loua L, Rödel MO, Feldhaar H (2018) Gene-flow in the clouds: landscape genetics of a viviparous, montane grassland toad in the tropics. *Conservation Genetics*, **19**, 169-180.

Schmidt BR, Itin E, Schaub M (2014) Seasonal and annual survival of the salamander *Salamandra salamandra salamandra*. *Journal of Herpetology*, **48**, 20–23.

Schulte U, Küsters D, Steinfartz S (2007) A PIT tag based analysis of annual movement patterns of adult fire salamanders (*Salamandra salamandra*) in a Middle European habitat. *Amphibia-Reptilia*, **28**, 531–536.

Segev O, Blaustein L (2014) Influence of water velocity and predation risk on fire salamander (*Salamandra infraimmaculata*) larval drift among temporary pools in ephemeral streams. *Freshwater Science*, **33**, 950–957.

Semlitsch RD (2008) Differentiating migration and dispersal processes for pond-breeding amphibians. *Journal of Wildlife Management*, **72**, 260–267.

Shine R (1980) "Costs" of reproduction in reptiles. *Oecologia*, **46**, 92–100.

Shine R (2015) The evolution of oviparity in squamate reptiles: an adaptationist perspective. *Journal of Experimental Zoology Part B: Molecular and Developmental Evolution*, **324**, 487-492.

Smith MA, Green DM (2005) Dispersal and the metapopulation in amphibian and paradigm ecology are all amphibian conservation: populations metapopulations? *Ecography*, **28**, 110–128.

Smouse PE, Peakall R (1999) Spatial autocorrelation analysis of individual multiallele and multilocus genetic structure. *Heredity*, **82**, 561-573.

Smouse PE, Peakall R, Gonzales E (2008) A heterogeneity test for fine-scale genetic structure. *Molecular Ecology*, **17**, 3389–3400.

Steinfartz S, Kuesters D, Tautz D (2004) Isolation and characterization of polymorphic tetranucleotide microsatellite loci in the Fire salamander *Salamandra salamandra* (Amphibia: Caudata). *Molecular Ecology Resources*, **4**, 626-628.

Stevens VM, Pavoine S, Baguette M (2010) Variation within and between closely related species uncovers high intra-specific variability in dispersal. *PLoS ONE*, **5**, e11123.

Tilley SG (2016) Patterns of genetic differentiation in woodland and dusky salamanders. *Copeia*, **104**, 8-20.

Thiesmeier B, Schuhmacher H (1990) Causes of larval drift of the fire salamander, *Salamandra salamandra terrestris*, and its effects on population dynamics. *Oecologia*, **82**, 259–263.

Trochet A, Courtois EA, Stevens VM *et al.* (2016) Evolution of sex-biased dispersal. *The Quarterly Review of Biology*, **91**, 297–320.

van Dyke JU, Brandley MC, Thompson MB (2014) The evolution of viviparity: molecular and genomic data from squamate reptiles advance understanding of live birth in amniotes. *Reproduction*, **147**, R15–R26.

Velo-Antón G, Buckley D (2015) Salamandra común – *Salamandra salamandra*. *In*: Carrascal LM, Salvador A (eds) *Enciclopedia Virtual de los Vertebrados Españoles*. Museo Nacional de Ciencias Naturales, Madrid. http://www.vertebradosibericos.org/anfibios/salsal.html

Velo-Antón G, Cordero-Rivera A (2017) Ethological and phenotypic divergence in insular fire salamanders: diurnal activity mediated by predation? *Acta Ethologica*, **20**, 243-253.

Velo-Antón G, García-París M, Galán P, Cordero Rivera A (2007) The evolution of viviparity in holocene islands: ecological adaptation versus phylogenetic descent along the transition from aquatic to terrestrial environments. *Journal of Zoological Systematics and Evolutionary Research*, **45**, 345–352.

Velo-Antón G, Parra JL, Parra-Olea G, Zamudio KR (2013) Tracking climate change in a dispersal-limited species: reduced spatial and genetic connectivity in a montane salamander. *Molecular Ecology*, **22**, 3261–3278.

Velo-Antón G, Santos X, Sanmartín-Villar I, Cordero-Rivera A, Buckley D (2015) Intraspecific variation in clutch size and maternal investment in pueriparous and larviparous *Salamandra salamandra* females. *Evolutionary Ecology*, **29**, 185-204.

Velo-Antón G, Zamudio KR, Cordero-Rivera A (2012) Genetic drift and rapid evolution of viviparity in insular fire salamanders (*Salamandra salamandra*). *Heredity*, **108**, 410–418.

Wang IJ (2013) Examining the full effects of landscape heterogeneity on spatial genetic variation: a multiple matrix regression approach for quantifying geographic and ecological isolation. *Evolution*, **67**, 3403–3411.

Wang IJ, Shaffer HB (2017) Population genetic and field ecological analyses return similar estimates of dispersal over space and time in an endangered amphibian. *Evolutionary Applications*, **10**, 630–639.

Wang J (2011) Coancestry: A program for simulating, estimating and analysing relatedness and inbreeding coefficients. *Molecular Ecology Resources*, **11**, 141–145.

Wang J, Santure AW (2009) Parentage and sibship inference from multilocus genotype data under polygamy. *Genetics*, **181**, 1579–1594.

Wang Y, Lane A, Ding P (2012) Sex-biased dispersal of a frog (*Odorrana schmackeri*) is affected by patch isolation and resource limitation in a fragmented landscape. *PLoS ONE*, **7**, e47683.

Chapter 4

Comparative landscape genetics of larviparous and pueriparous populations

Paper III

Comparative landscape genetics reveals the evolution of viviparity reduces genetic connectivity in fire salamanders

André Lourenço[1,2], João Gonçalves[2], Filipe Carvalho[2,3], Ian J. Wang[4] and Guillermo Velo-Antón[2]

Article published in Molecular Ecology, 2019, 28, 4573-4591. doi: https://doi.org/10.1111/mec.15249

[1] Departamento de Biologia da Faculdade de Ciências da Universidade do Porto, Rua Campo Alegre, 4169-007 Porto, Portugal.

[2] CIBIO/InBIO, Centro de Investigacao em Biodiversidade e Recursos Genéticos da Universidade do Porto, Instituto de Ciências Agrárias de Vairão, Rua Padre Armando Quintas 7, 4485-661 Vairão, Portugal

[3] Department of Zoology and Entomology, School of Biological and Environmental Sciences, University of Fort Hare, Private Bag X1314, Alice 5700, South Africa

[4] Department of Environmental Science, Policy and Management, University of California, 130 Mulford Hall #3114, Berkeley, CA 94705 USA

4.1 – Abstract

Evolutionary changes in reproductive mode may affect co-evolving traits, such as dispersal, although this subject remains largely underexplored. The shift from aquatic oviparous or larviparous reproduction to terrestrial viviparous reproduction in some amphibians entails skipping the aquatic larval stage and, thus, greater independence from water. Accordingly, amphibians exhibiting terrestrial viviparous reproduction may potentially disperse across a wider variety of suboptimal habitats and increase population connectivity in fragmented landscapes compared to aquatic-breeding species. We investigated this hypothesis in the fire salamander (*Salamandra salamandra*), which exhibits both aquatic- (larviparity) and terrestrial-breeding (viviparity) strategies. We genotyped 426 larviparous and 360 viviparous adult salamanders for 13 microsatellite loci and sequenced a mitochondrial marker for 133 larviparous and 119 viviparous individuals to compare population connectivity and landscape resistance to gene flow within a landscape genetics framework. Contrary to our predictions, viviparous populations exhibited greater differentiation and reduced genetic connectivity compared to larviparous populations. Landscape genetic analyses indicate viviparity may be partially responsible for this pattern, as water courses comprised a significant barrier only in viviparous salamanders, probably due to their fully terrestrial life cycle. Agricultural areas and, to a lesser extent, topography also decreased genetic connectivity in both larviparous and viviparous populations. This study is one of very few to explicitly demonstrate the evolution of a derived reproductive mode affects patterns of genetic connectivity. Our findings open avenues for future research to better understand the eco-evolutionary implications underlying the emergence of terrestrial reproduction in amphibians.

Keywords: genetic structure, haplotypes, landscape genetics, larviparity, pueriparity, *Salamandra salamandra*.

4.2 – Introduction

The evolution of derived phenotypic traits enables individuals to exploit novel resources and colonise new areas, often entailing profound eco-evolutionary implications to taxa (Losos 2010). One remarkable life-history adaptation is the transition from egg-laying (oviparous) reproduction to live-bearing (viviparous) reproduction, which occurred more than 150 times in vertebrates (mostly in reptiles) and involved major phenotypic, genetic, and ecological changes, especially in females (*e.g.* Pincheira-Donoso *et al.* 2013; Blackburn 2015; Wake 2015; Helmstetter *et al.* 2016; Halliwell *et al.* 2017; Gao *et al.* 2019). Strong environmental

pressures on offspring (*e.g.* stressful environmental conditions or predation) generally selected for longer periods of embryo retention (*i.e.* viviparity) to increase offspring survival rates, thus allowing viviparous taxa to thrive in harsher environments and disperse to areas previously inaccessible (*e.g.* Pincheira-Donoso *et al.* 2013; Helmstetter *et al.* 2016; Ma *et al.* 2018).

The phenotypic and ecological changes underlying the evolution of viviparity may also affect co-evolving traits, such as dispersal. This is because the dispersal ecology of organisms is intimately linked with reproductive biology, as it comprises a key mechanism for finding mates and breeding sites (Bonte *et al.* 2012; Pittman *et al.* 2014; Cosgrove *et al.* 2018). Additionally, individuals must also adjust dispersal decisions and pathways in accordance with environmental conditions encountered during the dispersal process to increase reproductive success (Bonte *et al.* 2012). Hence, the changes in reproductive biology and behaviour entailed by the evolution of viviparity can alter the ways individuals interact with the surrounding environment (Shine 2015), which in turn may affect overall patterns of dispersal, gene flow, and population dynamics. However, the effects of reproductive mode on dispersal ecology remain largely underexplored.

For amphibians in particular, shifts to viviparous or pueriparous reproduction (hereafter we use “pueriparous” for amphibians; see Greven 2003) result in significant life-history changes, making amphibians good systems in which to examine the effects of changes in reproductive mode on dispersal and genetic connectivity. Most amphibians exhibit a biphasic life cycle, in which an aquatic larval stage is followed by metamorphosis into terrestrial juveniles (Wells 2007). In aquatic-breeding amphibians, dispersal behaviour and success are largely driven by the quality and availability of aquatic breeding sites for the deposition and development of offspring (Pittman *et al.* 2014). However, some amphibians shifted from ancestral oviparous or larviparous aquatic reproduction (delivery of eggs or larvae in water, respectively) to pueriparous terrestrial reproduction (parturition of juveniles), possibly in response to a lack of suitable water bodies in their environments for depositing offspring (Velo-Antón *et al.* 2015; Liedtke *et al.* 2017). Their fully terrestrial lifestyle enables them to cope better with the challenges imposed by water-limited environments and to potentially disperse successfully across a wider variety of unsuitable habitats in comparison to aquatic-breeding amphibians (Liedtke *et al.* 2017; Lourenço *et al.* 2017).

Previous studies in aquatic- and terrestrial-breeding amphibians (including pueriparous and direct-developing species) have indeed suggested a lower dependency on water may reduce population genetic divergence in heterogeneous and fragmented landscapes (Measey *et al.* 2007; Mims *et al.* 2015; Sandberger-Loua *et al.* 2018), although other studies on direct-developing amphibians have reported substantial levels of genetic differentiation among

populations (*e.g.* Peterman *et al.* 2014a; Paz *et al.* 2015). Comparative studies involving species showing intraspecific variation in reproductive modes are crucial (*e.g.* aquatic vs. terrestrial reproduction), as they can overcome the potentially confounding factors involved in comparisons of species with pronounced phenotypic and ecological differences (*e.g.* Garcia *et al.* 2017; Hendrix *et al.* 2017).

Here, we examine patterns of gene flow among populations of the fire salamander (*Salamandra salamandra*, Linnaeus 1758), which, with its sister species, the North-African fire salamander (*S. algira*, Bedriaga 1883), is one of the only known amphibians exhibiting both aquatic and terrestrial reproduction (Velo-Antón *et al.* 2015; Dinis and Velo-Antón 2017). *Salamandra salamandra* exhibits two reproductive strategies: larviparity, in which females deliver up to *ca.* 90 larvae in water bodies after a gestation period of approximately 90 days; and pueriparity, in which the larval aquatic stage is skipped and females deliver 1–35 fully metamorphosed terrestrial juveniles after the same gestation period (Buckley *et al.* 2007; Velo-Antón *et al.* 2015). The ancestral reproductive mode, larviparity, is present throughout most of its range, while pueriparity is currently restricted to a section of northern Spain in the subspecies *S. s. bernardezi* and *S. s. fastuosa* (**Figure 4.1A**; Velo-Antón *et al.* 2015). Pueriparity probably arose in *S. s. bernardezi* in the Cantabrian Mountains during the Pleistocene, possibly in response to the lack of surface water in karstic limestone substrates (García-París *et al.* 2003). This trait later introgressed eastwards with *S. s. fastuosa* during population expansions following cycles of warm and cold climates (García-París *et al.* 2003). More recently (Holocene, <8 kya), pueriparity has also emerged independently in two insular populations of *S. s. gallaica* in north-western Spain (Velo-Antón *et al.* 2007; Velo-Antón *et al.* 2012).

A previous study contrasting patterns of fine-scale genetic structure and dispersal between larviparous and pueriparous fire salamanders on intact, natural landscapes (1-km transects) did not find significant differences in spatial genetic autocorrelation between reproductive modes (Lourenço *et al.* 2018a). However, whether such patterns hold at broader scales in heterogeneous and fragmented landscapes remains unknown. For instance, water bodies may be important dispersal corridors for larviparous populations, while water-limited habitats may be less resistant to dispersal for pueriparous salamanders, as they can survive in harsher environments (Lourenço *et al.* 2017). The field of landscape genetics has comprised a useful analytical framework for inferring the potential role of phenotypic traits and environmental heterogeneity in maintaining genetic connectivity among different taxa (*e.g.* Richardson 2012; Manel and Holderegger 2013; Garcia *et al.* 2017). These approaches may help us to determine whether a shift to pueriparity altered the way fire salamanders disperse across the landscape.

Here, we use a mitochondrial marker and a set of nuclear microsatellite loci in a comparative landscape genetics framework to: (i) characterise and evaluate differences in patterns of genetic diversity and structure between pueriparous and larviparous populations; and (ii) identify the environmental variables governing genetic connectivity in populations exhibiting different reproductive strategies. Because pueriparous individuals are expected to survive and disperse across a greater range of habitats, we expect to observe reduced genetic structure and higher genetic connectivity among pueriparous populations compared to their larviparous counterparts across two fragmented and heterogeneous focal landscapes.

4.3 – Materials and methods

4.3.1 – Study system

We focused on two *Salamandra salamandra* subspecies distributed in the north-western Iberian Peninsula: (i) *S. s. gallaica*, which is larviparous in mainland populations; and (ii) *S. s. bernardezi*, which is pueriparous (**Figure 4.1B**; Velo-Antón *et al.* 2015). The insular pueriparous populations of *S. s. gallaica* were not included in our comparative framework due to their independent origin of pueriparity (Velo-Antón *et al.* 2007) and population-specific characteristics (isolated populations, low genetic diversity, and divergent behaviour; Velo-Antón *et al.* 2012; Velo-Antón and Cordero-Rivera 2017; Lourenço *et al.* 2018b).

In northern Spain, individuals of both subspecies inhabit mostly humid and shaded environments, particularly deciduous woodlands (*Quercus* spp. and *Fagus* spp.) containing a high availability of shelters (*e.g.* underground cavities, fallen logs, and rocks) and nearby aquatic systems (streams or ponds) where larviparous females can give birth to aquatic larvae (Velo-Antón and Buckley 2015). However, they can also be found in a wide range of terrestrial habitats, including native coniferous forests, scrublands, and occasionally pine (*Pinus* spp.) and eucalyptus (*Eucalyptus* spp.) plantations (Cordero *et al.* 2007; Velo-Antón and Buckley 2015). Agricultural and urban areas generally comprise strong barriers to gene flow (Lourenço *et al.* 2017; Antunes *et al.* 2018), although pueriparous salamanders can survive in water-limited and harsh environments, such as small gardens and urban parks (Álvarez *et al.* 2015; Lourenço *et al.* 2017).

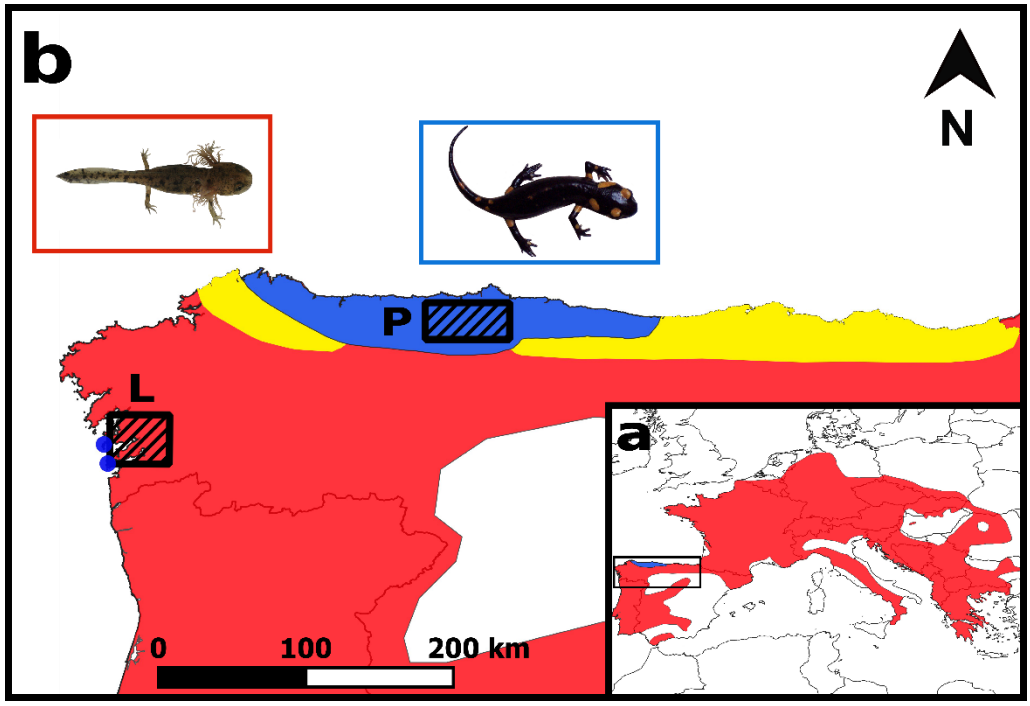

Fig. 4.1 Study areas. (a) Distribution of *Salamandra salamandra* in Europe, with larviparous and pueriparous populations highlighted in red and blue, respectively. (b) Distribution of larviparity and pueriparity in *S. salamandra* in the north-west corner of Iberian Peninsula. Both studied landscape plots (L – larviparous plot; P – pueriparous plot) are represented by black dashed rectangles. The yellowed areas illustrate roughly the contact zones between pueriparous and larviparous populations, in which, preliminary data has shown that there is substantial phenotypic and genetic admixture. The two blue dots represented in the west coast correspond to the insular pueriparous populations of *S. s. gallaica* not included in this study (see main text).

4.3.2 – Study sites and sampling

We studied two landscape plots, one for larviparous and one for pueriparous populations, that are located in northwestern Spain (**Figure 4.1B**). Larviparous salamanders of *S. s. gallaica* were sampled in a region (*ca.* 1,400 km^2) located on the western coast of the province of Galicia (hereafter "larviparous plot"; longitude: −8.61005; latitude: 42.42410), while pueriparous individuals of *S. s. bernardezi* were sampled in an area (*ca.* 1,800 km^2) situated in the province of Asturias (hereafter "pueriparous plot"; longitude: −6.03219; latitude: 43.36512). Both plots were selected because genetic admixture between different reproductive modes is absent (**Figure C1 in Appendix C**) and because they are similar in climate, topography, and landscape composition (**Figure C2 in Appendix C**). Climate in both regions is Atlantic, with an annual mean temperature of 14.8 and 13.3°C in the larviparous and pueriparous plots, respectively; the mean annual total precipitation, although high in both regions, is higher in the larviparous plot (1613 vs. 960 mm; AEmet 2010). Topography is complex, with altitude ranging from 1 m up to 1676 m in the pueriparous plot and from 1 m up

to 873 m in the larviparous plot. To account for these differences in topographic variation, we only sampled localities in low-elevation areas (<700 m) in both regions (**Figure C3 in Appendix C**). Furthermore, the landscape in both areas is highly heterogeneous and fragmented (**Figure C4 in Appendix C**; see **Supplementary Text C1** and **Table C1 in Appendix C** for details about land use reclassification). Both are dominated by five main habitat types: natural forests (*ca.* 17%–19%), scrublands (*ca.* 24% in both plots), plantations of exotic trees (*ca.* 22% and 7% in the larviparous and pueriparous plots, respectively), agricultural areas (*ca.* 22% and 40% in the larviparous and pueriparous plots, respectively), and urban settlements and infrastructures (*ca.* 5%–9%). Other minor land use types occupy cumulatively ≤5% (**Table C2 in Appendix C**). Focal regions do not differ substantially in the spatial configuration of putatively suitable and unsuitable habitats for fire salamanders, with most landscape metrics showing similar values (see **Supplementary Text C2 and Table C3 in Appendix C**).

The ideal comparison would be to sample larviparous and pueriparous salamanders from the same area to control for potential confounding effects of environmental variation across different sampling regions. However, while there are indeed areas where *S. s. bernardezi* and larviparous populations of other subspecies (including *S. s. gallaica* at north-west) are codistributed (**Figure 4.1B**), we did not sample these contact zones because there is substantial genetic and phenotypic admixture between larviparous and pueriparous salamanders (Galán 2007; unpublished data). This hinders not only the identification of an individual's reproductive mode in the field but also the assessment of the effects of reproductive mode on dispersal and gene flow.

Sampling was carried out during rainy nights from November 2013 until May 2018. We sampled a total of 428 adult larviparous salamanders from 22 sites (sample size per locality: 17-25) and 362 adult pueriparous individuals from 18 localities (sample size per locality: 15-25; **Table 4.1** and **Figure C4 in Appendix C**). Tail or toe clip samples were collected from individuals and preserved in ethanol. This procedure has a minimal impact on individual fitness, as fire salamanders are capable of regenerating limbs within a few weeks (Blaustein *et al.* 2018). Following tissue collection, sampled individuals were released at their place of capture. Because a few localities were sampled during multiple nights and several months apart, we conducted two procedures to avoid including recaptured individuals in genetic analyses. First, we inspected toes/tails from all encountered individuals. Second, because fire salamanders are capable of regenerating tissues, we used the option Multilocus Matches implemented in GENALEX v6.5 (Peakall and Smouse 2012) to check for genotype matches within each sampled locality based on microsatellite data.

4.3.3 - Molecular markers and laboratory procedures

We extracted genomic DNA using Genomic DNA Tissue Kits (EasySpin), following the manufacturer's protocol. Quantity and quality of extracted products were verified in a 0.8% agarose gel. To examine deeper levels of population divergence, we amplified and sequenced a fragment of the mitochondrial DNA (mtDNA) gene cytochrome b (cyt b) for a representative subsample of our data set (133 larviparous and 119 pueriparous salamanders). We amplified cyt b using the primers Glu14100L and Pro15500H (Zhang *et al.* 2008), following the protocol described by Beukema *et al.* (2016). DNA sequencing was outsourced to Genewiz Inc., and the resulting chromatograms were inspected and aligned using geneious v11.1.4 (http://www.genei ous.com). The aligned cyt b sequences were trimmed to avoid missing data, resulting in a consensus sequence of 665 bp. Following the protocol used by Lourenço *et al.* (2018a), we also amplified 14 microsatellites (SST-A6-I, SST-A6-II, SST-B11, SST-C3, and SST-G9; Hendrix *et al.* 2010; SalE14, Sal29, SalE12, SalE7, SalE5, SalE2, SalE06, Sal3, and SalE8; Steinfartz *et al.* 2004), distributed in four optimised multiplexes, to compare contemporary (short-term) patterns of genetic diversity and structure between larviparous and pueriparous populations.

We tested for deviations from Hardy–Weinberg equilibrium (HWE) and linkage equilibrium (LE) in these microsatellites by performing exact tests in GENEPOP 4.2 (Rousset 2008; dememorization = 5000, batch length = 10000, batch number = 1000). The p-values from HWE and LE multiple exact tests were corrected using the false discovery rate (Benjamini and Hochberg 1995). We tested the presence of null alleles in INEST 2.0 (Chybicki and Burczyk 2009) with 200,000 iterations, thinned every 200 iterations and with a burnin of 10% for the full individual inbreeding model.

4.3.4 – Patterns of genetic variation

We used the amplified cyt b fragment to infer long-term patterns of genetic variation. We calculated the number of unique haplotypes in each landscape plot and constructed haplotype networks using statistical parsimony, as implemented in TCS 1.21 (Clement *et al.* 2000).

We used microsatellites genotypes to estimate several summary statistics for each sampling site, including the mean number of alleles (N_A), number of private alleles (P_A), observed (H_O) and expected (H_E) heterozygosity, allelic richness (A_R), population mean inbreeding coefficient (F), and average relatedness (R_L). The first four genetic parameters were calculated in GENALEX, while A_R corrected for the smallest locality's sample size was estimated in R 3.5.1 (R Core Team 2018) with the package *diveRsity* 1.9.90 (Keenan *et al.*

2013). F was calculated in INEST, and R_L was estimated using the triadic likelihood estimator implemented in COANCESTRY 1.0.1.5, assuming no inbreeding (Wang 2011).

Table 4.1 Locality information and population (Pop) genetic statistics of populations sampled in the larviparous and pueriparous plots. These statistics were estimated with 13 microsatellite loci. Lat – latitude; Long – longitude; Code – population code; n – sample size; N_A – mean number of alleles; P_A – number of private alleles; H_O – observed heterozygosity; H_E – observed heterozygosity; A_R – allelic richness; F – mean inbreeding coefficient; R – relatedness.

Pop	Lat	Long	Code	n	N_A	P_A	H_O	H_E	A_R	F	R_L
Larviparous plot											
PEGA	42.320	-8.716	1	25	11.08	7	0.78	0.79	8.39	0.02	0.04
BORB	42.284	-8.532	2	20	8.69	1	0.73	0.76	7.09	0.03	0.06
REDO	42.291	-8.572	3	20	9.08	1	0.74	0.77	7.35	0.02	0.05
XUST	42.324	-8.606	4	18	9.77	4	0.77	0.79	7.86	0.02	0.04
SOUT	42.340	-8.557	5	17	9.00	1	0.82	0.80	7.49	0.01	0.06
EIRA	42.351	-8.489	6	19	9.08	4	0.79	0.81	7.48	0.01	0.05
COTO	42.360	-8.677	7	20	10.00	5	0.81	0.79	7.93	0.01	0.03
CANI	42.364	-8.606	8	21	9.62	2	0.77	0.79	7.61	0.02	0.06
TABU	42.370	-8.559	9	17	8.38	1	0.76	0.78	6.95	0.02	0.05
LOUR	42.408	-8.670	10	17	9.69	3	0.80	0.79	7.66	0.01	0.04
CAMP	42.406	-8.594	11	18	9.08	0	0.78	0.79	7.37	0.02	0.05
PARA	42.409	-8.510	12	20	9.54	1	0.80	0.80	7.73	0.02	0.04
XENX	42.421	-8.853	13	20	6.69	1	0.62	0.70	5.57	0.02	0.11
OVAO	42.448	-8.661	14	20	9.92	4	0.82	0.82	7.87	0.01	0.04
LREZ	42.452	-8.620	15	19	9.77	6	0.78	0.81	7.76	0.03	0.04
CALV	42.453	-8.558	16	19	8.54	1	0.77	0.77	6.87	0.02	0.05
CAST	42.463	-8.711	17	20	9.38	0	0.75	0.78	7.44	0.03	0.02
RIBA	42.511	-8.743	18	18	7.69	1	0.70	0.75	6.42	0.03	0.06
PTCT	42.516	-8.624	19	18	7.77	0	0.73	0.74	6.38	0.02	0.07
LOBE	42.562	-8.765	20	17	7.08	1	0.65	0.74	5.88	0.04	0.06
BARO	42.558	-8.626	21	24	9.08	2	0.68	0.77	7.16	0.04	0.05
LAME	42.548	-8.550	22	19	8.54	6	0.76	0.78	7.11	0.04	0.05
mean				**19.4**	**8.98**	**2.36**	**0.75**	**0.78**	**7.24**	**0.02**	**0.05**
Pueriparous plot											
INFA	43.359	-6.262	1	25	11.08	2	0.73	0.82	8.29	0.04	0.08
VNUE	43.358	-6.215	2	20	9.00	1	0.77	0.81	8.28	0.02	0.11
CORN	43.402	-6.192	3	19	8.46	3	0.76	0.77	6.55	0.04	0.14
REST	43.299	-6.191	4	18	9.85	4	0.70	0.78	6.11	0.03	0.08
YERN	43.273	-6.124	5	20	8.77	4	0.77	0.75	6.72	0.02	0.11
CUTI	43.358	-6.143	6	20	9.62	3	0.78	0.81	8.37	0.03	0.07
PADR	43.334	-6.120	7	20	9.15	2	0.78	0.80	7.41	0.02	0.09
PZAL	43.357	-6.064	8	19	7.54	1	0.79	0.77	6.89	0.01	0.15
BASE	43.309	-6.059	9	20	9.69	10	0.80	0.78	7.64	0.01	0.09
BOHI	43.435	-6.034	10	20	10.69	3	0.83	0.84	6.98	0.02	0.05
BOLG	43.404	-6.025	11	20	6.92	2	0.70	0.71	7.78	0.03	0.20
CCES	43.348	-5.999	12	20	9.31	3	0.82	0.81	7.46	0.02	0.07
TRUB	43.329	-5.953	13	20	10.23	3	0.83	0.83	6.35	0.01	0.06
BRAN	43.409	-5.922	14	25	10.69	2	0.74	0.81	7.49	0.03	0.06
POSA	43.461	-5.863	15	25	8.08	2	0.74	0.75	8.45	0.03	0.12
VMAR	43.369	-5.911	16	17	7.15	3	0.69	0.71	5.63	0.02	0.20
LILL	43.381	-5.858	17	19	8.85	3	0.73	0.82	8.29	0.04	0.08
BEND	43.333	-5.802	18	15	8.08	1	0.77	0.81	8.28	0.02	0.10
mean				**20.1**	**9.06**	**2.89**	**0.76**	**0.78**	**7.28**	**0.02**	**0.10**

We also employed genotypic data to examine short-term genetic structure through several independent approaches. Two measures of genetic differentiation and respective 95% confidence intervals (CIs) were calculated between sampled localities within each landscape plot: (i) pairwise F_{ST} (Weir *and* Cockerham 1984); and (ii) pairwise Jost's D_{EST} (Jost 2008). These measures were computed in the R package *diveRsity* using 5000 bootstrap replicates. Pairwise values were acknowledged as significant when 95% CIs did not overlap with zero, as recommended by Keenan *et al.* (2013).

We also inferred and visualized patterns of contemporary population genetic structure through two methods, which present different model assumptions: (i) the Bayesian clustering algorithm implemented in STRUCTURE 2.3.4 (Pritchard *et al.* 2000); and (ii) the Discriminant Analysis of Principal Components (DAPC; Jombart *et al.* 2010) implemented in the R package *adegenet* 2.1.1 (Jombart *et al.* 2008). These analyses were performed independently for each landscape plot.

Preliminary analyses in structure using the standard models (*i.e.* no sampling location information), together with the low pairwise genetic differentiation values (see Results), suggest that larviparous populations exhibit weak genetic structure (**Figure C5 in Appendix C**). Under these circumstances, incorporating sampling information in structure (*i.e.* including the LOCPRIOR parameter) provides more accurate detection of subtle patterns of genetic structure (Hubisz *et al.* 2009). Accordingly, analyses using standard and LOCPRIOR models were performed for both the pueriparous and larviparous populations to provide optimal comparisons. Analyses were carried out with the admixture model and correlated allele frequencies. We performed ten independent runs for K genetic clusters ranging from 1 to 20, which accounts for both potential substructure within pueriparous populations and the low genetic divergence exhibited by larviparous populations. A burnin period of 5×10^4 iterations followed by 5×10^5 Markov chain Monte Carlo iterations were set for each run. The output generated from multiple independent runs across each K was summarised and graphically represented using the main pipeline implemented in CLUMPAK with default advanced options (Kopelman *et al.* 2015). We used the software KFINDER 1.0 (Wang 2019) to determine the most supported K using three different criteria: (i) the K value that maximises the mean logarithmic posterior probability (ln[X|K]; Pritchard et al. 2000); (ii) the rate of change of ln[X|K] among K values (ΔK; Evanno *et al.* 2005); and (iii) the parsimony index (PI) parameter, which identifies the K that yields the most consistent and minimal average admixture (Wang 2019). Extensive simulations showed PI more accurately infers the correct number of genetic clusters under a variety of scenarios, including unbalanced sampling, low numbers of loci, reduced genetic divergence, and inbreeding (Wang 2019).

DAPC is a multivariate method that summarizes the data to minimize genetic differentiation within groups while maximizing it between groups. Unlike STRUCTURE, it does not rely in HWE and LE assumptions. We first executed the k-means algorithm to identify the optimal K value between an interval of K=1-20. The K exhibiting the lowest Bayesian Information Criterion was considered the most supported one. Then, to perform the DAPC, we followed *adegenet*'s guidelines to choose the adequate number of retained principal components and discriminant functions to avoid overfitting (Jombart *et al.* 2010).

4.3.5 – Landscape variables

To test the effects of landscape factors on genetic differentiation, we produced 17 environmental raster layers (**Table 4.2**) associated with land use, topography, and vegetation variables in each study area that are ecologically relevant to *S. salamandra* (Velo-Antón and Buckley 2015; Lourenço *et al.* 2017; Antunes *et al.* 2018) and other amphibians (*e.g.* Richardson, 2012; Velo-Antón *et al.* 2013; Alton and Franklin 2017; Gutiérrez-Rodríguez *et al.* 2017; McCartney-Melstad *et al.* 2018; Waraniak *et al.* 2019). These layers were cropped to the extent of each landscape plot, resampled to a 100 m resolution to make optimisation of resistance surfaces tractable and checked for collinearity ($|r| > 0.7$). Details of the post-processing procedures carried out to derive these 17 layers are explained in **Supplementary Text C3 in Appendix C**.

We generated five categorical binary layers representing presence/absence of the most abundant land use classes (*i.e.* natural forests, scrublands, plantations of exotic trees, agricultural areas, and urban settlements) for evaluating the impacts of each class on genetic connectivity in landscape resistance analyses. These layers were produced using a land use reclassification of vector layers downloaded from the *Centro Nacional de Información Geográfica* (CNIG; http://centrodedescargas.cnig.es/CentroDescargas/index.jsp) for 2011. These binary layers were used because preliminary analyses showed they exhibit higher statistical support than a layer representing all nine reclassified land use classes (see **Supplementary Text C3 and Table C4 in Appendix C**). We also derived three raster layers representing: (i) the density of paved roads (obtained from CNIG); (ii) the density of water courses, which includes both small streams and large rivers (accessed from the Ministerio para la Transición Ecológica; https://www.miteco.gob.es/es/cartografia-y-sig/ide/descargas/agua/red-hidrografi ca.aspx); and (ii) the density of water courses exhibiting a Strahler rank ≥3 (*i.e.* large rivers), which was derived from the european environment agency catchments and rivers network system v1.1 database (https ://www.eea.europa.eu/data-and-maps/data/european-catchments-and-rivers-network#tab-european-data).

We also produced five layers describing topographic complexity and climatic conditions directly associated with topography, namely: (i) altitude (downloaded from CNIG); (ii) slope; (iii) topographic wetness index (TWI), which describes patterns of water accumulation on the landscape; (iv) wind exposition index; and (v) potential incoming solar radiation.

To characterise vegetation and its spatial configuration, we obtained annual time series of Landsat-8 images for 2017 from Google Earth Engine (Gorelick *et al.* 2017). These images were used to derive two continuous indices of vegetation: (i) the Enhanced Vegetation Index (EVI); and (ii) the Normalized Difference Water Index (NDWI). EVI characterises patterns of vegetation cover and is more responsive to canopy structural variation and less sensitive to soil and atmospheric effects than the Normalized Difference Vegetation Index (Huete *et al.* 2002), while NDWI quantifies water content in leaves. We calculated these indices from remote sensing data at a spatial resolution of 30 m and later resampled the resulting layers to 100 m resolution using both the average (describes the amount) and the standard deviation (characterises spatial heterogeneity). Hence, we generated a total of four vegetation-related rasters for use in downstream analyses: (i) mean EVI; (ii) standard deviation of EVI; (iii) mean NDWI; and (iv) standard deviation of NDWI.

In addition to these 17 layers, we used neutral landscape models (NLMs) to simulate landscape patterns based on theoretical null distributions. Among other applications, NLMs can be used as null models to evaluate the effects of real landscapes on ecological processes (Gardner and Urban 2007). We used the R package *NLMR* 0.4 (Sciaini, Fritsch, & Scherer, 2018) to generate four NLM layers: (i) random; (ii) random cluster; (iii) distance gradient; and (iv) fractional brownian motion (**Figure C6 in Appendix C**). Default options were always used, with the exception of the random cluster model, in which five discrete land use types were processed to simulate land cover heterogeneity.

4.3.6 – Landscape genetic analyses

We applied the genetic optimisation algorithm framework implemented in the R package *ResistanceGA* 4.0-14 (Peterman 2018) to determine which environmental layers best explain genetic structure in larviparous and pueriparous populations. Briefly, this algorithm adaptively explores parameter space to find the combination of resistance surface values and transformations that maximise the statistical relationship between matrices of pairwise cost-distances (predictor) and genetic distances (response). Statistical relationships were assessed through a linear mixed effects model with maximum likelihood population effects (MPLE; Clarke *et al.* 2002), as implemented in the R package *lme4* (Bates *et al.* 2015). This regression technique accounts for nonindependence among the pairwise data and has been shown to

perform better than other regression methods commonly employed in landscape genetic studies (Shirk *et al.* 2018). See **Supplementary Text C4** and Peterman (2018) for more details about the algorithm.

Table 4.2 Environmental variables used in landscape genetic analyses. These variables are related with land use, topography, vegetation, and neutral landscape models (NMLs). The column "Hyp" denotes the predicted effects of the increase of a specific variable on genetic connectivity ("-", hinders gene flow; "+", facilitates gene flow). The mean ($\bar{x}$) and respective range of values for each environmental variable is also displayed per landscape plot (L – larviparous; P – pueriparous; LP – both plots), with the exception of categorical variables. NA – not applicable

Type	Variable	Acronym	Units	Hyp	Plot: $\bar{x}$ (range)
Land use					
	Agricultural	AGRIC	unitless	-	2 classes
	Forest	FOREST	unitless	+	2 classes
	Exotic plantations	PLANT	unitless	-	2 classes
	Scrublands	SCRUB	unitless	+	2 classes
	Urban	URBAN	unitless	-	2 classes
	Road density	ROAD_D	km/km^2	-	L: 3.81 (0 – 51.96)
					P: 2.88 (0 – 28.08)
	Water course density	WATER_D	km/km^2	-	L: 1.02 (0 - 4.38)
					P: 1.00 (0 - 4.50)
	Large river density	RIVER_D	km/km^2	-	L: 0.12 (0 – 3.08)
					P: 0.18 (0 – 2.75)
Topography					
	Altitude	ALT	metres	-	L: 241.3 (0.3 – 873.1)
					P: 401.2 (1.83 – 1676.5)
	Slope	SLP	angle	-	L: 14.8 (0 – 64.2)
					P: 27.6 (0.06 – 152.0)
	TWI	TWI	unitless	+	L: 12.3 (8.2 – 20.9)
					P: 11.1 (7.8 – 20.4)
	WEI	WEI	unitless	-	L: 1.02 (0.77 – 1.33)
					P: 1.01 (0.76 – 1.33)
	Solar radiation	SOLAR	kWh/m^2	-	L: 14357 (6993 – 16877)
					P: 7561 (2565 – 9741)
Vegetation					
	EVI (average)	EVI_avg	unitless	+	L: 0.54 (-0.05 – 0.99)
					P: 0.57 (-0.11 – 0.96)
	EVI (SD)	EVI_sd	unitless	+	L: 0.06 (0 – 0.52)
					P: 0.06 (0 – 0.62)
	NDWI (average)	NDWI_avg	unitless	+	L: 0.55 (-0.27 – 0.84)
					P: 0.30 (-0.17 – 0.59)
	NDWI (SD)	NDWI_sd	unitless	+	L: 0.05 (0 – 0.24)
					P: 0.04 (0 – 0.19)
NMLs					
	Random	RAND_nlm	unitless	NA	LP: 0.50 (0 – 1)
	Random Cluster	RCLUST_nlm	unitless	NA	5 classes
	Distance Gradient	DIST_nlm	unitless	NA	LP: 0.51 (0 – 1)
	Fraction Brownian	FBM_nlm	unitless	NA	L: 0.55 (0 – 1)
					P: 0.52 (0 – 1)

We first performed a single surface optimisation for each of the 21 layers using as a response variable the pairwise F_{ST} and, as predictors, pairwise cost-distance matrices calculated using the *commuteDistance* function implemented in the R package *gdistance* 1.2-2 (van Etten 2017), which is functionally equivalent to resistance distances (McRae 2006; Kivimäki *et al.* 2014). In addition to the NLMs, we also incorporated two null models to examine model performance: (i) a distance model, to test for isolation-by-distance (IBD); and (ii) an intercept-only model. Model performance was examined through the Akaike Information Criterion corrected for small sample sizes (AICc), and models were ranked according to ΔAICc (the difference in AICc between a given model and the top-ranked model). Input parameter details are included in **Supplementary Text C5 and Figure C7 in Appendix C**. We then performed a multiple surface optimisation to evaluate whether multivariate models (*i.e.* combinations of variables) better explain the observed patterns of genetic differentiation than univariate models. Ideally, this analysis should have included all possible model combinations; however, due to computational constraints, instead we built a candidate model set comprised of the most supported models. Univariate models exhibiting a ΔAICc < 7 were included in the candidate model set for multiple surface optimisation, as Richards (2005) showed that this conservative threshold retains the true best model with an approximate 95% confidence. We conducted one run using the same optimisation parameters described in **Supplementary Text C5 in Appendix C**. We used a total of 1000 bootstrap iterations in which individuals, sampling locations, and cost-distance matrices are subsampled in each iteration, to estimate each model's averaged Akaike weight (w_i; relative likelihood of a model) and the frequency that a model was top-ranked across each bootstrap iteration. To visualise patterns of genetic connectivity, we used the pairwise cost-distances estimated from the full multivariate models to generate a current map for each landscape plot in CIRCUITSCAPE 4.0.5 (McRae 2006).

4.4 - Results

4.4.1 – Genotype matches and marker validation

Almost all individuals exhibited a minimum of four allele mismatches with each other; only two larviparous individuals from the locality of SOUT and two pueriparous salamanders (one from PADR and one from LILL) had equivalent genotypes to other individuals sampled in the same localities. These four individuals probably comprised recaptured animals and were discarded, which means 426 and 360 salamanders from the larviparous and pueriparous plots, respectively, were included in downstream analyses. Additionally, we did not find evidence for deviations from LE, but one locus (SST-C3) showed consistent deviations from HWE and clear

evidence for null alleles in 10 pueriparous populations. To make genetic data sets comparable, we removed this locus from all populations; therefore, genetic analyses were performed with 13 loci.

4.4.2 – Patterns of genetic variation

We found a total of 11 and 21 distinct haplotypes among the studied larviparous and pueriparous populations, respectively (**Table C5 in Appendix C**). All samples in the larviparous plot were clustered into a single haplogroup (haplogroup A; **Figure 4.2**). Haplotype 24 was widespread and at high frequency across most larviparous populations, being absent only in population XENX (**Figure 4.2**). Conversely, genetic structure in pueriparous populations was higher and more complex than in larviparous ones, with pueriparous salamanders being grouped into two haplogroups (haplogroups B and C; **Figure 4.3**). Haplotype 13, which was assigned to haplogroup B, and haplotypes 1 and 8, assigned to haplogroup C, were the most common in the pueriparous plot (**Figure 4.3**). The remaining haplotypes in the pueriparous plot generally were found in few populations and at low frequencies. Furthermore, pueriparous populations often exhibited a higher number of haplotypes (up to 5) than larviparous ones (up to 3; **Table C5 in Appendix C**; **Figures 4.2 and 4.3**). Among the haplotypes found in the pueriparous plot, four haplotypes with very low frequencies grouped with the larviparous haplogroup A. Specifically, haplotypes 20 and 24 are shared with the sampled larviparous salamanders, while haplotypes 19 and 21 were not recorded in the larviparous plot.

Genetic diversity was high overall and similar between larviparous and pueriparous populations (mean values in the larviparous plot vs. pueriparous plot, respectively; N_A - 8.98 vs. 9.06; P_A - 2.36 vs. 2.89; H_O - 0.75 vs. 0.76; H_E - 0.78 vs. 0.78; A_R - 7.24 vs. 7.28; **Table 4.1**). Inbreeding coefficients were very low (range F in both plots: 0.01 – 0.04), while relatedness was considerably higher in the pueriparous plot (R_L: 0.10 [0.05 – 0.20]) than the larviparous plot (R_L: 0.05 [0.02 – 0.11]; **Table 4.1**). Population pairwise genetic differentiation was substantially higher in pueriparous populations (mean F_{ST}: 0.07 [0.02 – 0.16]; mean D_{EST}: 0.24 [0.03 – 0.52]) than larviparous ones (mean F_{ST}: 0.03 [0 – 0.08]; mean D_{EST}: 0.06 [0 – 0.18] **Tables C6-C7 in Appendix C**). The pueriparous populations CORN, BOLG, and VILL exhibited the highest mean pairwise genetic differentiation ($F_{ST} \geq 0.09$; $D_{EST} > 0.32$), while the population of XENX was significantly differentiated among larviparous populations (mean $F_{ST} = 0.06$; mean $D_{EST} > 0.13$).

LOCPRIOR models in STRUCTURE also revealed stronger patterns of genetic structure in pueriparous populations (**Figure 4.4**). The best supported numbers of clusters were K = 4 and K = 16 in the larviparous and pueriparous plots, respectively. These analyses corroborate the

larviparous population of XENX is substantially differentiated from the other larviparous populations, while in the pueriparous plot, many populations (especially in the north) appear to be genetically isolated to a large extent from other sampled populations (**Figure 4.4**). Estimates of these optimal K values were consistent among the three metrics (*i.e.* ln[X|K], ΔK, and PI) employed in this study (**Figure C8 in Appendix C**). The only exception was the ΔK method for pueriparous populations (K = 3), which roughly delimited three population groups across an east-west axis (**Figure C9 in Appendix C**). Standard models in structure also showed that pueriparous populations are significantly differentiated, while in the larviparous plot, they were not able to recover any signs of population structure (**Figure C10 in Appendix C**). Because the optimal K inferred from standard models was highly incongruent among the tested metrics (**Figure C11 in Appendix C**), we discuss the results yielded by LOCPRIOR models.

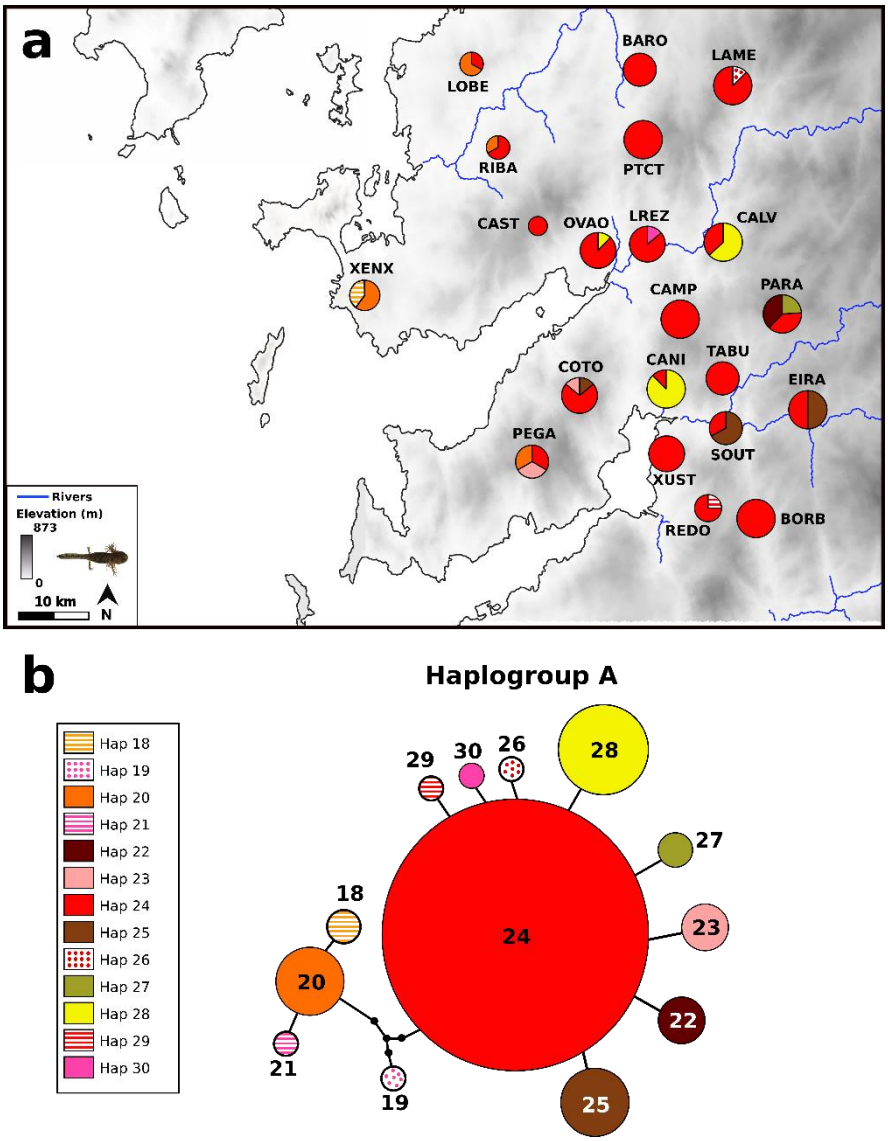

Fig. 4.2 Haplotype proportions and haplotype networks in the larviparous plot inferred from the amplified cyt b fragment. (A) Frequency of haplotypes found in each sampled locality. Each colour corresponds to a distinct haplotype. Population labels are also represented. The only exception is population LOUR, in which haplotypic data is not available. (B) Haplotype network inferred from the sampled larviparous populations. In total, 11 haplotypes were detected in this region and were clustered into a single haplogroup (haplogroup A). In addition to these 11 unique haplotypes, two other haplotypes (19 and 21) were assigned to haplogroup A, although both were only found at very low frequencies in the pueriparous plot. See **Table C5 in Appendix C** for more details concerning the haplotypic distribution in each sampled locality.

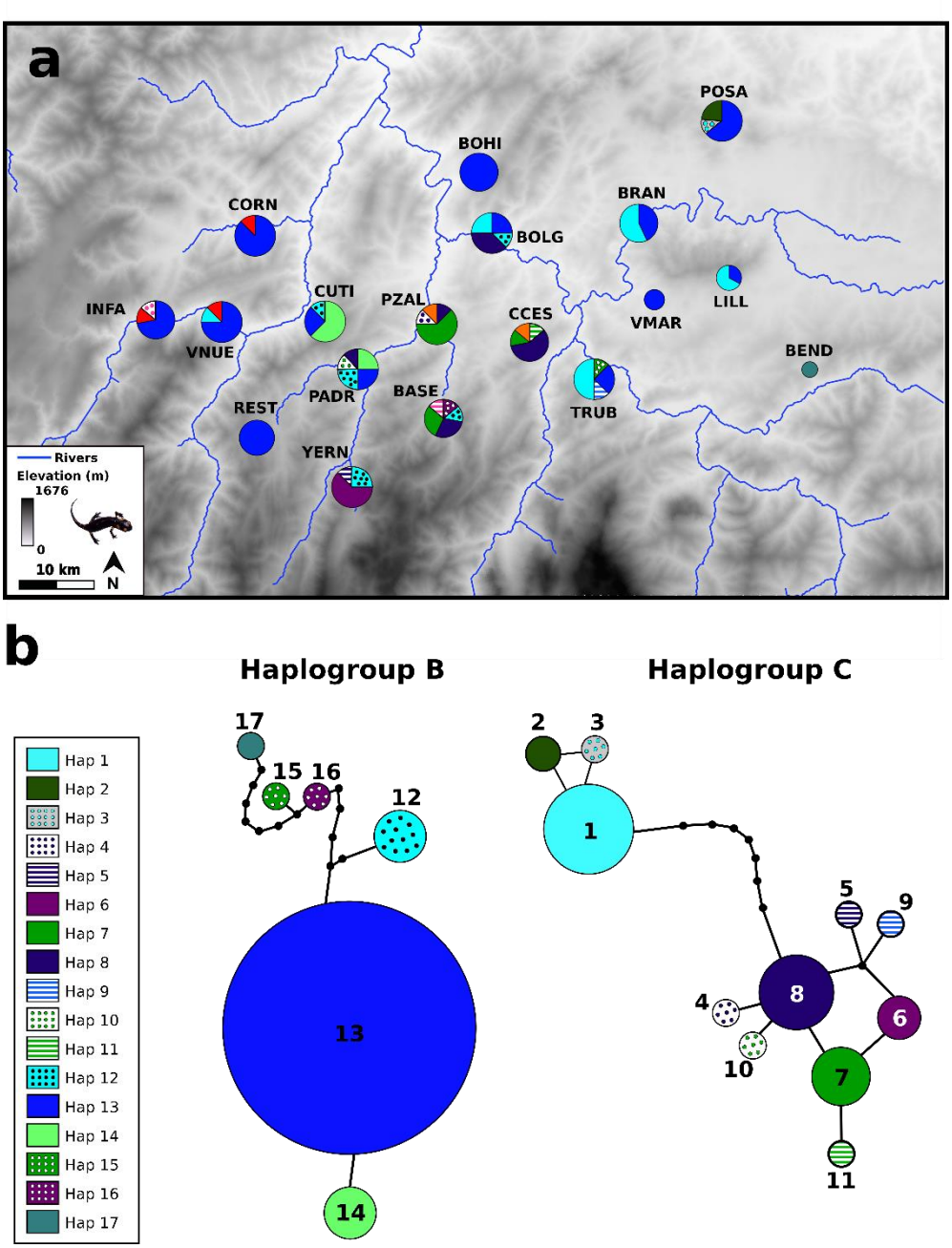

Fig. 4.3 Haplotype proportions and haplotype networks in the pueriparous plot inferred from the amplified cyt b fragment. (A) Frequency of haplotypes found in each sampled locality. Each colour corresponds to a distinct haplotype. Population labels are also represented. (B) Haplotype network inferred from the sampled larviparous populations. In total, 21 haplotypes were detected in this region. Seventeen of these haplotypes were clustered into two divergent haplogroups (haplogroups B and C). Haplotypes 19, 20, 21 and 24 were found in the pueriparous plot at very low frequencies, though they were assigned to haplogroup A, which contains all sampled larviparous populations. See **Table C5 in Appendix C** for more details concerning the haplotypic distribution in each sampled locality.

DAPC also demonstrated that pueriparous populations are more genetically structured in space than their larviparous counterparts, although this difference was not so clear as in STRUCTURE (optimal K=4 for both study areas; **Figure C12 in Appendix C**). Nonetheless, pueriparous populations appeared to be differentiated across an east-west axis, while larviparous populations were composed of individuals assigned to multiple genetic clusters.

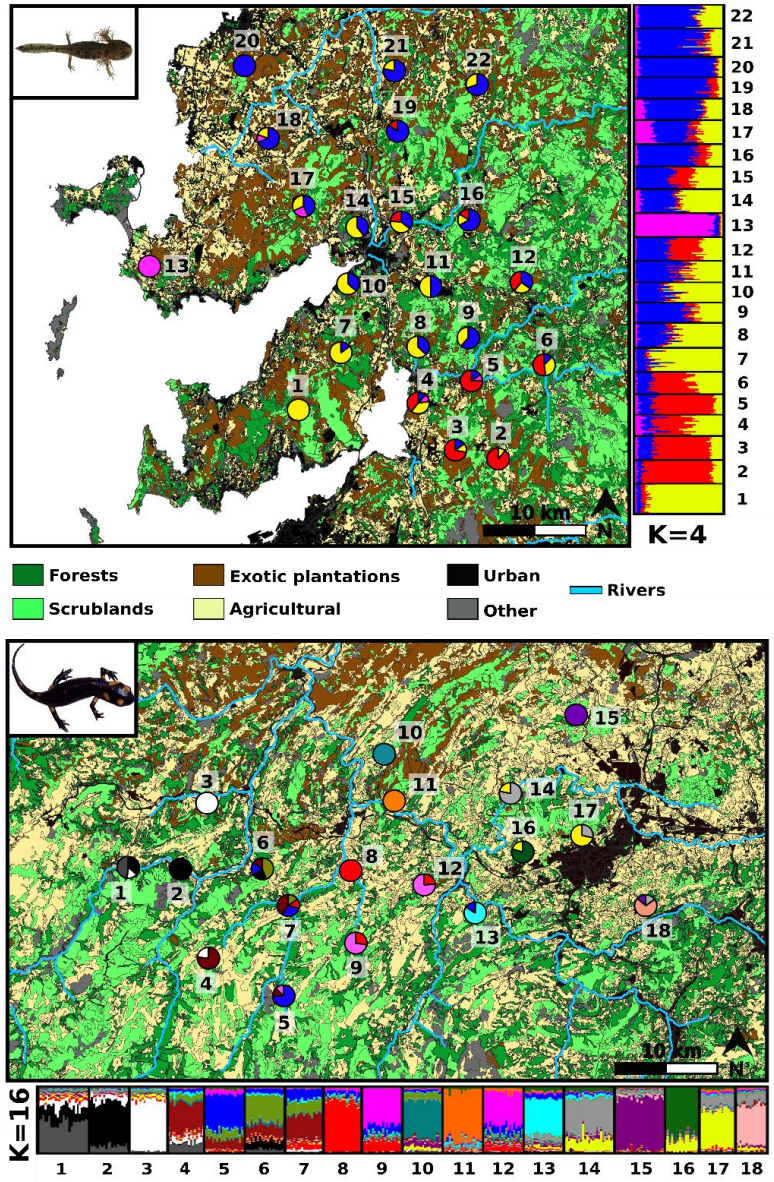

Fig. 4.4 Patterns of genetic structure in larviparous (top panel) and pueriparous (bottom panel) populations estimated by LOCPRIOR models in STRUCTURE. Barplots display the individual genetic membership for the most supported and congruent number of clusters, namely, K=4 and K=16 for the larviparous and pueriparous plots, respectively. Population membership for these K values is also summarized in the pie charts. The placement of pie charts corresponds to sampling locations and each pie chart is labelled with respective population codes, which are correspondent to the numbers displayed adjacently to barplots (see also **Table 4.1** regarding population codes). Additionally, this figure illustrates landscape composition and configuration. The most abundant reclassified land use classes are represented (*i.e.* natural forests, scrublands, plantations of exotic trees, agricultural areas, and urban settlements), while the class "Other" corresponds to minor reclassified land use classes showing a small percentage of occupied area (< 3%; **Table C2 in Appendix C**). Main rivers (Strahler rank ≥ 3) are also illustrated in each study region.

4.4.3 – Landscape genetic analyses

Correlation analyses showed that slope and TWI were the only highly correlated variables in the larviparous plot (**Tables C8-C9 in Appendix C**). We discarded TWI from optimization procedures because preliminary analyses in *ResistanceGA* showed lower statistical support for TWI than slope (TWI, AICc: −1628.5; slope, AICc: −1630.7). Single surface optimisation and model selection revealed that the variables best explaining genetic differentiation (ΔAICc < 7) were agricultural areas and wind exposure in both study plots and, additionally, the density of water courses and slope in the pueriparous plot (**Table 4.3**). The presence of agricultural areas was the top-ranked model in both plots, generating high resistance to gene flow in fire salamanders. For the remaining supported continuous surfaces, *ResistanceGA* identified several nonlinear relationships with resistance to gene flow (**Figure C13 in Appendix C**). Intermediate values of water course density appeared negatively related to gene flow in pueriparous populations, while both low and high values of wind exposure (both plots) and slope (pueriparous plot) were found to impose higher resistance to gene flow (**Figure C13 in Appendix C**). Multiple surface optimisation showed the univariate models received considerably higher statistical support than any of the multivariate models we tested (**Table 4.4**). Corroborating the results yielded by the single surface optimisation, agricultural areas were the top-ranked model in both larviparous ($w_I = 0.71$) and pueriparous ($w_I = 0.52$) plots. Wind exposure ($w_I = 0.24$) and water course density ($w_I = 0.23$) also received some support in the larviparous and pueriparous plots, respectively, while slope and wind exposure exhibited a $w_I \leq 0.11$ in pueriparous salamanders. Finally, the current maps generated by the full multivariate models show population connectivity across space is lower in pueriparous populations (**Figure 4.5**).

4.5 – Discussion

Given the greater independence from water exhibited by pueriparous fire salamanders (Velo-Antón *et al.* 2015), we hypothesized they are capable of successfully dispersing across a wider variety of suboptimal habitats, and thus, experience higher levels of population connectivity in fragmented landscapes compared to their larviparous counterparts. Contrary to our predictions, our analyses indicate genetic connectivity is lower among pueriparous populations, partially because pueriparity increases the barrier effects of certain landscape features, such as water courses. This study is one of the very few explicitly demonstrating that a shift in reproductive strategy influences genetic connectivity.

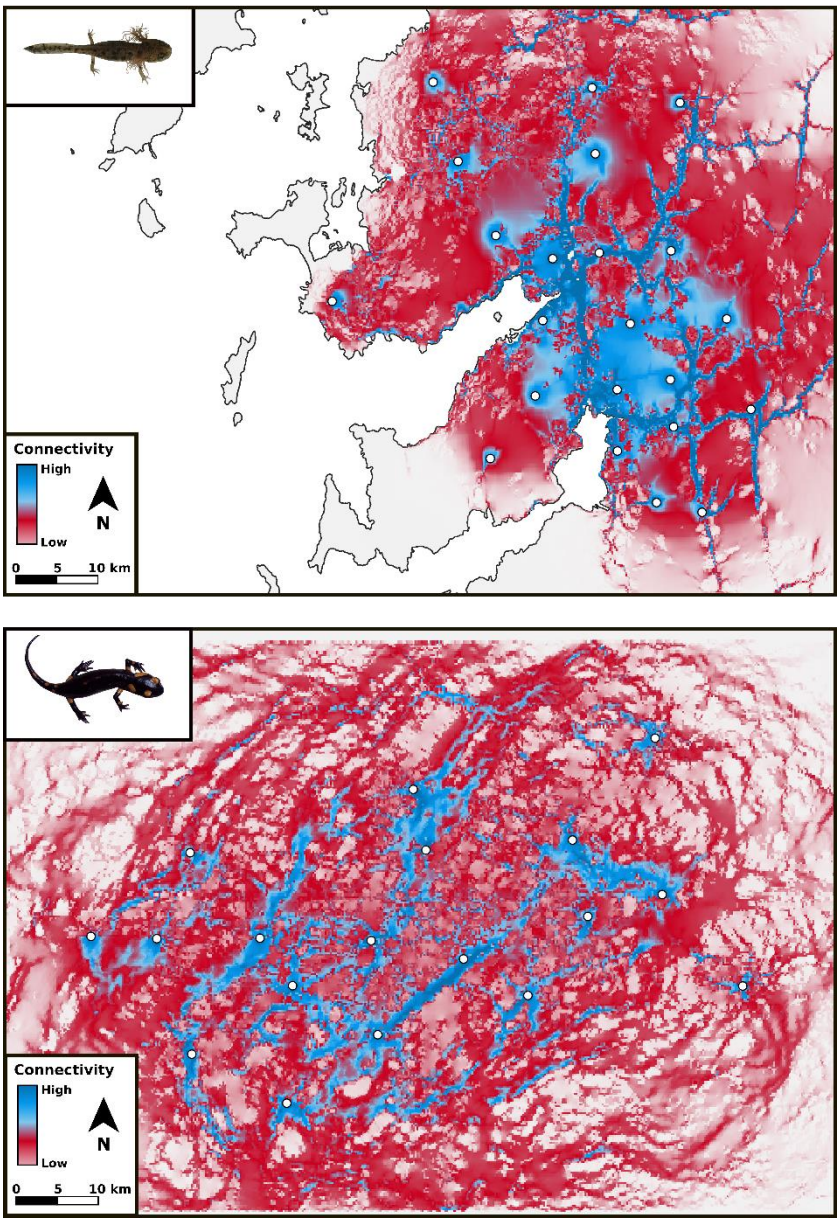

Fig. 4.5 Current maps illustrating patterns of genetic connectivity among larviparous (top panel) and pueriparous (bottom panel) populations. The pairwise cost-distance matrices obtained from the full multivariate models (*i.e.* AGRI+WEI in the larviparous plot and AGRI+WATER_D+WEI+SLP in the pueriparous plot; **Table 4.4**) were employed to generate these maps.

Table 4.3 Results of the single surface optimization carried out in *ResistanceGA* for the 21 resistance surfaces and the distance (Distance), and intercept-only (Null) models. The column "Type" denotes if a surface is continuous (C), categorical (CAT), or uniform (U), while the column "Transf" shows the data transformation applied to continuous layers (see **Figure C7 in Appendix C**) or the resistance values assigned to binary categorical land use layers (A – absence of a specific land use; P – presence). Model performance was examined through the difference in the values of the Akaike Information Criterion corrected for finite sample sizes (AICc) between the top ranked model and each tested model (ΔAICc). Bolded values indicate variables included in the multiple surface optimization analysis (ΔAICc < 7).

Larviparous plot					Pueriparous plot				
Surface	**Type**	**Transf**	**AICc**	**ΔAICc**	**Surface**	**Type**	**Transf**	**AICc**	**ΔAICc**
AGRIC	**CAT**	**A – 1; P – 17.6**	**-1643.3**	**0**	**AGRIC**	**CAT**	**A – 1; P – 11.8**	**-859.7**	**0**
WEI	**C**	**Inverse Ricker**	**-1639.0**	**4.33**	**WATER_D**	**C**	**Ricker**	**-855.8**	**3.85**
ROAD_D	C	Inverse-Reverse Ricker	-1635.0	8.36	**WEI**	**C**	**Inv.-Rev. Ricker**	**-854.6**	**5.12**
Distance	U		-1634.9	8.41	**SLP**	**C**	**Inverse Ricker**	**-854.0**	**5.71**
EVI_avg	C	Inverse Ricker	-1634.4	8.97	ALT	C	Inverse Ricker	-852.4	7.26
PLANT	CAT	A – 1; P – 1.7	-1634.0	9.35	EVI_avg	C	Inverse Ricker	-852.1	7.61
ALT	C	Ricker	-1633.9	9.45	SCRUB	CAT	A – 9.7; P – 1	-851.7	8.02
SCRUB	CAT	A – 2.5; P – 1	-1633.5	9.78	NDWI_avg	C	Inv.-Rev. Ricker	-851.0	8.74
RAND_nlm	C	Ricker	-1633.1	10.18	Distance	U		-850.8	8.88
FOREST	CAT	A – 1.4; P – 1	-1633.1	10.23	TWI	C	Reverse Ricker	-850.3	9.34
NDWI_avg	C	Inverse Ricker	-1632.8	10.52	FOREST	CAT	A – 1; P – 1.15	-847.9	11.77
SOLAR	C	Inverse Ricker	-1632.1	11.22	PLANT	CAT	A – 1; P – 1.14	-847.6	12.04
RIVER_D	C	Inverse Ricker	-1632.0	11.28	SOLAR	C	Reverse Ricker	-847.2	12.46
DIST_nlm	C	Inverse monomolecular	-1631.0	12.33	FBM_nlm	C	Ricker	-847.0	12.65
SLP	C	Ricker	-1630.7	12.66	DIST_nlm	C	Inv.-Rev. Ricker	-846.9	12.76
EVI_sd	C	Ricker	-1630.2	13.16	RAND_nlm	C	Monomolecular	-845.1	14.54
NDWI_sd	C	Inverse Ricker	-1629.4	13.89	ROAD_D	C	Reverse Ricker	-844.9	14.76
FBM_nlm	C	Inverse monomolecular	-1629.4	13.95	EVI_sd	C	Inv.-Rev. Monomolecular	-844.9	14.80
WATER_D	C	Inverse-Reverse Ricker	-1628.7	14.66	RIVER_D	C	Reverse Ricker	-844.8	14.88
URBAN	CAT	A – 1; P – 1.5	-1628.5	14.80	NDWI_sd	C	Ricker	-844.7	14.94
RCLUST_nlm	CAT		-1628.3	15.05	URBAN	CAT	A – 1; P – 6.2	-844.4	15.27
Null			-1623.8	19.47	RCLUST_nlm	CAT		-832.5	27.23
			-1546.9	96.44	Null			-793.9	65.80

Table 4.4 Results of the multiple surface optimization carried out in *ResistanceGA* for the variables that showed a ΔAICc < 7 in the univariate optimization. All model combinations among these variables were evaluated. A bootstrap analysis (1000 iterations) was conducted to examine model performance. Models' parameters (*i.e.* averaged AICc – Avg.AICc; averaged Akaike weight – Avg.w_i) correspond to the averaged values obtained in each bootstrap iteration. Top.boot represents the number of times (%) during the 1000 bootstrap iterations that each model was the top-ranked model. NA – not available.

Larviparous plot				Pueriparous plot			
Model	**Avg.AICc**	**Avg.w_i**	**Top.boot**	**Model**	**Avg.AICc**	**Avg.w_i**	**Top.boot**
AGRI	-840.8	0.71	81.6	AGRI	-427.3	0.52	62.9
WEI	-837.6	0.24	18.4	WATER_D	-423.1	0.23	24.0
AGRI+WEI	-835.3	0.05	0	SLP	-422.9	0.11	6.0
				WEI	-422.0	0.10	7.0
				AGRI+WATER_D	-420.5	0.03	0.1
				AGRI+WEI	-419.5	0.01	0
				AGRI+SLP	-416.0	0	0
				WATER_D+SLP	-410.8	0	0
				WATER_D+WEI	-408.7	0	0
				SLP+WEI	-406.6	0	0
				AGRI+WATER_D+WEI	-376.3	0	0
				AGRI+WATER_D+SLP	-373.7	0	0
				AGRI+SLP+WEI	-373.4	0	0
				WATER_D+SLP+WEI	-321.5	0	0
				AGRI+WATER_D+SLP+WEI	NA	0	0

4.5.1 – Does reproductive mode influence genetic connectivity and landscape resistance?

Contrary to our predictions, population genetic differentiation was much higher in pueriparous salamanders (mean F_{ST}: 0.07 [0.02– 0.16]; **Table C7 in Appendix C**) than larviparous ones (mean F_{ST}: 0.03 [0–0.08]; **Table C6 in Appendix C**), even over similar landscape distances. Analyses assessing both mtDNA and microsatellite genetic structure further corroborate that pueriparous populations show greater genetic divergence (**Figures 4.2 – 4.4**). Because the ocean is an effective barrier to dispersal in *Salamandra salamandra* (Lourenço *et al.* 2018b), these results become even more surprising, as the ocean in the larviparous plot may comprise an additional obstacle limiting gene flow, especially in the westernmost larviparous populations (**Figure 4.4**). We argue these genetic differences between larviparous and pueriparous populations are at least partially due to reproductive mode, as it appears to determine the extent to which specific environmental variables affect gene flow.

The density of water courses was significantly associated with higher resistance to gene flow only in pueriparous populations (**Tables 4.3 and 4.4**), despite both study landscape plots having dense hydric networks (mostly first- and second-order streams; **Table 4.2 and Figure C3 in Appendix C**). This potentially indicates reproduction largely governs the effects of lotic waters on genetic connectivity in *S. salamandra*, with pueriparity increasing the barrier effects imposed by these aquatic systems. This result appears to corroborate the elevated genetic differentiation found in other terrestrial-breeding amphibians across rivers and streams (Marsh *et al.* 2007; Fouquet *et al.* 2015), which suggests, in general, water courses comprise significant barriers to dispersal for terrestrial-breeding amphibians in particular. The relationship between this variable and landscape resistance was nonlinear (**Figure C13 in Appendix C**) and, thus, some caution is warranted when interpreting this effect, since it could potentially represent a statistical artefact arising from the underrepresentation of raster cells with very high density values.

The loss of the aquatic stage in pueriparous salamanders probably renders even small streams as relevant physical or behavioural barriers. Although the barrier effects of streams in terrestrial-breeding amphibians have been largely underexplored (Emel and Storfer 2012), Marsh *et al.* (2007) used fine-scale genetic and movement data to demonstrate that streams comprise significant, but not impermeable, barriers to dispersal in a terrestrial-breeding (direct-developer) salamander (the red-backed salamander, *Plethodon cinereus*). The broader spatial scale of our study does not enable us to infer the magnitude to which streams hamper gene flow; however, previous observations of pueriparous individuals traversing streams through

objects spanning their entire width (*e.g.* small stone and wood bridges, fallen tree logs) and crossing dry temporary streams during the first rains of the wet season (A. Lourenço and G. Velo-Antón, personal observations) indicate these lotic systems are not fully impermeable to dispersal.

The adverse effect of water courses on gene flow also appears to be supported by the inferred effect of slope. Optimisation analyses predicted that zones where slope is smoother impose higher resistance to dispersal in pueriparous populations (**Figure C13 in Appendix C**). This seems counterintuitive, as flat landscapes generally do not constrain movement in amphibians (*e.g.* Richardson 2012; Coster *et al.* 2015). We suggest this result is actually due to the common association between smoother terrains and lotic systems (85% of streams flow in zones where slope <30° in the pueriparous plot).

In contrast to the pueriparous populations, the density of water courses was one of the variables with the lowest contribution to explaining genetic differentiation in larviparous populations (**Table 4.3**). Unlike terrestrial-breeding amphibians, streams are expected to be relatively permeable to dispersal in aquatic amphibians, as they use streams (and other freshwater habitats) in all phases of their life cycle (Smith and Green 2006; Mims *et al.* 2015; Reinhardt *et al.* 2018). Although adult larviparous fire salamanders show a marked terrestrial life style, connectivity across streams is probably high because: (i) females enter into ponds and streams to lay aquatic larvae; (ii) females from opposite sides of streams may deposit larvae in the same stream; and (iii) crossing rates are probably high during the aquatic larval stage (Velo-Antón and Buckley 2015).

Aside from the increased barrier effects of water courses for pueriparous salamanders, we do not have clear evidence of other landscape variable imposing a marked difference in landscape resistance between larviparous and pueriparous salamanders. Although our sampling design tried to account for any potential confounding effects of landscape differences between study areas, there are some we could not control for and which limits our inferences. For instance, agricultural areas substantially hinder gene flow in both larviparous and pueriparous populations, though it remains unclear whether the greater independence on water entailed by pueriparity reduces their resistance. Although optimised resistance values assigned to agricultural fields are higher in larviparous salamanders (17.6 vs. 11.8; **Table 4.3**), our inferences are limited due to the higher proportion of agricultural fields in the pueriparous plot (40% vs. 22.5%; **Table C2 in Appendix C**). Moreover, similar to other amphibians (*e.g.* Richardson 2012; Coster *et al.* 2015), our results also suggest that moving upslope entails greater resistance to gene flow, but we found moderate support for this effect only in pueriparous populations. This could have led us to conclude pueriparous salamanders are

more susceptible to variations in the terrain than larviparous individuals, perhaps because the costs of locomotion are potentially higher due to their smaller size (see Hein *et al.* 2012; see also next paragraph). However, we suggest this result is probably an artefact of the higher topographic complexity found in the pueriparous plot compared to the larviparous one.

We cannot also discount the influence of non-environmental factors in explaining the greater genetic structure found in pueriparous populations. First, it is unclear whether pueriparity also promoted changes in dispersal behaviour. A previous study in *S. salamandra* showed that changes in reproductive behaviour (*i.e.* adaptation to deliver larvae either in streams or ponds) can indeed lead to modifications in dispersal behaviour (Hendrix *et al.* 2017). Because pueriparous salamanders do not need to search for water bodies to reproduce, they may have less motivation to move longer distances compared to their larviparous counterparts, though a previous genetic study did not find significant differences in patterns of dispersal at a very fine-scale (<1 km; Lourenço *et al.* 2018a). Second, the physical capacity for dispersal may differ between the studied subspecies. Larviparous *S. s. gallaica* individuals are generally larger (body size up to 250 mm) than *S. s. bernardezi* individuals (body size up to 180 mm; Velo-Antón and Buckley, 2015; Velo-Antón *et al.* 2015), and body size is often positively correlated with locomotor performance and individual dispersal distances (Paz *et al.* 2015; Garcia *et al.* 2017; Denoël *et al.* 2018). Fine-scale studies employing tracking methodologies (e.g., radio-telemetry or mark-recapture) could provide additional information on how salamanders with different reproductive modes interact with the landscape.

4.5.2 – What is the effect of the environment on genetic structure in *Salamandra salamandra*?

Land use and, to a lesser extent, topography were found to influence genetic connectivity in fire salamanders irrespective of their reproductive mode. Specifically, agricultural areas were identified as the best predictors of genetic differentiation in fire salamanders, promoting higher resistance to gene flow for both pueriparous and larviparous populations. This reinforces the findings of Antunes *et al.* (2018), who suggested agricultural fields comprise strong barriers to gene flow in a southern Iberian subspecies (*S. s. longirostris*). The narrow habitat tolerance generally exhibited by amphibians (*e.g.* high dependence on humid environments, ectothermic physiology), together with the severe habitat degradation caused by agricultural practices (*e.g.* pollution, loss of native vegetation, high exposure to UVB radiation), usually renders agricultural fields as impervious habitat matrices to dispersal (*e.g.* Cushman 2006; Johansson *et al.* 2007; Costanzi *et al.* 2018). Other land use types known to negatively affect movement and population density in *S. salamandra*, such as plantations of exotic trees (*Eucalyptus* spp.;

Cordero *et al.* 2007) and urban settlements (Lourenço *et al.* 2017), were not found to have significant effects. This may be due to the underrepresentation of these land uses in the study areas (**Table C2 in Appendix C**), with the only exception being the large area occupied by cultivated trees (*Eucalyptus* and *Pinus* spp.) in the larviparous plot. Plantations are particularly unsuitable habitats for fire salamanders when the soil is highly degraded and shrub cover is removed (Velo-Antón and Buckley 2015). However, it is possible most planted areas retained some structural characteristics (*e.g.* presence of shrub layer) to allow for the maintenance of genetic connectivity among larviparous populations.

Wind exposure was also found to have higher resistance to gene flow in both reproductive modes, though the magnitude of this relationship varies across both plots (**Figure C13 in Appendix C**). Amphibians are susceptible to dehydration (Hillyard 1999), and wind is one factor increasing rates of evaporative water loss. Amphibians, including *S. salamandra*, tend to reduce terrestrial activity under windy conditions to maintain hydric balance (Andreone *et al.* 1999; Peterman and Semlitsch 2014; Velo-Antón and Buckley 2015). This suggests dispersal rates are limited across terrains highly exposed to the wind. Despite the detrimental effects of wind on amphibian movement, it is rarely considered in landscape genetics studies. Future research including wind exposure may provide valuable information about its effects on genetic connectivity in amphibians.

4.5.3 – Why is genetic diversity similar between larviparous and pueriparous populations?

Restricted gene flow and low fecundity are two factors that often reduce population genetic diversity (Ellegren and Galtier 2016; Cosgrove *et al.* 2018). Considering pueriparous populations are generally more isolated and have lower reproductive output (Velo-Antón *et al.* 2015), the similar levels of nuclear genetic diversity shown by larviparous and pueriparous populations are surprising. We suggest this could have resulted from differences in population history. Pronounced climatic oscillations during the Pleistocene, coupled with the physiographic heterogeneity of the Iberian Peninsula, caused cyclic range contractions and expansions of many species, which shaped current patterns of biodiversity and genetic variation (Abellán and Svenning 2014). In northern Iberia, the Cantabrian mountains provided multiple refugia for fire salamanders, in particular for *S. s. bernardezi*, thus allowing population persistence, the maintenance of genetic diversity, and subsequent allopatric divergence from neighbouring isolated populations (García-París *et al.* 2003; Velo-Antón *et al.* 2007; Beukema *et al.* 2016). While the Western Iberian coast probably acted as climatic refuge for *S. s. gallaica*, the number of refuges and patterns of postglacial recolonization across NW Iberia are still

unclear for this subspecies. However, the shallower genetic structure and the lower number of haplotypes observed in this region for *S. s. gallaica* (García-París *et al.* 2003; Velo-Antón *et al.* 2007; this study) potentially suggest a recent recolonization through range expansions from adjacent refugia, during which the enhanced effects of drift and allele surfing along the expansion front could have caused an initial reduction of genetic diversity (see Martínez-Freiría *et al.* 2015; Pereira *et al.* 2018 for examples in reptiles across Northern Iberia).

Although we sampled pueriparous populations distant from known hybrid and introgressed areas, we found evidence of *S. s. gallaica* mtDNA (haplotypes 19, 20, 21, and 24) at very low frequencies in six localities across the pueriparous plot (**Figures 4.2 and 4.3**; **Table C5 in Appendix C**). This result could question whether the pueriparous plot exclusively contains pueriparous fire salamanders or a mixture of pueriparous and larviparous individuals. We find the latter explanation highly implausible because previous and ongoing field studies in this region have never recorded larviparity (Velo-Antón *et al.* 2015; unpublished data). Additionally, the phenotypes of sampled and nonsampled adults in this area clearly matched *S. s. bernardezi* (*i.e.* small body size, stripe coloration pattern, and round snout). Hence, the low frequency of *S. s. gallaica* mtDNA haplotypes probably results from incidental genetic leaks (historical or recent) from larviparous regions into this pueriparous area or variation that was present in a common ancestor, with the Cantabrian Mountains being a relatively efficient barrier to dispersal and gene flow between both phenotypes (García-París *et al.* 2003).

4.5.4 – Conclusions

Our study is one of the very few explicitly demonstrating that a shift in reproductive strategy influences population connectivity. Specifically, we show that pueriparity in *S. salamandra* reduces genetic connectivity due to increased barrier effects of lotic systems, suggesting these landscape features are significant obstacles to gene flow in terrestrial amphibians. This study also opens exciting avenues for future research that will contribute to better understanding the eco-evolutionary implications underlying the shifts in reproductive mode. Investigating the landscape contexts in which terrestrial reproduction promotes or constrains gene flow in amphibians is key to predicting the effects of environmental changes on genetic connectivity. For instance, the lower dependency on water entailed by pueriparity may benefit dispersal in arid environments, where water bodies between patches are absent or scarce (Mims *et al.*

2015; Sandberger-Loua *et al.* 2018). Future studies should also examine other potential outcomes from changes in reproductive strategy, such as lineage diversification. For example, the long-term effects of water courses on pueriparous salamanders possibly contributed to the high phylogeographic structure observed in *S. s. bernardezi* (García-París *et al.* 2003; Velo-Antón *et al.* 2007; Beukema *et al.* 2016), even though its range is among the smallest of *S. salamandra* subspecies. Finally, future research might benefit from the inclusion of high-resolution genomic data, which can be useful in uncovering hidden fine-scale genetic patterns (*e.g.* McCartney-Melstad *et al.* 2018) and, thus, may be important for detecting subtle differences in genetic structure between populations exhibiting different life-history traits.

4.6 – Acknowledgments

We thank A. Anagnostopoulou, A. Paoletti, B. Antunes, B. Correia, B. Santos, C. Figueiredo-Vázquez, F. Sousa, I. Pazos, L. Alarcón-Ríos, M. Henrique, P. Alves, and S. Rosa for their help during field work. S. Lopes provided laboratory assistance, while K. Mulder helped with *ResistanceGA* analyses. Dr. Bill Peterman provided advice about *ResistanceGA*. Fieldwork for obtaining tissue samples was done with the corresponding permits from the regional administrations (Xunta de Galicia, Ref. EB016/2018; Gobierno del Principado de Asturias, Ref. 2018/2115). Sampling procedures were carried out following the Guidelines for Use of Live Amphibians and Reptiles in Field and Laboratory Research, 2nd Edition, revised by the Herpetological Animal Care and Use Committee (HACC) of the American Society of Ichthyologists and Herpetologists, 2004. This work was supported by FEDER funds through the Operational Programme for Competitiveness Factors – COMPETE (FCOMP-01-0124-FEDER-028325 and POCI-01- 0145-FEDER-006821); and by National Funds through FCT – Foundation for Science and Technology (EVOVIV: PTDC/BIA-EVF/3036/2012; SALOMICS: PTDC/BIA-EVL/28475/2017). AL, FC, and GVA are supported by FCT (PD/BD/106060/2015, SFRH/BPD/115228/2016, IF/01425/2014, respectively). J.G. is supported by FCT CEEC Individual Contracts (2017). We thank Professor Loren Rieseberg, Professor François Balloux and two anonymous referees for constructive comments on earlier versions of the manuscript.

4.7 – References

Abellán P, Svenning J-C (2014) Refugia within refugia–patterns in endemism and genetic divergence are linked to Late Quaternary climate stability in the Iberian Peninsula. *Biological Journal of the Linnean Society*, **113**, 13–28.

Agencia Estatal de Meteorologia (2010) Standard climate values. Ministerio para la Transición Ecológica. Retrieved from http://www.aemet.es/en/serviciosclimaticos/datosclimatologicos/valoresclimatologicos

Alton LA, Franklin CE (2017) Drivers of amphibian declines: effects of ultraviolet radiation and interactions with other environmental factors. *Climate Change Responses*, **4**, 6.

Álvarez D, Lourenço A, Oro D, Velo-Antón G (2015) Assessment of census (*N*) and effective population size (*Ne*) reveals consistency of *Ne* single-sample estimators and a high *Ne*/*N* ratio in an urban and isolated population of fire salamanders. *Conservation Genetics Resources*, **7**, 705–712.

Andreone F, Clima V, De Michelis S (1999) On the ecology of *Salamandra lanzai*. Number and movements of individuals, and influence of climate on activity in a population of the upper Po Valley (Caudata: Salamandridae). *Herpetozoa*, **12**, 3-10.

Antunes B, Lourenço A, Caeiro-Dias G *et al.* (2018) Combining phylogeography and landscape genetics to infer the evolutionary history of a short-range Mediterranean relict, *Salamandra salamandra longirostris*. *Conservation Genetics*, **19**, 1411–1424.

Bates D, Mächler M, Bolker B, Walker S (2015) Fitting linear mixed-effects models using lme4. *Journal of Statistical Software*, **67**, 1-48.

Benjamini Y, Hochberg Y (1995) Controlling the false discovery rate: a practical and powerful approach to multiple testing. *Journal of the Royal Statistical Society. Series B.*, **57**, 289–300.

Beukema W, Nicieza AG, Lourenço A, Velo-Antón G (2016) Colour polymorphism in *Salamandra salamandra* (Amphibia: Urodela), revealed by a lack of genetic and environmental differentiation between distinct phenotypes. *Journal of Zoological Systematics and Evolutionary Research*, **54**, 127–136.

Blackburn DG (2015) Evolution of vertebrate viviparity and specializations for fetal nutrition: a quantitative and qualitative analysis. *Journal of Morphology*, **276**, 961–990.

Blaustein L, Segev O, Rovelli V *et al.* (2018) Compassionate approaches for the conservation and protection of fire salamanders. *Israel Journal of Ecology and Evolution*, **63**, 43–51.

Bonte D, van Dyck H, Bullock JM *et al.* (2012) Costs of dispersal. *Biological Reviews*, **87**, 290–312.

Buckley D, Alcobendas M, García-París M, Wake MH (2007) Heterochrony, cannibalism, and the evolution of viviparity in *Salamandra salamandra*. *Evolution and Development*, **9**, 105–115.

Chybicki IJ, Burczyk J (2009) Simultaneous estimation of null alleles and inbreeding coefficients. *The Journal of Heredity*, **100**, 106–113.

Clarke RT, Rothery P, Raybould AF (2002) Confidence limits for regression relationships between distance matrices: estimating gene flow with distance. *Journal of Agricultural, Biological, and Environmental Statistics*, **7**, 361–372.

Clement M, Posada DCKA, Crandall KA (2000) TCS: A computer program to estimate gene genealogies. *Molecular Ecology*, **9**, 1657–1659.

Cordero A, Velo-Antón G, Galán P (2007) Ecology of amphibians in small coastal Holocene islands: local adaptations and the effect of exotic tree plantations. *Munibe*, **25**, 94-103.

Cosgrove AJ, McWhorter TJ, Maron M (2018) Consequences of impediments to animal movements at different scales: a conceptual framework and review. *Diversity and Distributions*, **24**, 448–459.

Costanzi J-M, Mège P, Boissinot A *et al.* (2018) Agricultural landscapes and the Loire River influence the genetic structure of the marbled newt in Western France. *Scientific Reports*, **8**, 14177.

Coster SS, Babbitt KJ, Cooper A, Kovach AI (2015) Limited influence of local and landscape factors on finescale gene flow in two pond-breeding amphibians. *Molecular Ecology*, **24**, 742–758.

Cushman SA (2006) Effects of habitat loss and fragmentation on amphibians: a review and prospectus. *Biological Conservation*, **128**, 231–240.

Denoël M, Dalleur S, Langrand E, Besnard A, Cayuela H (2018) Dispersal and alternative breeding site fidelity strategies in an amphibian. *Ecography*, **41**, 1543–1555.

Dinis M, Velo-Antón G (2017) How little do we know about the reproductive mode in the north African salamander, *Salamandra algira*? Pueriparity in divergent mitochondrial lineages of *S. a. tingitana*. *Amphibia-Reptilia*, **38**, 540–546.

Ellegren H, Galtier N (2016) Determinants of genetic diversity. *Nature Reviews Genetics*, **17**, 422-433.

Emel SL, Storfer A (2012) A decade of amphibian population genetic studies: synthesis and recommendations. *Conservation Genetics*, **13**, 1685–1689.

Evanno G, Regnaut S, Goudet J (2005) Detecting the number of clusters of individuals using the software STRUCTURE: a simulation study. *Molecular Ecology*, **14**, 2611–2620.

Fouquet A, Courtois EA, Baudain D *et al.* (2015) The trans-riverine genetic structure of 28 Amazonian frog species is dependent on life history. *Journal of Tropical Ecology*, **31**, 361–373.

Galán P (2007) Viviparismo y distribución de *Salamandra salamandra bernardezi* en el norte de Galicia. *Boletín de La Asociación Herpetológica Española*, **18**, 44–49.

Gao W, Sun Y-B, Zhou W-W *et al.* (2019) Genomic and transcriptomic investigations of the evolutionary transition from oviparity to viviparity. *Proceedings of the National Academy of Sciences*, **116**, 3646–3655.

Garcia VOS, Ivy C, Fu J (2017) Syntopic frogs reveal different patterns of interaction with the landscape: a comparative landscape genetic study of *Pelophylax nigromaculatus* and *Fejervarya limnocharis* from central China. *Ecology and Evolution*, **7**, 9294–9306.

García-París M, Alcobendas M, Buckley D, Wake D (2003) Dispersal of viviparity across contact zones in Iberian populations of Fire salamanders (*Salamandra*) inferred from discordance of genetic and morphological traits. *Evolution*, **57**, 129–143.

Gardner RH, Urban DL (2007) Neutral models for testing landscape hypotheses. *Landscape Ecology*, **22**, 15–29.

Gorelick N, Hancher M, Dixon M *et al.* (2017) Google Earth Engine: planetary-scale geospatial analysis for everyone. *Remote Sensing of Environment*, **202**, 18–27.

Greven H (2003) Larviparity and pueriparity. In: *Reproductive Biology and Phylogeny of Urodela* (eds. Jamieson BGM, Sever DM), pp 447-475. Science Publishers. Enfield, NH, USA.

Gutiérrez-Rodríguez J, Gonçalves J, Civantos E, Martínez-Solano I (2017) Comparative landscape genetics of pond-breeding amphibians in Mediterranean temporal wetlands: the positive role of structural heterogeneity in promoting gene flow. *Molecular Ecology*, **26**, 5407–5420.

Halliwell B, Uller T, Holland BR, While GM (2017) Live bearing promotes the evolution of sociality in reptiles. *Nature Communications*, **8**, 2030.

Hein AM, Hou C, Gillooly JF (2012) Energetic and biomechanical constraints on animal migration distance. *Ecology Letters*, **15**, 104-110.

Helmstetter AJ, Papadopulos AST, Igea J, van Dooren TJM, Leroi AM, Savolainen V (2016) Viviparity stimulates diversification in an order of fish. *Nature Communications*, **7**, 11271.

Hendrix R, Schmidt BR, Schaub M, Krause ET, Steinfartz S (2017) Differentiation of movement behaviour in an adaptively diverging salamander population. *Molecular Ecology*, **26**, 6400–6413.

Hendrix R, Hauswaldt JS, Veith M, Steinfartz S (2010) Strong correlation between cross-amplification success and genetic distance across all members of 'True salamanders' (Amphibia: Salamandridae) revealed by *Salamandra salamandra*-specific microsatellite loci. *Molecular Ecology Resources*, **10**, 1038–1047.

Hillyard SD (1999) Behavioral, molecular and integrative mechanisms of amphibian osmoregulation. *Journal of Experimental Zoology*, **283**, 662-674.

Hubisz MJ, Falush D, Stephens M, Pritchard JK (2009) Inferring weak population structure with the assistance of sample group information. *Molecular Ecology Resources*, **9**, 1322–1332.

Huete A, Didan K, Miura T, Rodriguez EP, Gao X, Ferreira LG (2002) Overview of the radiometric and biophysical performance of the MODIS vegetation indices. *Remote Sensing of Environment*, **83**, 195-213.

Johansson M, Primmer CR, Merilä J. (2007) Does habitat fragmentation reduce fitness and adaptability? A case study of the common frog (*Rana temporaria*). *Molecular Ecology*, **16**, 2693–2700.

Jombart T, Devillard S, Balloux F (2010) Discriminant analysis of principal components: a new method for the analysis of genetically structured populations. *BMC Genetics*, **11**, 94.

Jombart T, Devillard S, Dufour A-B, Pontier D (2008) Revealing cryptic spatial patterns in genetic variability by a new multivariate method. *Heredity*, **101**, 92–103.

Jost L (2008) G_{ST} and its relatives do not measure differentiation. *Molecular Ecology*, **17**, 4015–4026.

Keenan K, McGinnity P, Cross TF, Crozier WW, Prodöhl PA (2013) diveRsity: an R package for the estimation of population genetics parameters and their associated errors. *Methods in Ecology and Evolution*, **4**, 782-788.

Kivimäki I, Shimbo M, Saerens M (2014) Developments in the theory of randomized shortest paths with a comparison of graph node distances. *Physica A: Statistical Mechanics and Its Applications*, **393**, 600–616.

Kopelman NM, Mayzel J, Jakobsson M, Rosenberg NA, Mayrose I (2015) CLUMPAK: a program for identifying clustering modes and packaging population structure inferences across K. *Molecular Ecology Resources*, **15**, 1179-1191.

Liedtke HC, Müller H, Hafner J *et al.* (2017) Terrestrial reproduction as an adaptation to steep terrain in African toads. *Proceedings of the Royal Society B*, **284**, 20162598.

Losos JB (2010) Adaptive Radiation, ecological opportunity, and evolutionary determinism. *The American Naturalist*, **175**, 623–639.

Lourenço A, Álvarez D, Wang IJ, Velo-Antón G (2017) Trapped within the city: integrating demography, time since isolation and population-specific traits to assess the genetic effects of urbanization. *Molecular Ecology*, **26**, 1498–1514.

Lourenço A, Antunes B, Wang IJ, Velo-Antón G (2018) Fine-scale genetic structure in a salamander with two reproductive modes: does reproductive mode affect dispersal? *Evolutionary Ecology*, **32**, 699-732.

Lourenço A, Sequeira F, Buckley D, Velo-Antón G (2018) Role of colonization history and species-specific traits on contemporary genetic variation of two salamander species in a Holocene island-mainland system. *Journal of Biogeography*, **45**, 1054–1066.

Ma L, Buckley LB, Huey RB, Du W-G (2018) A global test of the cold-climate hypothesis for the evolution of viviparity of squamate reptiles. *Global Ecology and Biogeography*, **27**, 679–689.

Manel S, Holderegger R (2013) Ten years of landscape genetics. *Trends in Ecology and Evolution*, **28**, 614–621.

Marsh DM, Page RB, Hanlon TJ *et al.* (2007) Ecological and genetic evidence that low-order streams inhibit dispersal by red-backed salamanders (*Plethodon cinereus*). *Canadian Journal of Zoology*, **85**, 319–327.

Martínez-Freiría F, Velo-Antón G, Brito JC (2015) Trapped by climate: interglacial refuge and recent population expansion in the endemic Iberian adder *Vipera seoanei*. *Diversity and Distributions*, **21**, 331–344.

McCartney-Melstad E, Vu J, Shaffer HB (2018) Genomic data recover previously undetectable fragmentation effects in an endangered amphibian. *Molecular Ecology*, **27**, 4430–4443.

McRae BH (2006). Isolation by resistance. *Evolution*, **60**, 1551–1561.

Measey GJ, Galbusera P, Breyne P, Matthysen E (2007) Gene flow in a direct-developing, leaf litter frog between isolated mountains in the Taita Hills, Kenya. *Conservation Genetics*, **8**, 1177–1188.

Mims MC, Phillipsen IC, Lytle DA *et al.* (2015) Ecological strategies predict associations between aquatic and genetic connectivity for dryland amphibians. *Ecology*, **96**, 1371–1382.

Paz A, Ibáñez R, Lips KR, Crawford AJ (2015) Testing the role of ecology and life history in structuring genetic variation across a landscape: a trait-based phylogeographic approach. *Molecular Ecology*, **24**, 3723–3737.

Peakall R, Smouse PE (2012) GenAlEx 6.5: genetic analysis in Excel. Population genetic software for teaching and research – an update. *Bioinformatics*, **28**, 2537–2539.

Pereira P, Teixeira J, Velo-Antón G (2018). Allele surfing shaped the genetic structure of the European pond turtle via colonization and population expansion across the Iberian Peninsula from Africa. *Journal of Biogeography*, **45**, 2202–2215.

Peterman WE (2018) ResistanceGA: An R package for the optimization of resistance surfaces using genetic algorithms. *Methods in Ecology and Evolution*, **9**, 1638–1647.

Peterman WE, Connette GM, Semlitsch RD, Eggert LS (2014) Ecological resistance surfaces predict fine-scale genetic differentiation in a terrestrial woodland salamander. *Molecular Ecology*, **23**, 2402–2413.

Peterman W, Semlitsch RD (2014) Spatial variation in water loss predicts terrestrial salamander distribution and population dynamics. *Oecologia*, **176**, 357–369.

Pincheira-Donoso D, Tregenza T, Witt MJ, Hodgson DJ (2013) The evolution of viviparity opens opportunities for lizard radiation but drives it into a climatic cul-de-sac. *Global Ecology and Biogeography*, **22**, 857–867.

Pittman SE, Osbourn MS, Semlitsch RD (2014) Movement ecology of amphibians: a missing component for understanding population declines. *Biological Conservation*, **169**, 44–53.

Pritchard JK, Stephens M, Donnelly P (2000) Inference of population structure using multilocus genotype data. *Genetics*, **155**, 945–959.

R Core Team (2018) R: A language and environment for statistical computing. R Foundation for Statistical Computing, Vienna, Austria. https://www.R-project.org/

Reinhardt T, Bauldauf L, Ilić M, Fink P (2018) Cast away: drift as the main determinant for larval survival in western fire salamanders (*Salamandra salamandra*) in headwater streams. *Journal of Zoology*, **306**, 171-179.

Richards SA (2005) Testing ecological theory using the information-theoretic approach: examples and cautionary results. *Ecology*, **86**, 2805–2814.

Richardson JL (2012). Divergent landscape effects on population connectivity in two co-occurring amphibian species. *Molecular Ecology*, **21**, 4437–4451.

Rousset F (2008) GENEPOP'007: a complete re-implementation of the GENEPOP software for Windows and Linux. *Molecular Ecology Resources*, **8**, 103–106.

Sandberger-Loua L, Rödel M-O, Feldhaar H (2018) Gene-flow in the clouds: landscape genetics of a viviparous, montane grassland toad in the tropics. *Conservation Genetics*, **19**, 169–180.

Sciaini M, Fritsch M, Scherer C (2018) NLMR and landscapetools: an integrated environment for simulating and modifying neutral landscape models in R. *Methods in Ecology and Evolution*, **9**, 2240–2248.

Shine R (2015) The evolution of oviparity in squamate reptiles: an adaptationist perspective. *Journal of Experimental Zoology Part B: Molecular and Developmental Evolution*, **324**, 487–492.

Shirk AJ, Landguth EL, Cushman SA (2018) A comparison of regression methods for model selection in individual-based landscape genetic analysis. *Molecular Ecology Resources*, **18**, 55–67.

Smith MA, Green DM (2006) Sex, isolation and fidelity: unbiased long-distance dispersal in a terrestrial amphibian. *Ecography*, **29**, 649-658.

Steinfartz S, Kuesters D, Tautz D (2004) Isolation and characterization of polymorphic tetranucleotide microsatellite loci in the fire salamander *Salamandra salamandra* (Amphibia: Caudata). *Molecular Ecology Notes*, **4**, 626–628.

van Etten J (2017) R Package gdistance: Distances and routes on geographical grids. *Journal of Statistical Software*, **76**, 1-21.

Velo-Antón G, Buckley D (2015) Salamandra común – *Salamandra salamandra*. *In: Enciclopedia Virtual de los Vertebrados Españoles* (eds Carrascal LM, Salvador A). Museo Nacional de Ciencias Naturales, Madrid. http://www.vertebradosibericos.org

Velo-Antón G, Cordero-Rivera A (2017) Ethological and phenotypic divergence in insular fire salamanders: diurnal activity mediated by predation? *Acta Ethologica*, **20**, 243–253.

Velo-Antón G, García-París M, Galón P, Cordero Rivera A (2007) The evolution of viviparity in holocene islands: ecological adaptation versus phylogenetic descent along the transition from aquatic to terrestrial environments. *Journal of Zoological Systematics and Evolutionary Research*, **45**, 345–352.

Velo-Antón G, Parra JL, Parra-Olea G, Zamudio KR (2013) Tracking climate change in a dispersal-limited species: reduced spatial and genetic connectivity in a montane salamander. *Molecular Ecology*, **22**, 3261–3278.

Velo-Antón G, Santos X, Sanmartín-Villar I, Cordero-Rivera A, Buckley D (2015) Intraspecific variation in clutch size and maternal investment in pueriparous and larviparous *Salamandra salamandra* females. *Evolutionary Ecology*, **29**, 185–204.

Velo-Antón G, Zamudio KR, Cordero-Rivera A (2012) Genetic drift and rapid evolution of viviparity in insular fire salamanders (*Salamandra salamandra*). *Heredity*, **108**, 410–418.

Wake MH (2015) Fetal adaptations for viviparity in amphibians. *Journal of Morphology*, **276**, 941–960.

Wang J (2011) Coancestry: A program for simulating, estimating and analysing relatedness and inbreeding coefficients. *Molecular Ecology Resources*, **11**, 141–145.

Wang J (2019) A parsimony estimator of the number of populations from a STRUCTURE-like analysis. *Molecular Ecology Resources*, **19**, 970-981.

Waraniak JM, Fisher JDL, Purcell K, Mushet DM, Stockwell CA (2019) Landscape genetics reveal broad and fine-scale population structure due to landscape features and climate history in the northern leopard frog (*Rana pipiens*) in North Dakota. *Ecology and Evolution*, **9**, 1041–1060.

Weir BS, Cockerham CC (1984). Estimating F-statistics for the analysis of population structure. *Evolution*, **38**, 1358-1370.

Wells KD (2007) *The ecology and behavior of amphibians*. The University of Chicago Press, Chicago.

Zhang P, Papenfuss TJ, Wake MH, Qu L, Wake DB (2008) Phylogeny and biogeography of the family Salamandridae (Amphibia: Caudata) inferred from complete mitochondrial genomes. *Molecular Phylogenetics and Evolution*, **49**, 586–597.

Chapter 5

General discussion

5.1 – Eco-evolutionary implications of pueriparity in fire salamanders and other key findings

The evolution of a derived viviparous reproduction (pueriparous in amphibians) occurred multiple times across several vertebrate taxa, with individuals experiencing pronounced phenotypic, physiological, genetic, and ecological changes. While many studies have addressed the morphological, physiological and genomic alterations caused by viviparity (see section 1.1), the impact of this trait in the ecology of individuals (*e.g.* survival, dispersal) and, by extension, its evolutionary implications at the population level (*e.g.* genetic connectivity) have received comparatively less attention, and the few studies that have examined this subject were performed in viviparous reptiles (*e.g.* Pincheira-Donoso *et al.* 2013; Zúñiga-Vega *et al.* 2016; Cornetti *et al.* 2017; Halliwell *et al.* 2017; Ma *et al.* 2018; Gao *et al.* 2019). In the present doctoral thesis, I explored some of the potential eco-evolutionary implications (*i.e.* long-term persistence in stressful environments, dispersal behaviour, and population connectivity) arising from the shift from a larviparous aquatic reproduction to a pueriparous terrestrial reproduction in *S. salamandra*. The major findings obtained in this thesis with regard to this topic are discussed in the present section, as well as other findings associated with the ecology and evolution of *S. salamandra*.

5.1.1 – Patterns of dispersal and gene flow

Transitions in reproductive modes are expected to be accompanied by evolutionary changes in dispersal and gene flow due to their correlated nature (see section 1.2.3.1.2 for more details). This topic has been underexplored and the present thesis provides relevant insights about it.

5.1.1.1 – Lotic waters

Dispersal and gene flow in amphibians are largely governed by the availability and distribution of water bodies (Semlitsch 2008; Pittman *et al.* 2014). Because the transition from

a semi-aquatic to a fully terrestrial life cycle entails greater independence from water for reproduction (Velo-Antón *et al.* 2015), it is reasonable to assume the degree of dependence on aquatic systems may be responsible for dispersal asymmetries between larviparous and pueriparous salamanders. Previous landscape studies proposed greater independence from water may help individuals to disperse successfully across sub-optimal habitats (Measey *et al.* 2007; Mims *et al.* 2015; Sandberger-Loua *et al.* 2018), although highly stressful environments may still constitute impermeable obstacles to dispersal for pueriparous amphibians. For example, analyses of genetic differentiation performed in chapter 2 showed pueriparous urban populations of *S. salamandra* are isolated to a large extent, including those that are only tens of metres apart (**Figure 2.2**).

A major finding of this dissertation is that skipping the aquatic larval stage (pueriparity) changes the way fire salamanders interact with lotic waters (streams and rivers). Evidence collected from chapters 3 and 4 suggest that reproductive mode influences the extent to which lotic systems affect the distances traveled by individuals and gene flow rates. Parentage analyses performed in chapter 3, jointly with other empirical studies (Thiesmeier and Schuhmacher 1990; Reinhardt *et al.* 2018; Veith *et al.* 2019), indicate small streams may promote passive long-distance movements of individuals during the larval stage, particularly, due to strong discharges after heavy rain. An approximate proportion of individuals that are dragged across a stream cannot be determined, although empirical data seems to suggest only a small proportion of larvae successfully disperse through this process due to elevated mortality rates caused by downstream drift after strong rains (Reinhardt *et al.* 2018). In addition to this, retaining the aquatic larval stage enables larviparous individuals to cross lotic waters (especially small streams) more efficiently and, thus, increase genetic connectivity in areas characterized by dense hydric networks (**Figure 4.5**; **Figure C3 in Appendix C**). Landscape genetic analyses carried out in chapter 4 clearly support this premise, as the variable density of water courses was associated with a greater landscape resistance only in pueriparous salamanders (**Table 4.3**). The greater barrier effects imposed by lotic waters to terrestrial-breeding amphibians was previously suggested as an important driver of higher genetic differentiation in direct-developing Amazonian frog species (Fouquet *et al.* 2015), and is likely the potential cause of the significant genetic differentiation observed in plethodontid salamanders located on opposite sides of small streams (Marsh *et al.* 2007). The results obtained in chapter 4, jointly with other circumstantial evidence (Marsh *et al.* 2007; Fouquet *et al.* 2015), stresses the importance of including data on both small streams and large rivers to better understand the patterns of population connectivity in amphibians exhibiting terrestrial reproduction.

5.1.1.2 – Differentiated movement behaviour

Since pueriparous salamanders exhibit higher independence from water, I hypothesized, in chapter 3, they would disperse farther on average at local scales, while larviparous individuals (especially females) would display a more philopatric behaviour given their need to remain nearby water bodies for reproduction (Velo-Antón and Buckley 2015). Genetic spatial autocorrelation analyses did not reveal significant differences in dispersal between reproductive modes, although the exact causal mechanisms for these patterns could not be inferred (see Discussion in chapter 3). Despite this, it should be mentioned the statistical tests underlying the above genetic analyses are suited for examining differences in dispersal between groups of individuals within a given distance class, while their statistical power to evaluate sporadic movements carried out by a small proportion of individuals is very limited (Banks and Peakall 2012). Individual movement behaviour and, by extension, the distances traveled by individuals may significantly vary within populations of vertebrates, including amphibians. Despite this variation, a general pattern found in nature is that a large proportion of individuals disperse over short distances, while a few others undergo long-distance dispersal due to social (*e.g.* seeking a territory during the juvenile stage or due to mating behaviour), ecological (*e.g.* searching for better environmental conditions), and phenotypic (*e.g.* bolder dispersal behaviour) factors (*e.g.* Smith and Green 2006; Bonte *et al.* 2012; Pittman *et al.* 2014; Hendrix *et al.* 2017; Denoël *et al.* 2018; Ousterhout and Semlitsch 2018). The case study presented by Hendrix *et al.* (2017) in *S. salamandra* neatly illustrates this issue. These authors used mark-recapture techniques and telemetry to compare patterns of movement between two co-distributed larviparous subpopulations, in which individuals of each subpopulation deliver larvae either in ponds or streams. They found individuals of both ecotypes displayed overall similar dispersal tendencies, with most individuals moving up to 500 m. However, a few salamanders potentially adapted to reproduce in ponds dispersed farther and exhibited higher variation in dispersal distances than salamanders reproducing in streams, possibly to cope with the spatio-temporal availability of pond habitats in the focal region. If the evolution of pueriparity has hypothetically produced changes in long-distance dispersal behaviour of at least some individuals, then the employed genetic analyses would most likely be unable to detect the above pattern, especially considering the relatively small sample size used in this study.

Genetic analyses in chapter 3 point to a lack of general differences in dispersal between reproductive modes. However, circumstantial evidence potentially suggests the dispersal behaviour of larviparous females may be more variable depending on the availability of water

bodies. Specifically, larviparous females sampled in a locality (SGAL_Larv), where nearby aquatic systems are absent, exhibited a positive relatedness at > 700 m, while larviparous females from other localities displayed a low (negative) relatedness at this distance class (**Figure 3.5**). This pattern may indicate females adjust their dispersal behaviour (*i.e.* increase dispersal rates and distances) under a scenario of scarcity of water bodies to increase the likelihood of finding breeding sites, as previously found for females of an anuran species (Wang *et al.* 2012). Despite these values of relatedness being positive, they are not significant and are based on low sample size, therefore, they should be interpreted with caution.

5.1.1.3 – Sex-biased dispersal

Whether there are sex-specific differences in dispersal in *S. salamandra* was unclear (see introduction in chapter 3). Clarifying this subject is key for a better understanding of not only (i) the dispersal ecology of this species, but also (ii) the demographic dynamics of *S. salamandra* populations, (iii) the influence of reproductive mode on dispersal behaviour, and (iv) for an accurate interpretation of phylogeographic and evolutionary patterns observed across the range of this species. Genetic spatial autocorrelation analyses performed in chapter 3 revealed males displayed higher relatedness values than females for a distance class of 701-1000 m and greater variation in dispersal distances (**Figures 3.4 and 3.5**). Conversely, females were genetically more structured in space and exhibited a marked philopatric behaviour (*i.e.* high relatedness values for short distances; **Figures 3.4 and 3.5**)**.** These results partially support male-biased dispersal in both reproductive modes, though evidence for this pattern achieved, overall, low statistical support.

Male-biased dispersal is usually suggested as a potential explanation for patterns of mito-nuclear discordances in many vertebrate groups (Toews and Brelsford 2012). However, multiple causes of mito-nuclear discordances are often suggested due to a lack of complementary data, which lead authors to base their interpretations of these genetic patterns on the biogeographic patterns themselves. The results obtained in chapter 3 provide additional support for the male-biased dispersal hypothesis proposed by biogeographic studies to justify the mito-nuclear discordances found in the Iberian Peninsula for *S. salamandra* (García-París *et al.* 2003; Pereira *et al.* 2016). This stresses the importance of exploring the role of sex-biased dispersal in explaining mito-nuclear discordances in animals, as this process is often suggested as a potential driver of these genetic discordances (see Table 1 in Toews and Brelsford 2012). It should be emphasized, however, that in some cases, sex-biased dispersal may vary at the intra-specific level (Wang *et al.* 2012; Trochet *et al.* 2016). This is because the drivers of dispersal, such as phenotypic and environmental variation, can vary substantially

across the range of a species, thus potentially contributing to variation in dispersal asymmetries between genders. For amphibians in particular, movement is largely influenced by the distribution and availability of water bodies (Pittman *et al.* 2014); therefore, a shift to terrestrial reproduction putatively reduces the interaction between individuals and aquatic systems. I cannot discard, for instance, sex-specific asymmetries in dispersal are more variable in larviparous individuals due to their hydric requirements. The high relatedness values for farther distances (> 700 m) exhibited by the larviparous females sampled in a locality (SGAL_Larv), where nearby aquatic systems are absent, seem to suggest reproductive mode impacts sex-biased dispersal under specific conditions (Wang *et al.* 2012). This raises the possibility that sex-biased dispersal may be more context-dependent in aquatic-breeding amphibians, although other factors (*e.g.* distribution of landscape barriers) should be taken into consideration. Certainly, future studies testing explicitly this hypothesis are warranted (see section 5.2.2).

5.1.1.4 – Environmental drivers of genetic connectivity in S. salamandra

Environmental changes may affect gene flow rates among populations and, consequently, entail significant demographic and evolutionary consequences for populations (Cosgrove *et al.* 2018). Assessing patterns of population genetic connectivity is thus an important task, especially, under a scenario of rapid changes in land cover and climate caused by anthropogenic activities (Pecl *et al.* 2017; Cosgrove *et al.* 2018; Pflüger *et al.* 2019). Studies explicitly linking patterns of genetic structure and environmental variation in *S. salamandra* are scarce (*e.g.* Antunes *et al.* 2018). Most data describing how dispersal and gene flow are influenced by the environment in *S. salamandra* was obtained from previous ecological studies (see Velo-Antón and Buckley 2015 and references therein) and descriptive genetic studies (Pisa *et al.* 2015; Straub *et al.* 2015; Konowalik *et al.* 2016; Vörös *et al.* 2017). The thorough landscape genetics framework used in chapter 4 provided relevant information about the landscape ecology of fire salamanders. Specifically, aside from lotic waters (see section 5.1.1.1), these analyses showed land cover, wind, and topography also influence genetic connectivity in *S. salamandra*.

Landscape genetic analyses carried out in chapter 4 revealed agricultural areas are the best predictor of genetic differentiation in both pueriparous and larviparous populations, being associated with higher resistance to gene flow. Whether pueriparity comprises a trait that minimizes the barrier genetic effects of this land use is unclear, as my inferences regarding the extent to which agricultural land affects gene flow in both larviparous and pueriparous populations are limited due to the much larger area occupied by agricultural fields in the

pueriparous plot. Additional studies are necessary to examine this issue in more detail (see also section 5.2.1). Moreover, the higher landscape resistance to gene flow imposed by agricultural land was also reported for a southern Iberian *S. salamandra* subspecies (*S. s. longirostris*; Antunes *et al.* 2018) and other amphibian species (*e.g.* Johansson *et al.* 2007; Nowakowski *et al.* 2015; Costanzi et al. 2018), thus reinforcing the notion that agricultural practices are a pervasive threat to the long-term persistence of many amphibians (*e.g.* Cushman 2006; Ferreira and Beja 2013). Throughout the range of *S. salamandra*, a large proportion of land has been converted for agricultural practices and, in addition to this, reports from the European Union predict an expansion of agricultural land, particularly, in southern and southeastern Europe (Perpiña Castillo *et al.* 2018). The continued expansion of agricultural fields may further isolate and cause demographic bottlenecks that may seriously compromise the long-term persistence of fire salamander populations. Subspecies presenting a fragmented and restricted distribution (*e.g. S. s. longirostris*; Antunes *et al.* 2018) are expected to be more vulnerable to such modifications in land cover and, therefore, they are of great conservation concern (Kuzmin *et al.* 2009).

No other land use variable was statistically associated with genetic differentiation, though previous descriptive studies have suggested man-made infrastructures (urban settlements and roads) hinder gene flow in *S. salamandra* (Pisa *et al.* 2015; Straub *et al.* 2015; Konowalik *et al.* 2016). Additionally, the study carried out in chapter 2 neatly demonstrates that urbanization (*e.g.* buildings and roads within Oviedo) substantially constrain dispersal in *S. salamandra*, as the studied urban pueriparous populations were genetically isolated despite the small distances separating them. Considering this, I argue the lack of statistical support for the negative impact of urban areas on genetic connectivity in *S. salamandra* is due to low statistical power arising from the small area occupied by urban settlements in both study landscape plots (see Discussion in chapter 4). This underscores the importance of accounting for sampling scheme and landscape structure to test specific hypotheses regarding the effects of particular land use types on genetic differentiation (see Short Bull *et al.* 2011; Oyler-McCance *et al.* 2013). Additionally, the way researchers measure and incorporate land cover in landscape genetic analyses also requires thoughtful considerations. I showed, in chapter 4, that using a single variable describing the total land cover or multiple land use variables, each characterizing a specific land use type, may lead to different outcomes. This is because including multiple land use classes in a single variable, which hypothetically influence gene flow in different ways, may obscure significant statistical relationships between specific land use types and genetic connectivity. This may potentially explain why some landscape genetic studies failed to detect a significant effect of land cover in patterns of gene flow (*e.g.* Ruiz-

Lopez *et al.* 2016; Garcia *et al.* 2017; Gutiérrez-Rodríguez *et al.* 2017). Based on the results obtained in this study, I suggest that future landscape genetic studies incorporating land cover should perform exploratory analyses to determine the best approach to represent this variable.

Besides land cover, wind exposition was also a significant predictor of genetic structure in both reproductive modes, with higher values of this variable being associated with a higher landscape resistance to gene flow. Amphibians are susceptible to the wind because it increases the rate of evaporative water loss (*e.g.* Peterman and Semlitsch 2014). As a response to windy conditions, amphibians tend to decrease activity to prevent water loss, including *S. salamandra* (Velo-Antón and Buckley 2015). Landscapes highly exposed to the wind likely hamper individual dispersal rates and distances, and this reduction in movement rates may translate into reduced genetic connectivity over these areas. Despite the acknowledged negative impact of wind in amphibians, it is surprising this variable has been overlooked in landscape genetic studies. The results obtained in this study highlight the importance of considering wind exposition in future landscape genetic studies to better understand the environmental factors governing genetic connectivity in amphibian populations.

Similarly to other studies, which found topography is an important driver of gene flow in amphibians (*e.g.* Velo-Antón *et al.* 2013; Coster *et al.* 2015; Burkhart *et al.* 2017; Gutiérrez-Rodríguez *et al.* 2017; Sánchez-Montes *et al.* 2018), chapter 4 also confirmed this variable plays a relevant role in shaping genetic structure in fire salamanders. Specifically, moving upslope entails greater resistance to gene flow, but I found moderate support for this effect only in pueriparous populations. The lack of an effect of topography on gene flow among larviparous populations is likely an artifact of the higher topographic complexity in the pueriparous plot compared to the larviparous one, as in other mountainous regions, neighbouring larviparous populations also present high levels of genetic differentiation (*e.g.* Vörös *et al.* 2017). These differences in topography between landscape plots, among other discussed factors (lotic waters, greater proportion of agricultural fields), possibly contributed to the higher genetic structure observed in pueriparous populations.

5.1.2 – Long-term persistence in urban environments

5.1.2.1 – Salamandra salamandra in Oviedo

Human activities have been largely responsible for habitat loss and fragmentation of extensive regions worldwide and, in particular, urbanization has been acknowledged as a rapid and pervasive driver of landscape changes, causing isolation and local extirpations of vulnerable species, such as amphibians (McKinney 2006). While pueriparity allowed survival of amphibians in natural water-limited environments (*e.g.* karstic limestones, García-París *et*

al. 2003; islands, Velo-Antón *et al.* 2012; steep terrains, Liedtke *et al.* 2017), I showed this reproductive mode also constitutes a key trait for survival in areas subjected to pronounced and rapid changes in land cover, such as urbanized landscapes. In chapter 2, I studied patterns of genetic variation in urban pueriparous populations of *S. salamandra* inhabiting the historical city of Oviedo (Spain). These populations inhabit small patches of vegetation (*e.g.* urban parks and gardens) scattered across the city, in which some of them, have putatively persisted for several hundreds of generations (*e.g.* fire salamanders located in Oviedo's cathedral; **Figure 2.1**). One especially relevant attribute of these patches is the lack of surface water for the development of aquatic larvae. Unlike other urbanized areas where aquatic breeding sites are available (*e.g.* Munshi-South *et al.* 2013; Furman *et al.* 2016), the extreme conditions found within Oviedo would render aquatic-breeding strategies unviable. This implies the fully terrestrial life cycle derived from a pueriparous reproduction has been crucial for the survival of fire salamanders under these stressful conditions, thus comprising a clear example of greater endurance of pueriparous amphibians in harsh habitats.

My thesis also revealed the studied urban populations are isolated to a large extent and exhibit a low *Ne* (most populations show a *Ne* < 50), which makes them potentially vulnerable to the detrimental effects of drift on genetic diversity (Frankham 2005). However, genetic diversity in these urban populations is moderately high and comparable to the estimates obtained for rural populations (**Table 2.2**). The processes responsible for this pattern are unclear, though the role of pueriparity in maintaining genetic diversity cannot be discarded. Previous studies performed in aquatic-breeding and direct-developing (which are more susceptible to desiccation) amphibians from highly urbanized areas reported reduced genetic diversity levels (*e.g.* Noël and Lapointe 2010; Munshi-South *et al.* 2013). Since pueriparous amphibians have putatively fewer habitat requirements than aquatic-breeding species, it is possible the high abundance of crevices and holes, which are used as refuges by fire salamanders, together with the virtual absence of predators in Oviedo, have been sufficient to assure reduced mortality rates and minimize the loss of genetic diversity through maintenance of a stable *Ne*. Other not mutually exclusive factors may also help to explain the elevated diversity estimates in the studied urban populations. For instance, the existence of mechanisms of genetic compensation (see Palstra and Fraser 2012) could explain the very high *Ne/N* ratios (>0.50) found in Álvarez *et al.* (2015) for a single urban fire salamander population in Oviedo. The capacity of females to store sperm from multiple males (Caspers *et al.* 2014; Velo-Antón unpublished data) and deliver offspring with multiple sires in a single parturition event may be an example of such mechanisms, as it potentially increases the reproductive success of males in such a small area, possibly boosting *Ne* and genetic diversity.

We cannot discard these high *Ne/N* ratios are also caused by associative overdominance (linkage of neutral loci to adaptive ones), which may be responsible for the maintenance of genetic diversity at neutral loci in genomic regions where recombination rates are low. This was neatly demonstrated by Schou *et al.* (2017), who experimentally showed that small-sized populations of *Drosophila melanogaster* experience a slower than expected loss of genetic diversity.

5.1.2.2 – Factors influencing genetic drift in urban environments

Urbanization can be a major driver of adaptive and neutral evolutionary processes in natural populations (Alberti *et al.* 2017; Johnson and Munshi-South 2017). Specifically, at the level of neutral genetic variation, many studies have shown urban settlements not only reduce gene flow among populations (*i.e.* increase genetic differentiation), but also reduce genetic diversity due to the exacerbated negative effects of drift in small and isolated populations (*e.g.* Noël and Lapointe 2010; Munshi-South *et al.* 2013; Munshi-South *et al.* 2016). However, the magnitude to which cities shape neutral genetic variation depends on how the migration-drift equilibrium is affected by different structural (*e.g.* urban development and planning), historical (*e.g.* age, past demography), biotic (*e.g.* presence of predators), and abiotic (*e.g.* pollution, disturbance, geographical context) factors (see Johnson and Munshi-South 2017). Data about the latter topic is scarce; therefore, under an increasingly urbanized world, obtaining such information may help researchers to better predict the direction and magnitude of evolutionary changes in urbanized landscapes.

I used the fire salamanders in Oviedo to examine some of the structural (patch size) and historical (time since isolation, past demography) factors that may govern the effects of genetic drift on genetic variation in urban environments. Regression analyses in this study revealed patch size is an important predictor of *Ne*, with larger patches holding larger populations because they house a greater availability of resources. Genetic variation and *Ne* are intimately linked (Ellegren and Galtier 2016) and, by extension, patch size plays also an important role on genetic diversity and differentiation, as shown by previous studies (urban areas, Delaney *et al.* 2010; natural habitats, Wang *et al.* 2011; simulations, Jackson and Fahrig 2016). Managing suitable patches of habitat within cities may thus comprise an effective conservation measure to help preserve the urban wildlife in the long-term. This may be particularly relevant for those species incapable of moving efficiently through the urban matrix (*i.e.* species with limited dispersal abilities, such as reptiles and amphibians), which may explain why the reduction in genetic diversity is often more severe in these groups (see Johnson and Munshi-South 2017). Additionally, the importance of patch size for *Ne* and genetic diversity observed

in chapter 2 may also extend to small-sized natural populations. For instance, patch size may be a good surrogate of population size and genetic variation (Wang *et al.* 2011; Henle *et al.* 2017; Denoël *et al.* 2018) for species that use discrete and well-delimited resource patches, such as pond-breeding amphibians. It should be noted, however, that many other factors likely play a crucial role in maintaining genetic variation of small-sized populations (*e.g.* habitat quality, biotic interactions) and, therefore, they should be considered accordingly.

5.2 – On-going and future studies

Although the present thesis has provided important insights about the eco-evolutionary implications of pueriparity in fire salamanders, there are still many questions related to the above studied topics that remain to be answered. In this section, I highlight exciting avenues for future research.

5.2.1 – Does pueriparity always constrains genetic connectivity?

The greater persistence shown by pueriparous populations of *S. salamandra* in Oviedo and in other highly fragmented and small forested patches in the pueriparous plot (*e.g.* populations CORN and BOHI; **Figure 4.4**), as well as by other terrestrial-breeding amphibians, potentially suggests terrestrial reproduction may help these species in maintaining higher levels of population connectivity in heterogeneous and fragmented landscapes compared to aquatic-breeding species (Marsh *et al.* 2004; Measey *et al.* 2007; Sandberger-Loua *et al.* 2018; see also Mims *et al.* 2015). Contrary to these predictions, data collected from chapters 3 and 4 show that dense hydric networks constrain dispersal and gene flow in pueriparous fire salamanders, while larviparous ones can transverse and disperse along lotic waters more efficiently during the aquatic larval stage. Whether pueriparity promotes higher dispersal success rates across other types of sub-optimal habitats (*e.g.* agricultural fields) is unclear, and future landscape studies with a more appropriate experimental design may help testing properly this hypothesis. Moreover, pueriparity may increase genetic connectivity under environmental contexts that differ from the ones studied in this thesis. For example, Mims *et al.* (2015) and Sandberger-Loua *et al.* (2018) observed reduced population genetic divergence in species displaying a lower dependency on water for survival and reproduction. These studies were performed in areas characterized by high levels of aridity or where the dry season imposes significant constraints to amphibians highly dependent on aquatic systems. It can thus be hypothesized that pueriparity may indeed favour genetic connectivity in semi-arid environments where water bodies between patches are absent or scarce. The sister species *S. algira* may be a good system to evaluate the influence of reproductive mode in population

connectivity under more extreme (*i.e.* drier) conditions. This species exhibits both an aquatic- (larviparity) and terrestrial-breeding (pueriparity) strategies (Dinis and Velo-Antón 2017), with pueriparous populations inhabiting karstic areas in the northern Rif Mountains of Morocco, where water bodies are absent or temporary, while larviparous populations are patchily distributed across the thermic or mesothermic Mediterranean forests from Morocco to Algeria.

5.2.2 – Has dispersal behaviour been affected by pueriparity?

The data collected in this thesis about the movement behaviour of larviparous and pueriparous salamanders are not conclusive. Genetic spatial autocorrelation analyses seem to suggest little differentiation in dispersal behaviour between reproductive modes, though the lack of resolution of the genetic methodologies employed here prevents me from inferring whether this is a general pattern or if some pueriparous individuals do show a differentiated movement behaviour. Future studies should include field methodologies (*e.g.* mark-recapture, radio tracking) to address more adequately this topic, as they can provide more detailed information on individual dispersal trajectories (although at greater costs; Lowe and Allendorf 2010). In addition to this, other methodological considerations should be taken into account to better understand the impact of pueriparity in the dispersal ecology of fire salamanders and other amphibians. First, it would be valuable to acknowledge life stage in movement studies. In many species of vertebrates (including amphibians), juveniles and subadults exhibit greater variation in dispersal compared to adults (Semlitsch 2008; Bonte *et al.* 2012; Pittman *et al.* 2014). Because natal dispersal is largely governed by reproductive biology, I cannot rule out that pueriparity has affected mostly dispersal in subadults. Second, future research should also test specific hypotheses regarding the local environmental context. For instance, patterns of movement of larviparous and pueriparous salamanders in areas containing low vs. high densities of water bodies could be compared. This may potentially (i) clarify the influence of reproductive mode on individual dispersal, and (ii) help evaluate if terrestrial-breeding strategies entail a lower variation on sex-biased dispersal within species due to its lower dependency on aquatic resources.

5.2.3 – Why is the distribution of pueriparity spatially restricted?

Pueriparity in *S. s. bernardezi* emerged during the Pliocene-Pleistocene period in the Cantabrian mountains (northern Spain), possibly, in response to the lack of surface water in karstic limestone substrates (García-París *et al.* 2003). However, pueriparity in *S. salamandra* has remained restricted to a relatively small section of northern Spain despite its potential advantages. Preliminary data seems to suggest the Cantabrian mountains are an effective

barrier to gene flow between *S. s. bernardezi* and *S. s. bejarae* (**Figures 1.13 and 1.14**; Velo-Antón unpublished). However, no apparent topographic barriers seem to explain the limited expansion of pueriparity, particularly, to the west. In fact, it appears that haplotypes from *S. s. gallaica* are introgressing within the range of the pueriparous *S. s. bernardezi*, but the opposite pattern has not been observed yet (see chapter 4; Velo-Antón unpublished data). Again, one potential factor explaining the small range of pueriparity in *S. salamandra* may be the greater barrier effects imposed by lotic waters to gene flow, as demonstrated in chapter 4. The northern part of Iberian Peninsula is characterized by dense networks of rivers and streams, which may have reduced the spread of this trait into across northern Spain (especially at west), although hybrid zones between northern lineages were detected and are presently been studied (Velo-Antón unpublished).

5.2.4 – Does pueriparity increases population diversification rates in *S. salamandra*?

Previous studies have demonstrated the evolution of a derived reproductive mode may affect lineage diversification rates (Helmstetter *et al.* 2016; see also section 1.1.3). The complex demographic history of *S. s. bernardezi* in the Cantabrian Mountains resulted in a greater phylogeographic structure compared with other subspecies (García-París *et al.* 2003; Velo-Antón *et al.* 2007; Beukema *et al.* 2016), even though its range is among the smallest of *S. salamandra* subspecies. The increased barrier effects of lotic systems on pueriparous salamanders suggest pueriparity may have also contributed to the long-term isolation of many populations and, consequently, lineage diversification within *S. s. bernardezi*. On-going work integrating molecular and environmental data at different time scales will elucidate the complex evolutionary history of *S. s. bernardezi* and, thus, help inferring the potential impact of pueriparity in population diversification rates.

5.2.5 – Evolution in urban environments

The urban populations of fire salamanders in Oviedo exhibited higher than expected genetic diversity levels. Some ecological (low dependence on water), demographic (low mortality rates), and genetic (mechanisms of genetic compensation, associative overdominance) factors were proposed as potential drivers of these genetic patterns, though the available data prevents me from establishing precise causal relationships. The inclusion of genomic tools to examine more accurately neutral and adaptive genetic variation may help to identify the factors governing genetic diversity in these small and isolated populations. Such information would

also be valuable not only to help explain the high genetic diversity levels reported in rural pueriparous populations inhabiting small and isolated patches (*e.g.* pueriparous populations in CORN and BOHI; see chapter 4), but also it could provide a better understanding of how isolation affects genomic diversity throughout time (Shaffer *et al.* 2015; Díez-del-Molino *et al.* 2018). In addition to genetic variation, the studied urban populations of *S. salamandra* in Oviedo have the potential to provide further insights about phenotypic evolution and fitness constraints in urbanized landscapes, which certainly can be valuable to other groups affected by urbanization (see Johnson and Munshi-South 2017).

These pueriparous populations offer also an excellent opportunity to study the structural and historical factors influencing genetic drift in urban environments. Aside from patch size, which was a significant predictor of *Ne*, I did not find clear support for the other tested variables (time since isolation, bottleneck magnitude, and post-bottleneck time). This is probably because the sample size used (n = 12 populations) is not adequate to perform robust regression analyses. Sampling more urban populations scattered across Oviedo can potentially add interesting insights about this subject and, by extension, help researchers to better predict the effects of urbanization in wildlife.

5.3 – Concluding remarks

The eco-evolutionary implications underlying the emergence of pueriparity in amphibians have been largely underexplored. The main aim of this thesis was to contribute additional insights to this subject by using a salamander species (*S. salamandra*) that exhibits two remarkably distinct reproductive strategies. Below I summarize the major contributions of the present thesis:

1. Pueriparity constrains genetic connectivity in fire salamanders, as a fully terrestrial life cycle increases the barrier effects of lotic waters (*e.g.* streams and rivers). Additionally, lotic systems may promote active or passive long-distance movements during the aquatic larval stage;
2. This thesis provided relevant information regarding the environmental drivers of genetic connectivity in this species, a topic that had remained underexplored until now. Agricultural fields were the best predictors of genetic connectivity in both larviparous and pueriparous salamanders, being strong barriers to gene flow. This supports the pervasive effects of agricultural land on amphibians regardless of their dependency on water. Wind exposition was also a relevant predictor of genetic differentiation for both reproductive modes. This variable has been overlooked in landscape genetic studies, and this result stresses the importance of incorporating this variable to better

understand how the environment shapes population connectivity in amphibian populations. Moving upslope entailed also greater costs only in pueriparous salamanders, though a more robust sampling design is required to clarify the effects of topography in both reproductive modes. Collectively, these can be valuable for the conservation of *S. salamandra*, particularly, for those subspecies exhibiting fragmented and restricted distributions.

3. The evolution of pueriparity enabled the long-term persistence of fire salamanders in habitats (urban environments) that are unsuitable for larviparous salamanders due to the lack of water bodies for the development of larvae. This implies pueriparity comprises an advantageous trait for survival under a scenario of rapid and pronounced changes in the landscape (*e.g.* loss of water bodies, urbanization);
4. Patch size is an important predictor of *Ne* and, by extension, of genetic variation in urbanized landscapes, at least, for species with limited dispersal abilities.
5. At local scales and in pristine habitats, the dispersal ecology of fire salamanders was likely unaffected by a shift to pueriparity, although the causes responsible for this pattern deserve further investigation;
6. Dispersal in *S. salamandra* is probably male-biased, although it is possible sex-specific differences in dispersal vary according to environmental context (*e.g.* availability of water bodies for reproduction in larviparous salamanders);
7. This thesis also opened interesting avenues for future research that promise to contribute to a better understanding of the ecological and evolutionary effects underlying the evolution of a derived reproduction.

5.4 – References

Alberti M, Correa C, Marzluff JM *et al.* (2017) Global urban signatures of phenotypic change in animal and plant populations. *Proceedings of the National Academy of Sciences*, **114**, 8951–8956.

Álvarez D, Lourenço A, Oro D, Velo-Antón G (2015) Assessment of census (*N*) and effective population size (*Ne*) reveals consistency of *Ne* single-sample estimators and a high *Ne*/*N* ratio in an urban and isolated population of fire salamanders. *Conservation Genetics Resources*, **7**, 705–712.

Antunes B, Lourenço A, Caeiro-Dias G *et al.* (2018) Combining phylogeography and landscape genetics to infer the evolutionary history of a short-range Mediterranean relict, *Salamandra salamandra longirostris*. *Conservation Genetics*, **19**, 1411–1424.

Banks SC, Peakall R (2012) Genetic spatial autocorrelation can readily detect sex-biased dispersal. *Molecular* Ecology, **21**, 2092–2105.

Beukema W, Nicieza AG, Lourenço A, Velo-Antón G (2016) Colour polymorphism in *Salamandra salamandra* (Amphibia: Urodela), revealed by a lack of genetic and environmental differentiation between distinct phenotypes. *Journal of Zoological Systematics and Evolutionary Research*, **54**, 127–136.

Bonte D, van Dyck H, Bullock JM *et al.* (2012) Costs of dispersal. *Biological Reviews*, **87**, 290–312.

Burkhart JJ, Peterman WE, Brocato ER *et al.* (2017) The influence of breeding phenology on the genetic structure of four pond-breeding salamanders. *Ecology and Evolution*, **7**, 4670–4681.

Caspers BA, Krause ET, Hendrix R *et al.* (2014) The more the better - polyandry and genetic similarity are positively linked to reproductive success in a natural population of terrestrial salamanders (*Salamandra salamandra*). *Molecular Ecology*, **23**, 239–250.

Cornetti L, Griffith OW, Benazzo A *et al.* (2017) Candidate genes involved in the evolution of viviparity: a RAD sequencing experiment in the lizard *Zootoca vivipara* (Squamata: Lacertidae). *Zoological Journal of the Linnean Society*, **183**, 196–207.

Cosgrove AJ, McWhorter TJ, Maron M (2018) Consequences of impediments to animal movements at different scales: a conceptual framework and review. *Diversity and Distributions*, **24**, 448–459.

Costanzi J-M, Mège P, Boissinot A *et al.* (2018). Agricultural landscapes and the Loire River influence the genetic structure of the marbled newt in Western France. *Scientific Reports*, **8**, 14177.

Coster SS, Babbitt KJ, Cooper A, Kovach AI (2015) Limited influence of local and landscape factors on finescale gene flow in two pond-breeding amphibians. *Molecular Ecology*, **24**, 742–758.

Cushman SA (2006) Effects of habitat loss and fragmentation on amphibians: a review and prospectus. *Biological Conservation*, **128**, 231-240.

Delaney KS, Riley SPD, Fisher RN (2010) A rapid, strong, and convergent genetic response to urban habitat fragmentation in four divergent and widespread vertebrates. *PLoS ONE*, **5**, e12767.

Denoël M, Dalleur S, Langrand E, Besnard A, Cayuela H (2018) Dispersal and alternative breeding site fidelity strategies in an amphibian. *Ecography*, **41**, 1543–1555.

Díez-del-Molino D, Sánchez-Barreiro F, Barnes I, Gilbert MTP, Dalén L (2018) Quantifying temporal genomic erosion in endangered Species. *Trends in Ecology and Evolution*, **33**, 176–185.

Dinis M, Velo-Antón G (2017) How little do we know about the reproductive mode in the north African salamander, *Salamandra algira*? Pueriparity in divergent mitochondrial lineages of *S. a. tingitana*. *Amphibia-Reptilia*, **38**, 540–546.

Ellegren H, Galtier N (2016) Determinants of genetic diversity. *Nature Reviews Genetics*, **17**, 422-433.

Ferreira M, Beja P (2013) Mediterranean amphibians and the loss of temporary ponds: are there alternative breeding habitats? *Biological Conservation*, **165**, 179–186.

Fouquet A, Courtois EA, Baudain D *et al.* (2015) The trans-riverine genetic structure of 28 Amazonian frog species is dependent on life history. *Journal of Tropical Ecology*, **31**, 361–373.

Frankham R (2005) Genetics and extinction. *Biological Conservation*, **126**, 131–140.

Furman BLS, Scheffers BR, Taylor M, Davis C, Paszkowski CA (2016) Limited genetic structure in a wood frog (*Lithobates sylvaticus*) population in an urban landscape inhabiting natural and constructed wetlands. *Conservation Genetics*, **17**, 19–30.

Gao W, Sun Y-B, Zhou W-W *et al.* (2019) Genomic and transcriptomic investigations of the evolutionary transition from oviparity to viviparity. *Proceedings of the National Academy of Sciences*, **116**, 3646–3655.

Garcia VOS, Ivy C, Fu J (2017) Syntopic frogs reveal different patterns of interaction with the landscape: a comparative landscape genetic study of *Pelophylax nigromaculatus* and *Fejervarya limnocharis* from central China. *Ecology and Evolution*, **7**, 9294–9306.

García-París M, Alcobendas M, Buckley D, Wake D (2003) Dispersal of viviparity across contact zones in Iberian populations of Fire salamanders (*Salamandra*) inferred from discordance of genetic and morphological traits. *Evolution*, **57**, 129–143.

Gutiérrez-Rodríguez J, Gonçalves J, Civantos E, Martínez-Solano I (2017) Comparative landscape genetics of pond-breeding amphibians in Mediterranean temporal wetlands: the positive role of structural heterogeneity in promoting gene flow. *Molecular Ecology*, **26**, 5407–5420.

Halliwell B, Uller T, Holland BR, While GM (2017) Live bearing promotes the evolution of sociality in reptiles. *Nature Communications*, **8**, 2030.

Helmstetter AJ, Papadopulos AST, Igea J, van Dooren TJM, Leroi AM, Savolainen V (2016) Viviparity stimulates diversification in an order of fish. *Nature Communications*, **7**, 11271.

Hendrix R, Schmidt BR, Schaub M, Krause ET, Steinfartz S (2017) Differentiation of movement behaviour in an adaptively diverging salamander population. *Molecular Ecology*, **26**, 6400–6413.

Henle K, Andres C, Bernhard D *et al.* (2017) Are species genetically more sensitive to habitat fragmentation on the periphery of their range compared to the core? A case study on the sand lizard (*Lacerta agilis*). *Landscape Ecology*, **32**, 131–145.

Jackson ND, Fahrig L (2016) Habitat amount, not habitat configuration, best predicts population genetic structure in fragmented landscapes. *Landscape Ecology*, **31**, 951–968.

Johansson M, Primmer CR, Merila J (2007) Does habitat fragmentation reduce fitness and adaptability? A case study of the common frog (*Rana temporaria*). *Molecular Ecology*, **16**, 2693-2700.

Johnson MTJ, Munshi-South J (2017) Evolution of life in urban environments. *Science*, **358**, eaam8327.

Konowalik A, Najbar A, Babik W, Steinfartz S, Ogielska M (2016) Genetic structure of the fire salamander *Salamandra salamandra* in the Polish Sudetes. *Amphibia Reptilia*, **37**, 405–415.

Kuzmin S, Papenfuss T, Sparreboom M *et al.* (2009). *Salamandra salamandra*. In: *The IUCN Red List of Threatened Species 2009*.

Lowe WH, Allendorf FW (2010) What can genetics tell us about population connectivity? *Molecular Ecology*, **19**, 3038–3051.

Ma L, Buckley LB, Du RBHW (2018) A global test of the cold-climate hypothesis for the evolution of viviparity of squamate reptiles. *Global Ecology and Biogeography*, **27**, 679–689.

Marsh DM, Page RB, Hanlon TJ *et al.* (2007) Ecological and genetic evidence that low-order streams inhibit dispersal by red-backed salamanders (*Plethodon cinereus*). *Canadian Journal of Zoology*, **85**, 319–327.

Marsh DM, Thakur KA, Bulka KC, Clarke LB (2004) Dispersal and colonization through open fields by a terrestrial, woodland salamander. *Ecology*, **85**, 3396–3405.

McKinney ML (2006) Urbanization as a major cause of biotic homogenization. *Biological Conservation*, **127**, 247–260.

Measey GJ, Galbusera P, Breyne P, Matthysen E (2007) Gene flow in a direct-developing, leaf litter frog between isolated mountains in the Taita Hills, Kenya. *Conservation Genetics*, **8**, 1177–1188.

Mims MC, Phillipsen IC, Lytle DA *et al.* (2015) Ecological strategies predict associations between aquatic and genetic connectivity for dryland amphibians. *Ecology*, **96**, 1371–1382.

Munshi-South J, Zak Y, Pehek E (2013) Conservation genetics of extremely isolated urban populations of the northern dusky salamander (*Desmognathus fuscus*) in New York City. *PeerJ*, **1**, e64.

Noël S, Lapointe FJ (2010) Urban conservation genetics: study of a terrestrial salamander in the city. *Biological Conservation*, **143**, 2823–2831.

Nowakowski AJ, Dewoody JA, Fagan ME, Willoughby JR, Donnelly MA (2015) Mechanistic insights into landscape genetic structure of two tropical amphibians using field-derived resistance surfaces. *Molecular Ecology*, **24**, 580–595.

Ousterhout BH, Semlitsch RD (2018) Effects of conditionally expressed phenotypes and environment on amphibian dispersal in nature. *Oikos*, **127**, 1142-1151.

Oyler-McCance SJ, Fedy BC, Landguth EL (2013) Sample design effects in landscape genetics. *Conservation Genetics*, **14**, 275–285.

Palstra FP, Fraser DJ (2012) Effective/census population size ratio estimation: a compendium and appraisal. *Ecology and Evolution*, **2**, 2357–2365.

Pecl GT, Araújo MB, Bell J *et al.* (2017) Biodiversity redistribution under climate change: impacts on ecosystems and human well-being. *Science*, **355**, eaai9214.

Pereira RJ, Martínez-Solano I, Buckley D (2016) Hybridization during altitudinal range shifts: nuclear introgression leads to extensive cyto-nuclear discordance in the fire salamander. *Molecular Ecology*, **25**, 1551–1565.

Perpiña Castillo CP, Kavalov B, Diogo V *et al.* (2018) *Trends in the EU agricultural land within 2015-2030*. JRC113717, European Commission 2018.

Peterman W, Semlitsch RD (2014) Spatial variation in water loss predicts terrestrial salamander distribution and population dynamics. *Oecologia*, **176**, 357–369.

Pflüger FJ, Signer J, Balkenhol N (2019) Habitat loss causes non-linear genetic erosion in specialist species. *Global Ecology and Conservation*, *17*(1), e00507.

Pincheira-Donoso D, Tregenza T, Witt MJ, Hodgson DJ (2013) The evolution of viviparity opens opportunities for lizard radiation but drives it into a climatic cul-de-sac. *Global Ecology and Biogeography*, **22**, 857–867.

Pisa G, Orioli V, Spilotros G *et al.* (2015) Detecting a hierarchical genetic population structure: The case study of the Fire Salamander (*Salamandra salamandra*) in Northern Italy. *Ecology and Evolution*, **5**, 743–758.

Pittman SE, Osbourn MS, Semlitsch RD (2014) Movement ecology of amphibians: a missing component for understanding population declines. *Biological Conservation*, **169**, 44–53.

Reinhardt T, Bauldauf L, Ilić M, Fink P (2018) Cast away: drift as the main determinant for larval survival in western fire salamanders (*Salamandra salamandra*) in headwater streams. *Journal of Zoology*, **306**, 171-179.

Ruiz-Lopez M. J, Barelli C, Rovero F *et al.* (2016) A novel landscape genetic approach demonstrates the effects of human disturbance on the Udzungwa red colobus monkey (*Procolobus gordonorum*). *Heredity*, **116**, 167–176.

Sánchez-Montes G, Wang J, Ariño AH, Martínez-Solano I (2018) Mountains as barriers to gene flow in amphibians: quantifying the differential effect of a major mountain ridge on the genetic structure of four sympatric species with different life history traits. *Journal of Biogeography*, **45**, 318–331.

Sandberger-Loua L, Rödel M-O, Feldhaar H (2018) Gene-flow in the clouds: landscape genetics of a viviparous, montane grassland toad in the tropics. *Conservation Genetics*, **19**, 169–180.

Schou MF, Loeschcke V, Bechsgaard J, Schlötterer C, Kristensen TN (2017) Unexpected high genetic diversity in small populations suggests maintenance by associative overdominance. *Molecular Ecology*, **26**, 6510–6523.

Semlitsch RD (2008) Differentiating migration and dispersal processes for pond-breeding amphibians. *Journal of Wildlife Management*, **72**, 260–267.

Shaffer HB, Gidiş M, McCartney-Melstad E *et al.* (2015) Conservation genetics and genomics of amphibians and reptiles. *Annual Review of Animal Biosciences*, **3**, 23.1-23.26.

Short Bull RA, Cushman SA, Mace R *et al.* (2011) Why replication is important in landscape genetics: American black bear in the Rocky Mountains. *Molecular Ecology*, **20**, 1092–1107.

Smith MA, Green DM (2006) Sex, isolation and fidelity: unbiased long-distance dispersal in a terrestrial amphibian. *Ecography*, **29**, 649-658.

Straub C, Pichlmüller F, Helfer V (2015) Population genetics of fire salamanders in a pre-Alpine urbanized area (Salzburg, Austria). *Salamandra*, **51**, 245–251.

Thiesmeier B, Schuhmacher H (1990) Causes of larval drift of the fire salamander, *Salamandra salamandra terrestris*, and its effects on population dynamics. *Oecologia*, **82**, 259–263.

Toews DPL, Brelsford A (2012) The biogeography of mitochondrial and nuclear discordance in animals. *Molecular Ecology*, **21**, 3907–3930.

Trochet A, Courtois EA, Stevens VM *et al.* (2016) Evolution of sex-biased dispersal. *The Quarterly Review of Biology*, **91**, 297–320.

Veith M, Baubkus M, Kugel S *et al.* (2019). Drift compensation in larval European fire salamanders, *Salamandra salamandra* (Amphibia: Urodela)? *Hydrobiologia*, **828**, 315–325.

Velo-Antón G, Buckley D (2015) Salamandra común – *Salamandra salamandra*. *In: Enciclopedia Virtual de los Vertebrados Españoles* (eds Carrascal LM, Salvador A). Museo Nacional de Ciencias Naturales, Madrid. http://www.vertebradosibericos.org

Velo-Antón G, García-París M, Galón P, Cordero Rivera A (2007) The evolution of viviparity in holocene islands: ecological adaptation versus phylogenetic descent along the transition from aquatic to terrestrial environments. *Journal of Zoological Systematics and Evolutionary Research*, **45**, 345–352.

Velo-Antón G, Parra JL, Parra-Olea G, Zamudio KR (2013) Tracking climate change in a dispersal-limited species: reduced spatial and genetic connectivity in a montane salamander. *Molecular Ecology*, **22**, 3261–3278.

Velo-Antón G, Santos X, Sanmartín-Villar I, Cordero-Rivera A, Buckley D (2015) Intraspecific variation in clutch size and maternal investment in pueriparous and larviparous *Salamandra salamandra* females. *Evolutionary Ecology*, **29**, 185-204.

Velo-Antón G, Zamudio KR, Cordero-Rivera A (2012) Genetic drift and rapid evolution of viviparity in insular fire salamanders (*Salamandra salamandra*). *Heredity*, **108**, 410–418.

Vörös J, Ursenbacher S, Kiss I *et al.* (2017) Increased genetic structuring of isolated *Salamandra salamandra* populations (Caudata: Salamandridae) at the margins of the Carpathian Mountains. *Journal of Zoological Systematics and Evolutionary Research*, **55**, 138–149.

Wang IJ, Johnson JR, Johnson BB, Shaffer HB (2011) Effective population size is strongly correlated with breeding pond size in the endangered California tiger salamander, *Ambystoma californiense*. *Conservation Genetics*, **12**, 911–920.

Wang Y, Lane A, Ding P (2012) Sex-biased dispersal of a frog (*Odorrana schmackeri*) is affected by patch isolation and resource limitation in a fragmented landscape. *PLoS ONE*, **7**, e47683.

Wourms JP, Lombardi J (1992) Reflections on the evolution of piscine viviparity. *American Zoologist*, **32**, 276–293.

Zúñiga-Vega JJ, Fuentes-G JA, Ossip-Drahos AG, Martins EP (2016) Repeated evolution of viviparity in phrynosomatid lizards constrained interspecific diversification in some life-history traits. *Biology Letters*, **12**, 20160653.

Chapter 6

Appendices and other publications

Appendix A

Supplementary Text A1

The access to maps and documents about urbanization on Oviedo provide us with relevant information to infer time since isolation on sampled urban populations of fire salamander. Readers who are interested in learning more about the history of fire salamanders in Oviedo can access the documentary *The last urban dragons* (Chachero and Álvarez 2016) in http://www.documentazul.com/info/dvd-los-ultimos-dragones-de-oviedo-contacto. Below, historical information concerning sampled localities is presented:

FC (Facultad Biología) – The construction of the Biology faculty building and surrounding streets was completed around 1992. Thus, we assume that this population has been isolated for 20-30 years.

PT (Plaza Toros) – The bullring was constructed in 1948. The old hospital which connects to one section of this patch was constructed in 1961. Therefore, this is the probable date of isolation. Accordingly, this population has been isolated for roughly 60 years.

CSF (Campo San Francisco) – This population likely became isolated around 1850-1900. Maps from 1900 confirmed that the San Francisco park was already surrounded by adjacent streets, and hence has been isolated for at least 100-120 years.

TEN (Club Tenis) – The Oviedo tennis club was built in 1950, but the small palace separating the club from the city was erected in 1902. Therefore, we estimate that this population became isolated during the period of 1902-1950 (about 60-100 years).

ARC (San Pedro de los Arcos) – The school which is connected with the park was constructed in 1985. In a city map of 1917, this location appears isolated from the city center after the construction of several streets and railways. Therefore, this population was isolated from external populations for almost 30 years and from the city centre since at least 100 years ago.

JAR (Jardines Seminário) – This population inhabits the gardens located between the walls of the old cemetery and the new seminary, both constructed at the beginning of the 20th century. Consequently, this population has putatively been isolated for more than 100 years.

OTE (Calle Muérdago-Otero) – This neighbourhood was urbanized in the 1970s, and in 1984 the construction of a beltway isolated the neighbourhood from the rest of the city, isolating this population for at least 35-40 years.

IND (Induráin-Tenderina) –The first construction in the Tenderina neighbourhood were built in the mid-1930s, but the urbanization of this neighbourhood took place mainly in 1960. Hence, this population has been isolated for 50-60 years ago.

MIL (Campus Milán) – The first building was constructed at the beginning of the 19th century as an ecclesiastical building (Seminario conciliar de Oviedo). In 1921, this building was taken by the army and the monks were moved to other monasteries. The urbanization of the Pumarin neighbourhood and the construction of the streets that surround the population of "Campus Milán" occurred in the mid-twentieth century. We estimated here that this population has been isolated for 60-70 years.

Populations located within historical walls – In 768 AD, the first of Oviedo's walls were erected, isolating the populations CAT (Catedral Patio; cathedral's courtyard) and MON (Monasterio; Monastery). In 852 AD, the Monastery was built, but since the construction of the first wall isolated this population from the rest of Oviedo, in this study we considered that both populations became isolated at the same time. A second wall was constructed in 1258, separating the population SAC (Casa Sacerdotal; Priests' Building) from the rest of the city. Thus, for the first two populations, we estimated an isolation period of about 1250 years, while for SAC we estimated that it has been isolated for about 700-800 years.

Supplementary Text A2

After assessing collinearity, employing logarithmic transformations, and standardizing predictors, we needed to determine the most suitable regression technique to model our response variables. We followed recommendations provided by Zuur *et al.* (2009) to carry out regression models for each response variable. We checked whether assumptions of normality and homogeneity of variances (critical features for linear regression) were violated. The former was inspected by making a histogram of the residuals and through Shapiro-Wilk normality tests, while the latter was assessed by plotting the residuals vs. the fitted values. In models where both assumptions were not violated, we used a multiple linear regression model with ordinary-least square estimates. On the other hand, when there was evidence for heterogeneity of variances, we employed a generalised least squares (GLS) method. This particular technique allows for a larger spread in the residuals by incorporating variance structures. The first step consists of the identification of the explanatory variables exhibiting heterogeneity. We plotted each predictor with the model's residuals to identify which variables showed a large spread. After identifying these variables, we chose the variance structure that minimized the model's Akaike Information Criterion (see Chapter 4 in Zuur *et al.* 2009). The most suitable variance structure was then included in GLS models. Finally, models exhibiting non-normally distributed residuals and large spread of residuals were initially fit with a generalised linear model (GLM) with a Poisson distribution. However, we found evidence for overdispersion (variance larger than the mean) through the calculation of a dispersion parameter (see chapter 9 in Zuur *et al.* 2009). Therefore, we applied a GLM with a negative binomial distribution, a method more robust to overdispersion (Zuur *et al.* 2009). Information concerning which models were used for each response variable is displayed in **Table A4 in Appendix A**.

Supplementary Table A1

Table A1 Descriptive information about sampling sites in Oviedo. Code Population acronym; Long and Lat – longitude and latitude coordinates, respectively; Size - patch size (m^2) for the sampling site; Time isolation – number of generations in which a population is putatively isolated (based on a generation time of 4 years for fire salamanders); DNP – distance to nearest population (m). NA – not applicable.

Code	Long	Lat	Size (m^2)	Time isolation	DNP (m)
FC	-5.8731	43.3564	248	6	541
PT	-5.8667	43.3577	7525	15	541
CSF	-5.8582	43.3621	155	25	459
TEN	-5.8571	43.3664	7560	20	481
ARC	-5.8463	43.3571	3948	25	481
JAR	-5.8463	43.3571	8698	25	566
OTE	-5.8366	43.3564	2917	10	665
IND	-5.8339	43.3621	204	15	658
MIL	-5.8397	43.3682	828	15	642
SAC	-5.8419	43.3610	596	190	178
CAT	-5.8433	43.3624	526	310	93
MON	-5.8436	43.3632	970	310	93
LIL	-5.8571	43.3803	NA	NA	1550
VIL	-5.9096	43.3683	NA	NA	3238
BEN	-5.8027	43.3334	NA	NA	3658
TIN	-5.7511	43.3668	NA	NA	5591

Supplementary Table A2

Table A2 Details of the 15 microsatellites used in this study. Information regarding multiplex arrangement, original published primers and fluorescently labelled oligonucleotides used as template for modified forward primers is displayed. The primer volume used to create a multiplex with a total volume of 100 µl (distilled H_2O plus the volumes of the unlabelled and fluorescently labelled primers) is also represented (PVM). The forward and reverse primers were concentrated at 10 µM and 100 µM respectively. This table is adapted from Supplementary Material of Álvarez *et al.* (2015).

Locus	Multiplex	Label*	Primer forward (5' – 3')	Primer reverse (5' – 3')	PVM (µl)
SST-A6-I [2]	S1	NED	TTCAGTGCTCTTGCAGGTTG	AGTCTGCAAGGATAGAAAGATCG	2.0
SST-A6-II [2]	S1	PET	ATTCTCTCTGACAAGGATTGTGG	GGTAGACAGACATCAAGGCAGAC	1.2
SalE14 [1]	S2	VIC	GCTGCCCTCTCTGCCTACTGACCAT	GCCAAGACATGGAACACCCTCCCGC	0.8
Sal29 [1]	S2	6-FAM	CTCTTTGACTGAACCAGAACCCC	GCCTGTCGGCTCTGTGTAACC	8.0
SST-B11 [2]	S3	PET	TCAAACGGTGCCAAAGTTATTAG	TTAATTGGCAGTTTTCTTTCCAG	2.0
SalE12 [1]	S3	VIC	CTCAGGAACAGTGTGCCCCAAATAC	CTCATAATTTAGTCTACCCTCCCAC	0.8
Sal23 [1]	S3	6-FAM	TCACTGTTTATCTTTGTTCTTTTAT	AATTATTTGTTTGAGTCGATTTTCT	9.2
SST-C3 [2]	S4	PET	CCGTTTGAGTCACTTCTTTCTTG	TTGCTTTACCAACCAGTTATTGTC	1.4
SalE7 [1]	S4	NED	TTTCAGCACCAAGATACCTCTTTTG	CTCCCTCCATATCAAGGTCACAGAC	0.8
SalE5 [1]	S4	6-FAM	CCACATGATGCCTACGTATGTTGTG	CTCCTGTTTACGCTTCACCTGCTCC	0.6
SalE2 [1]	S4	VIC	CACGACAAAATACAGAGAGTGGATA	ATATTTGAAATTGCCCATTTGGTA	3.0
SalE06 [1]	S5	VIC	GGACTCATGGTCACCCAGAGGTTCT	ATGGATTGTGTCGAAATAAGGTATC	1.2
Sal3 [1]	S5	6-FAM	CTCAGACAAGAAATCCTGCTTCTTC	ATAAATCTGTCCTGTTCCTAATCAG	1.2
SalE8 [1]	S5	NED	GCAAAGTCCATGCTTTCCCTTTCTC	GACATACCAAAGACTCCAGAATGGG	0.8
SST-G9 [2]	S5	NED	CCTCGTCAGGGGTTGTAGG	CTTTCCAGGAAGAAACTGAGATG	0.8

*An extra number of base pairs were added at the 5' end of the original sequence of forward primers in order to allow binding of four different fluorescent labelled oligonucleotides (6-FAM TGT AAA ACG ACG GCC AGT; VIC TAA TAC GAC TCA CTA TAG GG; NED TTT CCC AGT CAC GAC GTT G; PET GAT AAC AAT TTC ACA CAG G);

[1] Steinfartz *et al.* (2004)

[2] Hendrix *et al.* (2010)

Supplementary Table A3

Table A3 Input parameters in VarEff for each population (Pop). The number of loci (LOC) was 13 except in population MIL (12 loci; see main text). The mutation rate (0.00127) and mutation model (two-phased with proportion of 0.22 for multi-step mutations) were set in all populations. Parameters related to demographic trajectories are shown: the number of times that *Ne* changed in the past (JMAX), maximum distance (in motifs) between alleles (DMAX), correlation between *Ne* among successive intervals (COR), the prior for Ne (Prior *Ne*), and the number of generations since population origin (Prior G), along with respective prior variances for *Ne* (VAR *Ne*) and number of generations (VAR G). The diagonal (D; a smoothing parameter) and acceptance rate (ACP) were set following Nikolic and Chevalet's (2014) recommendations. Runs were carried out using 10000 batches with a length of 10, saved every 200 batches in the MCMC chain and with a burn-in period of 10000 batches.

Pop	LOC	JMAX	DMAX	Prior *Ne*	VAR *Ne*	COR	Prior *G*	VAR *G*	D	ACP
FC	13	4	20	15110	2	0.5	500	2	0.5	0.25
PT	13	4	22	16340	2	0.5	500	2	0.5	0.25
CSF	13	4	24	10430	2	0.5	500	2	0.5	0.25
TEN	13	4	19	17238	2	0.5	500	2	0.5	0.25
ARC	13	4	22	14760	2	0.5	500	2	0.5	0.25
JAR	13	4	21	17844	2	0.5	500	2	0.5	0.25
OTE	13	4	22	11952	2	0.5	500	2	0.5	0.25
IND	13	4	22	10040	2	0.5	500	2	0.5	0.25
MIL	12	4	21	16535	2	0.5	500	2	0.5	0.25
SAC	13	4	24	16228	2	0.5	500	2	0.5	0.25
CAT	13	4	20	13580	2	0.5	500	2	0.5	0.25
MON	13	4	13	10629	2	0.5	500	2	0.5	0.25
LIL	13	4	24	17520	2	0.5	500	2	0.5	0.25
VIL	13	4	22	16535	2	0.5	500	2	0.5	0.25
BEN	13	4	21	16141	2	0.5	500	2	0.5	0.25
TIN	13	4	19	13228	2	0.5	500	2	0.5	0.25

Supplementary Table A4

Table A4 Regression techniques used to model each response variable (R – relatedness; A_R – allelic richness; Ho – observed heterozygosity; DIFF – genetic cluster membership; Ne_SA – *Ne* estimated through the SA method; Ne_LD – *Ne* estimated through the LD method; Ne_mean – average between estimates generated by the SA and LD approaches) against different groups of predictor variables (PS – patch size; TI – time since isolation; MG – bottleneck's magnitude; POST – post-bottleneck time). MLR – multiple linear regression; GLS – generalised least squares; nbGLM – negative binomial generalised linear model

Models	R	A_R	H_O	DIFF	Ne_SA	Ne_LD	Ne_mean
TI+PS	GLS	GLS	MLR	MLR	MLR	nbGLM	nbGLM
TI+MG	GLS	GLS	MLR	MLR	MLR	nbGLM	nbGLM
TI+POST	GLS	GLS	MLR	MLR	MLR	nbGLM	nbGLM
PS+MG	GLS	MLR	MLR	MLR	MLR	nbGLM	nbGLM
PS+POST	GLS	GLS	MLR	MLR	MLR	nbGLM	nbGLM
MG+POST	GLS	GLS	MLR	MLR	MLR	nbGLM	nbGLM

Supplementary Table A5

Table A5 Genotyping errors and deviations from Hardy-Weinberg Equilibrium (HWE) for each locus. The parameters displayed are allele dropout (Ad), false alleles (Fa), mean null alleles frequencies (nf) and respective standard deviation (nf SD) and loci showing deviations from HWE in more than two populations (DHW). Markers with high null alleles frequencies are in bold (nf > 0.05).

Locus	Ad	Fa	nf	nf SD	DHW
SST-A6-II	0	0	**0.076**	0.051	No
SalE14	0	0	0.023	0.019	No
SST-A6-I	0	0	0.028	0.018	No
Sal29	0	0	**0.070**	0.049	No
SST-B11	0	0	0.043	0.043	No
SalE12	0	0	0.023	0.021	No
Sal23	0	0	**0.087**	0.065	No
SST-C3	0.032	0	**0.164**	0.099	Yes
SalE7	0	0	0.024	0.021	No
SalE5	0	0	0.028	0.020	No
SalE2	0	0	**0.072**	0.106	No
SalE06	0	0	**0.160**	0.163	Yes
Sal3	0	0	0.036	0.028	No
SalE8	0	0	0.025	0.020	No
SST-G9	0	0	0.026	0.017	No

Supplementary Table A6

Table A6 Relatedness (R) estimates obtained in COANCESTRY when accounting for genotyping errors (R-E), inbreeding (R-I) and both parameters (R-EI). The 95% CIs are in parentheses.

Population	R-E	R-I	R-EI
FC	0.103 (0.024-0.348)	0.145 (0.041-0.431)	0.154 (0.044-0.456)
PT	0.106 (0.016-0.408)	0.164 (0.030-0.502)	0.175 (0.037-0.521)
CSF	0.241 (0.088-0.522)	0.295 (0.132-0.608)	0.309 (0.141-0.630)
TEN	0.137 (0.034-0.398)	0.172 (0.050-0.463)	0.182 (0.054-0.484)
ARC	0.153 (0.033-0.419)	0.200 (0.062-0.493)	0.214 (0.069-0.512)
JAR	0.145 (0.025-0.450)	0.194 (0.054-0.545)	0.206 (0.058-0.566)
OTE	0.150 (0.047-0.418)	0.184 (0.063-0.489)	0.198 (0.069-0.511)
IND	0.143 (0.043-0.446)	0.210 (0.075-0.534)	0.224 (0.081-0.549)
MIL	0.286 (0.132-0.559)	0.334 (0.180-0.611)	0.351 (0.191-0.631)
SAC	0.134 (0.034-0.398)	0.176 (0.053-0.471)	0.186 (0.059-0.486)
CAT	0.126 (0.040-0.380)	0.168 (0.058-0.459)	0.181 (0.063-0.482)
MON	0.308 (0.132-0.590)	0.358 (0.188-0.666)	0.370 (0.194-0.677)
LIL	0.085 (0.016-0.340)	0.112 (0.025-0.415)	0.127 (0.028-0.443)
VIL	0.207 (0.058-0.471)	0.249 (0.092-0.539)	0.271 (0.107-0.573)
BEN	0.083 (0.006-0.361)	0.123 (0.015-0.439)	0.133 (0.018-0.461)
TIN	0.216 (0.077-0.464)	0.250 (0.110-0.523)	0.271 (0.128-0.561)

Supplementary Table A7

Table A7 Standard population genetic statistics from the 16 studied populations of fire salamanders, estimated using 13 loci: N_A – mean number of alleles per locus; P_A – number of private alleles; N_{PA} – number of individuals with private alleles; H_O – observed heterozygosity; H_E – expected heterozygosity; A_R – allelic richness; R – mean relatedness and respective 95%CIs in parentheses.

Population	N_A	P_A	N_{PA}	H_O	H_E	A_R	R
FC	8.6	7	12	0.714	0.760	3.52	0.094 (0.020 – 0.315)
PT	7.8	5	5	0.694	0.760	3.77	0.082 (0.013 – 0.375)
CSF	5.0	2	3	0.669	0.658	2.89	0.240 (0.088 – 0.536)
TEN	7.2	1	1	0.772	0.765	4.33	0.120 (0.024 – 0.376)
ARC	6.8	1	1	0.674	0.700	4.00	0.141 (0.028 – 0.411)
JAR	7.3	0	0	0.647	0.712	3.34	0.138 (0.019 – 0.446)
OTE	7.1	3	4	0.745	0.743	3.50	0.142 (0.040 – 0.414)
IND	6.6	0	0	0.689	0.724	3.64	0.135 (0.037 – 0.426)
MIL	4.6	1	1	0.686	0.641	3.33	0.274 (0.118 – 0.545)
SAC	6.6	4	9	0.708	0.724	3.95	0.125 (0.025 – 0.389)
CAT	7.6	4	4	0.712	0.735	3.78	0.113 (0.031 – 0.354)
MON	4.8	3	16	0.678	0.648	2.89	0.299 (0.124 – 0.583)
LIL	8.5	5	3	0.749	0.780	4.46	0.072 (0.013 – 0.313)
VIL	7.1	3	10	0.727	0.731	4.40	0.151 (0.029 – 0.395)
BEN	7.7	1	1	0.754	0.777	4.87	0.073 (0.004 – 0.338)
TIN	6.8	5	7	0.708	0.739	4.88	0.179 (0.060 – 0.402)

Supplementary Table A8

Table A8 *Ne* estimates and respective 95% CIs (in parentheses) obtained through the SA method when accounting for inbreeding (*Ne* I), genotyping errors (*Ne* E) and both parameters (*Ne* I+E).

Population	*Ne* I	*Ne* E	*Ne* I+E
FC	60 (37-104)	41 (25-73)	42 (25-72)
PT	58 (32-132)	45 (26-110)	45 (25-96)
CSF	23 (13-50)	19 (10-42)	20 (11-43)
TEN	36 (20-69)	33 (19-63)	36 (20-71)
ARC	45 (25-97)	33 (19-72)	35 (19-74)
JAR	65 (37-154)	42 (25-81)	49 (27-97)
OTE	27 (15-55)	22 (13-47)	26 (15-53)
IND	34 (19-73)	23 (12-47)	27 (14-58)
MIL	18 (10-39)	21 (11-45)	21 (11-45)
SAC	38 (21-80)	33 (18-67)	36 (20-74)
CAT	39 (22-75)	29 (16-58)	29 (17-58)
MON	26 (15-50)	19 (10-38)	17 (9-38)
LIL	68 (37-184)	53 (28-120)	68 (36-196)
VIL	109 (53-1001)	109 (50-1259)	109 (50-1259)
BEN	140 (55-Inf)	140 (53-Inf)	140 (55-Inf)
TIN	44 (19-3492)	21 (10-54)	21 (10-52)

Supplementary Table A9

Table A9 *Ne* estimates obtained with 13 loci based on two methods (Linkage Disequilibrium, LD; Sibship Assignment, SA) and their mean (*Ne* mean) with respective 95% CIs in parenthesis. The results of the SA analysis were generated with a model excluding inbreeding and genotyping errors.

Population	*Ne* LD	*Ne* SA	*Ne* mean
FC	35 (26 - 51)	45 (29 - 82)	40 (28 – 67)
PT	198 (31 - Inf)	48 (28 - 104)	123 (30 – Inf)
CSF	18 (9 - 56)	20 (11 - 42)	19 (10 – 49)
TEN	26 (17 - 44)	36 (21 - 74)	31 (19 – 59)
ARC	102 (38 - Inf)	32 (17 - 66)	67 (28 – Inf)
JAR	127 (34 - Inf)	44 (26 - 90)	86 (30 – Inf)
OTE	14 (9 - 24)	22 (12 - 43)	18 (10 – 34)
IND	22 (14 - 44)	26 (15 - 53)	24 (14 – 48)
MIL	10 (6 - 17)	19 (10 - 38)	14 (8 -28)
SAC	36 (21 - 89)	31 (18 - 64)	34 (20 – 76)
CAT	13 (11 - 17)	27 (15 - 64)	20 (13 – 40)
MON	10 (6 - 18)	19 (10 - 41)	14 (8 – 30)
LIL	30 (20 - 55)	36 (20 - 71)	33 (20 – 63)
VIL	Inf (168 - Inf)	68 (35 - 190)	Inf (102 – Inf)
BEN	Inf (107 - Inf)	70 (35 - 341)	Inf (71 – Inf)
TIN	16 (11 - 27)	28 (14 - 97)	22 (12 – 62)

Supplementary Table A10

Table S10 Values of the magnitude of demographic decline (MG) and post-bottleneck time (POST) calculated in VarEff are displayed for 13 loci and 11 loci. Population TIN was demographically stable throughout time. NA – not applicable

Population	13 loci		11 loci	
	MG	POST	MG	POST
FC	302.1	50	57.2	210
PT	881.1	90	696.4	80
CSF	348.9	110	307.6	110
TEN	529.9	70	486.5	80
ARC	1516.0	30	680.0	70
JAR	372.7	70	358.7	90
OTE	1007.5	80	884.3	90
IND	250.6	30	126.0	40
MIL	101.9	130	1.2	50
SAC	273.2	180	284.7	160
CAT	168.0	490	340.7	490
MON	400.4	450	142.7	300
LIL	767.2	50	168.7	490
VIL	670.3	30	1895.5	70
BEN	240.6	130	216.2	110
TIN	NA	NA	NA	NA

Supplementary Table A11

Table A11 Matrix of pairwise genetic differentiation between populations calculated from 13 loci. Below and above the diagonal are pairwise F_{ST} and Jost's D_{EST}, respectively. Significant pairwise values are in bold.

Pop	FC	PT	CSF	TEN	ARC	JAR	OTE	IND	MIL	SAC	CAT	MON	LIL	VIL	BEN	TIN
FC	0	0.037	**0.228**	0.054	0.072	0.113	**0.203**	**0.323**	**0.357**	**0.298**	0.125	**0.341**	0.117	**0.271**	0.118	**0.334**
PT	0.016	0	**0.185**	0.057	0.106	0.090	**0.243**	0.143	**0.386**	**0.201**	0.061	**0.214**	0.110	**0.362**	0.040	**0.276**
CSF	**0.117**	**0.101**	0	**0.220**	**0.251**	0.128	**0.199**	**0.188**	**0.442**	**0.292**	**0.228**	**0.405**	**0.151**	**0.326**	**0.215**	**0.380**
TEN	**0.054**	0.042	**0.092**	0	0.106	0.083	**0.174**	**0.175**	**0.293**	0.119	0.097	**0.221**	0.045	**0.203**	0.125	**0.234**
ARC	**0.057**	0.057	**0.121**	**0.072**	0	0.057	**0.229**	**0.174**	**0.214**	**0.183**	0.091	**0.285**	0.064	**0.191**	0.097	**0.383**
JAR	**0.070**	0.046	0.063	0.037	0.046	0	**0.276**	**0.148**	**0.256**	**0.171**	0.082	**0.358**	0.019	**0.187**	0.040	**0.363**
OTE	**0.096**	**0.092**	**0.124**	**0.099**	**0.107**	**0.109**	0	**0.194**	**0.351**	**0.263**	**0.217**	**0.303**	**0.143**	**0.308**	**0.233**	**0.198**
IND	**0.113**	0.056	**0.118**	**0.081**	**0.092**	**0.069**	**0.103**	0	**0.320**	**0.126**	**0.138**	**0.380**	0.129	**0.318**	**0.270**	**0.290**
MIL	**0.132**	**0.130**	**0.185**	**0.137**	**0.106**	**0.111**	**0.153**	**0.159**	0	**0.288**	**0.252**	**0.296**	**0.352**	**0.295**	**0.364**	**0.488**
SAC	**0.108**	**0.075**	**0.124**	**0.076**	**0.084**	0.057	**0.115**	**0.076**	**0.128**	0	0.122	**0.261**	0.065	**0.287**	**0.169**	**0.364**
CAT	**0.059**	0.047	**0.096**	**0.058**	0.052	0.034	**0.102**	**0.069**	**0.100**	**0.065**	0	**0.314**	0.074	**0.198**	0.094	**0.317**
MON	**0.137**	**0.103**	**0.215**	**0.145**	**0.149**	**0.141**	**0.168**	**0.183**	**0.181**	**0.144**	**0.150**	0	**0.267**	**0.445**	**0.387**	**0.410**
LIL	0.048	0.040	**0.065**	0.033	0.040	0.009	**0.058**	**0.060**	**0.115**	0.029	0.040	**0.111**	0	**0.131**	0.045	**0.260**
VIL	**0.092**	**0.104**	**0.146**	**0.099**	**0.086**	**0.082**	**0.126**	**0.136**	**0.124**	**0.121**	**0.097**	**0.186**	**0.059**	0	**0.269**	**0.484**
BEN	**0.059**	0.044	**0.116**	**0.068**	**0.062**	0.047	**0.110**	**0.116**	**0.130**	**0.081**	**0.063**	**0.146**	0.033	**0.090**	0	**0.230**
TIN	**0.109**	**0.105**	**0.157**	**0.100**	**0.140**	**0.102**	**0.112**	**0.121**	**0.192**	**0.140**	**0.118**	**0.174**	**0.079**	**0.156**	**0.085**	0

Supplementary Table A12

Table A12 Top-ranked models (TRM) from the six tested candidate models (in bold and underlined) that were within a 95% confidence interval and ranked according to Akaike weight (w_i) are shown, along with the difference in Akaike Information Criterion (ΔAICc) corrected for small sample sizes for genetic diversity and differentiation response variables (R – relatedness; A_R – allelic richness; H_O – observed heterozygosity; DIFF – genetic cluster membership). A total of four predictors are represented (PS – patch size; TI – time since isolation; MG – bottleneck's magnitude; POST – post-bottleneck time). NULL – null model

Candidate models	R			A_R			H_O			DIFF		
	TRM	ΔAICc	w_i	TRM	ΔAICc	w_i	TRM	ΔAICc	w_i	TRM	ΔAICc	w_i
TI+PS												
	NULL	0	0.96	NULL	0	0.77	NULL	0	0.50	NULL	0	0.69
				TI	3.59	0.13	PS	1.16	0.28	TI	2.64	0.18
TI+MG												
	NULL	0	0.96	NULL	0	0.60	NULL	0	0.59	NULL	0	0.68
				TI	1.12	0.34	TI	2.21	0.20	TI	2.64	0.18
TI+POST												
	NULL	0	0.98	NULL	0	0.80	NULL	0	0.64	NULL	0	0.63
				TI	3.85	0.12	TI	2.21	0.21	TI	2.43	0.19
PS+MG												
	NULL	0	0.97	NULL	0	0.63	NULL	0	0.52	NULL	0	0.74
				MG	2.17	0.21	PS	1.16	0.29	MG	3.53	0.13
PS+POST												
	NULL	0	0.95	NULL	0	0.78	NULL	0	0.55	NULL	0	0.67
				POST	3.79	0.12	PS	1.16	0.31	POST	2.43	0.20
MG+POST												
	NULL	0	0.98	NULL	0	0.78	NULL	0	0.65	NULL	0	0.67
				POST	3.31	0.15	MG	2.31	0.20	POST	2.43	0.20

Supplementary Table A13

Table A13 Top-ranked models (TRM) from the six tested candidate models (in bold and underlined) that were within a 95% confidence interval and ranked according to Akaike weight (w_i) are shown, along with the difference in Akaike Information Criterion (ΔAICc) corrected for small sample sizes for contemporary *Ne* response variables (Ne_SA - *Ne* estimated through SA method; Ne_LD - *Ne* estimated through LD method; Ne_mean - average between estimates generated by SA and LD approaches). A total of four predictors are represented (PS – patch size; TI – time since isolation; MG – bottleneck's magnitude; POST – post-bottleneck time). NULL – null model

Candidate models	Ne_SA			Ne_LD			Ne_mean		
	TRM	**ΔAICc**	w_i	**TRM**	**ΔAICc**	w_i	**TRM**	**ΔAICc**	w_i
TI+PS									
	NULL	0	0.54	PS	0	0.84	PS	0	0.82
	PS	1.47	0.26				TI+PS	3.75	0.13
TI+MG									
	NULL	0	0.64	NULL	0	0.61	NULL	0	0.78
	TI	2.43	0.19	TI	2.34	0.19	MG	2.56	0.22
TI+POST									
	NULL	0	0.57	NULL	0	0.57	NULL	0	0.54
	POST	1.79	0.23	POST	0.54	0.43	POST	1.23	0.29
PS+MG									
	NULL	0	0.57	PS	0	0.89	PS	0	0.86
	PS	1.47	0.27				PS+MG	4.54	0.09
PS+POST									
	NULL	0	0.50	PS	0	0.70	PS	0	0.74
	PS	1.47	0.40				PS+POST	2.56	0.20
MG+POST									
	NULL	0	0.59	NULL	0	0.57	NULL		0.53
	POST	1.79	0.24	POST	0.54	0.43	POST	1.23	0.29

Supplementary Table A14

Table A14 Regression modelling results for models containing metrics descriptive of genetic diversity and differentiation as response variables (A_R – allelic richness; H_O – observed heterozygosity; DIFF – genetic cluster membership). Regression parameters were obtained by model averaging for each response variable. The following regression parameters are represented: regression coefficients (β), standard errors (SE), 95% CIs of β and variable relative importance (w_+). Intercept (null model) estimates are not shown and models exhibiting response variables significantly related with a predictor are underlined. Relatedness is not represented because only the null model was supported (see **Table A12 in Appendix A**). Predictor variables used were: time since isolation (TI), patch size (PS), bottleneck magnitude (MG) and post-bottleneck time (POST).

Model	β	SE	95%CI	w_+
A_R ~ TI+PS				
TI	-0.052	0.152	(-0.852, 0.123)	0.14
A_R ~ TI+MG				
TI	-0.164	0.242	(-0.845, -0.057)	0.36
A_R ~ TI+POST				
TI	-0.047	0.157	(-0.982; 0.246)	0.13
A_R ~ PS+MG				
MG	0.063	0.154	(-0.234, 0.734)	0.25
A_R ~ PS+POST				
POST	5.406	0.162	(-0.766, 0.141)	0.13
A_R ~ MG+POST				
POST	-0.051	0.136	(-0.706, 0.073)	0.16
H_O ~ TI+PS				
PS	0.005	0.009	(-0.007, 0.037)	0.36
H_O ~ TI+MG				
TI	-0.003	0.007	(-0.035, 0.011)	0.25
H_O ~ TI+POST				
TI	-0.003	0.007	(-0.035, 0.011)	0.25
H_O ~ PS+MG				
PS	0.015	0.010	(-0.007, 0.037)	0.36
H_O ~ PS+POST				
PS	0.005	0.009	(-0.007, 0.037)	0.36
H_O ~ MG+POST				
MG	0.003	0.007	(-0.012; 0.034)	0.24

Table A14 Continued.

Model	β	SE	95%CI	w_+
DIFF ~ TI+PS				
TI	-0.008	0.024	(-0.051, 0.126)	0.21
DIFF ~ TI+MG				
TI	0.008	0.24	(-0.051, 0.126)	0.21
DIFF ~ TI+POST				
POST	0.009	0.025	(-0.046, 0.128)	0.23
DIFF ~ PS+MG				
MG	-0.002	0.016	(-0.106, 0.077)	0.15
DIFF ~ PS+POST				
POST	0.009	0.025	(-0.046, 0.128)	0.23
DIFF ~ MG+POST				
POST	0.009	0.025	(-0.046, 0.128)	0.23

Supplementary Table A15

Table A15 Regression modelling results for models containing metrics descriptive of contemporary *Ne* as response variables (Ne_SA – *Ne* estimated through SA method; Ne_LD – *Ne* estimated through LD method; Ne_mean – average between estimates generated by SA and LD approaches). Regression parameters were obtained by model averaging for each response variable. The following regression parameters are represented: regression coefficients (β), standard errors (SE), 95% CIs of β and variable relative importance (w_+). Intercept (null model) estimates are not shown and models exhibiting response variables significantly related with a predictor are underlined. Predictor variables used were: time since isolation (TI), patch size (PS), bottleneck magnitude (MG) and post-bottleneck time (POST).

Model	β	SE	95%CI	w_+
Ne_SA ~ TI+PS				
PS	1.953	3.716	(-3.448, 15.500)	0.32
Ne_SA ~ TI+MG				
TI	-1.056	2.870	(-14.473, 5.247)	0.23
Ne_SA ~ TI+POST				
POST	-1.627	3.444	(-15.208, 3.994)	0.29
Ne_SA ~ PS+MG				
PS	1.953	3.716	(-3.448, 15.500)	0.32
Ne_SA ~ PS+POST				
PS	1.530	3.387	(-3.448, 15.500)	0.25
POST	-1.214	3.058	(-15.208, 3.994)	0.22
Ne_SA ~ MG+POST				
POST	-1.627	3.444	(-15.208, 3.994)	0.29
Ne_LD ~ TI+PS				
PS	1.049	0.264	(0.590, 1.516)	0.84
Ne_LD ~ TI+MG				
TI	-0.167	0.351	(-1.545, 0.139)	0.24
Ne_LD ~ TI+POST				
POST	-0.412	0.528	(-1.754, -0.151)	0.43
Ne_LD ~ PS+MG				
PS	1.080	0.334	(0.553, 1.644)	0.89
Ne_LD ~ PS+POST				
PS	1.021	0.250	(0.574, 1.468)	0.70
Ne_LD ~ MG+POST				
POST	-0.412	0.528	(-1.754, -0.151)	0.43

Table A15 Continued.

Model	β	SE	95%CI	w_+
Ne_mean ~ TI+PS				
TI	-0.028	0.105	(-0.684, 0.255)	0.13
PS	0.707	0.210	(0.239, 1.176)	1.00
Ne_mean ~ TI+MG				
MG	0.388	2.282	(-0.240, 1.016)	0.22
Ne_mean ~ TI+POST				
POST	-0.192	0.307	(-1.153, 0.057)	0.35
Ne_mean ~ PS+MG				
PS	0.712	0.216	(0.230, 1.194)	1.00
MG	-0.125	0.256	(-0.704, 0.454)	0.09
Ne_mean ~ PS+POST				
PS	0.703	0.208	(0.238, 1.168)	1.00
POST	-0.069	0.161	(-0.772, 0.135)	0.22
Ne_mean ~ MG+POST				
POST	-1.153	0.057	(-1.153, 0.057)	0.35

Supplementary Table A16

Table A16 Regression modelling results for models exhibiting genetic response variables, calculated using 13 loci, significantly related with a predictor (underlined). Regression parameters were obtained by model averaging for each response variable. The following regression parameters are represented: regression coefficients (β), standard errors (SE), 95% CIs of β and variable relative importance (w_+). Intercept (null model) estimates are not shown. Predictor variables used were: time since isolation (TI), patch size (PS), bottleneck magnitude (MG) and post-bottleneck time (POST). The latter two predictors were estimated in VarEff using 11 loci.

Model	β	SE	95%CI	w_+
Ne_LD ~ TI+PS				
TI	-0.041	0.127	(-0.746, 0.216)	0.15
PS	0.677	0.216	(0.194, 1.160)	1.00
Ne_LD ~ TI+MG				
TI	-0.102	0.228	(-1.023, 0.020)	0.20
MG	0.429	0.367	(0.062, 1.217)	0.67
Ne_LD ~ PS+MG				
PS	0.593	0.292	(0.165, 1.158)	0.90
MG	0.106	0.237	(-0.176, 1.079)	0.24
Ne_LD ~ PS+POST				
PS	0.675	0.218	(0.188, 1.162)	1.00
POST	-0.016	0.086	(-0.664, 0.347)	0.10
Ne_LD ~ MG+POST				
MG	0.300	0.360	(0.033, 1.206)	0.48
POST	-0.097	0.239	(-1.159, 0.046)	0.17
Ne_mean ~ TI+PS				
TI	-0.030	0.092	(-0.542, 0.164)	0.16
PS	0.465	0.158	(0.111, 0.819)	1.00
Ne_mean ~ PS+MG				
PS	0.403	0.213	(0.097, 0.820)	0.88
MG	0.021	0.082	(-0.204, 0.578)	0.11
Ne_mean ~ PS+POST				
PS	0.404	0.218	(0.112, 0.822)	0.86

Supplementary Table A17

Table A17 Regression modelling results for models exhibiting genetic response variables significantly related with a predictor (underlined) using a dataset without population CAT. Regression parameters were obtained by model averaging for each response variable. The following regression parameters are represented: regression coefficients (β), standard errors (SE), 95% CIs of β and variable relative importance (w_+). Intercept (null model) estimates are not shown. Predictor variables used were: time since isolation (TI), patch size (PS), bottleneck magnitude (MG) and post-bottleneck time (POST).

Model	β	SE	95%CI	w_+
A_R ~ TI+POST				
POST	-0.323	0.270	(-0.907, -0.031)	0.69
A_R ~ PS+POST				
PS	0.187	0.195	(-0.263, 0.636)	0.08
POST	-0.467	0.194	(-0.906, -0.028)	0.72
A_R ~ MG+POST				
MG	0.049	0.147	(-0.152, 0.845)	0.14
POST	-0.277	0.274	(-0.907, -0.031)	0.59
DIFF ~ TI+POST				
TI	0.074	0.036	(-0.006, 0.154)	0.36
POST	0.081	0.034	(0.004, 0.158)	0.64
DIFF ~ PS+POST				
POST	0.055	0.047	(0.004, 0.158)	0.68
DIFF ~ MG+POST				
POST	0.055	0.047	(0.004, 0.158)	0.68
Ne_LD ~ TI+PS				
PS	1.072	0.284	(0.573, 1.577)	0.88
Ne_LD ~ PS+MG				
PS	1.131	0.348	(0.563, 1.747)	0.88
Ne_LD ~ PS+POST				
PS	1.060	0.268	(0.580, 1.541)	0.79
Ne_mean ~ TI+PS				
PS	0.644	0.302	(0.200, 1.227)	0.90
Ne_mean ~ PS+MG				
PS	0.644	0.302	(0.200, 1.227)	0.90
Ne_mean ~ PS+POST				
PS	0.714	0.225	(0.204, 1.224)	1.00
POST	-0.052	0.147	(-0.825, 0.162)	0.16

Supplementary Figure A1

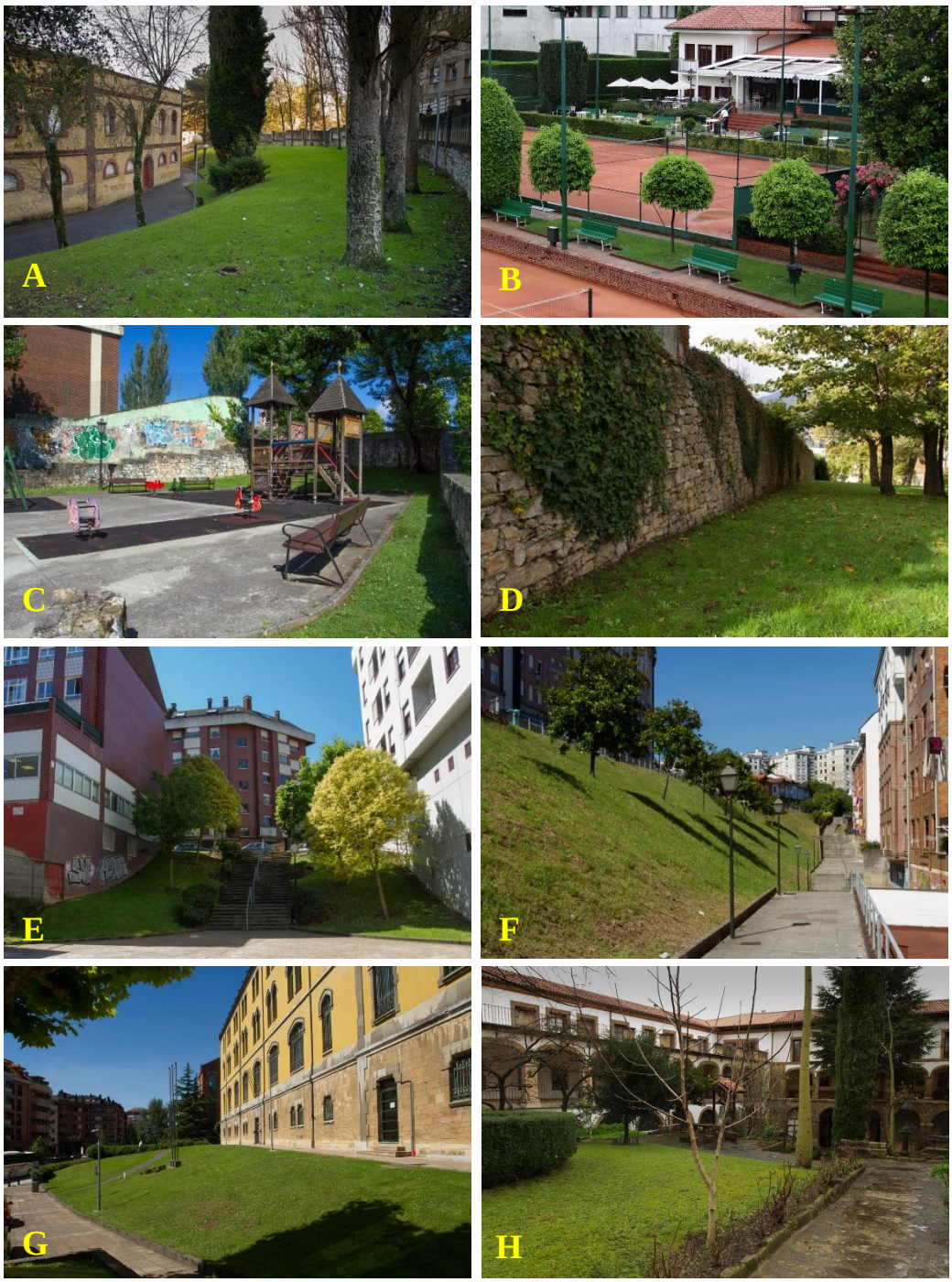

Fig. A1 Photographs showing the habitat from sampled localities in Oviedo. (A – PT; B – TEN; C – ARC; D – JAR; E – OTE; F – IND; G – MIL; H – MON).

Supplementary Figure A2

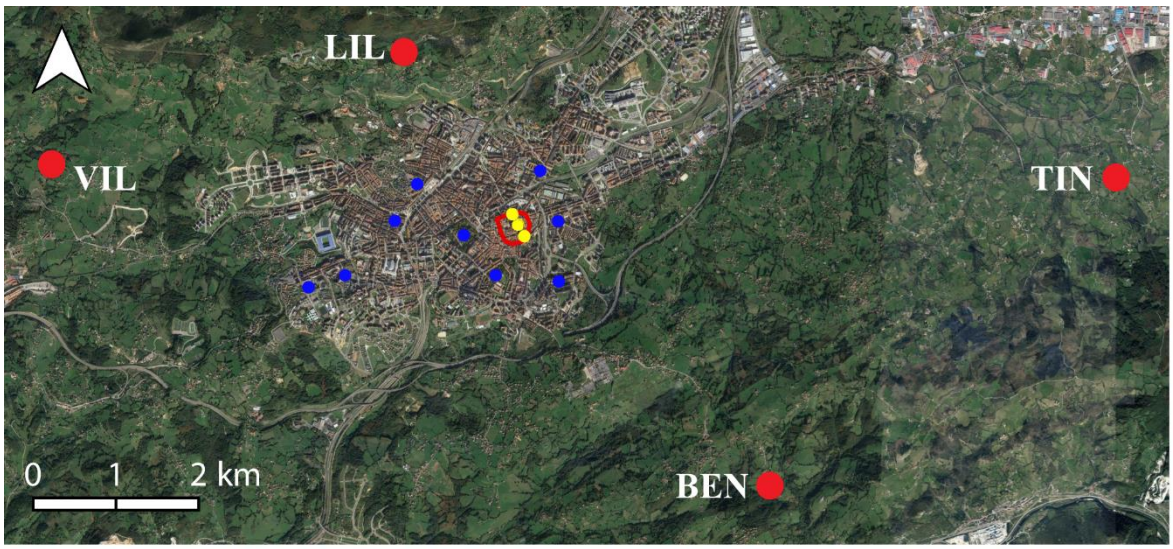

Fig. A2 Aerial photograph of the study area. Points denote the location of the 16 sampled populations. Yellow circles correspond to urban populations located inside walls (red line) while blue circles illustrate urban populations sampled outside walls. Red circles labelled with the respective population code represent rural populations sampled outside Oviedo. See Figure 3.2 in Chapter 3 for more details.

Supplementary Figure A3

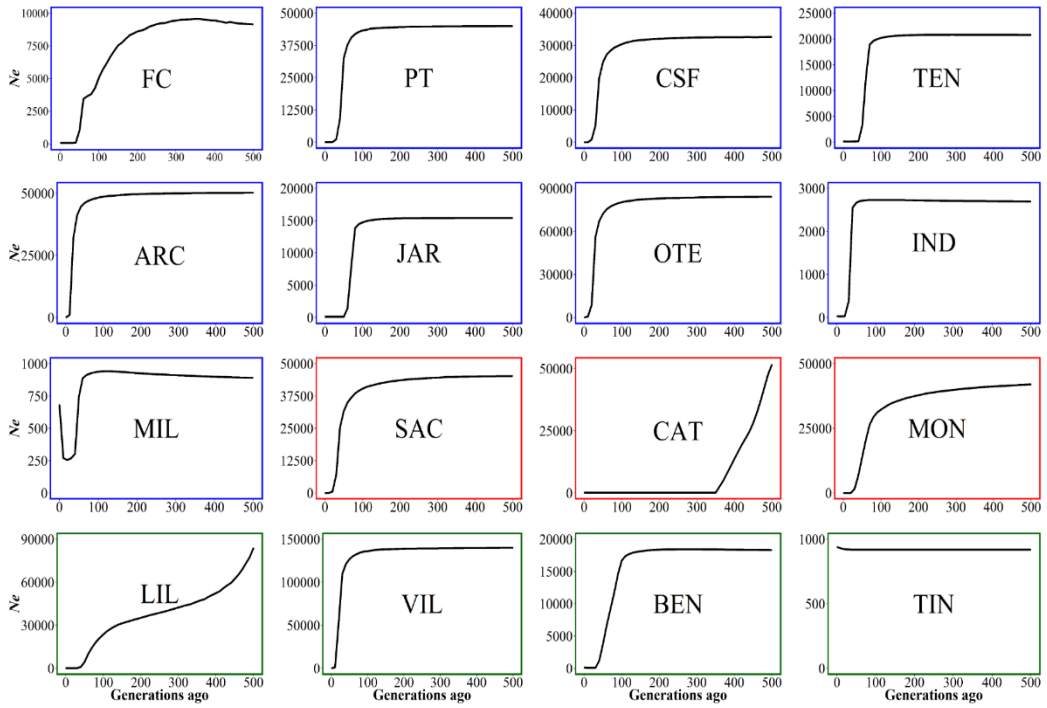

Fig. A3 *Ne* trajectories from present (0) to 500 generations ago for the 16 populations analysed in VarEff using 11 loci. Different colours in plots' borders represent the relative location of the population (blue – OW; red – IW; green – OC). Note that the y axis (*Ne*) has a different scale in each plot.

Supplementary Figure A4

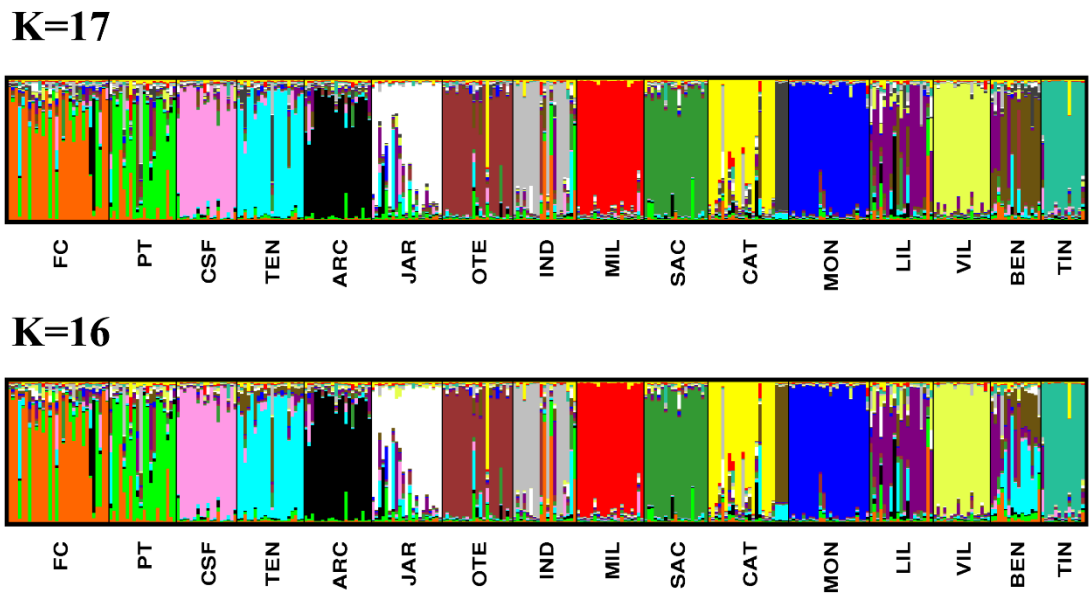

Fig. A4 STRUCTURE barplots of individual genetic assignment estimates using 15 loci. The top barplot shows the best K according to the MLPP method (K=17), while the bottom barplot represents the most supported K according to the ΔK approach (K=16).

Supplementary Figure A5

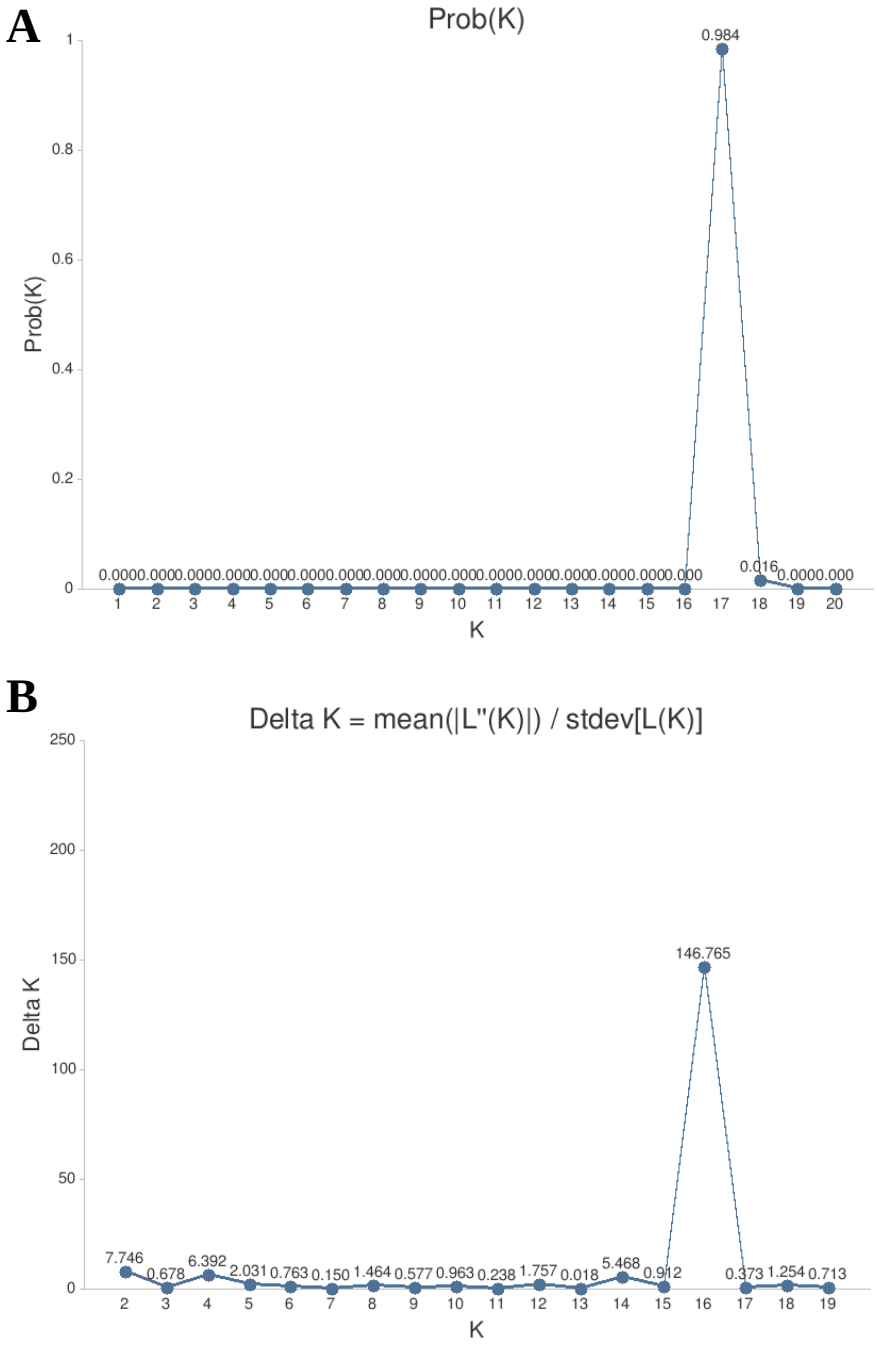

Fig. A5 Plots showing the best number of clusters according to two distinct approaches using 15 loci. A - plot of the mean logarithmic posterior probability (K=17); B – plot of the ΔK (K=16).

Supplementary Figure A6

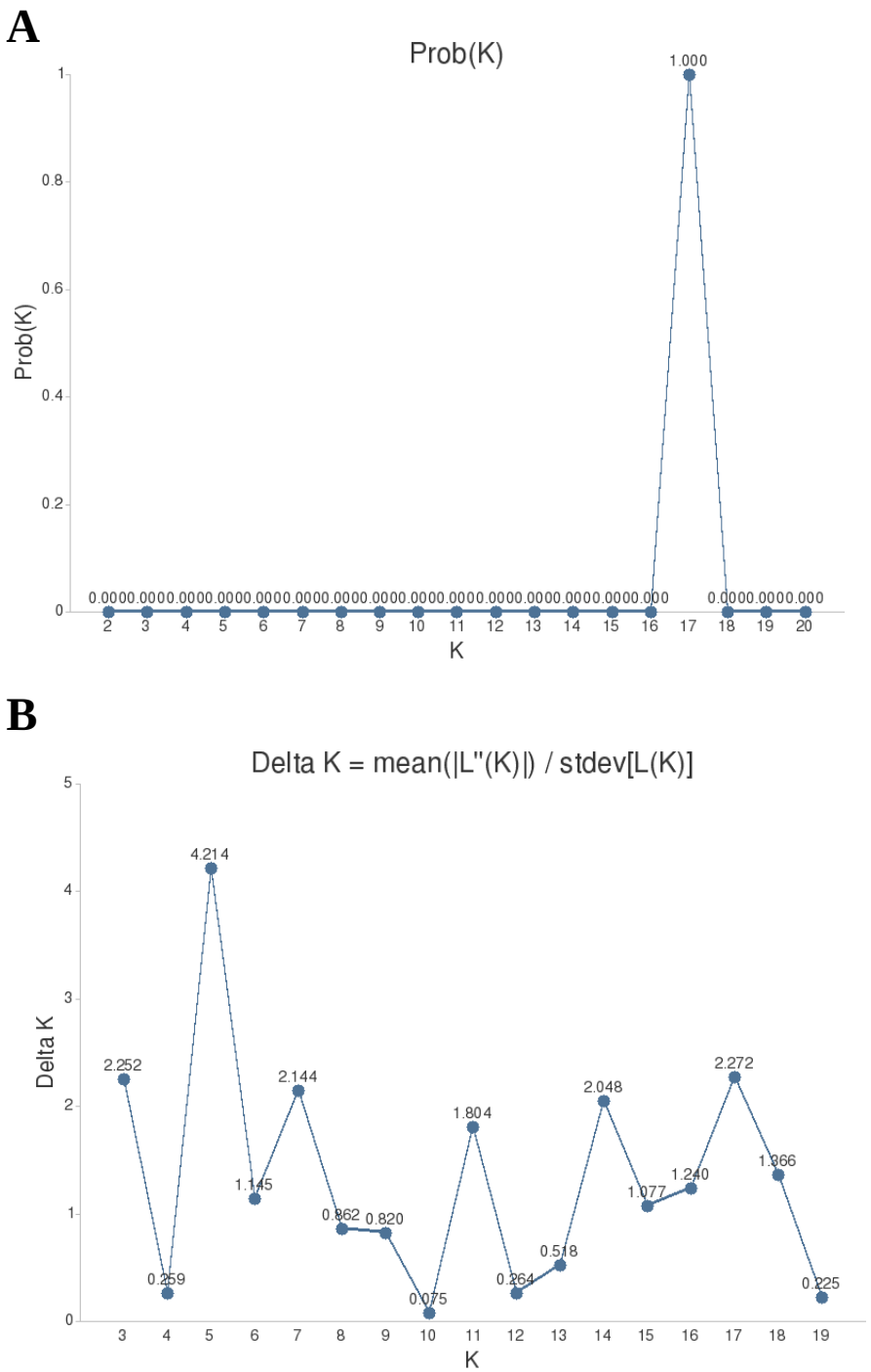

Fig. A6 Plots showing the best number of clusters according to two distinct approaches using 13 loci. A - plot of the mean logarithmic posterior probability (K=17); B – plot of the ΔK (K=5).

Supplementary Figure A7

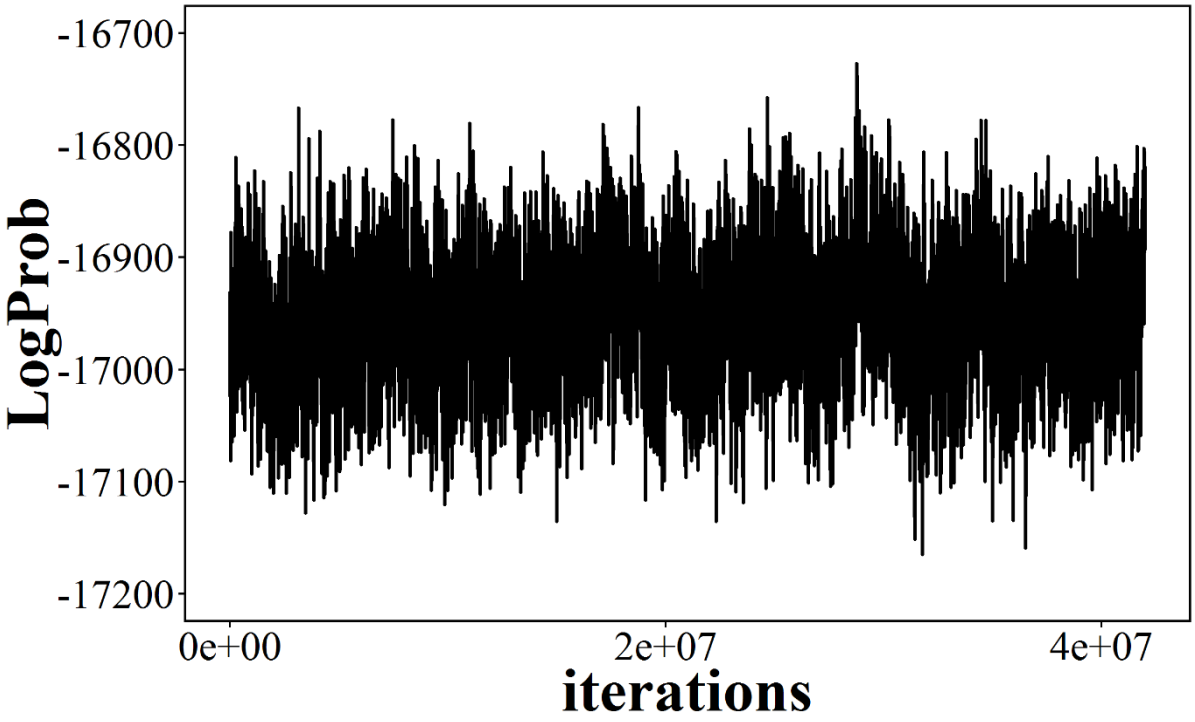

Fig. A7 Plot showing the combined MCMC chains (discarding burn-in iterations) from the three runs from BAYESASS. The plot clearly shows that the total log-likelihood (y axis) is stationary throughout the MCMC iterations (x axis).

References of Appendix A

Álvarez D, Lourenço A, Oro D, Velo-Antón G (2015) Assessment of census (*N*) and effective population size (*Ne*) reveals consistency of *Ne* single-sample estimators and a high *Ne/N* ratio in an urban and isolated population of fire salamanders. *Conservation Genetics Resources*, **7**, 705–712.

Chachero J, Álvarez D (2016) *The last urban dragons*. [DVD] Documentazul Producciones Audiovisuales S. L., Oviedo, Spain. Available at: http://www.documentazul.com/info/dvd-los-ultimos-dragones-de-oviedo-contacto

Hendrix R, Hauswaldt JS, Veith M, Steinfartz S (2010) Strong correlation between cross-amplification success and genetic distance across all members of 'True salamanders' (Amphibia: Salamandridae) revealed by *Salamandra salamandra*-specific microsatellite loci. *Molecular Ecology Resources*, **10**, 1038–1047.

Nikolic N, Chevalet C (2014) Detecting past changes of effective population size. *Evolutionary Applications*, **7**, 663–681.

Steinfartz S, Kuesters D, Tautz D (2004) Isolation and characterization of polymorphic tetranucleotide microsatellite loci in the fire salamander *Salamandra salamandra* (Amphibia: Caudata). *Molecular Ecology Notes*, **4**, 626–628.

Zuur AF, Ieno EN, Walker NJ, Saveliev AA, Smith GM (2009) *Mixed effects models and extensions in ecology*. Springer, New York.

Appendix B

Supplementary Text B1

Each PCR reaction contained a total volume of 10-11 µl: 5 µl of Multiplex PCR Kit Master Mix (QIAGEN), 3 µl of distilled water, 1 µl of primer multiplex mix and 1–2 µl of DNA extract (~50 ng/µl). To identify possible contaminations, a negative control was employed. PCR touchdown cycling conditions were equal in all multiplexes: the reaction started with an initial step at 95 ºC for 15 min, 19 cycles at 95 ºC for 30 s, 90 s of annealing at 65 ºC (decreasing 0.5 ºC each cycle), 72 ºC for 40 s, followed by 25 cycles of 95 ºC for 30 s, 56 ºC for 60 s, 72 ºC for 40 s, and ended with a final extension of 30 min at 60 ºC.

Prior to allele scoring in GENEMAPPER, allele fragment length binning was performed on a set of tissue samples of very high quality (ca. 50 samples) collected across northern Spain. The DNA Size Standard LIZ 500 DSMO-100 (MCLAB) was employed to determine the relative size of fragments. Following binning procedures, genotypes were checked and corrected by two persons to avoid potential erroneous scoring of alleles. Additionally, to reduce the potential influence of allele dropout and false alleles, we scored only alleles exhibiting clear fluorescence peaks higher than 100 relative fluorescent units. Microsatellite markers that failed to amplify or exhibited dubious allelic profiles (e.g. with high prevalence of peak artefacts) in samples containing more than 25% of missing data were reamplified in uniplex reactions (i.e. for a single microsatellite locus) to increase the likelihood of amplification. Each uniplex PCR contained a total volume of 10-11 µl: 5 µl of Multiplex PCR Kit Master Mix (QIAGEN), 2.8 µl of distilled water, 0.4 µl of forward primer (1 µM), 0.4 µl of reverse primer (10 µM), 0.4 µl of the respective fluorescently labelled oligonucleotides (10 µM; see **Supplementary Table B1**), and 1–2 µl of DNA extract. Cycling conditions are the same as those described for multiplexes.

Supplementary Text B2

The two geographic distance matrices obtained in locality EUME_Larv were subjected to additional pre-treatment procedures. This is because not all individuals along the transect were sampled in a straight path, particularly the westernmost individuals (**Figure 3.2**). Since a river that may comprise a barrier to dispersal is located adjacently to sampled individuals, the pairwise Euclidean distances involving these westernmost individuals are likely underestimated. To circumvent this issue, we digitized a shapefile adjacent to the river in QGIS (QGIS Development Team 2017). Then, we employed the R package *gdistance* (van Etten 2017) to rasterize the shapefile and calculate a pairwise “least-cost” distance that accounted for the river as a barrier to dispersal involving those individuals and remaining sampled individuals.

Supplementary Table B1

Table B1 Details of the 14 microsatellites used in this study. Information regarding multiplex arrangement, original published primers and fluorescently labelled oligonucleotides used as template for modified forward primers is displayed. The primer volume used to create a multiplex with a total volume of 100 µl (distilled H_2O plus the volumes of the unlabelled and fluorescently labelled primers) is also represented (PVM). The forward and reverse primers were concentrated at 10 µM and 100 µM, respectively. This table is adapted from Supplementary Material 2 of Álvarez *et al.* (2015) and Table S2 of Lourenço *et al.* (2017).

Locus	Multiplex	Label*	Primer forward (5' – 3')	Primer reverse (5' – 3')	PVM (µl)
SST-A6-I [2]	Ssal1	NED	TTCAGTGCTCTTGCAGGTTG	AGTCTGCAAGGATAGAAAGATCG	2.0
SST-A6-II [2]	Ssal1	PET	ATTCTCTCTGACAAGGATTGTGG	GGTAGACAGACATCAAGGCAGAC	1.2
SalE14 [1]	Ssal1	VIC	GCTGCCCTCTCTGCCTACTGACCAT	GCCAAGACATGGAACACCCTCCCGC	0.8
Sal29 [1]	Ssal2	6-FAM	CTCTTTGACTGAACCAGAACCCC	GCCTGTCGGCTCTGTGTAACC	8.0
SST-B11 [2]	Ssal2	PET	TCAAACGGTGCCAAAGTTATTAG	TTAATTGGCAGTTTTCTTTCCAG	2.0
SalE12 [1]	Ssal2	VIC	CTCAGGAACAGTGTGCCCCAAATAC	CTCATAATTTAGTCTACCCTCCCAC	0.8
SST-C3 [2]	Ssal3	PET	CCGTTTGAGTCACTTCTTTCTTG	TTGCTTTACCAACCAGTTATTGTC	1.4
SalE7 [1]	Ssal3	NED	TTTCAGCACCAAGATACCTCTTTTG	CTCCCTCCATATCAAGGTCACAGAC	0.8
SalE5 [1]	Ssal3	6-FAM	CCACATGATGCCTACGTATGTTGTG	CTCCTGTTTACGCTTCACCTGCTCC	0.6
SalE2 [1]	Ssal3	VIC	CACGACAAAATACAGAGAGTGGATA	ATATTTGAAATTGCCCATTTGGTA	3.0
SalE06 [1]	Ssal4	VIC	GGACTCATGGTCACCCAGAGGTTCT	ATGGATTGTGTCGAAATAAGGTATC	1.2
Sal3 [1]	Ssal4	6-FAM	CTCAGACAAGAAATCCTGCTTCTTC	ATAAATCTGTCCTGTTCCTAATCAG	1.2
SalE8 [1]	Ssal4	NED	GCAAAGTCCATGCTTTCCCTTTCTC	GACATACCAAAGACTCCAGAATGGG	0.8
SST-G9 [2]	Ssal4	NED	CCTCGTCAGGGGTTGTAGG	CTTTCCAGGAAGAAACTGAGATG	0.8

*An extra number of base pairs were added at the 5' end of the original sequence of forward primers in order to allow binding of four different fluorescent labelled oligonucleotides (6-FAM - TGT AAA ACG ACG GCC AGT; VIC - TAA TAC GAC TCA CTA TAG GG; NED - TTT CCC AGT CAC GAC GTT G; PET - GAT AAC AAT TTC ACA CAG G);

[1] Steinfartz *et al.* (2004)

[2] Hendrix *et al.* (2010)

Supplementary Table B2

Table B2 Summary statistics of spatial autocorrelation analyses comparing larviparous males and pueriparous males (see respective correlogram in **Figure 3.3A**) aimed at testing H1. The Omega test value (ω) and respective p-value (*p*) for each subsample is displayed. Significant ω values were declared when $p < 0.01$ (values in bold; Smouse *et al.*, 2008). Remaining parameters were estimated for each of the eight distance classes tested: 100 (0-100 m), 200 (101-200 m), 300 (201-300 m), 400 (301-400 m), 500 (401-500 m), 600 (501-600 m), 700 (601-700 m), and 1000 (701-1000 m). These parameters are: N (number of pairs of individuals analysed), r_{auto} (autocorrelation coefficient) and respective lower (r_{auto} lower 95% CI limit) and upper (r_{auto} upper 95% CI limit) bounds of the 95% CIs. The p-values of one-tailed tests to determine if r_{auto} values were significantly higher (*p (r-rand ≥ r-obs)*) or lower (*p (r-obs ≥ r-rand)*) than expected for a given distance class are also displayed, with significant *p* values ($p < 0.05$) in bold and underlined.

Data set and parameters	**ω (p_ω)**	**100**	**200**	**300**	**400**	**500**	**600**	**700**	**1000**
Larviparous males	28.4 (0.03)								
N		185	191	160	149	116	87	70	98
r_{auto}		-0.019	0.013	0.001	0.004	-0.008	-0.005	0.022	-0.001
r_{auto} lower 95% CI limit		-0.035	-0.007	-0.021	-0.019	-0.032	-0.031	-0.007	-0.028
r_{auto} upper 95% CI limit		0.001	0.033	0.024	0.028	0.017	0.022	0.053	0.024
p (*r-rand* ≥ *r-obs*)		0.979	0.068	0.446	0.336	0.733	0.662	0.079	0.551
p (*r-obs* ≥ *r-rand*)		**0.021**	0.932	0.554	0.664	0.267	0.338	0.921	0.449
Pueriparous males	21.7 (0.72)								
N		291	303	262	200	168	122	91	116
r_{auto}		-0.003	0.003	0.006	-0.007	-0.006	0.003	-0.007	0.009
r_{auto} lower 95% CI limit		-0.018	-0.010	-0.008	-0.024	-0.026	-0.021	-0.030	-0.012
r_{auto} upper 95% CI limit		0.011	0.017	0.022	0.011	0.015	0.026	0.017	0.030
p (*r-rand* ≥ *r-obs*)		0.699	0.319	0.186	0.806	0.744	0.382	0.699	0.187
p (*r-obs* ≥ *r-rand*)		0.301	0.681	0.814	0.194	0.256	0.618	0.301	0.813

Supplementary Table B3

Table B3 Summary statistics of spatial autocorrelation analyses comparing larviparous females and pueriparous females (see respective correlogram in **Figure 3.3B**) aimed at testing H1. The Omega test value (ω) and respective p-value (*p*) for each subsample is displayed. Significant ω values were declared when $p < 0.01$ (values in bold; Smouse *et al.* 2008). Remaining parameters were estimated for each of the eight distance classes tested: 100 (0-100 m), 200 (101-200 m), 300 (201-300 m), 400 (301-400 m), 500 (401-500 m), 600 (501-600 m), 700 (601-700 m), and 1000 (701-1000 m). These parameters are: N (number of pairs of individuals analysed), r_{auto} (autocorrelation coefficient) and respective lower (r_{auto} lower 95% CI limit) and upper (r_{auto} upper 95% CI limit) bounds of the 95% CIs. The p-values of one-tailed tests to determine if r_{auto} values were significantly higher (*p (r-rand ≥ r-obs)*) or lower (*p (r-obs ≥ r-rand)*) than expected for a given distance class are also displayed, with significant *p* values ($p < 0.05$) in bold and underlined.

Data set and parameters	**ω (p_ω)**	**100**	**200**	**300**	**400**	**500**	**600**	**700**	**1000**
Larviparous females	**38.4 (<0.01)**								
N		188	188	164	158	135	105	58	79
r_{auto}		0.020	-0.005	-0.008	-0.016	0.008	0.024	-0.018	-0.019
r_{auto} lower 95% CI limit		0.000	-0.027	-0.027	-0.037	-0.016	-0.001	-0.047	-0.051
r_{auto} upper 95% CI limit		0.040	0.016	0.013	0.006	0.031	0.048	0.015	0.011
p (*r-rand* ≥ *r-obs*)		**0.017**	0.714	0.782	0.941	0.210	**0.031**	0.858	0.917
p (*r-obs* ≥ *r-rand*)		0.983	0.286	0.218	0.060	0.790	0.970	0.142	0.083
Pueriparous females	**44.3 (<0.01)**								
N		280	281	241	186	134	100	64	75
r_{auto}		0.010	-0.017	0.003	0.006	-0.003	0.034	-0.038	-0.004
r_{auto} lower 95% CI limit		-0.004	-0.032	-0.014	-0.013	-0.024	0.007	-0.066	-0.039
r_{auto} upper 95% CI limit		0.025	-0.002	0.020	0.026	0.019	0.060	-0.010	0.033
p (*r-rand* ≥ *r-obs*)		0.077	0.992	0.354	0.242	0.602	**0.003**	0.994	0.612
p (*r-obs* ≥ *r-rand*)		0.923	**0.008**	0.646	0.758	0.398	0.997	**0.007**	0.389

Supplementary Table B4

Table B4 Summary statistics of spatial autocorrelation analyses comparing larviparous males and larviparous females (see respective correlogram in **Figure 3.4A**) aimed at testing H2. The Omega test value (ω) and respective p-value (*p*) for each subsample is displayed. Significant ω values were declared when $p < 0.01$ (values in bold; Smouse *et al.* 2008). Remaining parameters were estimated for each of the eight distance classes tested: 100 (0-100 m), 200 (101-200 m), 300 (201-300 m), 400 (301-400 m), 500 (401-500 m), 600 (501-600 m), 700 (601-700 m), and 1000 (701-1000 m). These parameters are: N (number of pairs of individuals analysed), r_{auto} (autocorrelation coefficient) and respective lower (r_{auto} lower 95% CI limit) and upper (r_{auto} upper 95% CI limit) bounds of the 95% CIs. The p-values of one-tailed tests to determine if r_{auto} values were significantly higher (*p (r-rand ≥ r-obs)*) or lower (*p (r-obs ≥ r-rand)*) than expected for a given distance class are also displayed, with significant *p* values ($p < 0.05$) in bold and underlined.

Data set and parameters	**ω (p_ω)**	**100**	**200**	**300**	**400**	**500**	**600**	**700**	**1000**
Larviparous males	28.4 (0.03)								
N		185	191	160	149	116	87	70	98
r_{auto}		-0.019	0.013	0.001	0.004	-0.008	-0.005	0.022	-0.001
r_{auto} lower 95% CI limit		-0.035	-0.007	-0.021	-0.019	-0.032	-0.031	-0.007	-0.028
r_{auto} upper 95% CI limit		0.001	0.033	0.024	0.028	0.017	0.022	0.053	0.024
p (*r-rand* ≥ *r-obs*)		0.979	0.068	0.446	0.336	0.733	0.662	0.079	0.551
p (*r-obs* ≥ *r-rand*)		**0.021**	0.932	0.554	0.664	0.267	0.338	0.921	0.449
Larviparous females	**38.4 (<0.01)**								
N		188	188	164	158	135	105	58	79
r_{auto}		0.020	-0.005	-0.008	-0.016	0.008	0.024	-0.018	-0.019
r_{auto} lower 95% CI limit		0.000	-0.027	-0.027	-0.037	-0.016	-0.001	-0.047	-0.051
r_{auto} upper 95% CI limit		0.040	0.016	0.013	0.006	0.031	0.048	0.015	0.011
p (*r-rand* ≥ *r-obs*)		**0.017**	0.714	0.782	0.941	0.210	**0.031**	0.858	0.917
p (*r-obs* ≥ *r-rand*)		0.983	0.286	0.218	0.060	0.790	0.970	0.142	0.083

Supplementary Table B5

Table B5 Summary statistics of spatial autocorrelation analyses comparing pueriparous males and pueriparous females (see respective correlogram in **Figure 3.4B**) aimed at testing H2. The Omega test value (ω) and respective p-value (*p*) for each subsample is displayed. Significant ω values were declared when $p < 0.01$ (values in bold; Smouse *et al.* 2008). Remaining parameters were estimated for each of the eight distance classes tested: 100 (0-100 m), 200 (101-200 m), 300 (201-300 m), 400 (301-400 m), 500 (401-500 m), 600 (501-600 m), 700 (601-700 m), and 1000 (701-1000 m). These parameters are: N (number of pairs of individuals analysed), r_{auto} (autocorrelation coefficient) and respective lower (r_{auto} lower 95% CI limit) and upper (r_{auto} upper 95% CI limit) bounds of the 95% CIs. The p-values of one-tailed tests to determine if r_{auto} values were significantly higher (*p (r-rand ≥ r-obs)*) or lower (*p (r-obs ≥ r-rand)*) than expected for a given distance class are also displayed, with significant *p* values ($p < 0.05$) in bold and underlined.

Data set and parameters	**ω (p_ω)**	**100**	**200**	**300**	**400**	**500**	**600**	**700**	**1000**
Pueriparous males	21.7 (0.72)								
N		291	303	262	200	168	122	91	116
r_{auto}		-0.003	0.003	0.006	-0.007	-0.006	0.003	-0.007	0.009
r_{auto} lower 95% CI limit		-0.018	-0.010	-0.008	-0.024	-0.026	-0.021	-0.030	-0.012
r_{auto} upper 95% CI limit		0.011	0.017	0.022	0.011	0.015	0.026	0.017	0.030
p (*r-rand* ≥ *r-obs*)		0.699	0.319	0.186	0.806	0.744	0.382	0.699	0.187
p (*r-obs* ≥ *r-rand*)		0.301	0.681	0.814	0.194	0.256	0.618	0.301	0.813
Pueriparous females	**44.3 (<0.01)**								
N		280	281	241	186	134	100	64	75
r_{auto}		0.010	-0.017	0.003	0.006	-0.003	0.034	-0.038	-0.004
r_{auto} lower 95% CI limit		-0.004	-0.032	-0.014	-0.013	-0.024	0.007	-0.066	-0.039
r_{auto} upper 95% CI limit		0.025	-0.002	0.020	0.026	0.019	0.060	-0.010	0.033
p (*r-rand* ≥ *r-obs*)		0.077	0.992	0.354	0.242	0.602	**0.003**	0.994	0.612
p (*r-obs* ≥ *r-rand*)		0.923	**0.008**	0.646	0.758	0.398	0.997	**0.007**	0.389

Supplementary Table B6

Table B6 Summary statistics of spatial autocorrelation analyses comparing males and females in each sampled larviparous population (PEGA_Larv, EUME_Larv, and SGAL_Larv; see respective correlograms in **Figure 3.5**). The Omega test value (ω) and respective p-value (*p*) for each sampled locality is displayed. Significant ω values were declared when $p < 0.01$ (values in bold; Smouse *et al.* 2008). Remaining parameters were estimated for each of the six distance classes tested: 100 (0-100 m), 200 (101-200 m), 300 (201-300 m), 500 (301-500 m), 700 (501-700 m), and 1000 (701-1000 m). These parameters are: N (number of pairs of individuals analysed), r_{auto} (autocorrelation coefficient) and respective lower (r_{auto} lower 95% CI limit) and upper (r_{auto} upper 95% CI limit) bounds of the 95% CIs. The p-values of one-tailed tests to determine if r_{auto} values were significantly higher (*p (r-rand ≥ r-obs)*) or lower (*p (r-obs ≥ r-rand)*) than expected for a given distance class are also displayed, with significant p values ($p < 0.05$) in bold and underlined.

Data set and parameters	ω (p_ω)	100	200	300	500	700	1000
PEGA_Larv							
Males	25.0 (0.01)						
N		71	76	58	99	62	41
r_{auto}		-0.035	0.010	0.009	0.011	-0.003	0.006
r_{auto} lower 95% CI limit		-0.063	-0.018	-0.021	-0.013	-0.032	-0.034
r_{auto} upper 95% CI limit		-0.007	0.040	0.035	0.036	0.025	0.050
p (*r-rand* ≥ *r-obs*)		0.997	0.210	0.277	0.153	0.597	0.372
p (*r-obs* ≥ *r-rand*)		**0.003**	0.790	0.723	0.847	0.403	0.628
Females	**30.9 (<0.01)**						
N		61	44	35	83	45	22
r_{auto}		0.007	0.042	-0.029	-0.006	0.002	-0.049
r_{auto} lower 95% CI limit		-0.022	0.005	-0.068	-0.031	-0.035	-0.095
r_{auto} upper 95% CI limit		0.038	0.075	0.016	0.019	0.043	-0.004
p (*r-rand* ≥ *r-obs*)		0.264	**0.009**	0.950	0.713	0.447	0.988
p (*r-obs* ≥ *r-rand*)		0.736	0.991	**0.049**	0.288	0.553	**0.013**

Table B6 Continued.

Data set and parameters	ω (p_ω)	100	200	300	500	700	1000
EUME_Larv							
Males	19.2 (0.11)						
N		64	64	59	93	33	12
r_{auto}		0.020	0.015	-0.001	-0.021	-0.021	0.035
r_{auto} lower 95% CI limit		-0.013	-0.026	-0.047	-0.052	-0.075	-0.066
r_{auto} upper 95% CI limit		0.062	0.063	0.045	0.012	0.031	0.102
p (*r-rand* ≥ *r-obs*)		0.157	0.210	0.514	0.910	0.779	0.214
p (*r-obs* ≥ *r-rand*)		0.844	0.790	0.486	0.091	0.221	0.786
Females	**30.9 (<0.01)**						
N		55	68	64	92	47	25
r_{auto}		0.056	-0.030	-0.014	-0.004	0.028	-0.040
r_{auto} lower 95% CI limit		0.016	-0.074	-0.042	-0.040	-0.015	-0.098
r_{auto} upper 95% CI limit		0.097	0.014	0.012	0.032	0.069	0.026
p (*r-rand* ≥ *r-obs*)		**0.006**	0.950	0.771	0.625	0.098	0.919
p (*r-obs* ≥ *r-rand*)		0.994	**0.049**	0.230	0.375	0.902	0.081
SGAL_Larv							
Males	**31.9 (<0.01)**	50	51	43	73	62	45
N		-0.042	0.015	-0.006	0.007	0.033	-0.019
r_{auto}		-0.070	-0.020	-0.046	-0.022	0.002	-0.052
r_{auto} lower 95% CI limit		-0.015	0.047	0.037	0.037	0.065	0.015
r_{auto} upper 95% CI limit		0.996	0.169	0.613	0.301	**0.012**	0.884
p (*r-rand* ≥ *r-obs*)		**0.004**	0.831	0.387	0.699	0.988	0.116
p (*r-obs* ≥ *r-rand*)							
Females	15.1 (0.24)	72	76	65	118	71	32
N		0.005	-0.011	0.009	-0.005	0.001	0.018
r_{auto}		-0.029	-0.038	-0.020	-0.028	-0.026	-0.030
r_{auto} lower 95% CI limit		0.035	0.017	0.038	0.018	0.028	0.073
r_{auto} upper 95% CI limit		0.353	0.788	0.264	0.678	0.479	0.173
p (*r-rand* ≥ *r-obs*)		0.647	0.212	0.736	0.322	0.521	0.827
p (*r-obs* ≥ *r-rand*)		50	51	43	73	62	45

Supplementary Table B7

Table B7 Summary statistics of spatial autocorrelation analyses comparing males and females in each sampled pueriparous population (INFA_Puer, BRAN_Puer, and VILL_Puer; see respective correlograms in **Figure 3.5**). The Omega test value (ω) and respective p-value (*p*) for each sampled locality is displayed. Significant ω values were declared when $p < 0.01$ (values in bold; Smouse *et al.* 2008). Remaining parameters were estimated for each of the six distance classes tested: 100 (0-100 m), 200 (101-200 m), 300 (201-300 m), 500 (301-500 m), 700 (501-700 m), and 1000 (701-1000 m). These parameters are: N (number of pairs of individuals analysed), r_{auto} (autocorrelation coefficient) and respective lower (r_{auto} lower 95% CI limit) and upper (r_{auto} upper 95% CI limit) bounds of the 95% CIs. The p-values of one-tailed tests to determine if r_{auto} values were significantly higher (*p (r-rand ≥ r-obs)*) or lower (*p (r-obs ≥ r-rand)*) than expected for a given distance class are also displayed, with significant p values ($p < 0.05$) in bold and underlined.

Data set and parameters	ω (p_ω)	100	200	300	500	700	1000
INFA_Puer							
Males	15.7 (0.22)						
N		107	105	83	86	63	48
r_{auto}		0.006	0.006	-0.008	0.003	-0.013	-0.006
r_{auto} lower 95% CI limit		-0.019	-0.018	-0.035	-0.025	-0.041	-0.041
r_{auto} upper 95% CI limit		0.030	0.031	0.019	0.032	0.017	0.027
p (*r-rand* ≥ *r-obs*)		0.245	0.293	0.751	0.380	0.834	0.653
p (*r-obs* ≥ *r-rand*)		0.755	0.707	0.250	0.620	0.166	0.347
Females	18.6 (0.12)						
N		88	86	66	93	40	27
r_{auto}		0.013	-0.019	-0.003	0.011	-0.006	0.003
r_{auto} lower 95% CI limit		-0.016	-0.049	-0.028	-0.015	-0.041	-0.050
r_{auto} upper 95% CI limit		0.040	0.011	0.021	0.036	0.034	0.056
p (*r-rand* ≥ *r-obs*)		0.140	0.943	0.584	0.163	0.632	0.444
p (*r-obs* ≥ *r-rand*)		0.860	0.058	0.416	0.837	0.369	0.556

Table B7 Continued.

Data set and parameters	ω (p_ω)	100	200	300	500	700	1000
BRAN_Puer							
Males	25.8 (0.02)						
N		71	84	72	117	65	26
r_{auto}		-0.028	0.001	0.035	-0.010	-0.004	0.029
r_{auto} lower 95% CI limit		-0.061	-0.030	-0.004	-0.037	-0.036	-0.021
r_{auto} upper 95% CI limit		0.009	0.032	0.072	0.019	0.029	0.081
p (*r-rand* ≥ *r-obs*)		0.962	0.467	**0.014**	0.795	0.606	0.133
p (*r-obs* ≥ *r-rand*)		**0.038**	0.533	0.987	0.205	0.394	0.867
Females	19.9 (0.14)						
N		84	92	92	127	74	27
r_{auto}		-0.002	-0.023	0.013	0.003	0.011	-0.004
r_{auto} lower 95% CI limit		-0.030	-0.052	-0.020	-0.021	-0.020	-0.075
r_{auto} upper 95% CI limit		0.026	0.005	0.045	0.030	0.043	0.070
p (*r-rand* ≥ *r-obs*)		0.538	0.953	0.183	0.388	0.220	0.575
p (*r-obs* ≥ *r-rand*)		0.462	**0.047**	0.817	0.612	0.780	0.425
VILL_Puer							
Males	16.5 (0.18)						
N		113	114	107	165	85	42
r_{auto}		0.002	0.002	-0.001	-0.009	0.011	0.014
r_{auto} lower 95% CI limit		-0.018	-0.018	-0.021	-0.027	-0.017	-0.021
r_{auto} upper 95% CI limit		0.021	0.023	0.019	0.008	0.037	0.049
p (*r-rand* ≥ *r-obs*)		0.414	0.414	0.542	0.895	0.173	0.184
p (*r-obs* ≥ *r-rand*)		0.586	0.586	0.458	0.105	0.827	0.816
Females	17.9 (0.14)						
N		108	103	83	100	50	21
r_{auto}		0.017	-0.010	-0.002	-0.006	0.006	-0.010
r_{auto} lower 95% CI limit		-0.007	-0.031	-0.029	-0.028	-0.031	-0.063
r_{auto} upper 95% CI limit		0.043	0.013	0.024	0.018	0.044	0.045
p (*r-rand* ≥ *r-obs*)		0.057	0.843	0.583	0.703	0.360	0.674
p (*r-obs* ≥ *r-rand*)		0.943	0.157	0.417	0.298	0.641	0.326

Supplementary Table B8

Table B8 Matrix of pairwise ω_{GROUPS} values (below diagonal) and respective p-values (above diagonal) between the compared subsamples (LM – larviparous males; LF – larviparous females; PM – pueriparous males; PF – pueriparous females) in the "combined correlograms" (see **Figures 3.3 and 3.4**). These analyses aimed at testing both of our hypotheses (i.e. differences in fine-scale genetic structure between reproductive modes [LM vs. PM and LF vs. PF] and sexes [LM vs. LF and PM vs. PF]) at global level. Comparisons between males and females were performed only within reproductive mode (NA – not applicable). No pairwise comparison was significant ($p < 0.01$; Banks and Peakall 2012).

subsample	**LM**	**LF**	**PM**	**PF**
LM	0	0.02	0.73	NA
LF	30.00	0	NA	0.57
PM	12.19	NA	0	0.14
PF	NA	14.35	22.22	0

Supplementary Table B9

Table B9 Pairwise t^2 values and respective p-values (p_{t2}) between the analysed subsamples (LM – larviparous males; LF – larviparous females; PM – pueriparous males; PF – pueriparous females) for the eight distance classes evaluated: 100 (0-100 m), 200 (101-200 m), 300 (201-300 m), 400 (301-400 m), 500 (401-500 m), 600 (501-600 m), 700 (601-700 m), and 1000 (701-1000 m). These analyses aimed at testing both of our hypotheses (i.e. differences in fine-scale genetic structure between reproductive modes [LM vs. PM and LF vs. PF] and sexes [LM vs. LF and PM vs. PF]) at distance class level. Significant pairwise comparisons ($p_{t2} < 0.01$; Banks and Peakall 2012) are in bold and underlined.

Comparison	100	200	300	400	500	600	700	1000
Hypothesis 1								
LM vs. PM								
t^2	1.22	0.53	0.12	0.53	0.01	0.20	2.12	0.30
p_{t2}	0.27	0.47	0.74	0.48	0.91	0.66	0.15	0.58
LF vs. PF								
t^2	0.61	0.75	0.59	1.93	0.41	0.29	0.85	0.37
p_{t2}	0.43	0.39	0.45	0.17	0.52	0.59	0.36	0.55
Hypothesis 2								
LM vs. LF								
t^2	**7.03**	1.37	0.35	1.51	0.83	2.33	3.20	0.72
p_{t2}	**<0.01**	0.24	0.56	0.22	0.37	0.13	0.07	0.39
PM vs. PF								
t^2	1.53	3.38	0.09	0.98	0.04	2.76	2.70	0.37
p_{t2}	0.21	0.07	0.77	0.32	0.84	0.10	0.10	0.55

Supplementary Table B10

Table B10 Matrix of pairwise ω_{GROUPS} values (below diagonal) and respective p-values (above diagonal) between males sampled from different sampled localities. These analyses aimed at testing if males from pairs of populations exhibiting the same or different (red shading) reproductive modes showed significant differences in fine-scale genetic structure at global level. No pairwise comparison was significant ($p < 0.01$; Banks and Peakall 2012).

population	PEGA_Larv	EUME_Larv	SGAL_Larv	INFA_Puer	BRAN_Puer	VILL_Puer
PEGA_Larv	0	0.18	0.74	0.56	0.75	0.49
EUME_Larv	16.29	0	0.04	0.78	0.30	0.83
SGAL_Larv	8.56	21.96	0	0.28	0.16	0.39
INFA_Puer	10.69	8.09	14.29	0	0.19	0.85
BRAN_Puer	8.43	14.13	16.80	16.01	0	0.54
VILL_Puer	11.37	7.38	12.81	7.17	10.87	0

Supplementary Table B11

Table B11 Matrix of pairwise ω_{GROUPS} values (below diagonal) and respective p-values (above diagonal) between females sampled from different sampled localities. These analyses aimed at testing if females from pairs of populations exhibiting the same or different (red shading) reproductive modes showed significant differences in fine-scale genetic structure at global level. No pairwise comparison was significant ($p < 0.01$; Banks and Peakall 2012).

population	PEGA_Larv	EUME_Larv	SGAL_Larv	INFA_Puer	BRAN_Puer	VILL_Puer
PEGA_Larv	0	0.09	0.31	0.23	0.16	0.54
EUME_Larv	18.96	0	0.14	0.28	0.20	0.50
SGAL_Larv	13.84	17.22	0	0.95	0.96	0.98
INFA_Puer	15.18	14.33	5.22	0	0.93	0.98
BRAN_Puer	16.56	15.83	4.82	5.77	0	0.86
VILL_Puer	10.86	11.28	4.05	4.23	6.84	0

Supplementary Table B12

Table B12 Matrices of pairwise t^2 values (below diagonal) and respective p-values (above diagonal) between males from different sampled localities. These analyses aimed at testing if males from populations exhibiting the same or different (red shading) reproductive modes showed significant differences in fine-scale genetic structure at distance class level. Six distance classes were evaluated: 100 (0-100 m), 200 (101-200 m), 300 (201-300 m), 500 (301-500 m), 700 (501-700 m), and 1000 (701-1000 m). No pairwise comparison was significant ($p_{t2} < 0.01$; Banks and Peakall 2012).

population	PEGA_Larv	EUME_Larv	SGAL_Larv	INFA_Puer	BRAN_Puer	VILL_Puer
100 m						
PEGA_Larv	0	0.02	0.76	0.04	0.75	0.07
EUME_Larv	5.66	0	0.01	0.55	0.04	0.45
SGAL_Larv	0.09	6.39	0	0.04	0.55	0.07
INFA_Puer	4.17	0.36	4.29	0	0.09	0.79
BRAN_Puer	0.11	4.15	0.36	2.86	0	0.15
VILL_Puer	3.16	0.58	3.17	0.07	2.05	0
200 m						
PEGA_Larv	0	0.83	0.84	0.83	0.67	0.70
EUME_Larv	0.04	0	1.00	0.68	0.53	0.58
SGAL_Larv	0.04	0.00	0	0.70	0.57	0.60
INFA_Puer	0.05	0.17	0.15	0	0.82	0.83
BRAN_Puer	0.18	0.37	0.32	0.05	0	0.97
VILL_Puer	0.16	0.31	0.27	0.04	0.00	0
300 m						
PEGA_Larv	0	0.83	0.84	0.83	0.67	0.70
EUME_Larv	0.04	0	1.00	0.68	0.53	0.58
SGAL_Larv	0.04	0.00	0	0.70	0.57	0.60
INFA_Puer	0.05	0.17	0.15	0	0.82	0.83
BRAN_Puer	0.18	0.37	0.32	0.05	0	0.97
VILL_Puer	0.16	0.31	0.27	0.04	0.00	0
500 m						
PEGA_Larv	0	0.69	0.59	0.46	0.27	0.66
EUME_Larv	0.16	0	0.85	0.76	0.14	1.00
SGAL_Larv	0.29	0.03	0	0.93	0.12	0.86
INFA_Puer	0.57	0.10	0.01	0	0.05	0.72
BRAN_Puer	1.23	2.22	2.34	3.90	0	0.10
VILL_Puer	0.19	0.00	0.03	0.13	2.76	0

Table B12 Continued.

population	PEGA_Larv	EUME_Larv	SGAL_Larv	INFA_Puer	BRAN_Puer	VILL_Puer
700 m						
PEGA_Larv	0	0.11	0.83	0.69	0.25	0.25
EUME_Larv	2.56	0	0.19	0.26	0.58	0.60
SGAL_Larv	0.04	1.74	0	0.87	0.42	0.46
INFA_Puer	0.16	1.27	0.02	0	0.48	0.47
BRAN_Puer	1.33	0.31	0.65	0.48	0	0.99
VILL_Puer	1.34	0.28	0.56	0.51	0.00	0
1000 m						
PEGA_Larv	0	0.53	0.12	0.66	0.96	0.52
EUME_Larv	0.40	0	0.05	0.77	0.54	0.26
SGAL_Larv	2.41	3.85	0	0.06	0.11	0.36
INFA_Puer	0.18	0.08	3.71	0	0.70	0.27
BRAN_Puer	0.00	0.37	2.62	0.15	0	0.49
VILL_Puer	0.40	1.24	0.87	1.20	0.47	0

Supplementary Table B13

Table B13 Matrices of pairwise t^2 values (below diagonal) and respective p-values (above diagonal) between females from different sampled localities. These analyses aimed at testing if females from populations exhibiting the same or different (red shading) reproductive modes showed significant differences in fine-scale genetic structure at distance class level. Six distance classes were evaluated: 100 (0-100 m), 200 (101-200 m), 300 (201-300 m), 500 (301-500 m), 700 (501-700 m), and 1000 (701-1000 m). No pairwise comparison was significant ($p_{t2} < 0.01$; Banks and Peakall 2012).

population	PEGA_Larv	EUME_Larv	SGAL_Larv	INFA_Puer	BRAN_Puer	VILL_Puer
100 m						
PEGA_Larv	0	0.05	0.92	0.82	0.68	0.68
EUME_Larv	3.95	0	0.03	0.06	0.01	0.08
SGAL_Larv	0.01	4.65	0	0.71	0.74	0.55
INFA_Puer	0.05	3.68	0.14	0	0.46	0.82
BRAN_Puer	0.16	6.18	0.11	0.52	0	0.32
VILL_Puer	0.17	3.13	0.36	0.05	1.00	0
200 m						
PEGA_Larv	0	**<0.01**	0.06	0.02	0.02	0.05
EUME_Larv	**6.95**	0	0.42	0.62	0.77	0.38
SGAL_Larv	3.70	0.66	0	0.71	0.56	0.98
INFA_Puer	5.37	0.25	0.14	0	0.82	0.68
BRAN_Puer	5.73	0.08	0.34	0.05	0	0.51
VILL_Puer	3.90	0.77	0.00	0.17	0.43	0

Table B13 Continued.

population	PEGA_Larv	EUME_Larv	SGAL_Larv	INFA_Puer	BRAN_Puer	VILL_Puer
300 m						
PEGA_Larv	0	0.59	0.18	0.34	0.13	0.34
EUME_Larv	0.29	0	0.33	0.63	0.23	0.61
SGAL_Larv	1.77	0.96	0	0.61	0.87	0.60
INFA_Puer	0.89	0.24	0.26	0	0.47	0.99
BRAN_Puer	2.25	1.43	0.03	0.51	0	0.45
VILL_Puer	0.92	0.27	0.27	0.00	0.57	0
500 m						
PEGA_Larv	0	0.94	0.96	0.46	0.68	1.00
EUME_Larv	0.01	0	0.98	0.48	0.70	0.93
SGAL_Larv	0.00	0.00	0	0.43	0.65	0.95
INFA_Puer	0.57	0.51	0.63	0	0.70	0.41
BRAN_Puer	0.18	0.14	0.20	0.14	0	0.62
VILL_Puer	0.00	0.01	0.00	0.68	0.25	0
700 m						
PEGA_Larv	0	0.38	0.96	0.79	0.74	0.91
EUME_Larv	0.80	0	0.29	0.25	0.52	0.42
SGAL_Larv	0.00	1.12	0	0.80	0.64	0.85
INFA_Puer	0.07	1.36	0.06	0	0.52	0.70
BRAN_Puer	0.11	0.40	0.23	0.43	0	0.81
VILL_Puer	0.01	0.65	0.04	0.16	0.06	0
1000 m						
PEGA_Larv	0	0.84	0.12	0.24	0.32	0.41
EUME_Larv	0.04	0	0.15	0.30	0.40	0.51
SGAL_Larv	2.45	2.06	0	0.70	0.59	0.50
INFA_Puer	1.38	1.04	0.15	0	0.87	0.77
BRAN_Puer	1.00	0.73	0.30	0.03	0	0.88
VILL_Puer	0.67	0.43	0.45	0.09	0.02	0

Supplementary Table B14

Table B14 Results of heterogeneity t^2 tests, as well as respective p-values, between males and females in each sampled locality. These tests aimed at examining differences in fine-scale genetic structure between sexes in each sampled locality at distance class levels. A total of six distance classes were evaluated: 100 (0-100 m), 200 (101-200 m), 300 (201-300 m), 500 (301-500 m), 700 (501-700 m), and 1000 (701-1000 m). No significant differences in genetic structure were found (pt2 < 0.01; Banks and Peakall 2012).

Pop (males vs. females)	**100**	**200**	**300**	**500**	**700**	**1000**
PEGA_Larv						
t^2 (p_{t2})	3.48 (0.06)	1.56 (0.21)	2.12 (0.15)	0.80 (0.37)	0.05 (0.81)	2.47 (0.12)
EUME_Larv						
t^2 (p_{t2})	1.44 (0.23)	1.84 (0.17)	0.20 (0.65)	0.42 (0.52)	1.99 (0.16)	1.94 (0.17)
SGAL_Larv						
t^2 (p)	3.99 (0.04)	1.22 (0.27)	0.35 (0.55)	0.33 (0.56)	2.17 (0.14)	1.46 (0.23)
INFA_Puer						
t^2 (p_{t2})	0.11 (0.75)	1.60 (0.21)	0.08 (0.77)	0.14 (0.71)	0.09 (0.77)	0.08 (0.77)
BRAN_Puer						
t^2 (p_{t2})	1.30 (0.25)	1.26 (0.26)	0.88 (0.35)	0.47 (0.50)	0.46 (0.49)	0.48 (0.49)
VILL_Puer						
t^2 (p)	0.84 (0.36)	0.57 (0.46)	0.01 (0.93)	0.05 (0.81)	0.05 (0.83)	0.56 (0.45)

References of Appendix B

Álvarez D, Lourenço A, Oro D, Velo-Antón G (2015) Assessment of census (*N*) and effective population size (*Ne*) reveals consistency of *Ne* single-sample estimators and a high *Ne/N* ratio in an urban and isolated population of fire salamanders. *Conservation Genetics Resources*, **7**, 705–712.

Banks SC, Peakall R (2012) Genetic spatial autocorrelation can readily detect sex-biased dispersal. *Molecular Ecology*, **21**, 2092–2105.

Hendrix R, Hauswaldt JS, Veith M, Steinfartz S (2010) Strong correlation between cross-amplification success and genetic distance across all members of 'True salamanders' (Amphibia: Salamandridae) revealed by *Salamandra salamandra*-specific microsatellite loci. *Molecular Ecology Resources*, **10**, 1038–1047.

Lourenço A, Álvarez D, Wang IJ, Velo-Antón G (2017) Trapped within the city: integrating demography, time since isolation and population-specific traits to assess the genetic effects of urbanization. *Molecular Ecolology*, **26**, 1498–1514.

QGIS Development Team (2017) QGIS Geographic Information System. Open Source Geospatial Foundation Project. http://qgis.osgeo.org

Smouse PE, Peakall R, Gonzales E (2008) A heterogeneity test for fine-scale genetic structure. *Molecular Ecology*, **17**, 3389–3400.

Steinfartz S, Kuesters D, Tautz D (2004) Isolation and characterization of polymorphic tetranucleotide microsatellite loci in the Fire salamander *Salamandra salamandra* (Amphibia: Caudata). *Molecular Ecolology Resources*, **4**, 626-628.

van Etten J (2017) R Package gdistance: Distances and routes on geographical grids. *Journal of Statistical Software*, **76**, 1-21.

Appendix C

Supplementary Text C1

Vectorial data (shapefile of polygons) representing the composition and configuration of land cover for the provinces of Galicia and Asturias in the year of 2011 were downloaded from the *Centro Nacional de Información Geográfica* (CNIG; http://centrodedescargas.cnig.es/CentroDescargas/index.jsp). These land cover data sets were generated by the Sistema de Información sobre Ocupación del Suelo de España (SIOSE; hereafter referred to as SIOSE_LC). Unlike other land use data sets, the SIOSE_LC not only provides a thorough qualitative classification of the landscape (more than 100 land use classes are discriminated), but also a detailed quantitative characterization of the landscape (i.e. the proportion of each land use class within a specific patch/polygon). These vectorial layers were cropped to the extent of both study plots (*i.e.* the larviparous and pueriparous plots).

Based on previous ecological and genetic studies, the SIOSE_LC for both study landscape plots were reclassified into a total of nine classes that are ecologically relevant to *S. salamandra* populations (*e.g.* Velo-Antón and Buckley 2015; Lourenço *et al.* 2017; Antunes *et al.* 2018; Lourenço *et al.* 2018a). This major simplification of the original SIOSE_LC was carried out because: (i) the combination of tens of land use classes and respective habitat proportions resulted in more than 9000 unique attributes (classes) in our study areas, thus rendering a manual reclassification intractable and error prone; and (ii) the genetic algorithm implemented in ResistanceGA (**Supplementary Text C4 in Appendix C**) to parameterize categorical resistance surfaces is computationally very intensive even with a small number of categorical classes (*e.g.* 5-10).

Based on the aforementioned studies in *S. salamandra*, the reclassified land use classes hypothesized to promote genetic connectivity were: (1) natural forests (LC_FORE); (2) scrublands (LC_SCRU); and (3) continental wetlands (LC_WET). Conversely, the reclassified land use classes hypothesized to hamper gene flow were: (4) plantations of exotic trees (LC_PLT); (5) open areas with little or no vegetation (LC_OPEN); (6) agricultural areas (LC_AGRI); and (7) urban areas (LC_URB). Additionally, we also devised two compound land use classes that represent different combinations of these seven land use categories: (8) heterogeneous areas exhibiting a mixture of habitat types putatively enhancing and hampering genetic connectivity (LC_HETE); and (9) disturbed areas containing a mixture of multiple land use classes that putatively hinder gene flow (LC_DTBR). We followed a hierarchical set of criteria to reclassify each polygon into one of the nine mentioned classes:

1 – A polygon containing > 50% of a particular land use class (see **Table C1 in Appendix C**) was reclassified into that specific class (LC_FORE, LC_SCRU, LC_WET, LC_AGRI, LC_URB, LC_PLT, or LC_OPEN). For instance, a polygon exhibiting >50% of natural forests was reclassified into LC_FORE.

2-A polygon exhibiting a cumulative proportion ≥ 50% of putatively suitable habitat types (*i.e.* LC_FORE, LC_SCRU, or LC_WET) was reclassified into LC_HETE.

3-A polygon containing a cumulative proportion >50% of putatively unsuitable habitat types (*i.e.* LC_AGRI, LC_URB, LC_PLT, or LC_OPEN) was reclassified into LC_DTBR.

4-Polygons exhibiting > 50% of land use classes describing brackish and/or saltwater aquatic systems (*e.g.* ocean, estuaries, coastal wetlands) were not included in our analyses and were coded as “no data”. This is because there is no evidence of dispersal (and tolerance) across saltwater systems in *S. salamandra* (see Velo-Antón and Buckley 2015; Lourenço *et al.* 2018b).

Moreover, additional modifications in the reclassified SIOSE_LC were performed for the landscape plot studied in Galicia (*i.e.* the larviparous plot). Galicia is extensively covered by plantations of exotic trees, such as eucalyptus (*Eucalyptus* spp.) and pine (*Pinus* spp.), because timber harvest is an important economic activity in NW Iberia (Ministerio de Medio Ambiente, y Medio Rural y Marino de España 2007; Deus *et al.* 2018). This information, together with in situ observations of the authors (AL and GVA), led to the conclusion that the reclassified SIOSE_LC for Galicia was largely underestimating the area covered by planted exotic trees (this land use class occupied only ca. 4%). To minimize this issue, a fine-scale vectorial land cover data from Información Xeográfica de Galicia was downloaded (http://mapas.xunta.gal/visores/ocupaciondosolo/; hereafter IXG). From the IXG, polygons representing exotic tree plantations were selected and used to create an independent vectorial layer illustrating solely this land use type in the larviparous plot. Polygons in the reclassified SIOSE_LC that overlapped > 50% in their extent with the plantations polygons derived from the IXG were reclassified into LC_PLT through the QGIS plugin Select Within (Vesanto 2018). Unfortunately, a similar procedure could not be performed for the pueriparous plot in Asturias, once vectorial data similar to the IXG is not available for this region. However, the percentage of area occupied by plantations of exotic trees in Asturias is about 2-3 times lower than Galicia, and mostly concentrated to north of our study area (Montero and Serrada 2013). Therefore,

the putative inability of the SIOSE_LC in correctly identifying areas of plantations is likely not so severe in Asturias as in Galicia. Finally, the vectorial data sets were rasterized for downstream landscape analyses using the option Rasterize in Quantum GIS v3.2.3 (QGIS Development Team 2018).

Supplementary Text C2

Besides landscape composition, landscape configuration (*i.e.* size and arrangement of patches) is also an important determinant of patterns of population genetic structure (*e.g.* Cushman *et al.* 2012; Millette and Keyghobadi 2015). Hence, this parameter should also be evaluated to assure that both larviparous and pueriparous plots show relatively analogous landscape contexts. We compared patch configuration in the studied regions from a functional perspective, *i.e.* we compared the arrangement of habitat types that putatively enhance gene flow and those that likely hinder genetic connectivity in *S. salamandra*. From the reclassified vectorial land use layer (nine categories in total; Supplementary Text C1 in Appendix C), we considered natural forests, scrublands, and continental wetlands as land use classes promoting dispersal in *S. salamandra*, while the six remaining land use classes were considered as hampering dispersal and gene flow (*e.g.* Velo-Antón and Buckley 2015; Lourenço *et al.* 2017; Antunes *et al.* 2018; Lourenço *et al.* 2018a). Following this classification, "suitable" habitat classes (*i.e.* forests, scrublands, and wetlands) were coded as 1, while land cover classes potentially hampering gene flow ("unsuitable") were coded as 2. Then, we generated binary raster layers (1-suitable habitat, 2-unsuitable habitat) at different pixel sizes (5 m, 20 m, 50 m, and 100 m) for each sampling region to compare patterns of habitat fragmentation at multiple scales between the larviparous and the pueriparous plots.

We used FRAGSTATS 4.2 (McGarigal *et al.* 2012) to calculate landscape metrics for the aforementioned binary raster layers. These metrics describe different spatial properties of the landscape, such as patch area and edges, patch shape, core areas, contrast, and aggregation (see FRAGSTATS's manual for more information about these landscape attributes). We compared a total of nine uncorrelated class-level landscape metrics: (i) edge density (ED); (ii) perimeter-area fractal dimension (PAFRAC); (iii) area-weighted mean of the core area index (CAI_AM); (iv) total edge contrast index (TECI); (v) area-weighted mean of the edge contrast index (ECON_AM); (vi) coefficient of variation of the proximity index (PROX_CV); (vii) clumpiness (CLUMPY); (viii) landscape shape index (LSI); and (ix) normalized landscape shape index (nLSI) (see Wang *et al.* 2014). We used default options to calculate them, with the exception of TECI, ECON_AM, and PROX_CV. The former two metrics describe landscape contrast, which refers to the magnitude of difference between adjacent habitat types

regarding ecological processes relevant to the organisms of interest (McGarigal *et al.* 2012). We set a high contrast value of 0.75 (ranges from 0 to 1) between "suitable" vs. "unsuitable" habitats. The latter metric (*i.e.* PROX_CV) requires the input of a search radius. We set a search radius of 500 m because previous ecological studies showed that most *S. salamandra* individuals disperse less than this distance threshold (Schulte *et al.* 2007; Ficetola *et al.* 2012; Hendrix *et al.* 2017). Comparisons were restricted to the same habitat type (*e.g.* "suitable" vs. "suitable") and pixel size between both landscape plots. Most of these metrics do not have any associated measure of error or confidence intervals, as only a single landscape per reproductive mode was analysed. To quantify the relative difference in a given metric between the larviparous and pueriparous plots, we calculated the percentage of difference between landscape metric values using the following formula:

$$\frac{|m_L - m_P|}{\frac{m_L + m_P}{2}} \times 100$$

where m_L and m_P are the values of a given landscape metric for the larviparous and pueriparous plots, respectively.

Supplementary Text C3

A total of 17 raster layers (environmental variables) representing land use, topography, and vegetation cover were generated for each landscape plot and analysed with the R (R Core Team 2018) package *ResistanceGA* 4.0-14 (Peterman 2018). Common to all variables, each raster layer was cropped to the extent of each landscape plot under study and resampled to a 100-m resolution to make optimization of resistance surfaces tractable. All methodological treatments were performed in Quantum GIS 3.2.3 unless stated otherwise.

1-Land use (8 environmental layers): Land use composition and configuration has a major impact on the genetic connectivity of many amphibian populations, with agricultural and urban areas often hindering gene flow (*e.g.* Cushman 2006; Johansson *et al.* 2007; Arntzen *et al.* 2017; Lourenço *et al.* 2017). Preliminary univariate optimization analyses in *ResistanceGA* showed that the final reclassified 9-class SIOSE_LC layer exhibited lower statistical support than the five categorical binary layers representing presence/absence of the most abundant land use classes (*i.e.* natural forests, scrublands, plantations of exotic trees, agricultural areas, and urban settlements; **Table C4 in Appendix C**). It is possible the SIOSE_LC layer contained

classes poorly associated with genetic differentiation and/or underrepresented in the study areas, which likely decreased the overall statistical support for this variable and could have led to spurious conclusions regarding the effects of land cover on population genetic differentiation. Bearing this in mind, and the fact that complex categorical layers (*i.e.* exhibiting several categories) increase substantially computational time in *ResistanceGA*, we discarded this variable and used instead the five binary layers for downstream landscape analyses.

Previous studies have also demonstrated that linear landscape features, such as roads and rivers, may impose strong barriers to gene flow (*e.g.* Marsh *et al.* 2007; Richardson, 2012; McCartney-Melstad *et al.* 2018). However, although the original SIOSE data set contains more than 100 land use classes, it does not represent adequately these linear features. In addition to this, the large pixel size (100 m) used in this study further contributes to a poor representation of these linear landscape elements in raster surfaces. Accordingly, we calculated three additional raster layers displaying: (i) the density of paved roads; (ii) density of water courses (includes small streams and large rivers); and (iii) density of water courses exhibiting a Strahler rank ≥ 3 (*i.e.* large rivers). We first downloaded polyline vectorial data sets from other sources representing more accurately these landscape features. A vectorial layer illustrating the network of paved roads in Spain was downloaded from the *Centro Nacional de Información Geográfica* (CNIG; http://centrodedescargas.cnig.es/CentroDescargas/index.jsp), while the hydric network of Spain was accessed from the Ministerio para la Transición Ecológica (https://www.miteco.gob.es/es/cartografia-y-sig/ide/descargas/agua/red-hidrografica.aspx). To identify large rivers, a vectorial layer representing the hydric network of Europe was obtained from the European Environment Agency (EEA Catchments and Rivers Network System v1.1 database; https://www.eea.europa.eu/data-and-maps/data/european-catchments-and-rivers-network#tab-european-data). From this data set, the Strahler stream order classification (Strahler 1957) was employed to identify large rivers. Water courses exhibiting a Strahler rank ≥ 3 were selected, as these water courses have generally a width > 5 m (Downing et al. 2012). Subsequently, the *Line density* tool, implemented in ArcGIS 10.1 (ESRI 2012), was used to estimate densities of these linear landscape elements within a cell search radius of 500 m. This distance threshold was chosen because previous ecological studies demonstrated that most *S. salamandra* individuals disperse less than 500 m (Schulte *et al.* 2007; Ficetola *et al.* 2012; Hendrix *et al.* 2017).

2-Topography (5 environmental layers): Topography is known to influence the distribution and genetic connectivity of a wide variety of amphibian populations (*e.g.* Velo-Antón *et al.* 2013; Gutiérrez-Rodríguez *et al.* 2017; Sánchez-Montes *et al.* 2018). We produced a total of

five raster layers displaying topographic complexity, and climatic conditions directly associated with topography, namely: (i) altitude; (ii) slope; (iii) topographic wetness index (TWI), which describes patterns of water accumulation on the landscape; (iv) wind exposition index, because wind can inhibit dispersal activity (Velo-Antón and Buckley, 2015); and (v) potential incoming solar radiation, which, at high levels, may negatively affect individual fitness (*e.g.* Alton and Franklin 2017). Digital elevation models (DEMs) at a 5-m resolution were downloaded from the CNIG for the areas of interest and resampled to a 100-m resolution to obtain a surface representing altitude (http://centrodedescargas.cnig.es/CentroDescargas/index.jsp). From these DEMs, slope was calculated using the QGIS tool *GDAL Slope* with default options. TWI was derived from two input layers: (1) slope; and (2) catchment area (describes the accumulation of water across the landscape). Catchment area was calculated from DEMs through the "deterministic" algorithm implemented in the QGIS tool SAGA *Catchment area*. Then, we used the QGIS tool *SAGA wetness index* (default options) to estimate TWI. Moreover, DEMs were also employed to create raster layers representing WEI and solar radiation in SAGA 2.3.2 (Conrad *et al.* 2015). The former was calculated using the tool *Wind exposition index* (default options), while the latter was estimated using the option *Potential Incoming Solar Radiation*. In this study, the averaged solar radiation layer in each landscape plot was estimated over the period in which sampling was performed (larviparous plot - from 1st January 2011 until 15th October 2018; pueriparous plot – from 21st November 2013 until 24th May 2018). Insolation values were extracted every two days within 2-hour intervals.

3-Vegetation cover (4 environmental layers): We used the Enhanced Vegetation Index (EVI) and the Normalized Difference Water Index (NDWI) to characterize patterns of vegetation cover and vegetation water content, respectively. These indexes have been applied successfully to unveil how aspects of vegetation structure and composition influence genetic connectivity in amphibians (*e.g.* Gutiérrez-Rodríguez *et al.* 2017). Both measures were derived from an annual time series of Landsat-8 images for the year 2017 and were processed in Google Earth Engine cloud-based platform (Gorelick *et al.* 2017). EVI was selected in detriment of the commonly employed Normalized Difference Vegetation Index, because it shows a higher sensitivity over high-biomass regions and a greater vegetation monitoring ability through the decoupling of the canopy background signal and reduction of the atmospheric influence (Huete *et al.* 2002; Didan *et al.* 2015). EVI spectral vegetation index is calculated as:

$$EVI = 2.5 \times \frac{NIR - Red}{NIR + 6 \times Red - 7.5 \times Blue + 1}$$

where NIR, Red, and Blue are the near-infrared band (B5), the red band (B4) and the blue band (B2) from Landsat-8, respectively. EVI is extensively used in ecological applications and provides a continuous measure related to vegetation canopy characteristics such as biomass, leaf area index, and percentage of vegetation cover. This index varies from -1 (non-vegetated/artificial surfaces) up to 1 (for densely vegetated areas).

Complementarily, we used the NDWI vegetation water content (VWC; Gao 1996) index which varies from -1 (indicative of low VWC) up to 1 (signalling high VWC). This spectral index is calculated as:

$$NDWI = \frac{NIR - MIR}{NIR + MIR}$$

This index captures the difference between reflectance levels in the near-infrared (NIR, band B5) and the mid-infrared channel (MIR, band B6; often known more generally as SWIR shortwave infrared) which is typically used for water detection and mapping.

The image time series, used to calculate both indices, was composed by 55 images in the larviparous plot and 21 image scenes for the pueriparous plot. These images were cloud-masked and temporally aggregated using a median reducer to improve signal and reduce seasonal influences. The original resolution of this multi-temporal image composite was 30 m. We aggregated the composite images of EVI and NDWI for each study area to a 100-m pixel size using both the spatial average (capturing vegetation and VWC amount) and the standard deviation (capturing heterogeneity in vegetation levels and land cover). Accordingly, a total of four raster layers were included in landscape genetics analyses: (i) averaged EVI; (ii) standard deviation of EVI; (iii) averaged NDWI; and (iv) standard deviation of NDWI.

Supplementary Text C4

Briefly, the genetic algorithm implemented in *ResistanceGA* processes one or more environmental layers simultaneously, as follows (see Peterman 2018 for more details):

Step 1 – if continuous, the raw input layer is rescaled to an interval of 0-10;

Step 2 – transformation of the rescaled continuous or categorical layer(s) into a resistance surface within a specified range of starting parameters (*e.g.* equation parameters, type of transformations, interval of resistance values to be assessed; see Peterman 2018). The

algorithm randomly chooses the starting parameters within the specified range. There are eight types of transformations (Monomolecular and Ricker) available in *ResistanceGA* that can be applied to continuous layers and convert them into resistance surfaces (**Supplementary Figure C7 in Appendix C**). Categorical variables (≤ 15 unique levels) are optimized by holding the resistance value of one level constant, while different resistance values are assigned to remaining levels.

Step 3 – the optimized resistance surface is used to calculate a pairwise cost-distance (*e.g.* least cost path or circuit-based) matrix between sampled locations;

Step 4 - fit of a linear mixed effects model with maximum likelihood population effects (MPLE) between matrices of pairwise cost-distances (predictor) and pairwise genetic (response) distances;

Step 5 - estimation of an objective function (*e.g.* Akaike Information Criterion, AIC) from the fitted MPLE model;

Step 6 - steps 2-5 are repeated until the specified number of optimized resistance surfaces have been generated in a given iteration;

Step 7 - optimized resistance surfaces exhibiting the best fit with genetic data are carried over to the next iteration (*e.g.* the 5% exhibiting the lowest AIC);

Step 8 - steps 2-7 are repeated until all specified iterations are processed.

Supplementary Text C5

We first performed a single surface optimization for each of the 17 environmental data layers and the four neutral landscape models. We evaluated all possible surface transformations for continuous layers (**Supplementary Figure C7 in Appendix C**), and the algorithm was allowed to explore resistance values up to 2000 for both categorical and continuous variables. The predictor pairwise cost-distance matrices were calculated using the *commuteDistance* function implemented in the R package *gdistance* 1.2-2 (van Etten 2017). Similarly to resistance distances (McRae 2006), the commute distances are estimated using the analogy with an electrical circuit. It was demonstrated that both distance measures are functionally equivalent in undirected graphs, differing only in their scaling (Kivimäki *et al.* 2014). Nonetheless, commute distances were chosen over resistance distances because the former is computationally more efficient (Peterman 2018). Moreover, because both genetic differentiation metrics (F_{ST} and D_{EST}) are highly correlated in the study regions (*Mantel's r* > 0.88), we used only the population pairwise F_{ST} as a response variable to make optimization tractable. The algorithm ran for a maximum of 500 iterations (200 in the case of multiple surface optimization) or 25 consecutive iterations without improvement in the Akaike Information

Criterion (AIC). The probability of mutation and crossover were set to 0.25 and 0.90, respectively, as preliminary runs showed the optimization was ending too quickly (see *ResistanceGA* manual). Finally, we incorporated two additional null models to examine model performance: (i) a distance model, to test for isolation-by-distance (IBD); and (ii) an intercept-only model. Model performance was examined through AIC corrected for small sample sizes (AICc), and models were ranked according to ΔAICc (the difference in AICc between a given model and the top-ranked model).

Supplementary Table C1

Table C1 SIOSE (Sistema de Información sobre Ocupación del Suelo de España) land use classes that were reclassified for the present study (Reclassified code).

SIOSE code	Description	Reclassified code
FDC	Broad-leaf forest	Natural forests (LC_FORE)
FDP	Perennial forests	Natural forests (LC_FORE)
CNF	Coniferous forests	Natural forests (LC_FORE)
MTR	Scrublands	Scrublands (LC_SCRU)
HPA	Marshes	Continental wetlands (LC_WET)
HTU	Peat bogs	Continental wetlands (LC_WET)
ACU	Water courses	Continental wetlands (LC_WET)
ALG	Lakes and lagoons	Continental wetlands (LC_WET)
AEM	Water reservoirs	Continental wetlands (LC_WET)
FDCpl	Plantations of exotic broad-leaf trees	Plantations of exotic trees (LC_PLT)
FDPpl	Plantations of exotic perennial trees	Plantations of exotic trees (LC_PLT)
CNFpl	Plantations of exotic conifers	Plantations of exotic trees (LC_PLT)
PDA	Beaches and dunes	Areas with little or no vegetation (LC_OPEN)
SDN	Bare soil	Areas with little or no vegetation (LC_OPEN)
ZQM	Burnt areas	Areas with little or no vegetation (LC_OPEN)
GNP	Glaciers / permanent snow	Areas with little or no vegetation (LC_OPEN)
RMB	Dry stream bed	Areas with little or no vegetation (LC_OPEN)
ACM	Marine cliffs	Areas with little or no vegetation (LC_OPEN)
ARR	Rocky outcrops	Areas with little or no vegetation (LC_OPEN)
CCH	Rocky outcrops	Areas with little or no vegetation (LC_OPEN)
CLC	Rocky outcrops	Areas with little or no vegetation (LC_OPEN)
PMX	Mines	Areas with little or no vegetation (LC_OPEN)
CHA	Rice plantations	Agricultural areas (LC_AGRI)
CHL	Other herbaceous plantations	Agricultural areas (LC_AGRI)

Table C1 Continued.

SIOSE code	Description	Reclassified code
LFC	Citrus orchards	Agricultural areas (LC_AGRI)
LFN	Non-citrus orchards	Agricultural areas (LC_AGRI)
LVI	Vine yards	Agricultural areas (LC_AGRI)
LOL	Olive yards	Agricultural areas (LC_AGRI)
LOC	Other cultivated woody plantations	Agricultural areas (LC_AGRI)
PRD	Meadow	Agricultural areas (LC_AGRI)
PST	Pastures	Agricultural areas (LC_AGRI)
OVD	Mosaic of vine and olive yards	Agricultural areas (LC_AGRI)
AAR	Residential agricultural settlement	Agricultural areas (LC_AGRI)
UER	Kitchen garden	Agricultural areas (LC_AGRI)
PAG	Agricultural / Livestock	Agricultural areas (LC_AGRI)
EDF	Buildings	Urban areas (LC_URB)
ZAU	Urban green areas	Urban areas (LC_URB)
LAA	Artificial water course	Urban areas (LC_URB)
VAP	Parking space and/or pedestrian areas	Urban areas (LC_URB)
OCT	Other buildings	Urban areas (LC_URB)
SNE	Bare soil without buildings	Urban areas (LC_URB)
ZEV	Dumping areas	Urban areas (LC_URB)
UCS/UEN/UDS	Mixed urban areas	Urban areas (LC_URB)
IPO/IPS/IAS	Industrial polygons	Urban areas (LC_URB)
PFT	Mixture of urban and forested areas	Urban areas (LC_URB)
PPS	Fish farms	Urban areas (LC_URB)
TCO/TCH	Recreational buildings	Urban areas (LC_URB)
TPR/TCG	Recreational areas	Urban areas (LC_URB)

Table C1 Continued.

SIOSE code	Description	Reclassified code
EAI/ESN/ECM	Other public and private buildings	Urban areas (LC_URB)
EDU/EPN/ERG	Other public and private buildings	Urban areas (LC_URB)
ECL/EDP/ECG	Other public and private buildings	Urban areas (LC_URB)
EPU	Other public and private buildings	Urban areas (LC_URB)
NRV	Roads	Urban areas (LC_URB)
NRF	Railways	Urban areas (LC_URB)
NPO	Harbours	Urban areas (LC_URB)
NAP	Airports	Urban areas (LC_URB)
NEO/NSL/NCL	Infrastructures related with energy	Urban areas (LC_URB)
NEL/NTM	Infrastructures related with energy	Urban areas (LC_URB)
NHD/NGO	Infrastructures related with energy	Urban areas (LC_URB)
NTC	Infrastructures related with communications	Urban areas (LC_URB)
NDP/NDS/NCC	Water treatment infrastructures	Urban areas (LC_URB)
NVE/NPT	Waste treatment infrastructures	Urban areas (LC_URB)
HMA/HSM	Coastal salt marshes	No data
ALC/AES/AMO	Coastal lagoons, estuaries, and ocean	No data

Supplementary Table C2

Table C2 Area occupied (in km^2 and percentage [%]) by the nine reclassified land use types in the larviparous and pueriparous plots. The asterisks denote land use classes differing in more than 5% in occupied area between the analysed landscape plots.

Class	Larviparous plot	Pueriparous plot
	Area (km^2 [%])	**Area (km^2 [%])**
Agricultural*	310.2 [22.5]	713.2 [40.0]
Scrublands	331.1 [24.1]	428.8 [24.0]
Forests	232.1 [16.9]	347.0 [19.5]
Plantations*	303.9 [22.1]	123.7 [6.9]
Urban	129.4 [9.4]	80.9 [4.5]
Open areas	21.9 [1.6]	30.1 [1.7]
Disturbed	32.0 [2.3]	28.0 [1.6]
Heterogeneous	10.5 [0.7]	23.5 [1.3]
Wetlands	5.3 [0.4]	8.6 [0.5]
Total	1376.4	1783.8

Supplementary Table C3

Table C3 Landscape metrics calculated for the binary raster layers representing putative unsuitable (U) and suitable (S) habitats for *S. salamandra*. These analyses were performed independently for each landscape plot (_larv – larviparous; _puer – pueriparous) and at multiple spatial grains (pixel size: 5 m, 20 m, 50 m, and 100 m). The percentage of difference in landscape metric values of unsuitable (U%) and suitable (S%) habitats between the larviparous and pueriparous plots is also displayed. Those values showing a percentage of difference ≥ 5 are in bold.

Hab_class	ED	LSI	PAFRAC	CAI_AM	PROX_CV	TECI	ECON_AM	CLUMPY	nLSI
5 m									
U_larv	45.0	70.6	1.4	89.2	205.5	71.3	70.9	0.98	0.01
U_puer	39.8	81.6	1.4	88.5	213.6	74.2	74.1	0.98	0.01
U%	**12.2**	**14.5**	0.1	0.8	3.9	3.9	4.4	0.2	6.3
S_larv	45.0	80.8	1.4	85.4	354.2	74.2	74.3	0.97	0.02
S_puer	39.8	91.9	1.4	85.5	394.0	74.3	74.2	0.98	0.02
S%	**12.2**	**12.8**	0.8	0.0	**10.6**	0.1	0.1	0.1	0.6
20 m									
U_larv	43.0	67.5	1.3	100.0	142.1	71.3	70.8	0.91	0.05
U_puer	38.2	78.4	1.3	100.0	149.7	74.1	74.1	0.92	0.05
U%	**11.8**	**14.9**	1.3	0.0	**5.2**	3.9	4.5	0.9	**7.0**
S_larv	43.0	77.3	1.4	100.0	242.4	74.2	74.2	0.90	0.06
S_puer	38.2	88.3	1.4	100.0	203.0	74.3	74.2	0.91	0.06
S%	**11.8**	**13.2**	0.7	0.0	**17.7**	0.2	0.0	0.6	0.2
50 m									
U_larv	35.9	56.6	1.4	100.0	124.4	71.0	70.7	0.81	0.10
U_puer	33.5	68.8	1.4	100.0	134.7	74.0	73.9	0.82	0.11
U%	**6.9**	**19.5**	1.5	0.0	**8.0**	4.2	4.4	1.1	**11.9**
S_larv	35.9	64.7	1.5	100.0	236.5	74.0	74.0	0.80	0.13
S_puer	33.5	77.4	1.5	100.0	170.9	74.2	74.1	0.80	0.14
S%	**6.9**	**17.8**	0.4	0.0	**32.2**	0.3	0.1	0.2	4.7
100 m									
U_larv	27.8	44.1	1.5	100.0	141.0	70.3	70.0	0.71	0.15
U_puer	26.6	54.9	1.5	100.0	151.3	73.7	73.7	0.72	0.18
U%	4.2	**21.8**	1.6	0.0	**7.0**	4.8	5.0	1.1	**14.4**
S_larv	27.8	50.4	1.5	100.0	250.6	73.6	73.8	0.69	0.21
S_puer	26.6	61.8	1.5	100.0	183.2	74.0	73.9	0.68	0.22
S%	4.2	**20.2**	0.7	0.0	**31.0**	0.6	0.2	0.8	**7.1**

ED – edge density; LSI – landscape shape index; PAFRAC – perimeter-area fractal dimension;
CAI_AM – area-weighted mean of the core area index; PROX_CV – coefficient of variation of the proximity index; TECI – total edge contrast index; ECON_AM – area-weighted mean of the edge contrast index;
CLUMPY – clumpiness; nLSI – normalized landscape shape index

Supplementary Table C4

Table C4 Model ranking of six land use layers preliminarily assessed in *ResistanceGA*. Variables were ranked according to the Akaike Information Criterion corrected for small sample sizes (AICc). We tested the following surfaces: AGRIC (presence/absence of agricultural areas), FOREST (presence/absence of forests), PLANT (presence/absence of plantations of exotic trees), SCRUB (presence/absence of scrublands), URBAN (presence/absence of urbanized areas), and TOTAL_LC9 (9-class reclassified land use layer). Binary categorical layers exhibited a higher support in both landscape plots compared to the 9-class layers.

Larviparous plot		**Pueriparous plot**	
Variable	**AICc**	**Variable**	**AICc**
AGRIC	-1642.7	AGRIC	-859.7
PLANT	-1634.0	URBAN	-847.9
SCRUB	-1633.5	FOREST	-847.9
FOREST	-1633.1	PLANT	-847.4
URBAN	-1628.3	SCRUB	-846.8
TOTAL_LC9	-1595.6	TOTAL_LC9	-801.0

Supplementary Table C5

Table C5 Number and distribution of haplotypes inferred from the amplified cyt b fragment (665 bp) for each sampled larviparous (L) and pueriparous (P) population. The following parameters are displayed: nseq (number of amplified sequences), nhap (number of distinct haplotypes), code_hap (numeric code of each haplotype found in a population), and hap_group (haplogroup assigned to each haplotype). No sequences were successfully amplified for population LOUR. For more information about the frequencies of haplotypes in each sampled locality check **Figures 4.2-4.3** in the main text.

locality	code	reproduction	nseq	nhap	code_hap	hap_group
Moaña (Rego da Pega)	PEGA	L	6	3	20, 23, 24	A
Cuartos de Borbén	BORB	L	8	1	24	A
Redondela	REDO	L	4	2	24, 29	A
Soutoxuste	XUST	L	7	1	24	A
Soutomaior	SOUT	L	6	2	24, 25	A
Encoro de Eiras	EIRA	L	8	2	24, 25	A
Cotorredondo	COTO	L	7	3	23, 24, 25	A
Canicouva	CANI	L	8	2	24, 28	A
Tabuadelo	TABU	L	6	1	24	A
Lourizán	LOUR	L	-	-	-	-
Pontevedra, El Campillo	CAMP	L	8	1	24	A
Paradela	PARA	L	8	3	22, 24, 27	A
Sanxenxo	XENX	L	5	2	18 ,20	A
Pontevedra, O Vao	OVAO	L	7	2	24, 28	A
Pontevedra, Río Lérez	LREZ	L	7	2	24, 30	A
Calvelo	CALV	L	8	2	24, 28	A
Castrove	CAST	L	2	1	24	A
Ribadumia	RIBA	L	3	2	20, 24	A
Pontillón de Castro	PTCT	L	8	1	24	A
Monte Lobeira	LOBE	L	3	2	20, 24	A
Río Barosa	BARO	L	6	1	24	A
Campo Lameiro	LAME	L	8	2	24, 26	A
	Total		**133**			
Soto de los Infantes	INFA	P	7	3	13, 19*, 24*	B, A*
Villanueva	VNUE	P	8	3	1§, 13, 24*	B, A*, C§
Cornellana	CORN	P	8	2	13, 24*	B, A*
Restiello	REST	P	6	1	13	B
Yernes	YERN	P	8	3	5§, 6§, 12	B, C§
Cutiellos	CUTI	P	8	3	12, 13, 14	B
San Padru	PADR	P	8	5	3§, 10§, 12, 13, 14	B, C§
Panizal	PZAL	P	8	4	4§, 7§, 8§, 20*	A*, C§
Baselgas	BASE	P	7	5	7§, 8§, 12, 16, 21*	B, A*, C§
Bohiles	BOHI	P	7	1	13	B
Bolgues	BOLG	P	8	4	1§, 8§, 12, 13	B, C§
Los Cruces	CCES	P	7	4	7§, 8§, 11§, 20*	A*, C§
Trubia	TRUB	P	8	4	1§, 9§, 13, 15	B, C§
Brañes	BRAN	P	7	2	1§, 13	B, C§
Posada	POSA	P	8	3	2§, 3§, 13	B, C§
Villamar	VMAR	P	2	1	13	B
Oviedo, San Miguel de Lillo	LILL	P	3	2	1§, 13	B, C§
Arroyo de Bendones	BEND	P	1	1	17	B
	Total		**119**			

Supplementary Table C6

Table C6 Matrix of pairwise genetic differentiation among larviparous populations. Below and above the diagonal are pairwise F_{ST} and Jost's D_{EST}, respectively. Significant values are in bold.

	PEGA	BORB	REDO	XUST	SOUT	EIRA	COTO	CANI	TABU	LOUR	CAMP	PARA	XENX	OVAO	LREZ	CALV	CAST	RIBA	PTCT	LOBE	BARO	LAME
PEGA	0	**0.07**	**0.09**	**0.07**	**0.13**	**0.12**	0.02	0.04	**0.09**	0.06	0.05	**0.08**	**0.16**	**0.08**	**0.10**	**0.06**	**0.05**	**0.08**	**0.11**	**0.15**	**0.07**	**0.09**
BORB	**0.03**	0	0.05	0.03	0.03	**0.06**	**0.10**	**0.09**	0.05	**0.10**	0.04	0.04	**0.12**	**0.08**	0.05	**0.06**	**0.05**	**0.07**	**0.08**	**0.14**	**0.09**	**0.10**
REDO	**0.03**	**0.03**	0	0.05	0.06	**0.07**	**0.11**	**0.08**	**0.08**	0.02	0.04	**0.08**	**0.19**	**0.08**	0.05	0.04	0.06	**0.11**	**0.10**	**0.12**	**0.07**	**0.08**
XUST	**0.02**	**0.02**	**0.02**	0	0.00	0.02	0.01	0.01	0.05	0.01	0.05	0.01	**0.14**	0.07	0.03	**0.06**	0.00	**0.06**	**0.08**	**0.12**	**0.07**	0.04
SOUT	**0.03**	0.01	0.02	0.01	0	0.02	**0.13**	0.04	**0.09**	0.06	**0.07**	0.00	**0.13**	0.06	0.04	0.06	0.07	**0.09**	**0.10**	0.04	**0.12**	0.07
EIRA	**0.03**	**0.02**	**0.03**	0.01	0.02	0	0.06	0.05	0.06	0.06	0.05	0.03	**0.16**	0.05	0.03	**0.10**	0.04	**0.09**	**0.09**	**0.16**	**0.08**	0.03
COTO	0.01	**0.04**	**0.03**	0.01	**0.04**	**0.03**	0	0.04	0.03	0.04	0.04	0.04	**0.14**	0.03	0.05	**0.06**	0.04	**0.12**	**0.07**	**0.10**	0.05	**0.07**
CANI	**0.02**	**0.04**	**0.03**	0.01	**0.02**	0.02	**0.02**	0	0.02	0.02	0.01	0.06	**0.13**	0.05	0.04	0.03	0.03	0.02	0.03	0.06	0.05	0.03
TABU	**0.03**	**0.03**	**0.03**	0.02	**0.03**	**0.02**	**0.02**	0.01	0	0.01	0.00	0.02	**0.08**	0.04	0.01	0.01	0.01	0.05	0.03	0.08	0.04	0.01
LOUR	0.02	**0.04**	**0.01**	0.01	0.02	**0.03**	0.02	0.01	0.01	0	0.00	0.02	**0.18**	0.02	0.03	0.01	0.02	0.01	0.04	0.05	0.03	0.01
CAMP	**0.02**	**0.02**	**0.02**	0.02	**0.02**	0.02	**0.02**	0.01	0.00	0.01	0	0.03	**0.14**	0.01	0.00	0.01	0.03	0.06	0.05	0.07	0.02	0.02
PARA	**0.02**	**0.03**	**0.02**	0.01	0.01	0.02	**0.02**	**0.02**	0.01	0.02	0.01	0	**0.13**	0.04	0.01	0.02	0.05	0.04	0.03	0.06	**0.06**	0.03
XENX	**0.06**	**0.08**	**0.07**	**0.06**	**0.07**	**0.08**	**0.06**	**0.06**	**0.07**	**0.07**	**0.06**	**0.07**	0	**0.17**	**0.13**	**0.09**	**0.07**	**0.12**	**0.11**	**0.11**	**0.09**	**0.14**
OVAO	**0.03**	**0.04**	**0.04**	**0.02**	**0.03**	**0.02**	**0.02**	0.02	**0.02**	0.02	0.01	0.02	**0.07**	0	0.04	0.05	0.01	0.02	0.05	0.06	**0.08**	0.05
LREZ	**0.03**	**0.02**	**0.02**	0.01	0.02	0.01	**0.02**	0.01	0.01	0.02	0.00	0.00	**0.07**	0.02	0	0.02	**0.06**	**0.10**	0.04	0.08	0.03	0.03
CALV	**0.03**	**0.03**	**0.02**	**0.02**	**0.02**	**0.03**	**0.03**	**0.02**	0.01	0.01	0.01	0.01	**0.05**	**0.02**	0.01	0	0.02	0.05	0.01	0.03	0.00	0.02
CAST	**0.02**	**0.03**	**0.03**	0.01	**0.03**	**0.02**	0.01	0.01	0.01	0.02	0.01	**0.02**	**0.04**	0.01	**0.02**	0.02	0	0.02	**0.06**	0.05	0.02	0.01
RIBA	**0.03**	**0.04**	**0.04**	**0.03**	**0.04**	**0.04**	**0.04**	0.01	0.02	0.01	**0.02**	0.02	**0.06**	0.02	**0.03**	0.02	0.01	0	0.02	0.02	**0.06**	0.05
PTCT	**0.03**	**0.04**	**0.03**	**0.03**	**0.04**	**0.04**	**0.03**	**0.03**	0.02	**0.03**	0.02	**0.02**	**0.06**	**0.04**	**0.02**	0.01	**0.02**	**0.02**	0	0.03	0.03	0.02
LOBE	**0.04**	**0.06**	**0.04**	**0.03**	**0.03**	**0.05**	**0.04**	0.02	**0.04**	0.02	**0.03**	0.02	**0.06**	0.03	**0.03**	0.02	0.01	0.01	0.03	0	0.02	0.05
BARO	**0.02**	**0.03**	**0.02**	**0.03**	**0.03**	**0.03**	**0.02**	**0.02**	0.02	**0.02**	0.01	**0.02**	**0.05**	**0.03**	0.01	0.00	0.01	**0.02**	0.01	0.01	0	0.02
LAME	**0.03**	**0.04**	**0.03**	0.02	**0.03**	0.02	**0.03**	0.01	0.00	0.02	0.01	0.02	**0.06**	**0.02**	0.01	0.01	0.01	**0.02**	0.02	0.02	0.01	0

Supplementary Table C7

Table C7 Matrix of pairwise genetic differentiation among pueriparous populations. Below and above the diagonal are pairwise FST and Jost's DEST, respectively. Significant values are in bold. All pairwise values are significant except pairwise F_{ST} in population pair BASE/CCES and pairwise D_{EST} in population pairs YERN/PADR, CUTI/PADR, CUTI/BOHI, and BRAN/LILL.

	INFA	VNUE	CORN	REST	YERN	CUTI	PADR	PZAL	BASE	BOHI	BOLG	CCES	TRUB	BRAN	POSA	VMAR	LILL	BEND
INFA	0	**0.09**	**0.18**	**0.17**	**0.24**	**0.20**	**0.30**	**0.21**	**0.23**	**0.19**	**0.37**	**0.19**	**0.21**	**0.22**	**0.26**	**0.46**	**0.20**	**0.33**
VNUE	**0.03**	0	**0.24**	**0.23**	**0.26**	**0.23**	**0.29**	**0.37**	**0.22**	**0.16**	**0.45**	**0.35**	**0.25**	**0.28**	**0.31**	**0.37**	**0.24**	**0.37**
CORN	**0.06**	**0.07**	0	**0.29**	**0.26**	**0.22**	**0.28**	**0.32**	**0.35**	**0.27**	**0.46**	**0.35**	**0.29**	**0.41**	**0.31**	**0.51**	**0.36**	**0.42**
REST	**0.05**	**0.07**	**0.07**	0	**0.20**	**0.11**	**0.08**	**0.17**	**0.22**	**0.16**	**0.39**	**0.20**	**0.29**	**0.28**	**0.24**	**0.48**	**0.30**	**0.24**
YERN	**0.10**	**0.10**	**0.10**	**0.08**	0	**0.10**	0.08	**0.18**	**0.06**	**0.15**	**0.28**	**0.10**	**0.18**	**0.23**	**0.20**	**0.37**	**0.25**	**0.25**
CUTI	**0.06**	**0.06**	**0.06**	**0.04**	**0.04**	0	0.04	**0.23**	**0.13**	0.06	**0.35**	**0.12**	**0.17**	**0.24**	**0.23**	**0.43**	**0.19**	**0.23**
PADR	**0.08**	**0.08**	**0.07**	**0.04**	**0.04**	**0.02**	0	**0.19**	**0.18**	**0.10**	**0.36**	**0.17**	**0.18**	**0.26**	**0.26**	**0.43**	**0.27**	**0.26**
PZAL	**0.08**	**0.10**	**0.10**	**0.09**	**0.06**	**0.07**	**0.06**	0	**0.12**	**0.27**	**0.42**	**0.13**	**0.24**	**0.23**	**0.30**	**0.52**	**0.28**	**0.33**
BASE	**0.08**	**0.08**	**0.10**	**0.08**	**0.03**	**0.04**	**0.05**	**0.04**	0	**0.09**	**0.27**	**0.03**	**0.16**	**0.15**	**0.22**	**0.34**	**0.18**	**0.23**
BOHI	**0.05**	**0.04**	**0.05**	**0.05**	**0.05**	**0.02**	**0.04**	**0.07**	**0.03**	0	**0.27**	**0.08**	**0.10**	**0.13**	**0.15**	**0.26**	**0.08**	**0.20**
BOLG	**0.12**	**0.13**	**0.14**	**0.12**	**0.11**	**0.10**	**0.11**	**0.13**	**0.09**	**0.08**	0	**0.18**	**0.26**	**0.28**	**0.32**	**0.34**	**0.19**	**0.35**
CCES	**0.07**	**0.08**	**0.10**	**0.07**	**0.04**	**0.04**	**0.05**	**0.06**	0.02	**0.03**	**0.07**	0	**0.12**	**0.12**	**0.16**	**0.34**	**0.13**	**0.18**
TRUB	**0.06**	**0.06**	**0.07**	**0.06**	**0.05**	**0.05**	**0.05**	**0.06**	**0.04**	**0.03**	**0.08**	**0.03**	0	**0.10**	**0.27**	**0.33**	**0.16**	**0.16**
BRAN	**0.06**	**0.06**	**0.09**	**0.07**	**0.07**	**0.05**	**0.07**	**0.07**	**0.05**	**0.03**	**0.08**	**0.03**	**0.03**	0	**0.17**	**0.23**	0.07	**0.13**
POSA	**0.08**	**0.09**	**0.09**	**0.08**	**0.08**	**0.07**	**0.08**	**0.10**	**0.07**	**0.05**	**0.10**	**0.06**	**0.06**	**0.05**	0	**0.32**	**0.16**	**0.18**
VMAR	**0.13**	**0.11**	**0.16**	**0.14**	**0.14**	**0.12**	**0.13**	**0.16**	**0.12**	**0.08**	**0.15**	**0.10**	**0.08**	**0.08**	**0.14**	0	**0.29**	**0.39**
LILL	**0.06**	**0.06**	**0.09**	**0.08**	**0.08**	**0.05**	**0.07**	**0.08**	**0.05**	**0.03**	**0.08**	**0.04**	**0.04**	**0.02**	**0.06**	**0.10**	0	**0.11**
BEND	**0.08**	**0.08**	**0.10**	**0.07**	**0.09**	**0.06**	**0.06**	**0.10**	**0.06**	**0.05**	**0.11**	**0.05**	**0.04**	**0.03**	**0.06**	**0.11**	**0.05**	0

Supplementary Table C8

Table C8 Matrix of pairwise correlation among the environmental raster layers tested in the larviparous plot. Information about these layers is displayed in Table 4.2. Values highlighted in bold indicate those pair of variables that are highly correlated (| r | > 0.7).

	AGRIC	ALT	EVI_avg	EVI_sd	FOREST	SOLAR	NDWI_avg	NDWI_sd	PLANT	RIVER_D	ROAD_D	SCRUB	SLP	WATER_D	TWI	URBAN	WEI
AGRIC	1	-0.29	0.23	0.17	-0.24	0.05	-0.20	0.03	-0.29	0.03	0.19	-0.30	-0.31	0.08	0.39	-0.17	-0.30
ALT	-0.29	1	-0.04	-0.37	0.07	0.04	0.19	-0.18	-0.05	-0.19	-0.47	0.41	0.35	-0.06	-0.52	-0.26	0.64
EVI_avg	0.23	-0.04	1	-0.11	0.13	0.23	0.60	-0.23	0.09	0.00	-0.24	-0.11	-0.03	0.17	0.08	-0.36	-0.12
EVI_sd	0.17	-0.37	-0.11	1	-0.05	0.05	-0.35	0.53	-0.13	0.09	0.37	-0.23	-0.26	0.04	0.30	0.30	-0.34
FOREST	-0.24	0.07	0.13	-0.05	1	-0.04	0.25	-0.10	-0.24	0.06	-0.11	-0.25	0.08	0.08	-0.04	-0.15	-0.09
SOLAR	0.05	0.04	0.23	0.05	-0.04	1	-0.15	0.08	-0.10	-0.02	0.00	0.05	-0.20	-0.01	0.08	0.01	0.04
NDWI_avg	-0.20	0.19	0.60	-0.35	0.25	-0.15	1	-0.37	0.34	0.01	-0.48	0.06	0.29	0.13	-0.26	-0.50	0.10
NDWI_sd	0.03	-0.18	-0.23	0.53	-0.10	0.08	-0.37	1	-0.09	-0.04	0.24	-0.03	-0.11	-0.10	0.06	0.23	-0.02
PLANT	-0.29	-0.05	0.09	-0.13	-0.24	-0.10	0.34	-0.09	1	-0.03	-0.13	-0.30	0.13	-0.02	-0.13	-0.17	0.08
RIVER_D	0.03	-0.19	0.00	0.09	0.06	-0.02	0.01	-0.04	-0.03	1	0.01	-0.05	-0.08	0.35	0.23	0.00	-0.35
ROAD_D	0.19	-0.47	-0.24	0.37	-0.11	0.00	-0.48	0.24	-0.13	0.01	1	-0.27	-0.28	-0.09	0.30	0.46	-0.31
SCRUB	-0.30	0.41	-0.11	-0.23	-0.25	0.05	0.06	-0.03	-0.30	-0.05	-0.27	1	0.23	-0.07	-0.33	-0.18	0.39
SLP	-0.31	0.35	-0.03	-0.26	0.08	-0.20	0.29	-0.11	0.13	-0.08	-0.28	0.23	1	-0.07	**-0.72**	-0.19	0.28
WATER_D	0.08	-0.06	0.17	0.04	0.08	-0.01	0.13	-0.10	-0.02	0.35	-0.09	-0.07	-0.07	1	0.34	-0.08	-0.42
TWI	0.39	-0.52	0.08	0.30	-0.04	0.08	-0.26	0.06	-0.13	0.23	0.30	-0.33	**-0.72**	0.34	1	0.20	-0.64
URBAN	-0.17	-0.26	-0.36	0.30	-0.15	0.01	-0.50	0.23	-0.17	0.00	0.46	-0.18	-0.19	-0.08	0.20	1	-0.15
WEI	-0.30	0.64	-0.12	-0.34	-0.09	0.04	0.10	-0.02	0.08	-0.35	-0.31	0.39	0.28	-0.42	-0.64	-0.15	1

Supplementary Table C9

Table C9 Matrix of pairwise correlation among the environmental raster layers tested in the pueriparous plot. Information about these layers is displayed in Table 4.2. No pairs of variables were correlated (i.*e.* | r | < 0.7 for all pairs of variables).

	AGRIC	ALT	EVI_avg	EVI_sd	FOREST	SOLAR	NDWI_avg	NDWI_sd	PLANT	RIVER_D	ROAD_D	SCRUB	SLP	WATER_D	TWI	URBAN	WEI
AGRIC	1	-0.16	0.48	0.15	-0.40	0.18	0.05	-0.03	-0.22	-0.01	0.10	-0.46	-0.34	0.01	0.22	-0.18	-0.10
ALT	-0.16	1	-0.19	-0.31	-0.03	-0.08	-0.20	-0.23	-0.11	-0.31	-0.39	0.31	0.42	-0.35	-0.47	-0.16	0.65
EVI_avg	0.48	-0.19	1	0.04	-0.11	0.56	0.26	-0.14	-0.01	-0.07	-0.09	-0.25	-0.28	0.04	0.11	-0.26	-0.12
EVI_sd	0.15	-0.31	0.04	1	-0.01	0.07	-0.10	0.46	-0.06	0.18	0.33	-0.25	-0.36	0.12	0.37	0.24	-0.28
FOREST	-0.40	-0.03	-0.11	-0.01	1	-0.18	0.15	-0.11	-0.13	0.09	-0.10	-0.28	0.18	0.14	-0.04	-0.11	-0.18
SOLAR	0.18	-0.08	0.56	0.07	-0.18	1	-0.26	0.14	0.03	-0.03	0.15	-0.08	-0.27	-0.01	0.14	0.05	0.02
NDWI_avg	0.05	-0.20	0.26	-0.10	0.15	-0.26	1	-0.28	0.27	-0.04	-0.29	-0.12	0.06	0.11	-0.15	-0.39	-0.08
NDWI_sd	-0.03	-0.23	-0.14	0.46	-0.11	0.14	-0.28	1	0.05	0.08	0.37	-0.11	-0.22	0.01	0.23	0.34	-0.12
PLANT	-0.22	-0.11	-0.01	-0.06	-0.13	0.03	0.27	0.05	1	-0.06	-0.05	-0.15	0.01	0.01	-0.09	-0.06	0.03
RIVER_D	-0.01	-0.31	-0.07	0.18	0.09	-0.03	-0.04	0.08	-0.06	1	0.21	-0.10	-0.01	0.40	0.27	0.10	-0.47
ROAD_D	0.10	-0.39	-0.09	0.33	-0.10	0.15	-0.29	0.37	-0.05	0.21	1	-0.22	-0.38	0.06	0.46	0.53	-0.31
SCRUB	-0.46	0.31	-0.25	-0.25	-0.28	-0.08	-0.12	-0.11	-0.15	-0.10	-0.22	1	0.28	-0.13	-0.29	-0.12	0.33
SLP	-0.34	0.42	-0.28	-0.36	0.18	-0.27	0.06	-0.22	0.01	-0.01	-0.38	0.28	1	-0.06	-0.69	-0.23	0.21
WATER_D	0.01	-0.35	0.04	0.12	0.14	-0.01	0.11	0.01	0.01	0.40	0.06	-0.13	-0.06	1	0.31	-0.01	-0.54
TWI	0.22	-0.47	0.11	0.37	-0.04	0.14	-0.15	0.23	-0.09	0.27	0.46	-0.29	-0.69	0.31	1	0.32	-0.63
URBAN	-0.18	-0.16	-0.26	0.24	-0.11	0.05	-0.39	0.34	-0.06	0.10	0.53	-0.12	-0.23	-0.01	0.32	1	-0.15
WEI	-0.10	0.65	-0.12	-0.28	-0.18	0.02	-0.08	-0.12	0.03	-0.47	-0.31	0.33	0.21	-0.54	-0.63	-0.15	1

Supplementary Figure C1

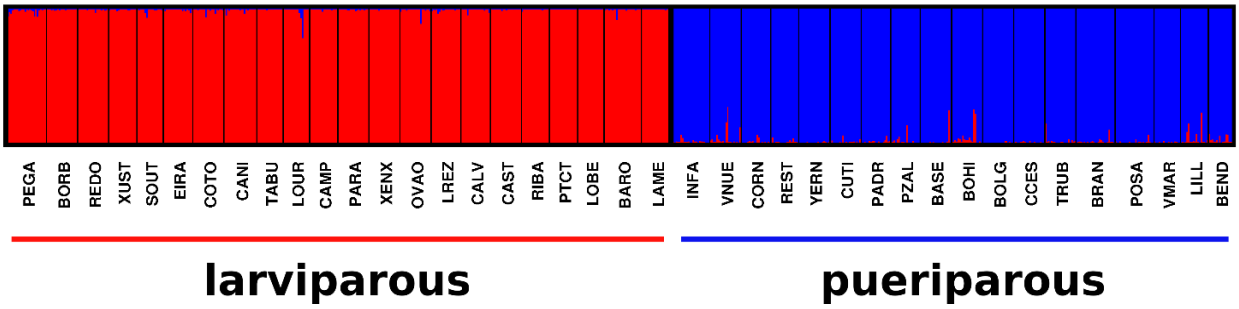

Fig. C1 STRUCTURE's barplot (K=2) displaying patterns of genetic structure between larviparous (red) and pueriparous (blue) fire salamanders. Sampled localities are separated by thin black lines, while the thick black line separates sites where individuals show different reproductive modes. Input parameters used in this preliminary analysis were equal to those described in the main text. This barplot shows that there is not genetic admixture between sampled larviparous and pueriparous populations.

Supplementary Figure C2

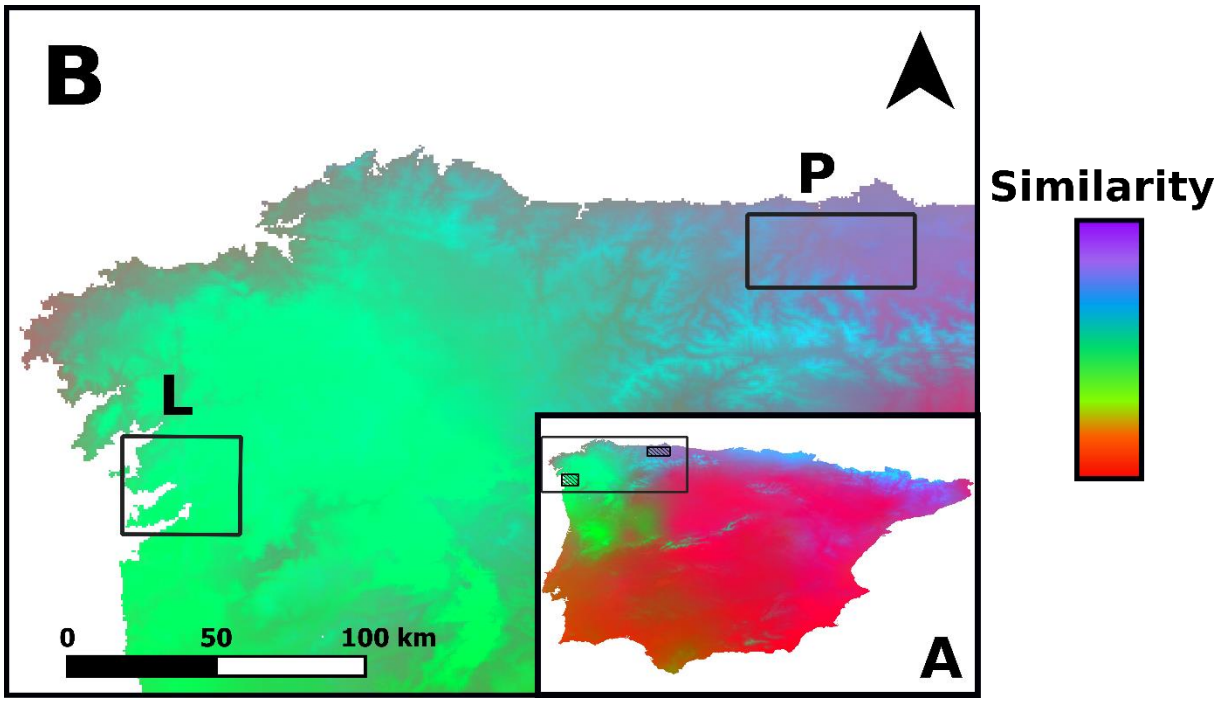

Fig. C2 Composite image of the first three axes (PC1, PC2, and PC3) of a Principal Component Analysis (PCA) performed on 19 bioclimatic layers (related with temperature and precipitation) for the Iberian Peninsula. These bioclimatic layers were downloaded from WorldClim 2.0 (Fick and Hijmans 2017) and the PCA was performed using the QGIS plugin Principal Components (Georgousis and Bruy 2019). (A) PCA of the Iberian Peninsula showing the great environmental heterogeneity of this region. (B) North-western corner of Iberian Peninsula showing climatic similarity in the studied regions (L – larviparous plot; P – pueriparous plot). Although there is some degree of climatic dissimilarity between sampling regions, they both present an Atlantic climate (mild summers and cool winters), which greatly contrast with the Mediterranean climate (dry summers and low annual precipitation) found in central and southern Iberian Peninsula at low elevations.

Supplementary Figure C3

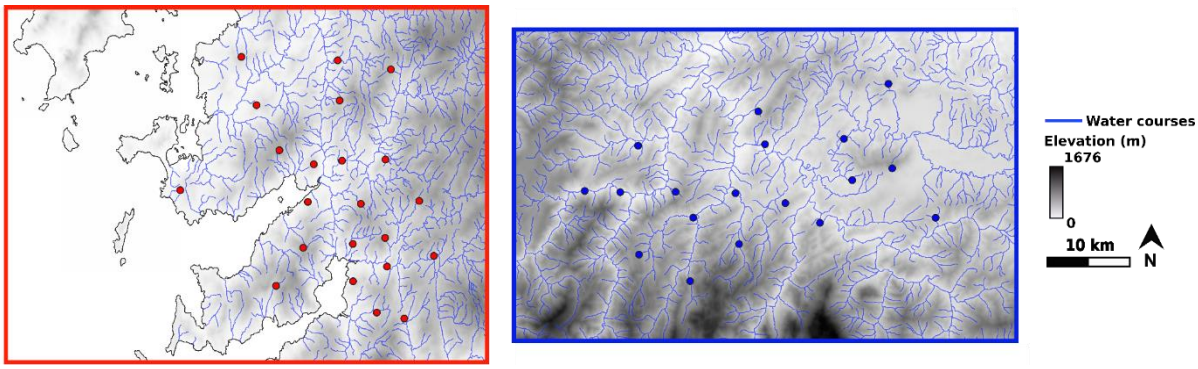

Fig. C3 Topography (elevation) in the larviparous (red box) and pueriparous (blue box) plots, along with respective sampled sites. The pueriparous plot shows a higher altitudinal gradient and topographic complexity, particularly, in its southern part. Hence, we avoided sampling pueriparous populations in the southern section to minimize the potential confounding effects of topographic variation between plots.

Supplementary Figure C4

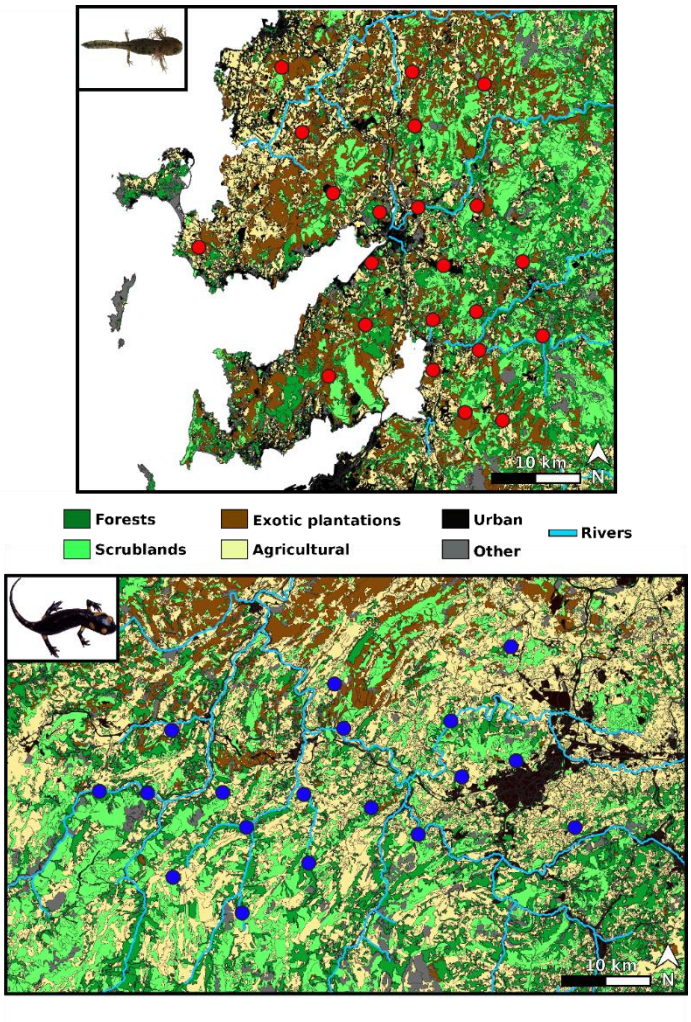

Fig. C4 Land cover composition and configuration of the larviparous (top panel) and pueriparous (bottom panel) plots, along with respective sampled localities (red – larviparous populations; blue – pueriparous populations). The most abundant reclassified land use classes are represented (*i.e.* natural forests, scrublands, plantations of exotic trees, agricultural areas, and urban settlements). The class "Other" represent reclassified land use classes showing a small percentage of occupied area (< 3%), such as open areas with little or no vegetation, continental wetlands, heterogeneous areas, and disturbed areas (see Supplementary Text C1 and Supplementary Table C2 in Appendix C). Finally, main rivers (Strahler rank ≥ 3) are also illustrated.

Supplementary Figure C5

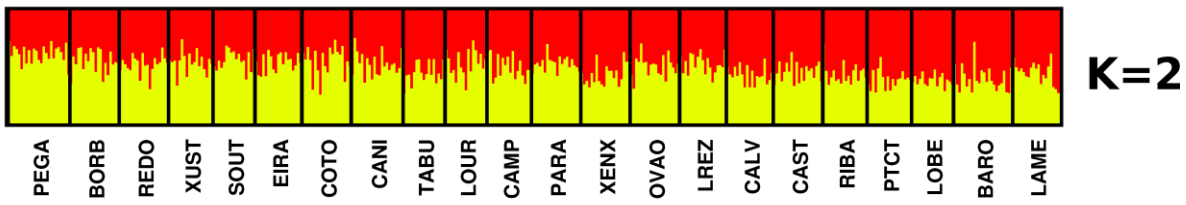

Fig. C5 STRUCTURE's barplot estimated through standard models (*i.e.* no sampling information) for larviparous populations. This barplot shows that larviparous populations exhibit a weak genetic structure.

Supplementary Figure C6

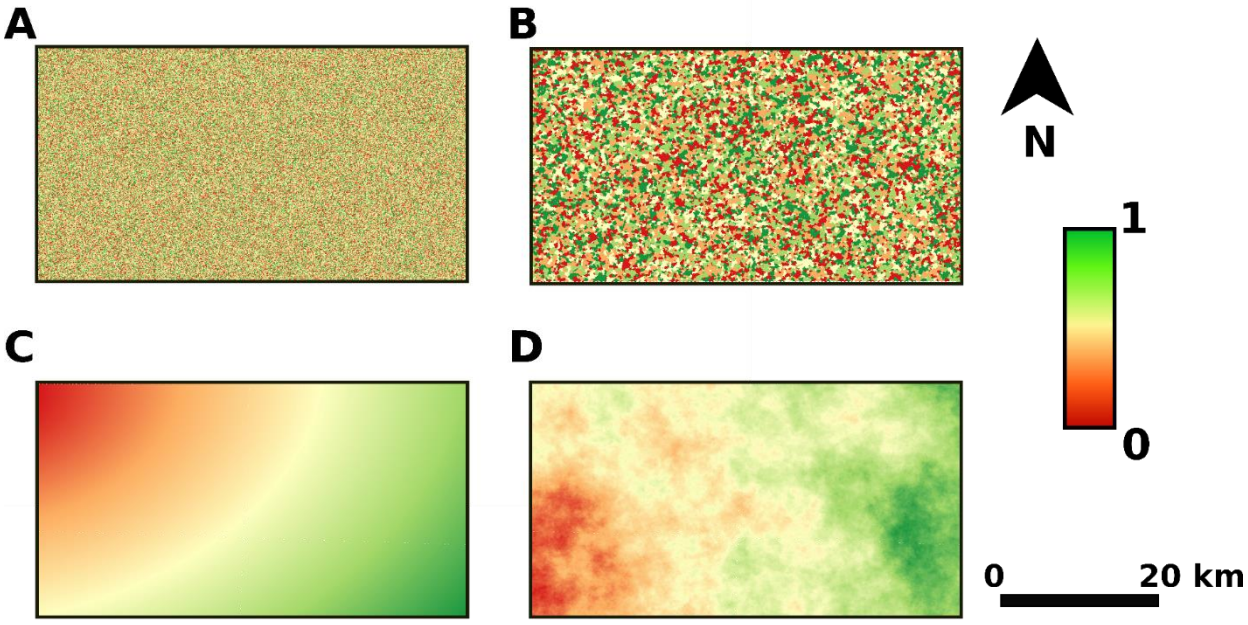

Fig. C6 Illustration of the landscape patterns simulated by the four neutral landscape models (NLMs) tested in landscape genetic analyses: (A) random; (B) random cluster; (C) distance gradient; and (D) fractional Brownian motion. These NLMs are represented in the pueriparous plot, though the same landscape patterns apply to the NLMs employed in the larviparous plot. Values in all models vary between 0 and 1, and all NLMs present a continuous gradient, with the exception of the random cluster model. The latter model was created with five different categories to simulate land cover heterogeneity. See Sciaini *et al.* (2018) for more details.

Supplementary Figure C7

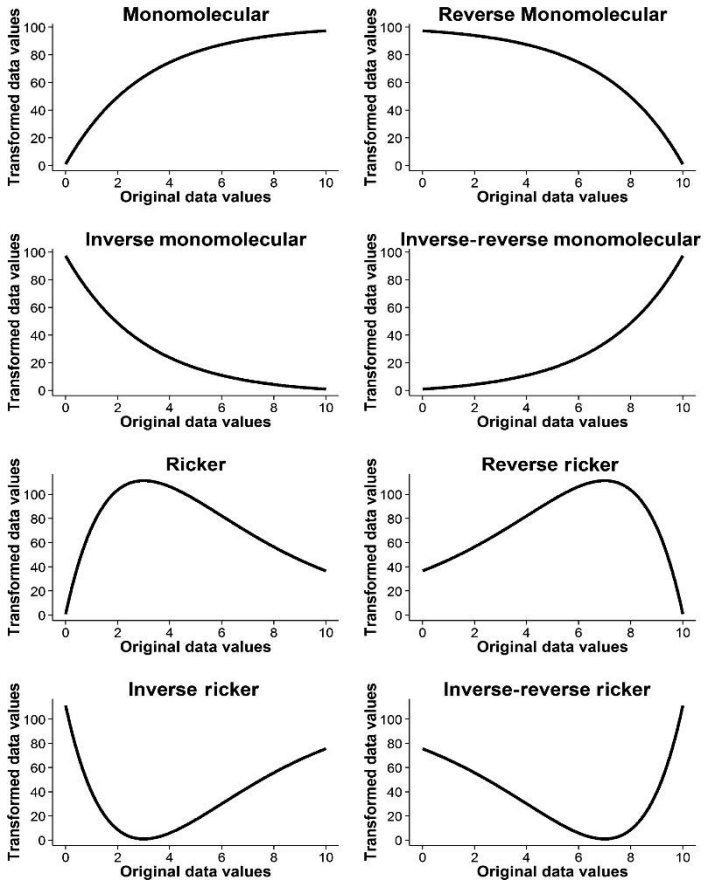

Fig. C7 Transformations that can be applied to continuous layers in *ResistanceGA* to transform raw layer values into optimized resistance values. Retrieved from Peterman (2018).

Supplementary Figure C8

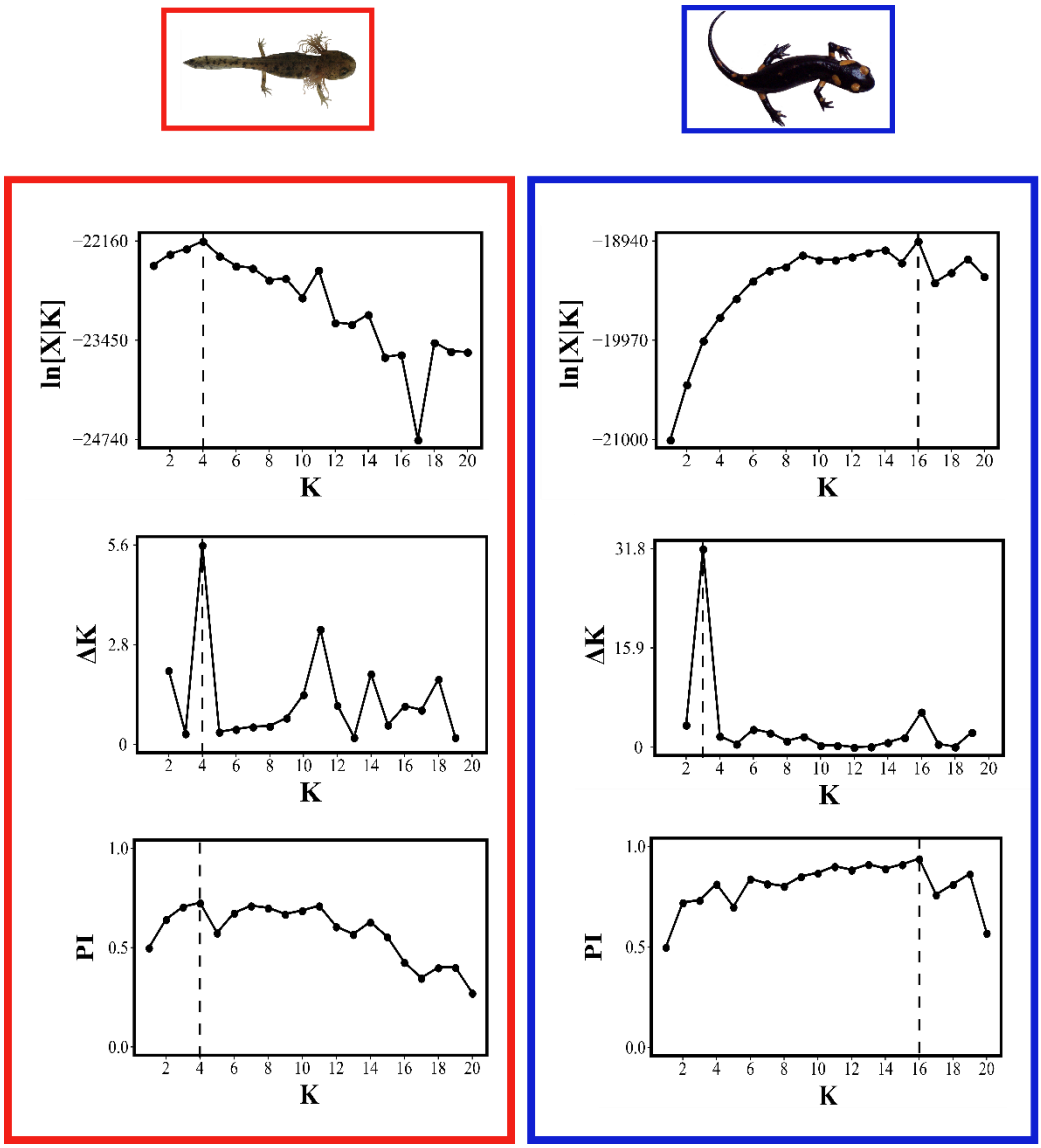

Fig. C8 Most supported number of genetic clusters for larviparous (red box) and pueriparous (blue box) populations, as inferred from STRUCTURE's output obtained with LOCPRIOR models. The dashed line corresponds to the optimal K. Three criteria were employed to determine optimal K values: (1) the mean logarithmic posterior probability (ln[X|K]); (2) the ΔK; and (3) the parsimony index (PI). K values were congruent among methods, with the exception of ΔK for the pueriparous plot.

Supplementary Figure C9

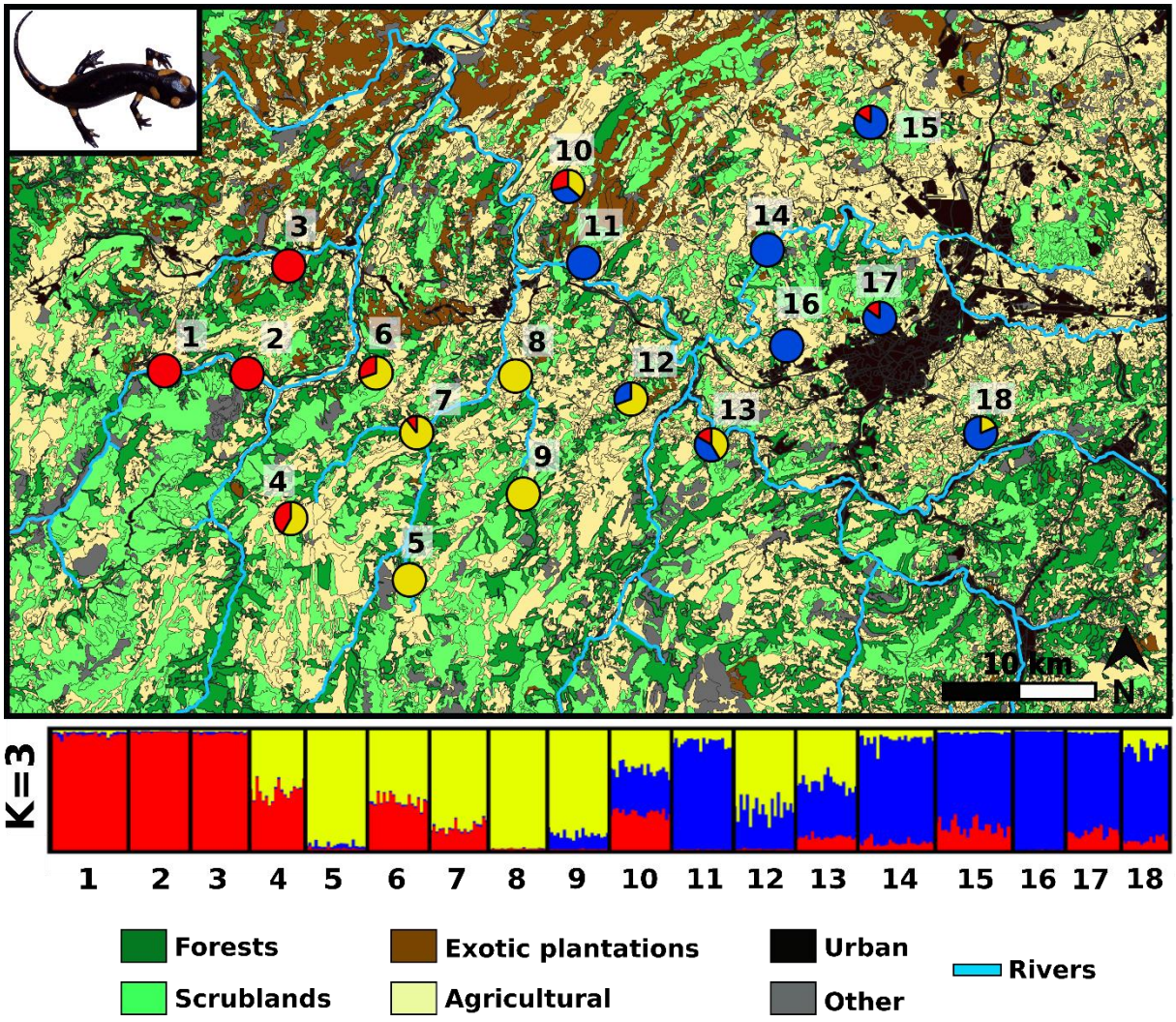

Fig. C9 Patterns of genetic structure obtained with LOCPRIOR models (STRUCTURE) in pueriparous populations for K=3. This K value was the most supported K according to the ΔK method. The most abundant reclassified land use classes are represented (i.e. natural forests, scrublands, plantations of exotic trees, agricultural areas, and urban settlements), along with main rivers (Strahler rank ≥ 3). The class "Other" represent minor reclassified land use classes, such as open areas with little or no vegetation, continental wetlands, heterogeneous areas, and disturbed areas.

Supplementary Figure C10

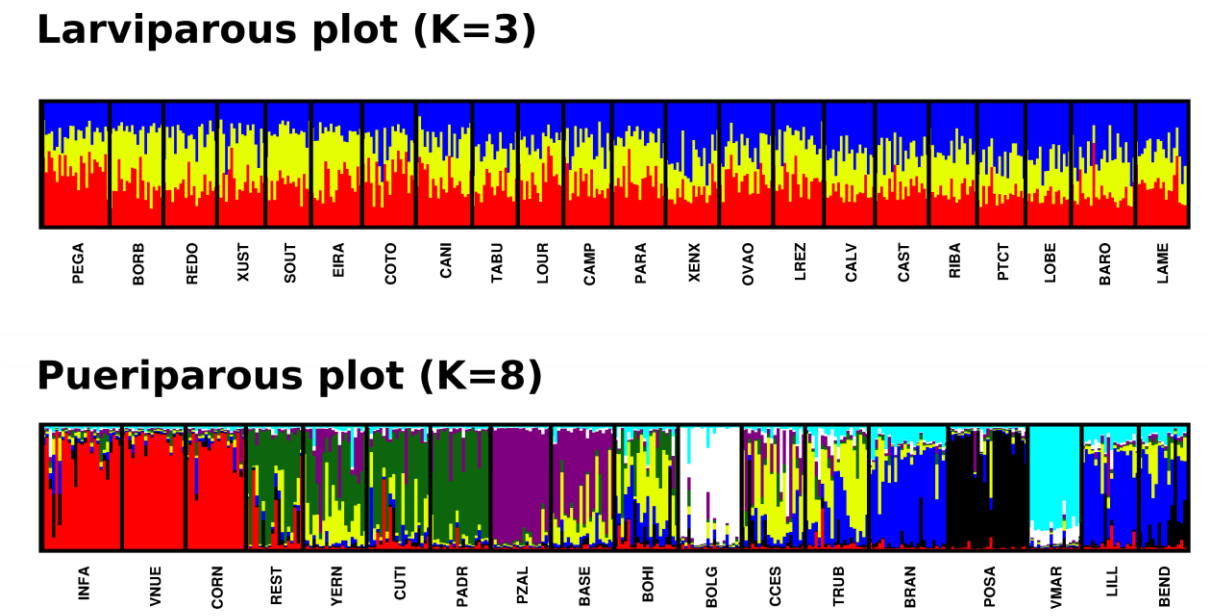

Fig. C10 STRUCTURE's barplots depicting patterns of genetic admixture among larviparous (top barplot) and pueriparous (bottom barplot) populations. These results were obtained through the standard models (*i.e.* no sampling information). These K values (K=3 and K=8) correspond to the most supported number of clusters according to the parsimony index method. This method was shown to outperform other approaches under many scenarios (*e.g.* unbalanced sampling, low number of loci, low genetic divergence, inbreeding; Wang 2019).

Supplementary Figure C11

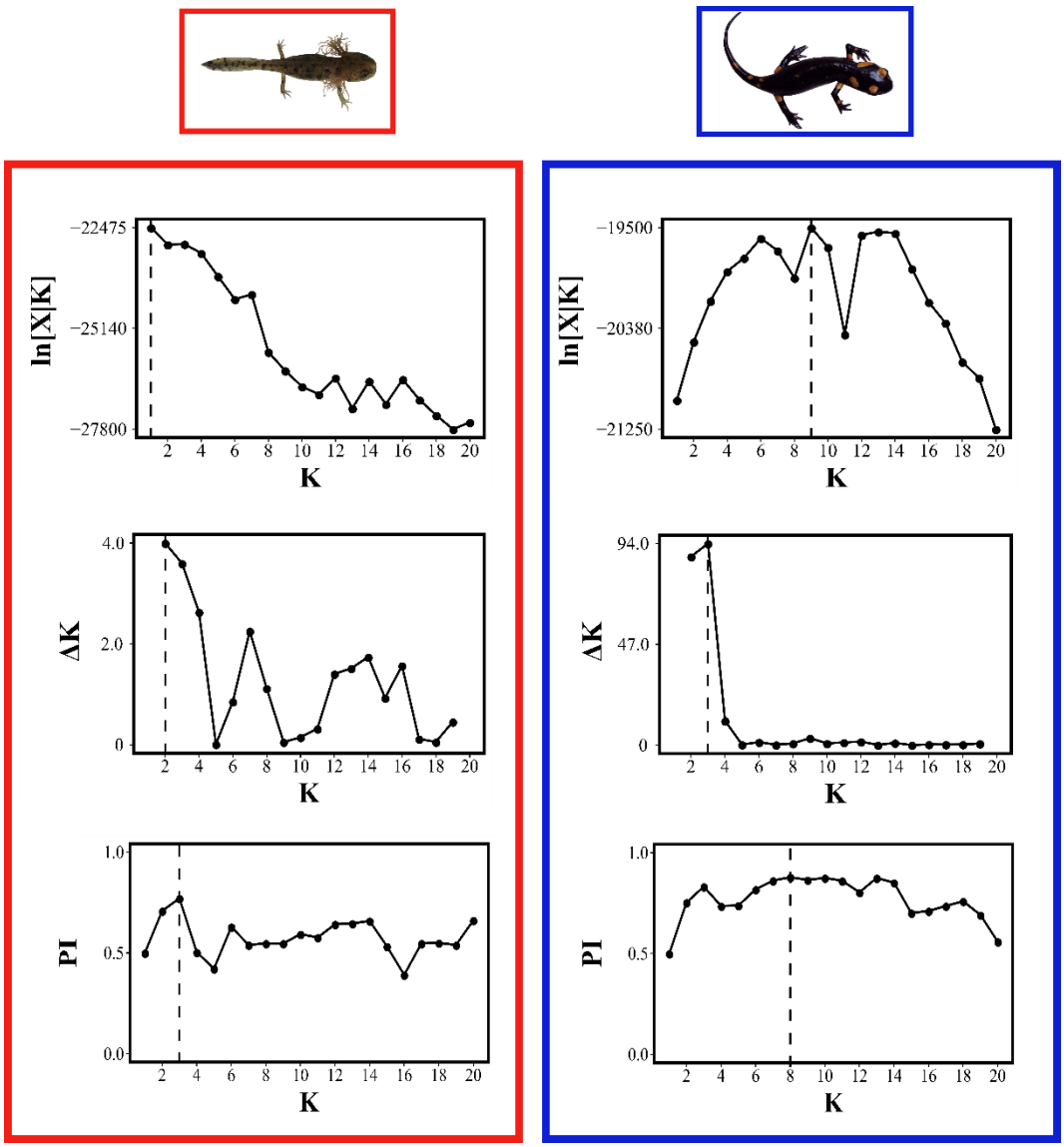

Fig. C11 Most supported number of genetic clusters for larviparous (red box) and pueriparous (blue box) populations, as inferred from STRUCTURE's output generated with standard models. The dashed line corresponds to the optimal K. Three criteria were employed to determine optimal K values: (1) the mean logarithmic posterior probability (ln[X|K]); (2) the ΔK; and (3) the parsimony index (PI). K values were highly incongruent among methods.

Supplementary Figure C12

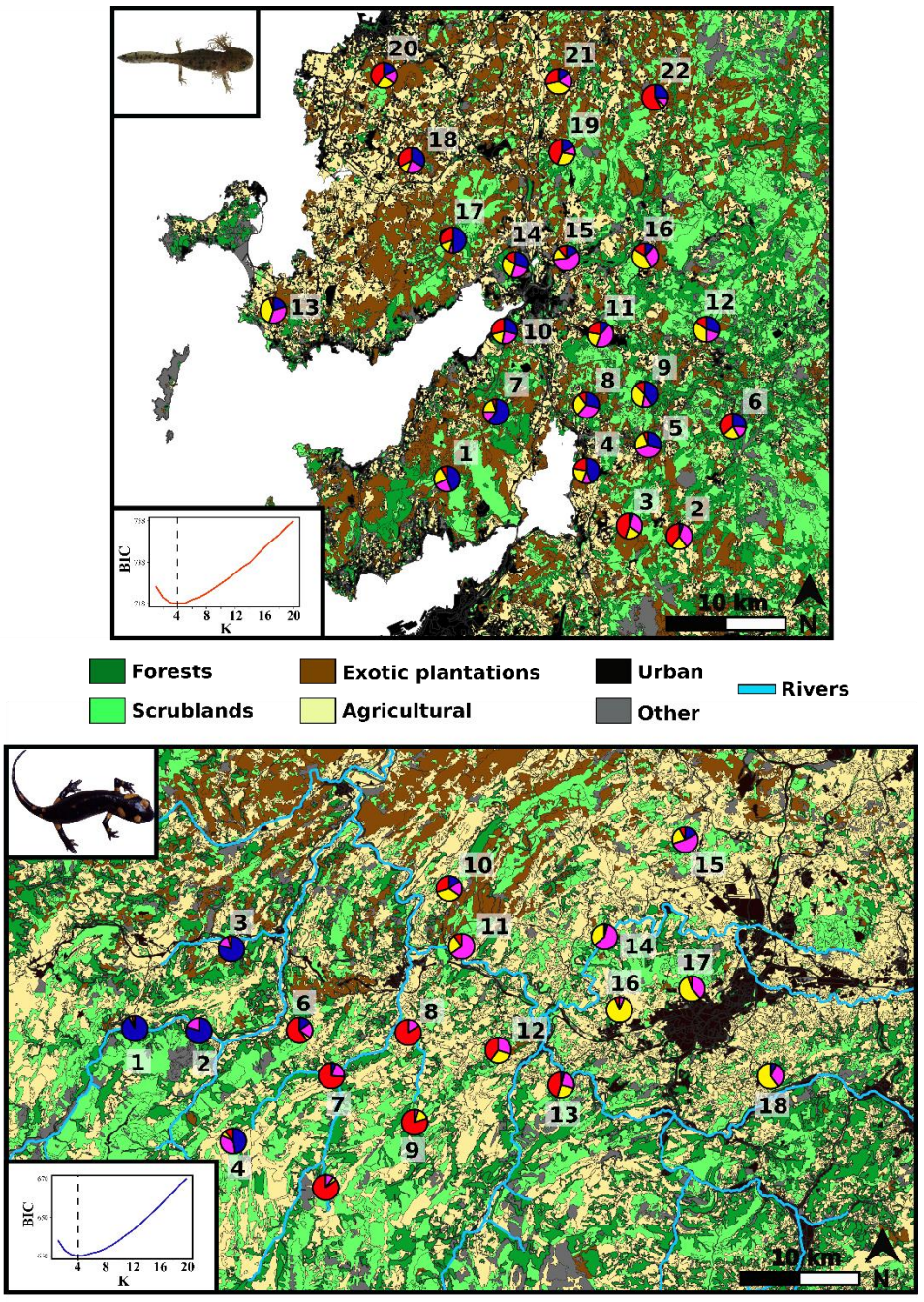

Fig. C12 Patterns of genetic structure in larviparous (top panel) and pueriparous (bottom panel) populations estimated in DAPC for the most supported K (K=4 in both study areas; see plots of the Bayesian Information Criterion in the bottom-left corner in each panel). Pie charts represent the proportion of individuals assigned to a particular cluster. The most abundant reclassified land use classes are represented (*i.e.* natural forests, scrublands, plantations of exotic trees, agricultural areas, and urban settlements), along with main rivers (Strahler rank ≥ 3). The class "Other" represent minor reclassified land use classes, such as open areas with little or no vegetation, continental wetlands, heterogeneous areas, and disturbed areas.

Supplementary Figure C13

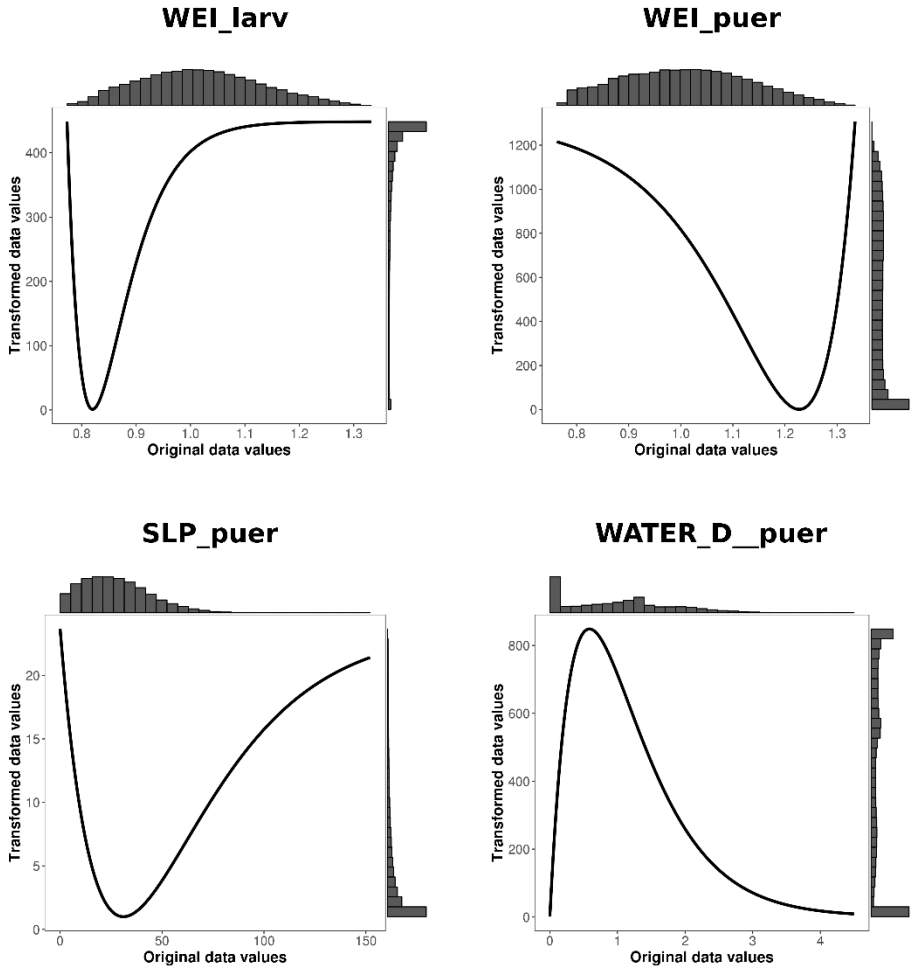

Fig. C13 Non-linear relationships between the original environmental values (*i.e.* raster layer values) and the optimized resistance values for the most supported continuous variables identified in the single surface optimization performed in *ResistanceGA*. The wind exposition index was supported in both the larviparous (WEI_larv) and pueriparous (WEI_puer) plots, while slope (SLP_puer), and the density of water coursers (WATER_D_puer) were supported only in pueriparous populations. WEI_larv and SLP_puer were optimized using an Inverse Ricker transformation, whereas WEI_puer and WATER_D_puer were transformed by an Inverse-Reverse Ricker and Ricker functions, respectively. Histograms of the distribution of the original environmental raster values (histograms above each plot) and the transformed resistance values (histograms to the right of each plot) are also displayed.

References of Appendix C

Alton LA, Franklin CE (2017) Drivers of amphibian declines: effects of ultraviolet radiation and interactions with other environmental factors. *Climate Change Responses*, **4**, 6.

Antunes B, Lourenço A, Caeiro-Dias G *et al.* (2018) Combining phylogeography and landscape genetics to infer the evolutionary history of a short-range Mediterranean relict, *Salamandra salamandra longirostris*. *Conservation Genetics*, **19**, 1411–1424.

Arntzen JW, Abrahams C, Meilink WRM, Iosif R, Zuiderwijk A (2017) Amphibian decline, pond loss and reduced population connectivity under agricultural intensification over a 38 year period. *Biodiversity and Conservation*, **26**, 1411–1430.

Conrad O, Bechtel B, Bock M *et al.* (2015) System for Automated Geoscientific Analyses (SAGA) v. 2.1.4. *Geoscientific Model Development*, **8**, 1991-2007.

Cushman SA, Shirk A, Landguth EL (2012) Separating the effects of habitat area, fragmentation and matrix resistance on genetic differentiation in complex landscapes. *Landscape Ecology*, **27**, 369–380.

Deus E, Silva JS, Castro-Díez P *et al.* (2018) Current and future conflicts between eucalypt plantations and high biodiversity areas in the Iberian Peninsula. *Journal for Nature Conservation*, **45**, 107–117.

Didan K, Munoz AB, Solano R, Huete A (2015) MODIS Vegetation Index User's Guide (MOD13 Series) - version 3.00, June 2015 (Collection 6). University of Arizona, Vegetation Index and Phenology Lab.

Environmental Systems Research Institute (ESRI) (2012). ArcGIS Release 10.1. Redlands, CA.

Ficetola GF, Manenti R, De Bernardi F, Padoa-Schioppa E (2012) Can patterns of spatial autocorrelation reveal population processes? An analysis with the fire salamander. *Ecography*, **35**, 693–703.

Fick SE, Hijmans RJ (2017) WorldClim 2: new 1-km spatial resolution climate surfaces for global land areas. *International Journal of Climatology*, **37**, 4302-4315.

Gao BC (1996) NDWI — A normalized difference water index for remote sensing of vegetation liquid water from space. *Remote Sensing of Environment*, **58**, 257-266.

Georgousis S, Bruy A (2019) Principal Components. QGIS plugin version 1.0.

Gorelick N, Hancher M, Dixon M *et al.* (2017) Google Earth Engine: planetary-scale geospatial analysis for everyone. *Remote Sensing of Environment*, **202**, 18–27.

Gutiérrez-Rodríguez J, Gonçalves J, Civantos E, Martínez-Solano I (2017) Comparative landscape genetics of pond-breeding amphibians in Mediterranean temporal wetlands: the

positive role of structural heterogeneity in promoting gene flow. *Molecular Ecology*, **26**, 5407–5420.

Hendrix R, Schmidt BR, Schaub M, Krause ET, Steinfartz S (2017). Differentiation of movement behaviour in an adaptively diverging salamander population. *Molecular Ecology*, **26**, 6400–6413.

Huete A, Didan K, Miura T, Rodriguez EP, Gao X, Ferreira LG (2002) Overview of the radiometric and biophysical performance of the MODIS vegetation indices. *Remote Sensing of Environment*, **83**, 195-213.

Johansson M, Primmer CR, Merilä J. (2007) Does habitat fragmentation reduce fitness and adaptability? A case study of the common frog (*Rana temporaria*). *Molecular Ecology*, **16**, 2693–2700.

Kivimäki I, Shimbo M, Saerens M (2014) Developments in the theory of randomized shortest paths with a comparison of graph node distances. *Physica A: Statistical Mechanics and Its Applications*, **393**, 600–616.

Lourenço A, Álvarez D, Wang IJ, Velo-Antón G (2017) Trapped within the city: integrating demography, time since isolation and population-specific traits to assess the genetic effects of urbanization. *Molecular Ecology*, **26**, 1498–1514.

Lourenço A, Antunes B, Wang IJ, Velo-Antón G (2018a) Fine-scale genetic structure in a salamander with two reproductive modes: does reproductive mode affect dispersal? *Evolutionary Ecology*, **32**, 699-732.

Lourenço A, Sequeira F, Buckley D, Velo-Antón G (2018b) Role of colonization history and species-specific traits on contemporary genetic variation of two salamander species in a Holocene island-mainland system. *Journal of Biogeography*, **45**, 1054–1066.

Marsh DM, Page RB, Hanlon TJ *et al.* (2007) Ecological and genetic evidence that low-order streams inhibit dispersal by red-backed salamanders (*Plethodon cinereus*). *Canadian Journal of Zoology*, **85**, 319–327.

McRae BH (2006). Isolation by resistance. *Evolution*, **60**, 1551–1561.

McGarigal K, Cushman SA, Ene E (2012) FRAGSTATS v4: spatial pattern analysis program for categorical and continuous Maps. University of Massachusetts, Amherst. Accessed on 24 November 2018. http:// www.umass.edu/landeco/research/fragstats/fragstats.html.

McCartney-Melstad E, Vu J, Shaffer HB (2018) Genomic data recover previously undetectable fragmentation effects in an endangered amphibian. *Molecular Ecology*, **27**, 4430–4443.

Millette KL, Keyghobadi N (2015) The relative influence of habitat amount and configuration on genetic structure across multiple spatial scales. *Ecology and Evolution*, **5**, 73-86.

Ministerio de Medio Ambiente, y Medio Rural y Marino de España, (2007) Anuario de estadística forestal 2007. https://www.pefc.es/documentacion/relacionada/anu_est_for_2007.pdf

Montero G, Serrada R (2013). La situación de los bosques y el sector forestal en España – ISFE 2013. Sociedad Española de Ciencias Forestales. Lourizán (Pontevedra). https://www.congresoforestal.es/fichero.php?t=12225&i=529&m=2185

Peterman WE (2018) ResistanceGA: An R package for the optimization of resistance surfaces using genetic algorithms. *Methods in Ecology and Evolution*, **9**, 1638–1647.

QGIS Development Team (2018) QGIS Geographic Information System. Open Source Geospatial Foundation Project. http://qgis.osgeo.org

R Core Team (2018) R: A language and environment for statistical computing. R Foundation for Statistical Computing, Vienna, Austria. https://www.R-project.org/

Richardson JL (2012) Divergent landscape effects on population connectivity in two co-occurring amphibian species. *Molecular Ecology*, **21**, 4437–4451.

Sánchez-Montes G, Wang J, Ariño AH, Martínez-Solano I (2018) Mountains as barriers to gene flow in amphibians: quantifying the differential effect of a major mountain ridge on the genetic structure of four sympatric species with different life history traits. *Journal of Biogeography*, **45**, 318–331.

Schulte U, Küsters D, Steinfartz S (2007) A PIT tag based analysis of annual movement patterns of adult fire salamanders (*Salamandra salamandra*) in a Middle European habitat. *Amphibia-Reptilia*, **28**, 531–536.

Sciaini M, Fritsch M, Scherer C (2018) NLMR and landscapetools: an integrated environment for simulating and modifying neutral landscape models in R. *Methods in Ecology and Evolution*, **9**, 2240–2248.

Strahler AN (1957) Quantitative analysis of watershed geomorphology. *Eos, Transactions American Geophysical Union*, **38**, 913-920.

van Etten J (2017) R Package gdistance: Distances and routes on geographical grids. *Journal of Statistical Software*, **76**, 1-21.

Velo-Antón G, Buckley D (2015) Salamandra común – *Salamandra salamandra*. In: L.M. Carrascal, A Salvador (eds) *Enciclopedia Virtual de los Vertebrados Españoles*. Museo Nacional de Ciencias Naturales, Madrid. Retrieved from http://www.vertebradosibericos.org/anfibios/salsal.html

Velo-Antón G, Parra JL, Parra-Olea G, Zamudio KR (2013) Tracking climate change in a dispersal-limited species: reduced spatial and genetic connectivity in a montane salamander. *Molecular Ecology*, **22**, 3261–3278.

Vesanto H (2018) Select Within. QGIS plugin version 0.4. https://plugins.qgis.org/plugins/SelectWithin/

Wang J (2019) A parsimony estimator of the number of populations from a STRUCTURE-like analysis. *Molecular Ecology Resources*, **19**, 970-981.

Wang X, Blanchet FG, Koper N (2014) Measuring habitat fragmentation: an evaluation of landscape pattern metrics. *Methods in Ecology and Evolution*, **5**, 634–646.

Appendix D

Assessment of census (*N*) and effective population size (*Ne*) reveals consistency of *Ne* single-sample estimators and a high *Ne*/*N* ratio in an urban and isolated population of fire salamanders

David Álvarez[1], André Lourenço[2,3], Daniel Oro[4] and Guillermo Velo-Antón[3]

Article published in *Conservation Genetics Resources*, 2015, **7**, 705-712. doi: 10.1007/s12686-015-0480-0

[1] Ecology Unit, Department of Organisms and Systems Biology, University of Oviedo, C/ Catedrático Rodrigo Uría, 33071 Oviedo, Spain

[2] Departamento de Biologia da Faculdade de Ciências da Universidade do Porto, Rua Campo Alegre, 4169-007 Porto, Portugal.

[3] CIBIO/InBIO, Centro de Investigacao em Biodiversidade e Recursos Genéticos da Universidade do Porto, Instituto de Ciências Agrárias de Vairão, Rua Padre Armando Quintas 7, 4485-661 Vairão, Portugal

[4] Population Ecology Group, IMEDEA (CSIC-UIB), Miquel Marque`s 21, Esporles, Majorca, Spain

D1 – Abstract

Amphibians are the most threatened vertebrates on Earth, and one of the main factors involved in their decline is the loss and fragmentation of their natural habitats. Contemporary urban development is a major cause of habitat fragmentation, and populations trapped within urban environments offer a unique opportunity to study effects of fragmentation. Here, we compared, for the first time in fire salamanders (*Salamandra salamandra*), estimates of census (*N*) and effective population size (*Ne*) in a small urban population in the city of Oviedo (Spain). We performed a 4 year capture-mark-recapture study and used three single-sample *Ne* estimators based on 58 individuals genotyped for 15 polymorphic microsatellite loci. Our study showed a small ($\widehat{N}$=113 salamanders; 95%CI 100–142) but dense population (mean 0.45 individuals per m^2), while single-sample estimators provided congruent *Ne* estimates. A high *Ne*/*N* population size ratio (range 0.50–0.84) obtained in this small and isolated population suggests the existence of mechanisms of genetic compensation (low reproductive variance and multiple paternity) in fire salamanders.

Keywords: demography, genetic compensation, inbreeding, *N*, *Ne*

D2 – Introduction

Amphibians are at the forefront of the so-called sixth mass extinction on Earth (Wake and Vredenburg 2008) and half of over 7000 amphibian species are in decline (http://amphibiaweb.org/declines/declines.html). Among other threats, the rampant loss and fragmentation of their habitats is the major cause of amphibian extinctions and declines (Cushman 2006). Habitat fragmentation has increased the isolation of populations, compromising their persistence due to reduced gene flow and associated loss of genetic diversity through genetic drift and inbreeding effects. As a consequence of these phenomena, the evolutionary potential of populations to cope with environmental changes can be greatly reduced (Frankham 2005). Contemporary urban development (mostly increased during the mid-twentieth century) has been a major cause of habitat fragmentation, restricting many species to small isolated patches embedded within a matrix of inhospitable habitat. Populations trapped within urban environments constitute an extreme case of habitat fragmentation, in which amphibian species are especially vulnerable since they largely depend on the availability of water bodies to reproduce. Therefore, it is crucial to obtain reliable estimates of key demographic parameters to better manage isolated populations and implement effective mitigation measures (Frankham 2010). Available methodologies to

estimate such parameters can be more rigorously assessed in small, controlled environments, like urban populations.

Effective population size (*Ne*) is one of the most important parameters in conservation, because it summarizes information on both contemporary and evolutionary dynamics (Luikart *et al.* 2010). When combined with population census size (*N*), *Ne*/*N* size ratios provide additional information concerning demographic (*e.g.* variance in reproductive success, population size fluctuations) and genetic (*e.g.* genetic erosion) population parameters, which have implications at evolutionary and conservation levels (Palstra and Ruzzante 2008). However, estimating *Ne* accurately in nature is not straightforward, although many methods have been recently proposed, with single-sample methods most popular at present (Luikart *et al.* 2010). Here, we studied a viviparous population of fire salamander (*Salamandra salamandra*) in the city of Oviedo (northern Spain). The species is mostly larviparous throughout its wide distribution in Europe, but some populations in the north of Spain have evolved viviparity (García-París *et al.* 2003; Velo-Antón *et al.* 2012a; Velo-Antón *et al.* 2015). This adaptation has allowed viviparous salamanders to survive in environments without permanent water bodies. The urban population under study is isolated from other populations within the city (Álvarez 2012), constituting an interesting case study to test the accuracy of single-sample methods and estimate *Ne*/*N* size ratios. Here, we compare different estimates of demographic parameters in *S. salamandra*. We first estimate *N* through capture-mark-recapture modeling, and then calculate the *Ne*/*N* ratio based on different estimates of *Ne* obtained from genotyping 58 individuals with 15 polymorphic microsatellite markers. The results are discussed with emphasis on the potential of single-sample methods to accurately estimate *Ne* in an isolated and potentially inbred population.

D3 – Materials and methods

D3.1 – Study area and salamander sampling

Our study was conducted in a plot of 248 m^2 located at the Biology Faculty in Oviedo University Campus (lat. 43.3564°, long. −5.8731°). This plot is surrounded on three sides by paved roads, while the fourth side is limited by a building (**Figure D1**). The walls of this building have numerous crevices and holes that provide shelter for salamanders during the day. The ground is covered with grass, and there are two medium sized trees at one end of the plot.

The study plot was sampled during rainy nights between October 2008 and October 2011. During this period, 216 adult individuals larger than 110 mm were captured and transferred to the laboratory, where they were weighed, sexed and photographed an overhead, dorsal view for posterior measurements. A tissue sample (tail or toe clips) was collected from 55 adult

individuals and three juveniles (58 individuals in total). All tissues were preserved in 100 % ethanol for microsatellite genotyping. All individuals were marked with passive integrated transponders (length 8 mm, diameter 2.1 mm; AVID ©) inserted subcutaneously. On the day following their capture, all individuals were released at their sites of initial capture. Each salamander captured was scanned with a Minitracker 3 hand scanner (AVID ©), and if a transponder was detected, transponder code and site of recapture were annotated. The nearby green patches that surrounded the study plot were also revisited during sampling events but no marked salamanders were found, suggesting no or low migration levels.

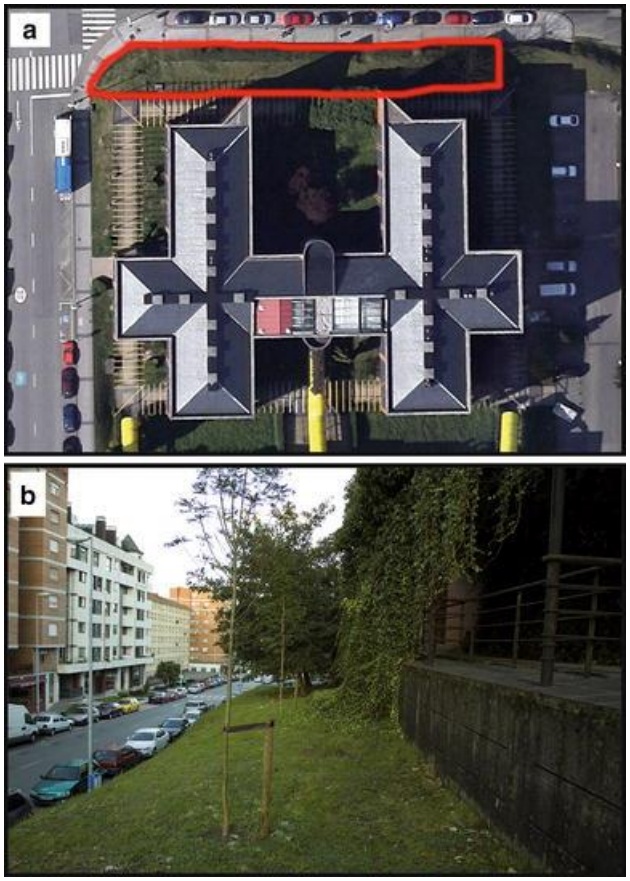

Fig. D1 A - Zenithal view of the Biology Faculty in the Oviedo Campus University. The line outlines the study plot where the study was performed. No PIT-tagged salamanders were found outside the study plot. B - Picture showing the habitat of the study population.

D3.2 – Estimation of census population size (*N*)

Because our samples include only adult individuals, our estimate of *N* reflects the number of breeding adults alive during a given period of time. To estimate *N* we used a particular capture-recapture model, the “robust design”, which is a combination of the Cormack–Jolly–Seber live recapture model and the “closed capture” models (model details are in

Supplementary Table D.ST1). Models were run using MARK software (White and Burnham 1999). Model selection was based on Akaike's Information Criterion corrected for small sample sizes (AICc, Burnham and Anderson 2002). The best model is that with the lowest AICc value, and models differing in AICc values by <2 (AICc < 2) are considered statistically equivalents (Burnham and Anderson 2002). The 216 adult salamanders captured were marked and monitored during 15 secondary occasions between 2008 and 2011 (late autumn for all years plus a spring fieldwork campaign in 2011).

D3.3 – Laboratory procedures

DNA was extracted from fresh tissue using Genomic DNA Tissue Kit (EasySpin), following the manufacturer's protocol. DNA quantity and quality were assessed visually on a 0.8 % agarose gel. Genotyping was carried out using a set of 15 microsatellites (**Supplementary Table D.ST2**).

Microsatellites were amplified in five different PCR multiplexes. Each multiplex mix contained distilled H_2O, fluorescently labelled forward (6-FAM, VIC, NED or PET; see **Supplementary Table D.ST2** for sequence details) and reverse primers modified with a "PIG-tail" (GTTT) at the 5′ end. Each PCR reaction contained a total volume of 10–11: 5 µl of Multiplex PCR Kit Master Mix (QIAGEN, Valencia, CA, USA), 3 µl of distilled H_2O, 1 µl of primer multiplex mix and 1–2 µl of DNA extract (~50 ng/µl). A negative control was always used to identify possible contaminations. PCR touchdown cycling conditions were equal in four of the five multiplex reactions (panelS1, panelS2, panelS4 and panelS5): the reaction started with an initial step at 95 °C for 15 min, 19 cycles at 95 °C for 30 s, 90 s of annealing at 65 °C (decreasing 0.5 °C each cycle), 72 °C for 40 s, followed by 25 cycles of 95 °C for 30 s, 56 °C for 60 s, 72 °C for 40 s, and ended with a final extension of 30 min at 60 °C. For panelS3, a similar protocol was performed but with 27 cycles instead of 19 and the annealing temperature during the last 25 cycles was set to 52 °C. PCR amplification quality was assessed by visual inspection in 2 % agarose gels. PCR products were run on an ABI3130XL capillary sequencer (Applied Biosystems), and allele scoring was performed using GeneMapper version 4.0 (Applied Biosystems).

D3.4 – Microsatellite data analyses

Six individuals (about 10 % of the full dataset) were genotyped twice to estimate allele dropout (AD) and false allele frequencies (FA), a widely accepted procedure for the analysis of fresh tissue samples (Guichoux *et al.* 2011). AD and FA were jointly estimated using software PEDANT 1.0 (Johnson and Haydon 2007), setting 10,000 steps for maximum

likelihood search iterations. Unbiased null allele frequencies and mean inbreeding coefficients were calculated with INEST 2.0 (Chybicki and Burczyk 2009) using the Individual Inbreeding Model. Parameters used were as follows: 200,000 total cycles, 20,000 burn-in cycles, and each iteration was saved every 100 cycles.

Each locus was tested for Hardy–Weinberg equilibrium (HWE) and linkage disequilibrium (LD) on GENEPOP 4.2 (dememorisation = 10,000, batch length = 50,000, batch number = 2000; Rousset 2008). P values from multiple HW and LD exact tests were adjusted using the false discovery rate (Benjamini and Hochberg 1995). Population mean relatedness (Queller and Goodnight 1989) and number of alleles and expected and observed heterozygosities were calculated for each locus with GENEALEX 6.5 (Peakall and Smouse 2012).

D3.5 – Estimation of effective population size (*Ne*)

Ne was estimated using three commonly used single-sample methods: (1) the linkage disequilibrium (LD) method implemented in NEESTIMATOR V2 (Do *et al.* 2014); (2) the Approximate Bayesian Computation (ABC) method based on summary statistics in ONESAMP 1.2 (Tallmon *et al.* 2008); and (3) the sibship assignment (SA; Wang 2009) method implemented in COLONY2 (Jones and Wang 2010).

Salamandra salamandra is an iteroparous species, meaning that individuals from different cohorts coexist in a given period of time. The single-sample estimators outlined on the previous paragraph assume discrete generations, and consequently, it is important to take into account possible biases when interpreting results. Unlike other studies (*e.g.* Skrbinšek *et al.* 2012), we did not use the estimator by parentage assignment (EPA) method (Wang *et al.* 2010), which is more suitable for species with overlapping generations, because we cannot accurately assign sampled animals to specific age groups based on their biometric measurements. Keeping in mind this potential bias, and in order to overcome the presence of different cohorts in our dataset, we accounted for the unique characteristics displayed by each method.

NEESTIMATOR V2 uses measures of linkage disequilibrium (*i.e.* non-random allele associations) to assess the magnitude of genetic drift in small populations, and thus, calculate contemporary *Ne*. Linkage disequilibrium is quantified using the unbiased estimator of Burrows' Δ method (Weir 1979) which was bias-corrected for sample size (Waples 2006). Calculations were performed using the random mating model. One run was carried out to estimate *Ne* along with parametric and jacknife 95 % confidence intervals (95% CIs), where rare alleles with a frequency below 0.02 were excluded. This threshold was chosen because Waples and Do (2010) have shown that this value represents a good compromise between accuracy and bias. The LD method was developed to estimate *Ne* for species with discrete

generations. However, previous studies have shown that in cases where *Ne* is small and the number of cohorts (containing only mature individuals) sampled is approximately equal to generation length, methods based on linkage disequilibrium will produce relatively unbiased estimates of *Ne* per generation (Robinson and Moyer 2013; Waples *et al.* 2014). Considering the small extent of our study area and the low estimated number of individuals (see Results section), we assume that different cohorts of mature individuals are well represented in our sample. Additionally, Robinson and Moyer (2013) demonstrated that the inclusion of immature individuals constitutes an additional source of bias (downward biased estimates), suggesting that the use of adult salamanders in our study is better justified.

ONESAMP 1.2 estimates eight summary statistics related to *Ne* in the reference microsatellite dataset through ABC, which are then compared with summary statistics estimated for 50,000 simulated populations with a range of *Ne* values specified by the user. Like LD method, ONESAMP assumes that genetic drift is the main evolutionary force shaping *Ne*. Four different prior combinations (lower and upper bounds for *Ne*) were chosen: 20–100, 20–150, 50–100, and 50–150. Although lower prior bounds were arbitrarily chosen, we used our *N* estimate and respective 95% CIs to choose more realistic upper bounds for priors of *Ne*, since *Ne* is generally lower than *N* (*i.e. Ne*/*N* < 1; Palstra and Ruzzante 2008). Three replicates were conducted for each combination of priors and means and 95% CIs of the resulting *Ne* estimates were subsequently calculated. Unlike LD method, we opted to maintain all genotyped individuals in the analyses since ONESAMP performed reasonably well with different cohorts included in the analyses (Barker 2011; Skrbinšek *et al.* 2012).

COLONY2 incorporates the sibship assignment method (SA). *Ne* is derived by estimating the frequencies of half-siblings and full-siblings of pairs of offspring drawn randomly from a population. This implies that populations with small *Ne* will have a greater proportion of full- and half-siblings. COLONY2 assumes that the offspring sample is taken from the same cohort. However, datasets may be partitioned into two cohorts (parent and offspring), which confers a greater flexibility regarding sampling than other single-sample estimators. By including parent generation, sibship relationships can be inferred more accurately, which, according to Wang (2009), confers more power for the analysis. To reduce bias associated with the presence of multiple cohorts in our dataset, we roughly approximated the age of each individual in the dataset using snout-vent length measurements and date of sampling. This allowed us to distribute more accurately individuals across three datasets (parent, n = 11; offspring, n = 4; both, n = 43) and obtain more reliable results. Although this approach was confined to the most evident cases due to lack of precise age information for most individuals, it allowed us to identify the oldest/youngest individuals which could or could not have contributed for the gene

pool of our sample. We used the full-likelihood method and specified high likelihood precision and medium run length under scenarios of polygamy and monogamy for both sexes, as well polygyny and polyandry. We tested three different probabilities of an individual in the offspring sample having a parent in our dataset—0.15, 0.30 and 0.60. No *a priori* information regarding known parents was provided. The genotyping error rates estimated in PEDANT 1.0 and INEST 2.0 were incorporated in calculations. For each combination of parameters, three independent runs (*i.e.* with different random seeds) were carried out and mean *Ne* and 95% CIs were calculated for each group of three replicates, assuming models of inbreeding and random mating.

D4 – Results

Most of the unique 216 marked salamanders were recaptured (70.4 %) at least once, and the number of recaptures of the same individual per occasion (*i.e.* without multiple recaptures within occasions) ranged from 1 to 15 (median: 3; mode: 2). The robust capture-recapture modelling showed that the best model (model 1; **Supplementary Table D.ST1**) was the one with time-varying survival and recapture probabilities but with constant population size during the 4 years of study. Population census size $\widehat{N}$ was estimated at 113 salamanders (SE 10.155; 95% CI 100–142), with an average of 0.45 individuals per m^2. Recaptures for the best ranked model were time-dependent and ranged from 0.055 (SE 0.019; 95% CI 0.028–0.106) to 0.682 (SE 0.043; 95% CI 0.593–0.759).

No microsatellite locus showed evidence for allele dropout or false alleles. However, four loci (SST-A6-II, Sal23, SST-C3 and SalE06) exhibited high frequencies of null alleles, two of which (SST-C3 and SalE06) also showed deviations from HWE, with Sal23 in LD with SalE7 (**Supplementary Table D.ST3**). Therefore, analyses were repeated excluding the four loci with high null allele frequencies. All loci were polymorphic, exhibiting high levels of genetic diversity, except for loci with evidence of null alleles. Mean number of alleles (±SE) was 9.133 ± 0.496, while average observed and expected heterozygosities were 0.680 ± 0.047 and 0.764 ± 0.035, respectively. No signs of strong inbreeding were detected in this population, with a mean inbreeding coefficient of F = 0.03 and mean population relatedness of R = 0.06.

Differences in $\widehat{Ne}$ estimates between analyses based on 15 and 11 markers were low for the LD and ABC methods, but they were slightly more pronounced when using the SA method (**Figure D2; Table D1; Supplementary Table D.ST4**). Although differences between the random mating and inbreeding models were very low, the SA method generated highly variable $\widehat{Ne}$ estimates across all tested scenarios: polygamy (range of $\widehat{Ne}$ 56–65), monogamy (range

of $\widehat{Ne}$ 111–146) and one sex monogamous (range of $\widehat{Ne}$ 73–89). The LD ($\widehat{Ne}$ = 91) and ABC (range among all priors: 63–95) methods also estimated high values for effective population size (**Figure D2**). ONESAMP generated more precise estimates than other methods (only prior 20–150 produced 95% CIs that overlapped mean $\widehat{N}$). *Ne*/*N* ratio estimates based on the different methods ranged from 0.50 to 1.29 (**Table D1**).

Table D1 Estimates of effective population size *(Ne*), 95% CIs and *Ne*/*N* ratios obtained from individuals genotyped at 15 microsatellites.

Method	**Scenario**	N_e	**95% CIs**	N_e/N
NEESTIMATOR[A]		91	72-123 (69-128)	0.80
ONESAMP				
	20-100	85	74-107	0.75
	20-150	95	81-128	0.84
	50-100	63	58-68	0.56
	50-150	66	60-74	0.58
COLONY2[B]				
	PG – 0.15	65 (64)	43-101 (40-107)	0.57
	PG – 0.30	59 (57)	41–92 (37–94)	0.52
	PG – 0.60	56 (54)	38–87 (35–89)	0.50
	PAND – 0.15	86 (86)	57–135 (55–143)	0.76
	PAND – 0.30	82 (82)	52–138 (55–143)	0.72
	PAND – 0.60	76 (77)	49–131 (51–122)	0.67
	PGYN – 0.15	74 (71)	50–114 (44–113)	0.65
	PGYN – 0.30	89 (90)	57–145 (56–164)	0.79
	PGYN – 0.60	73 (75)	47–133 (49–123)	0.65
	MG - 0.15	146 (160)	95–265 (98–367)	1.29
	MG - 0.30	142 (155)	92–256 (93–371)	1.26
	MG - 0.60	111 (116)	72–185 (73–219)	0.98

Mean *Ne* and respective 95% CIs are presented for ONESAMP and COLONY2 summarizing results from three replicate runs for all tested scenarios.

PG polygamy, PAND polyandry, PGYN polygyny, MG monogamy

[A] For NEESTIMATOR the jacknife confidence interval is in parenthesis

[B] For COLONY2 the *Ne* estimates and respective95 % CIs for the inbreeding model are in parenthesis

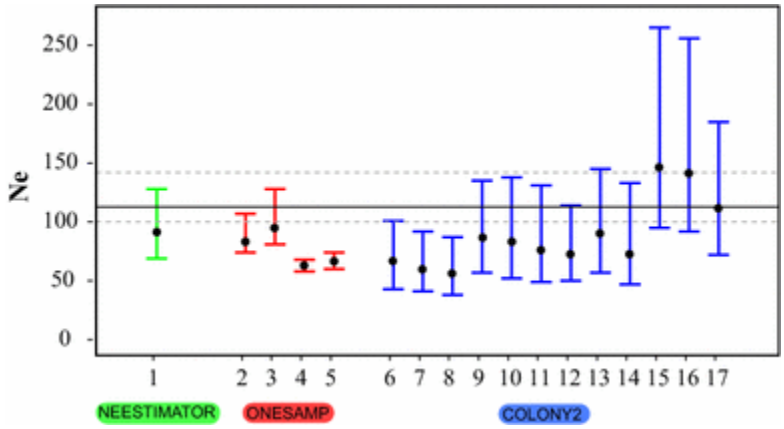

Fig. D2 *Ne* estimates and respective 95% CI for three single-sample estimators. Each number represents a different combination of input parameters for a particular method: NEESTIMATOR with jacknife 95% CI (1); ONESAMP and respective *Ne* priors 20–100 (2), 20–150 (3), 50–100 (4) 50–150 (5); COLONY2 under a random mating model, with a parent sampling probability of 0.15, 0.30 and 0.60 assuming polygamy (6, 7, 8), polyandry (9, 10, 11), polygyny (12, 13, 14) and monogamy (15, 16, 17), respectively. Horizontal lines represent mean $\widehat{N}$ estimate (solid) and 95% CI (dashed).

D5 – Discussion

In the studied population, *Ne* single-sample methods provided relatively concordant *Ne* estimates and did not yield unrealistic results given that we obtained ratios *Ne*/*N* <1 (Palstra and Ruzzante 2008; Palstra and Fraser 2012), except for the SA method under an assumption of monogamy for both sexes (see **Table D1**). Hence, we acknowledge the potential of these methods to estimate *Ne* for small populations in iteroparous species, assuming that the methods' assumptions and limitations are properly accounted for. Like other studies (*e.g.* Phillipsen *et al.* 2011; Holleley *et al.* 2014), ONESAMP delivered the most precise estimates, but similarly to Barker (2011), we detected some sensitivity to choice of priors. Having a reasonable expectation of population size (as in our study) helps in choosing adequate priors (see Holleley *et al.* 2014). However, more empirical studies evaluating ONESAMP performance under different priors and conditions are required. On the other hand, Waples *et al.* (2014) detected that LD method could yield downwardly biased estimates in iteroparous species. In our study, the LD method yielded a *Ne*/*N* ratio size higher than most ratios obtained by other methods, hence a high downward bias in our estimates is unlikely. The SA method estimated the highest *Ne* values when monogamy for both males and females was chosen (*Ne*/*N* > 1). Higher degrees of monogamy promote higher *Ne*/*N* ratios, mainly because variance of lifetime reproductive success is lower (meaning that, on average, individuals contribute similarly to a population's gene pool; see Palstra and Ruzzante 2008 and the review of Waples *et al.* 2013). However, assuming a scenario of monogamy for both sexes is unrealistic since fire salamander females are polyandrous (Caspers *et al.* 2014) and males are

thought to be polygynous (see Helfer *et al.* 2012 for *Salamandra atra*). COLONY2 analyses accounting for polygamy on both sexes generated the lowest *Ne* estimates among all tested methods. We do not exclude possible downward bias due to the presence of samples from different cohorts. Wang *et al.* (2010) stated that for iteroparous species, there is a higher probability of familial relationships with similar levels of relatedness to half-siblings (*e.g*. grandparent-offspring relationships). Since the SA method is also based on half-sibling frequencies, it is possible that *Ne* was underestimated in our study. Moreover, the frequency of polygamous matings from both sexes may be too low, and consequently, a scenario of polyandry or polygyny may describe our data more accurately. In fact, *Ne* estimates assuming polygyny or polyandry are closer to the ones obtained by the LD method and ONESAMP for some priors, but establishing which scenario is more realistic (polygamy, polyandry or polygyny) is not straightforward. Our results indicate the need for further genetic studies to confirm polygyny and to evaluate the extent to which multiple paternity occurs in fire salamanders.

The SA method also demonstrated a slightly higher sensitivity when different number of loci were used, presenting generally lower *Ne* estimates with 11 microsatellites. On one hand, it is possible that by using fewer markers, type I error rates increased (*i.e.* assignment of false sibship relationships), leading to lower *Ne* values. On the other hand, despite COLONY2 handling genotyping errors to avoid false exclusions of familiar relationships (Wang and Santure 2009), the effects of genotyping errors on *Ne* calculations using the SA method have not been thoroughly explored. Accordingly, studies testing simultaneously the effects of number of loci and genotyping error on the SA method's performance are required to tackle this issue.

Analyses of capture-mark-recapture models depicted a relatively low number of individuals inhabiting the studied patch, but contrary to our expectations, the population density was higher than expected given the small size and isolation of this habitat patch. Likely, the presence of sheltering features (*e.g.* wall's crevices and holes) and available food resources during subterranean activity may be crucial factors for the survival of this population. Interestingly, the studied urban population shows higher genetic diversity and smaller relatedness values when compared to two insular viviparous populations (San Martiño and Ons) (observed heterozygosity: 0.727 vs 0.56 and 0.66; relatedness = −0.019 vs 0.47 and 0.27; based on seven microsatellites used in Velo-Antón *et al.* 2012a). Moreover, the *N*, at least for the insular population Ons, is much larger than the studied urban population (Velo-Antón and Cordero-Rivera 2015). These results suggest that the potential recent bottleneck experienced by this urban population has not resulted in an evident loss of genetic diversity or

inbreeding depression. *Ne* estimates are also in line with this interpretation, because all methods yielded *Ne* >50, which is the minimal threshold considered in the literature to prevent, at least in the short-term, inbreeding depression (Jamieson and Allendorf 2012; but see also recommendations of higher thresholds by Frankham *et al.* 2014).

Additionally, the *Ne*/*N* ratios calculated in our study were higher than the median values calculated with genetic-based methods in amphibian literature (0.136–0.154; median values are variable due to studies employing multiple *Ne* estimators; Schmeller and Merilä 2007 and studies reported there; Beebee 2009; Ficetola *et al.* 2010). However, some authors also reported *Ne*/*N* >1 ratios using single-sample estimators in small populations (Schmeller and Merilä 2007; Beebee 2009). On *Bufo calamita*, Beebee (2009) attributed the high *Ne*/*N* ratios to mechanisms of genetic compensation, although he could not exclude bias due to insufficient sampling effort. However, Palstra and Ruzzante (2008) argue that mechanisms of genetic compensation may counteract reductions of *Ne* (and hence increase *Ne*/*N*) in small populations largely due to low reproductive variance. Contrarily, *Ne*/*N* ratios in large populations are generally lower because there is higher disparity in individual breeding success (for example, some individuals may reproduce more times than others during their lifespan). High degrees of polygamy may cause more pronounced reductions in *Ne*/*N* ratios. For example, Ficetola *et al.* (2010) showed that lower ratio sizes were associated with larger populations with greater levels of polygyny in *Rana latastei*. However, diverse systems of polygamy can differently influence *Ne*/*N* ratios. In the case of *Rana latastei*, male dominance behavior can impede other males from contributing to the gene pool of future generations and thus reduce *Ne*/*N* ratios. The same might hold true for dominant polygynous systems, but little is known about processes of reproductive behavior in species such as the fire salamanders. Although male–male agonistic behavior occurs in fire salamanders, this is rarely seen in nature and it is unclear whether this results from rival male combat during territorial defense or from mistaken matings (Velo-Antón *et al.* 2012b). We argue that the ability of polyandrous fire salamanders to store sperm from multiple males and generate progeny with multiple paternity in a single parturition event (Caspers *et al.* 2014), together with the potential existence of polygyny in this species in absence of social dominance, might induce low reproductive variance in males and thus, increasing *Ne*/*N* ratios.

Overall, the combination of small population census size, the mating mechanisms of female fire salamanders, and the reduced habitat patch in this isolated urban population may have played a greater role in determining *Ne*/*N* ratios than in most studies in amphibians. However, we do not dismiss that other factors, such as population size stability (Ficetola *et al.* 2010) or

the use of different *Ne* estimators in other studies (*e.g.* temporal methods; see discussion in Hoehn *et al.* 2012), could also explain the disparity observed between our study and others.

Here, we showed the utility of using a controlled urban system to obtain robust census and effective population size estimates. Overall, and despite the possible bias introduced by sampling multiple cohorts, this study shows consistent *Ne* estimates using different single-sample methods, suggesting that deviations from this assumption may not be critical in small and isolated populations. Finally, the high *Ne*/*N* ratio observed in our urban population might suggest mechanisms of genetic compensation (*e.g.* low reproductive variance or multiple paternity) that might help prevent inbreeding depression.

D6 – Acknowledgments

This work is funded by FEDER funds through the Operational Programme for Competitiveness Factors—COMPETE and by National Funds through FCT—Foundation for Science and Technology under the PTDC/BIA-EVF/3036/2012 and FCOMP-01-0124-FEDER-028325. GVA and AL are supported by FCT (IF/01425/2014 and PD/BD/106060/2015, respectively). We thank two anonymous reviewers for their helpful and constructive comments.

D7 – References

Álvarez D (2012) Las salamandras de la ciudad de Oviedo: una vida entre el asfalto. *Quercus*, **321**, 26-32.

Barker JSF (2011) Effective population size of natural populations of *Drosophila buzzatii*, with a comparative evaluation of nine methods of estimation. *Molecular Ecology*, **20**, 4452–4471.

Beebee TJC (2009) A comparison of single-sample effective size estimators using empirical toad (*Bufo calamita*) population data: genetic compensation and population size-genetic diversity correlations. *Molecular Ecology*, **18**, 4790–4797.

Benjamini Y, Hochberg Y (1995) Controlling the false discovery rate: a practical and powerful approach to multiple testing. *Journal of the Royal Statistical Society. Series B.*, **57**, 289–300.

Burnham KP, Anderson DR (2002) Model selection and multimodel inference: a practical information-theoretic approach. Springer, New York

Caspers BA, Krause ET, Hendrix R *et al.* (2014) The more the better- polyandry and genetic similarity are positively linked to reproductive success in a natural population of terrestrial salamanders (Salamandra salamandra). *Molecular Ecology*, **23**, 239–250.

Chybicki IJ, Burczyk J (2009) Simultaneous estimation of null alleles and inbreeding coefficients. *Journal of Heredity*, **100**, 106–113.

Cushman SA (2006) Effects of habitat loss and fragmentation on amphibians: a review and prospectus. *Biological Conservation*, **128**, 231–240.

Do C, Waples RS, Peel D, Macbeth GM, Tillett BJ, Ovenden JR (2014) NeEstimator v2: re-implementation of software for the estimation of contemporary effective population size (*Ne*) from genetic data. *Molecular Ecology Resources*, **14**, 209–214.

Ficetola GF, Padoa-Schioppa E, Wang J, Garner TW (2010) Polygyny, census and effective population size in the threatened frog, *Rana latastei*. *Animal Conservation*, **13**, 82–89.

Frankham R (2005) Genetics and extinction. *Biological Conservation*, **126**, 131–140.

FrankhamR(2010) Challenges and opportunities ofgenetic approaches to biological conservation. *Biological Conservation*, **143**, 1919–1927.

Frankham R, Bradshaw CJA, Brook BW (2014) Genetics in conservation management: revised recommendations for the 50/500 rules, Red List criteria and population viability analyses. *Biological Conservation*, **170**, 56–63.

García-París M, Alcobendas M, Buckley D, Wake D (2003) Dispersal of viviparity across contact zones in Iberian populations of Fire salamanders (*Salamandra*) inferred from discordance of genetic and morphological traits. *Evolution*, **57**, 129–143.

Guichoux E, Lagache L, Wagner S *et al.* (2011) Current trends in microsatellite genotyping. *Molecular Ecology*, **11**, 591–611.

Helfer V, Broquet T, Fumagalli L (2012) Sex-specific estimates of dispersal show female philopatry and male dispersal in a promiscuous amphibian, the alpine salamander (*Salamandra atra*). *Molecular Ecology*, **21**, 4706–4720.

Hendrix R, Hauswaldt JS, Veith M, Steinfartz S (2010) Strong correlation between cross-amplification success and genetic distance across all members of 'True salamanders' (Amphibia: Salamandridae) revealed by *Salamandra salamandra*-specific microsatellite loci. *Molecular Ecology Resources*, **10**, 1038–1047.

Hoehn M, Gruber B, Sarre SD, Lange R, Henle K (2012) Can genetic estimators provide robust estimates of the effective number of breeders in small populations? *PLoS ONE*, **7**, e48464.

Holleley CE, Nichols RA, Whitehead MR, Adamack AT, Gunn MR, Sherwin WB (2014) Testing single-sample estimators of effective population size in genetically structured populations. *Conservation Genetics*, **15**, 23–35.

Jamieson IG, Allendorf FW (2012) How does the 50/500 rule apply to MVPs? *Trends in Ecology and Evolution*, **27**, 578–584.

Johnson PCD, Haydon DT (2007) Maximum-likelihood estimation of allelic dropout and false allele error rates from microsatellite genotypes in the absence of reference data. *Genetics*, **175**, 827–842.

Jones O, Wang J (2010) COLONY: a program for parentage and sibship inference from multilocus genotype data. *Molecular Ecology Resources*, **10**, 551–555.

Luikart G, Ryman N, Tallmon DA, Schwartz MK, Allendorf FW (2010) Estimation of census and effective population sizes: the increasing usefulness of DNA-based approaches. *Conservation Genetics*, **11**, 355–373.

Palstra FP, Fraser DJ (2012) Effective/census population size ratio estimation: a compendium and appraisal. *Ecology and Evolution*, **2**, 2357–2365.

Palstra FP, Ruzzante DE (2008) Genetic estimates of contemporary effective population size: what can they tell us about the importance of genetic stochasticity for wild population persistence? *Molecular Ecology*, **17**, 3428–3447.

Peakall R, Smouse PE (2012) GenAlEx 6.5: genetic analysis in Excel. Population genetic software for teaching and research—an update. *Bioinformatics*, **28**, 2537–2539.

Phillipsen IC, Funk WC, Hoffman EA, Monsen KJ, Blouin MS (2011) Comparative analyses of effective population size within and among species: ranid frogs as a case study. *Evolution*, **65**, 2927–2945.

Queller D, Goodnight K (1989) Estimating relatedness using genetic markers. *Evolution*, **43**, 258–275.

Robinson JD, Moyer GR (2013) Linkage disequilibrium and effective population size when generations overlap. *Evolutionary Applications*, **6**, 290–302.

Rousset F (2008) GENEPOP'007: a complete re-implementation of the GENEPOP software for Windows and Linux. *Molecular Ecology Resources*, **8**, 103–106.

Schmeller DS, Merilä J (2007) Demographic and genetic estimates of effective population and breeding size in the amphibian *Rana temporaria*. *Conservation Biology*, **21**,142–151.

Skrbinšek T, Jelenčič M, Waits L, Kos I, Jerina K, Trontelj P (2012) Monitoring the effective population size of a brown bear (*Ursus arctos*) population using new single-sample approaches. *Molecular Ecology*, **21**, 862–875.

Steinfartz S, Kuesters D, Tautz D (2004) Isolation and characterization of polymorphic tetranucleotide microsatellite loci in the fire salamander *Salamandra salamandra* (Amphibia: Caudata). *Molecular Ecology Notes*, **4**, 626–628.

Tallmon DA, Koyuk A, Luikart G, Beaumont MA (2008) ONeSAMP: a program to estimate effective population size using approximate Bayesian computation. *Molecular Ecology Resources*, **8**, 299–301.

Velo-Antón G, Rivera AC (2015) La singular adaptación de las salamandras en el Parque Nacional de las Islas Atlánticas. *Quercus*, **353**, 32-39.

Velo-Antón G, Zamudio KR, Cordero-Rivera A (2012a) Genetic drift and rapid evolution of viviparity in insular fire salamanders (*Salamandra salamandra*). *Heredity*, **108**, 410–418.

Velo-Antón G, Galán P, Béjar X (2012b) *Salamandra salamandra gallaica* & *Salamandra salamandra europaea* (Fire salamander). Agonistic behaviour. *Herpetological Review*, **43**, 460–461.

Velo-Antón G, Santos X, Sanmartín-Villar I, Cordero-Rivera A, Buckley D (2015) Intraspecific variation in clutch size and maternal investment in pueriparous and larviparous *Salamandra salamandra* females. *Evolutionary Ecology*, **29**, 185-204.

Wake DB, Vredenburg VT (2008) Are we in the midst of the sixth mass extinction? A view from the world of amphibians. *Proceedings of the National Academy of Sciences USA*, **105** (Supplement 1), 11466–11473.

Wang J (2009) A new method for estimating effective population sizes from a single sample of multilocus genotypes. *Molecular Ecology*, **18**, 2148–2164.

Wang J, Santure AW (2009) Parentage and sibship inference from multilocus genotype data under polygamy. *Genetics*, **181**, 1579–1594.

Wang J, Brekke P, Huchard E, Knapp LA, Cowlishaw G (2010) Estimation of parameters of inbreeding and genetic drift in populations with overlapping generations. *Evolution*, **64**, 1704–1718.

Waples RS (2006) A bias correction for estimates of effective population size based on linkage disequilibrium at unlinked gene loci. *Conservation Genetics*, **7**, 167–184.

Waples RS, Do C (2010) Linkage disequilibrium estimates of contemporary *Ne* using highly variable genetic markers: a largely untapped resource for applied conservation and evolution. *Evolutionary Applications*, **3**, 244–262.

Waples RS, Luikart G, Faulkner JR, Tallmon DA (2013) Simple life history traits explain key effective population size ratios across diverse taxa. *Proceedings of the Royal Society B*, **280**, 20131339.

Waples RS, Antao T, Luikart G (2014) Effects of overlapping generations on linkage disequilibrium estimates of effective population size. *Genetics*, **197**, 769–780.

Weir BS (1979) Inferences about linkage disequilibrium. *Biometrics*, **35**, 235–254.

White GC, Burnham KP (1999) Program MARK: survival estimation from populations of marked animals. *Bird Study*, **46**(Supplement): 120–139.

D8 – Supplementary Information

Supplementary Table D.ST1

Table D.ST1 List of capture-recapture models to estimate population size of salamanders during 2008-2011 at Oviedo urban population. □AICc = difference in AICc value relative to the best model; wi = AICc weights of model i; MLi = likelihood of model i; np = number of parameters; Devi = deviance of model i. Selected model in bold. □ = survival; p = recapture probability; N: population size. t = time-dependent; · = constant.

Model #	Model	AICc	□AICc	w_i	ML_i	np	Dev_i
□	**□$_t$, p_t, $N_\cdot$**	**-482.810**	**0**	**0.824**	**1**	**19**	**249.287**
□	□$_t$, p_t, N_t	-479.462	3.348	0.155	0.188	22	246.159
□	□$_\cdot$, p_t, N_t	-475.394	7.416	0.020	0.025	20	254.552
□	□$_\cdot$, p_t, $N_\cdot$	-469.198	13.611	0.001	0.001	17	267.176
□	□$_t$, $p_\cdot$, N_t	-362.507	120.303	0	0.000	11	386.514
□	□$_\cdot$, $p_\cdot$, N_t	-360.416	122.394	0	0.000	9	392.759

Supplementary Table D.ST2

Table D.ST2 Characteristics of the 15 microsatellites used in this study. Information regarding multiplex arrangement, original published primer forward and reverse sequences, fluorescently labelled oligonucleotides used as template for modified forward primers and the concentration of primer forward (PF) and reverse (PR) used to construct multiplex mixes (_M) and on 10 µl PCR reactions are represented.

Locus	Multiplex	Label*	Primer forward (5' – 3')	Primer reverse (5' – 3')	PF_M/PCR (µM)	PR_M/PCR (µM)
SST-A6-I [2]	Panel S1	NED	TTCAGTGCTCTTGCAGGTTG	AGTCTGCAAGGATAGAAAGATCG	0.2 / 0.02	2.0 / 0.2
SST-A6-II [2]	Panel S1	PET	ATTCTCTCTGACAAGGATTGTGG	GGTAGACAGACATCAAGGCAGAC	0.12 / 0.012	1.2 / 0.12
SalE14 [1]	Panel S2	VIC	GCTGCCCTCTCTGCCTACTGACCAT	GCCAAGACATGGAACACCCTCCCGC	0.08 / 0.008	0.8 / 0.08
Sal29 [1]	Panel S2	6-FAM	CTCTTTGACTGAACCAGAACCCC	GCCTGTCGGCTCTGTGTAACC	0.8 / 0.08	8.0 / 0.8
SST-B11 [2]	Panel S3	PET	TCAAACGGTGCCAAAGTTATTAG	TTAATTGGCAGTTTTCTTTCCAG	0.2 / 0.02	2.0 / 0.2
SalE12 [1]	Panel S3	VIC	CTCAGGAACAGTGTGCCCCAAATAC	CTCATAATTTAGTCTACCCTCCCAC	0.08 / 0.008	0.8 / 0.08
Sal23 [1]	Panel S3	6-FAM	TCACTGTTTATCTTTGTTCTTTTAT	AATTATTTGTTTGAGTCGATTTTCT	0.92 / 0.092	9.2 / 0.92
SST-C3 [2]	Panel S4	PET	CCGTTTGAGTCACTTCTTTCTTG	TTGCTTTACCAACCAGTTATTGTC	0.14 / 0.014	1.4 / 0.14
SalE7 [1]	Panel S4	NED	TTTCAGCACCAAGATACCTCTTTTG	CTCCCTCCATATCAAGGTCACAGAC	0.08 / 0.008	0.8 / 0.08
SalE5 [1]	Panel S4	6-FAM	CCACATGATGCCTACGTATGTTGTG	CTCCTGTTTACGCTTCACCTGCTCC	0.06 / 0.006	0.6 / 0.06
SalE2 [1]	Panel S4	VIC	CACGACAAAATACAGAGAGTGGATA	ATATTTGAAATTGCCCATTTGGTA	0.3 / 0.03	3.0 / 0.3
SalE06 [1]	Panel S5	VIC	GGACTCATGGTCACCCAGAGGTTCT	ATGGATTGTGTCGAAATAAGGTATC	0.12 / 0.012	1.2 / 0.12
Sal3 [1]	Panel S5	6-FAM	CTCAGACAAGAAATCCTGCTTCTTC	ATAAATCTGTCCTGTTCCTAATCAG	0.12 / 0.012	1.2 / 0.12
SalE8 [1]	Panel S5	NED	GCAAAGTCCATGCTTTCCCTTTCTC	GACATACCAAAGACTCCAGAATGGG	0.08 / 0.008	0.8 / 0.08
SST-G9 [2]	Panel S5	NED	CCTCGTCAGGGGTTGTAGG	CTTTCCAGGAAGAAACTGAGATG	0.08 / 0.008	0.8 / 0.08

*An extra number of base pairs were added at 5' end of the original sequence of forward primers in order to allow binding of four different fluorescent labelled oligonucleotides (6-FAM - TGT AAA ACG ACG GCC AGT; VIC - TAA TAC GAC TCA CTA TAG GG; NED - TTT CCC AGT CAC GAC GTT G; PET - GAT AAC AAT TTC ACA CAG G);

[1] Steinfartz S *et al.* (2004)

[2] Hendrix R *et al.* (2010)

Supplementary Table D.ST3

Table D.ST3 Loci statistics for the 15 microsatellites used in this study and respective mean values (N – number of individuals genotyped; Na – number of alleles; Ho – observed heterozygosity; He – expected heterozygosity; NU – frequency of null alleles; HWD – deviations of HWE). Asterisks denote markers showing evidence for linkage disequilibrium (LD).

Locus	*N*	Na	Ho	He	NU	HWD
SST-A6-II	55	8	0.636	0.796	0.111	Yes
SalE14	58	9	0.879	0.846	0.008	No
SST-A6-I	55	13	0.855	0.856	0.010	No
Sal29	52	8	0.808	0.861	0.022	No
SST-B11	58	7	0.741	0.729	0.012	No
SalE12	58	12	0.724	0.786	0.025	No
Sal23*	56	4	0.482	0.647	0.129	Yes
SST-C3	54	6	0.463	0.705	0.200	Yes
SalE7*	57	11	0.772	0.864	0.037	No
SalE5	58	7	0.310	0.346	0.027	No
SalE2	58	17	0.828	0.879	0.013	No
SalE06	54	6	0.426	0.765	0.239	Yes
Sal3	56	14	0.893	0.877	0.007	No
SalE8	55	6	0.727	0.783	0.032	No
SST-G9	58	9	0.655	0.718	0.020	No
Mean	56.13	9.133	0.680	0.764	0.060	-

Supplementary Table D.ST4

Table D.ST4 Estimates of effective population size (*Ne*), 95% CIs and *Ne/N* ratios obtained from individuals genotyped at 11 microsatellites. Mean Ne and respective 95% CIs are presented for ONESAMP and COLONY2 summarizing results from three replicate runs for all tested scenarios. (PG – polygamy; PAND – polyandry; PGYN – polygyny; MG – monogamy).

Method	**Scenario**	N_e	**95% CIs**	N_e/N
NEESTIMATOR[A]		99	72-149 (74-149)	0.88
ONESAMP				
	20-100	75	66-92	0.66
	20-150	94	80-127	0.83
	50-100	63	80-127	0.56
	50-150	67	61-76	0.59
COLONY2[B]				
	PG – 0.15	49 (49)	32-80 (32-79)	0.43
	PG – 0.30	49 (49)	32-80 (31-78)	0.43
	PG – 0.60	46 (45)	29-72 (29-74)	0.41
	PAND – 0.15	70 (70)	46-111 (46-110)	0.62
	PAND – 0.30	71 (70)	46-114 (46-112)	0.63
	PAND – 0.60	61 (61)	41-97 (40-97)	0.54
	PGYN – 0.15	74 (74)	51-117 (48-120)	0.65
	PGYN – 0.30	68 (67)	45-108 (43-109)	0.60
	PGYN – 0.60	58 (57)	37-92 (37-92)	0.51
	MG - 0.15	125 (128)	81-211 (83-241)	1.11
	MG - 0.30	112 (114)	72-208 (72-211)	0.99
	MG - 0.60	94 (94)	62-153 (61-158)	0.83

[A] For NEESTIMATOR the jacknife confidence interval is in parenthesis

[B] For COLONY2 the N_e estimates and respective 95% CIs for the inbreeding model are in parenthesis